G protein-gated potassium channels in ventral tegmental area dopamine neurons temper behavioral sensitivity to cocaine

A THESIS
SUBMITTED TO THE FACULTY OF THE
UNIVERSITY OF MINNESOTA
BY

Nora Marie McCall

IN PARTIAL FULFILLMENT OF THE REQUIREMENTS
FOR THE DEGREE OF
DOCTOR OF PHILOSOPHY

Advisor: Kevin Wickman, PhD

February 2019

Acknowledgements

First and foremost, I must thank my advisor, Dr. Kevin Wickman. Thank you for providing an environment where I could thrive, guidance when I needed it, and independence when you knew it was time. I'm sorry, but I'm not sorry for all the powerpoints.

I thank my committee members: Dr. Mark Thomas (Chair), Dr. Robert Meisel, and Dr. Anna Lee. Thank you for your insight and encouragement throughout the years.

I thank my Wickman lab colleagues, past and present: Dr. Ezequiel Marron Fernandez de Velasco, Dr. Megan Tipps, Dr. Nicole Victoria, Dr. Lydia Kotecki, Dr. Nicole Wyedeven, Dr. Lei Zhang, Baovi Vo, Allison Anderson, Tim Rose, Margot DeBaker, Nicholas Carlblom, Hannah Oberle, Zhilian Xia, JingYing Zhang, and Melody Truong. This journey was made much more enjoyable having you all here with me. Drs. Marron Fernandez de Velasco and Tipps have been instrumental in my growth as a scientist, technically and intellectually, and as a person. I would especially like to thank our technicians, Nicholas Carlblom, Hannah Oberle, Zhilian Xia, JingYing Zhang, and Melody Truong, for their excellent care of the mouse colony, technical support, and assistance with experiments. I would not have been nearly as productive without your help.

I thank my co-authors who have contributed to my graduate publications: Drs. Lydia Kotecki, Segio Dominguez-Lopez, Ezequiel Marron Fernandez de Velasco, Amanda Sharpe, Michael Beckstead, and Kevin Wickman, and Nicholas Carlblom. Thanks to Dr. Victoria and Dr. William Engeland for help designing and performing the corticosterone radioimmunoassay experiments in Chapter 2, and to Dr. Yasushi

Nakagawa and the University Imaging Centers for their help in performing the immunohistochemistry experiments in Chapter 5.

I thank the Graduate Program in Neuroscience's Directors of Graduate Studies and Assistant Directors of Graduate Studies, past and present, for designing the graduate program curriculum; I think it is a good one. Special thanks to Dr. A. David Redish, for listening to me in times of decision making-induced emotional peril, and to Dr. Linda McLoon, for providing the perfect foil to Dave when I needed it. I thank my fellow students of Graduate Program in Neuroscience, particularly the wonderfully introverted class of 2013, for their community and support. We do not often get the opportunity to pick our colleagues, but I would have picked you.

I thank my scientific mentors prior to Minnesota who inspired and encouraged me to pursue this path. Dr. Melissa Glenn, thank you for instilling in me a sense of wonder and appreciation for the brain. Thank you for trying to ease us into the harder aspects of the job of neuroscience with vanilla scented trash bags; whenever I smell artificial vanilla, I think of you and the rats back in Maine. Dr. Chia Li, thank you for telling me I was enough when I needed to hear it, and for being one of the best examples of a scientist I know. Dr. Thomas Kash, thank you for seeing promise in me, and supporting me then and now.

I thank my family and friends. To my parents, Kevin and Jane McCall, and my sister Grace McCall, thank you for your unwavering support, even when it was unclear what I actually was doing with all those mice. I thank the friends I have made in Minnesota who have supported me so than I can say here and have made my time in Minnesota enjoyable, especially Megan Tipps, Mariah Wu, and Louis Prahl.

I thank running. While running, I have found much solace, and without it, I would not be who I am today, nor would I not be getting this degree. For bringing running into

my life, I must thank my first friend, Laura Tallerico, and my high school cross country coach, Tom Arnold, the standard by which all of my mentors are measured. I would also like the thank the community of runners I have joined in Minneapolis for enriching my life here and providing much needed balance.

I thank the University of Minnesota for providing mental health services in our health care. This is an incredibly worthwhile investment.

My thesis work was supported several NIH grants; as such, I thank the tax payer. My training was supported by appointments on the NIH training grants “Predoctoral Training of Neuroscientists” (T32-GM008471) and “Neuroscience Training in Drug Abuse Research” (T32-DA007234), as well as an individual National Research Service Award (F31-DA041767). My research was supported by grants award to my advisor, Dr. Kevin Wickman: R01 DA034696 and R01 MH061933. My work was also supported by DA007097 (LK) and DA032701 (MJB).

Finally, I would also like to thank you, the reader of this thesis, in part or in its entirety. Writing it brought me both stress and clarity; I hope it brings you the latter.

Dedication

This thesis is dedicated to the memories of Rachel Bentley (1988 – 2007) and Mark Sabatini (1989 – 2012). Your kindness is not forgotten.

Abstract

Drugs of abuse share the ability to enhance dopamine (DA) release in the mesocorticolimbic system. This increase in DA is thought to drive persistent adaptations in the brain and behavior that contribute to the progression of addiction. One such adaptation is a cocaine exposure-induced suppression of G protein-dependent inhibitory signaling in DA neurons of the ventral tegmental area (VTA), a cell population important for reward-related behavior. This cocaine-induced adaptation involves the internalization of G protein-gated inwardly rectifying K^+ (GIRK/Kir3) channels, a key contributor to inhibitory G protein pathways that normally temper DA neurotransmission in the mesocorticolimbic system. Dopamine 2 receptor (D_2R) activation mediates this adaptation. While methamphetamine, another psychostimulant, can induce a similar adaptation in inhibitory G protein signaling, other drugs of abuse, i.e. morphine, are unable to induce a GIRK channel adaptation. Thus, inhibitory G protein signaling in VTA DA neurons could be important for tempering the behavioral response to cocaine, and could represent an inhibitory "barrier" to addiction. The goal of this thesis research is to understand the impact of GIRK channel activity signaling on behavioral sensitivity to cocaine. The work in this thesis tests the hypothesis that the strength of inhibitory G protein signaling in VTA DA neurons is inversely related to behavioral sensitivity to cocaine.

This hypothesis predicts decreasing GIRK channel activity in DA neurons will increase behavioral sensitivity to cocaine. To test this, a genetic strategy was employed, to ablate GIRK channels in DA neurons using DATCre(+):*Girk2*$^{fl/fl}$ mice. The strength of two significant G protein receptor-dependent signaling dependent on GIRK channels were significantly reduced in a dopamine neuron-specific manner. DATCre(+):*Girk2*$^{fl/fl}$

mice displayed increased locomotor responding to both acute and repeated cocaine, as well as increased responding for, and intake of, cocaine in intravenous self-administration. The DATCre(+):*Girk2*$^{fl/fl}$ manipulation parallels the cocaine-induced suppression of GIRK-dependent signaling in VTA DA neurons, and suggests the GIRK channel in DA neurons temper behavioral sensitivity to cocaine.

This hypothesis was further tested in a VTA-specific manner using a Cre-dependent viral approach, overexpressing GIRK channels with opposing functional roles. The overexpression of GIRK2 increased inhibitory G protein signaling and decreased cocaine-induced locomotion, while conversely, overexpression of GIRK3 decreased inhibitory G protein signaling and increased cocaine-induced locomotion. Overall, this supports the hypothesis GIRK channel activity in VTA DA neurons tempers behavioral sensitivity to drugs of abuse.

In addition to addiction, VTA DA neurons have been implicated in negative affective behaviors, notably following stress. Interestingly, manipulating GIRK channel activity did not alter depression- and anxiety-related behavior, suggests that inhibitory signaling in VTA DA neurons mediated by GIRK channels plays a minimal role in negative affective behaviors, at least in non-stress conditions. However, footshock, a more severe form of stress, elicited adaptations in GIRK channel activity in VTA DA neurons, suggesting that GIRK channel activity could influence behavior following stress.

Taken together, the work in this thesis suggests the GIRK channel present in VTA DA neurons contributes to the behavioral effects of cocaine, and could represent a promising therapeutic target for psychostimulant addiction.

Table of Contents

List of Tables

List of Figures

List of Abbreviations

5-HTR	Serotonin receptor
AC	Adenylyl cyclase
ACSF	Artificial cerebrospinal fluid
ANOVA	Analysis of variance
BLA	Basolateral amygdala
BNST	Bed nucleus of the stria terminalis
cAMP	Cyclic adeonosine monophostate
Cas9	CRISPR-associated 9
CeA	Central amygdala
CGP	[S-(R*,R*)]-[3-[[1-(3,4-Dichlorophenyl)ethyl]amino]-2-hydroxypropyl](cyclohexylmethyl) phosphinic acid
Cm	Membrane capacitance
CNO	Clozipine-N-oxide
CPP	Conditioned place preference
CRF	Corticotropin-releasing factor
CRISPR	clustered regularly interspaced short palindromic repeats
D_1R	Dopamine 1 receptor
D_2R	Dopamine 2 receptor
DA	Dopamine
DAMGO	[D-Ala2, N-MePhe4, Gly-ol]-enkephalin
DAT	Dopamine transporter
DREADD	Designer receptor exclusively activated by designer drug
DRN	Dorsal raphe nucleus
dStr	Dorsal striatum
EC_{50}	Half maximal effective concentration
EPM	Elevated plus maze
FERM	4.1/ezrin/radixin/moesin-like domain
FR	Fixed ratio
FSS	Forced swim stress
FST	Forced swim test
GABA	γ-aminobutyric acid
$GABA_AR$	$GABA_A$ receptor
$GABA_BR$	$GABA_B$ receptor
GDP	Guanosine diphosphate
GIRK	G protein-gated inwardly-rectifying potassium channel
$GIRK2_{DA}KO$	DATCre(+):*Girk2*$^{flox/flox}$ mice
$GIRK2_{DA}WT$	DATCre(−):*Girk2*$^{flox/flox}$ mice
GPCR	G protein coupled receptor
GRK	G protein coupled receptor kinase
GTP	Guanosine triphosphate
HCN	Hyperpolarization-activated cyclic nucleotide gated channels
hM4Di	Modified form of the human M4 muscarinic (hM4) receptor
HPC	Hippocampus
I_h	Current through HCN channels
IL	Infralimbic
KCTD	Potassium channel tetramerization domain-containing protein

LC	Locus coeruleus
LDT	Laterodorsal tegmental nucleus
LH	Lateral hypothalamus
LHb	Lateral habenula
mAChR	Muscarinic acetylcholine receptor
mEPSC	Miniature excitatory postsynaptic currents
mGluR	Metabotropic glutamate receptor
MOR	Mu (μ) opioid receptor
MSN	Medium spiny neuron
NAc	Nucleus accumbens
NALCN	Sodium leak channel
NE	Norepinephrine
NET	Norepinephrine transporter
NT	Neurotransmitter
OFC	Orbitofrontal cortex
PAG	Periaqueductal gray
PB	Phosphate buffer
PBP	Parabrachial pigmental nucleus
PBS	Phosphate buffered saline
PDZ	Postsynaptic density -95, discs large, zona occludens domain
PFA	Paraformaldehyde
PFC	Prefrontal cortex
PIF	Parainterfasicular nucleus of the VTA
PIP_2	Phosphatidylinositol 4,5-bisphosphate
PKA	Protein kinase A
PKC	Protein kinase C
PL	Prelimbic
PN	Paranigral nucleus of the VTA
PP2A	Protein phosphatase 2A
PPTg	Pedunculopontine tegmental nucleus
PTX	Pertussis toxin
PX	Phox homology domain
Ref.	References
RGS	Regulator of G protein signaling
Rm	Membrane resistance
RMTg	Rostromedial tegmental nucleus
RT-PCR	Reverse transcription polymerase chain reaction
SERT	Serotonin transporter
SN	Substantia nigra
SNX27	Sorting nexin 27
SUD	Substance use disorder
TH	Tyrosine hydroxylase
VP	Ventral pallidum
VTA	Ventral tegmental area
VTAR	Ventral tegmental area, rostral part
β-ARR	β arrestin

Chapter 1

Introduction

1.1 Reward: behavior and circuitry

This thesis describes the contribution of inhibitory G protein signaling in ventral tegmental area dopamine neurons, a cell population important for reward and behavioral sensitivity to the addictive drug cocaine. To provide context for this work, reward behavior is explored, with an emphasis on the role of ventral tegmental area dopamine neurons and their interaction with other brain regions.

1.1.1 What is reward behavior?

The concept of reward is complex and multifaceted. These hedonic feature of reward, also described as “pleasure” or “liking,” are defined by positive affective reactions to stimuli and are key for the rewarding properties of “reinforcing” stimuli (Berridge et al., 2009; Volkow et al., 2017). Reward also encompasses the motivation to pursue rewarding stimuli, a facet described as “wanting” or “incentive salience” (Berridge, 2007; Berridge et al., 2009). The goal-directed actions to approach or pursue rewarding stimuli link motor activity and arousal to reward (Berridge and Robinson, 1998). Another key feature of reward behavior is its close interaction with learning (Hyman, 2005), as motivation for intrinsically reinforcing stimuli (*e.g.*, palatable food) can be transferred to associated context or cues, “conditioned reinforcement” (Schultz, 1998; Wise, 2004; Berridge et al., 2009; Volkow et al., 2017). Additionally, reward also involves behavioral economic computation and value (Flagel et al., 2009; Salamone and Correa, 2012). Together, these theories provide a broad overview of what “reward” means in neuroscience.

As with other aspects of biology, reward behavior generally takes place within a functional, homeostatic range. Rewarding stimuli, *e.g.*, food, are often necessary for survival. This often means the pursuit of rewarding stimuli, and the brain circuits underling this behavior, increases an individual's fitness and survival. However, when rewarding stimuli are pursued regardless of negative consequences, the function of brain regions associated with rewarding behavior is no longer advantageous. Indeed, the pursuit of rewarding stimuli, *e.g.*, drugs, despite negative consequences is a fundamental and debilitating feature of addiction. In this way, addiction can be conceptualized as a pathological extension of natural reward behavior. Additionally, many of the brain regions implicated in reward behavior have also been implicated in negative affective disorders, such as anxiety and depression. Negative affective disorders can be conceptualized as another disorder of reward circuitry. Overall, reward behavior exists on a spectrum, and pathological or disadvantageous behavior is found outside of the "ideal" middle range.

1.1.2 Anatomy of reward behaviors

Reward is complex and multifaceted; therefore, it follows that many brain regions are involved in the production and promotion of reward-related behaviors (**Figure 1.1**). Classically, reward behaviors are thought to be mediated primarily by the mesocorticlimbic system, which consists of the ventral tegmental area (VTA) – "meso" – and its reciprocal connections with the prefrontal cortex (PFC) – "cortico" – and the nucleus accumbens (NAc) – "limbic" (Lüscher and Malenka, 2011). However, a number of brain regions beyond the VTA, NAc, and PFC contribute to reward processing (**Figure 1.1**). In addition to striatal input, prominent projections to the VTA include the lateral hypothalamus (LH), which is involved in driving feeding behavior, and the dorsal raphe nucleus (DRN) (Qi et al., 2014; Castro et al., 2015; Nieh et al., 2015; Faget et al., 2016).

The ventral pallidum (VP), a common path for limbic output to the brainstem, also functions as a “hedonic hot-spot” and can promote drug seeking behavior and mediate aversion (Berridge et al., 2009; Root et al., 2015; Wulff et al., 2018). Other brain regions associated with positively modulating reward behaviors include the laterodorsal tegmental nucleus (LDT) (Carr and Sesack, 2000; Omelchenko and Sesack, 2005; Lammel et al., 2012) and the substantia nigra (SN; A9). The SN is a largely dopaminergic (~90%) (Margolis et al., 2006a) structure with reciprocal connections to the dorsal striatum (Watabe-Uchida et al., 2012) and is involved in movement control (Wise, 2009).

Other brain regions play a role in regulating the context- and state-dependent aspect of reward behavior. The locus coeruleus (LC), a brainstem nucleus containing norepinephrine (NE) and other neuropeptides, modulates a number of behaviors, including sleep cycles, attention, cognition, and stress responsiveness, which can influence reward-related behavior (Schwarz and Luo, 2015; Hurtubise and Howland, 2017). The hippocampus (HPC) receives dopaminergic input from the VTA and is involved in the representation of cues and context, as well as learning and memory (Lisman and Grace, 2005; McNamara et al., 2014), which can influence the learning aspect of reward. Similarly, the pedunculopontine tegmental nucleus (PPTg), an interface between the basal ganglia and motor systems, regulates environment-dependent arousal (Charara et al., 1996; Garzo´n et al., 1999; Mena-Segovia and Bolam, 2017), which can influence the perception of and response to rewarding stimuli.

Brain regions associated with negative valence impact reward seeking behavior are activated by aversive and fear- and stress-inducing stimuli. The amygdala, which consists of the central amygdala (CeA), the basolateral amygdala (BLA), and intercalated cells between the CeA and BLA, plays a key role in negative affective

behaviors, learning, fear, feeding, and emotion, and has been implicated in stress-induced reward seeking behavior (Janak and Tye, 2015). The bed nucleus of the stria terminalis (BNST) plays a key role in the integration of stress and anxiety and impacts reward (Avery et al., 2016). The lateral habenula (LHb) activates the rostral medial tegmental nucleus (RMTg), also referred to as the tail of the VTA, in response to aversive stimuli. RMTg activation provides inhibitory control over brain regions and cell types that promote reward-seeking, notably VTA neurons (Jhou et al., 2009; Omelchenko et al., 2009; Kaufling et al., 2010; Lecca et al., 2012). The periaqueductal gray (PAG) also promotes aversion and plays a role in analgesia, fear, and anxiety (Behbehani, 1995; Vander Weele et al., 2018).

Recent advances in tool development, *e.g.*, optogenetics (Kim et al., 2017), chemogenetics (Roth, 2016), and viral and genetic approaches allowing for cell type and brain region specificity, have facilitated a better understanding of the contribution of these brain regions and their connections to distinct aspects of reward behavior. The remainder of **Section 1.1.2** focuses on the VTA, with particular emphasis on dopamine (DA) neurons, as they are the experimental target of all studies in this thesis, and touches on the interaction between the NAc and PFC, the other classical components of the mesocorticolimbic system (Lüscher and Malenka, 2011), and the VTA.

Ventral Tegmental Area

The VTA, located in the medial, ventral, posterior part of the brain (**Figures 1.1 and 1.2**), contains dopaminergic (~55-65%), GABAergic (~30%), and glutamatergic neurons (~5%) (Hearing et al., 2012; Polter and Kauer, 2014; Pignatelli and Bonci, 2015). These VTA neuronal populations receive input from many of these same brain regions (Faget et al., 2016) and communicate with each other. The dopamine (DA)

neurons of the VTA generally play a central, but complicated role in the reinforcing effects of reward, while GABAergic neurons appear to oppose this function.

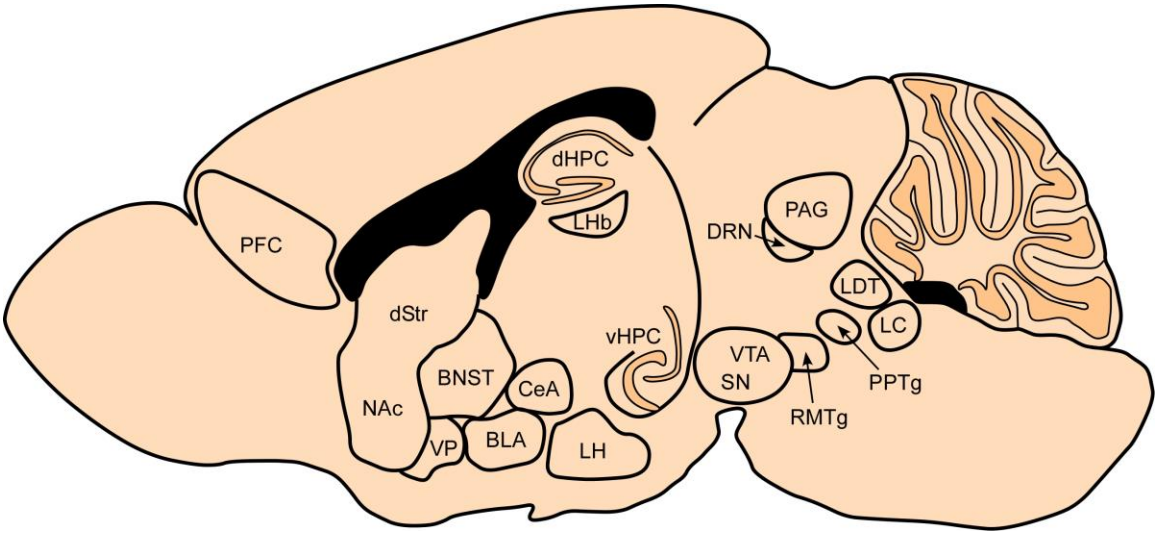

Figure 1.1. Brain regions implicated in reward-related behaviors.

Cartoon of sagittal brain section, depicting brain regions implicated in reward-related behavior, adapted from the Allen Brain Atlas (atlas.brain-map.org).

BLA (basolateral amygdala); BNST (bed nucleus of the stria terminalis); CeA (central amygdala); DRN (dorsal raphe nucleus); LDT (laterodorsal tegmental nucleus); LH (lateral hypothalamus); LHb (lateral habenula); HPC (hippocampus, dorsal and ventral); NAc (nucleus accumbens); PAG (periaqueductal grey); PFC (prefrontal cortex); PPTg (pedunculopontine tegmental nucleus)**;** RMTg (rostromedial tegmental nucleus); dStr (dorsal striatum); SN (substantia nigra); VP (ventral pallidum); VTA (ventral tegmental area)

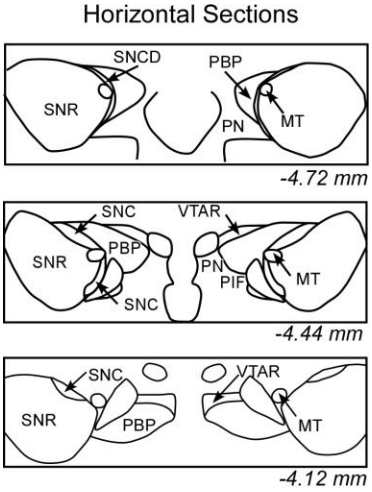

Figure 1.2. Detail of VTA subregions.

Horizontal sections of the VTA, adapted from *The Mouse Brain in Stereotaxic Coordinates, 3rd edition* (Franklin and Paxinos, 2008). Subregions considered part of the VTA include: PBP, parabrachial pigmented nucleus of the VTA; PIF, parainterfasicular nucleus of the VTA; PN, paranigral nucleus of the VTA; VTAR, ventral tegmental area, rostral part. Other landmarks include: MT, medial terminal nucleus of the accessory optic tract; SNC, substantia nigra, compact part; SNCD, substantia nigra, compact part, dorsal tier; SNR, substantia nigra, reticular part.

Dopamine neurons

Dopamine (DA) neurons of the VTA, also known as nucleus A10 cells, are the most prevalent cell type in the VTA (~55%) (Margolis et al., 2006b, 2010; Nair-Roberts et al., 2008). DA neurons can be identified by the presence of tyrosine hydroxylase (TH), Pitx3, and the dopamine transporter (DAT). TH is an enzyme involved in catecholamine synthesis (Daubner et al., 2011), and antibodies against TH, THeGFP(+) mice, and THCre(+) mice are used to identify and manipulate DA neurons in the VTA (Lammel et al., 2015; Stuber et al., 2015). DA neurons also express the homeobox transcription factor Pitx3, which is important for the development and maintenance of DA neurons, and Pitx3eGFP(+) and Pitx3Cre(+) mice are also used to identify and manipulate DA neurons (Zhao et al., 2004; Smidt et al., 2012). DAT pumps DA from the synaptic cleft into the cytosol of DA neurons. DATCre(+) mice are also widely used to manipulate DA neurons (Lammel et al., 2015; Stuber et al., 2015).

VTA DA neurons have classically been described as a homogeneous neuron population with well-defined electrophysiological properties and behavioral roles. Putative DA neurons were identified by the presence of I_h currents, which are mediated by hyperpolarization-activated cyclic nucleotide–gated (HCN) inwardly rectifying non-specific cation channels (Margolis et al., 2006b); a slower spontaneous firing rate; a larger size compared to surrounding putative GABAergic neurons' and inhibition by activators of dopamine 2 receptors (D_2Rs) (Margolis et al., 2012). These "classical" DA neurons were thought to be excited by reward and reward-related cues and inhibited by aversive cues (Schultz et al., 1997).

A rich body of recent work has revealed that DA neurons have diverse electrophysiological properties and broad influences on behavior (Lammel et al., 2014; Holly and Miczek, 2016; Juarez and Han, 2016; Morales and Margolis, 2017) (**Table**

1.1). The classic putative DA neurons are likely a single subpopulation of DA neurons: a lateral VTA population that projects to the lateral shell of NAc (Lammel et al., 2008). Indeed, DA neurons with other projection targets possess different electrophysiological properties. More medial DA neurons lack prominent I_h currents and project to the core and medial shell aspects of the NAc as well as the BLA and PFC. In particular, the PFC-projecting VTA DA neurons appear to have distinct electrophysiological properties, such as a lack of D_2R-mediated inhibition (Lammel et al., 2008). Additionally some VTA DA neuron subpopulations, including those projecting to the HPC and VP (**Table 1.1**) have not been electrophysiologically characterized. Further adding to the diversity of VTA DA neuron function is the wide variety of local and afferent input (Watabe-Uchida et al., 2012; Faget et al., 2016) (**Table 1.2**). The most prominent afferent inputs are from the striatum, DRN, and LH (Faget et al., 2016), but a variety of regions and neurotransmitters influence the excitability of, and behavior modulated by, VTA DA neurons.

There are a number of hypotheses about the role DA plays in reward behavior. Attempts to determine the meaning of DA have relied on lesioning or inhibiting DA neurons, or infusing DA receptor antagonists to determine the behavioral functions for which DA is necessary, and exciting DA neurons or infusing DA receptor agonists to determine the behavioral functions DA is sufficient to drive. Other studies observe DA neuron activity or DA release during behavior, and use the correlation of physiology with behavior to infer the role of DA. From these studies, it is clear that DA plays a role in pleasure, motivation, learning, value, incentive salience, and reward prediction error (**Section 1.1.1**). Indeed, the release of DA in the NAc appears to be linked to reward and reward-predictive cues (Schultz, 1998; Phillips et al., 2003). DA also plays a role in motor activity associated with the approach, attention, and arousal related to the pursuit

of reward (Berridge and Robinson, 1998). While DA modulates these experiences, it is, interestingly, not necessary for them. Indeed, rats with dopaminergic lesions display typical liking reactions (Berridge and Robinson, 1998) and dopamine deficient mice are able to learn (Hnasko et al., 2005). Additionally, while aversive stimuli elicit inhibition in some DA neurons, other midbrain DA neurons are activated by aversive and stressful events (Brischoux et al., 2009; Bromberg-Martin et al., 2010; Zweifel et al., 2011; Cohen et al., 2012; Schultz, 2013). Together, this constellation of data suggests the valence and behaviors associated with DA are likely brain region- and DA neuron subpopulation-dependent.

Table 1.1. VTA DA neuron electrophysiological and behavioral diversity, based on projection target.

Description	Location within the VTA	Electrophysiological and molecular properties	Behavior
VTA^{DA} → NAc lateral shell	Lateral, primarily PBP (Lammel et al., 2008)	"Classical" DA neuron I_h > 100 pA Slower firing frequency *ex vivo* Larger neuron cell body Higher DAT, VMAT expression Respond to opioid receptor activation (Ford et al., 2006)	Rewarding, promotes reinforcement (Lammel et al., 2012)
VTA^{DA} → NAc core	Medial posterior, in the PN and the most medial aspect of PBP (Lammel et al., 2008)	No I_h (sag) current Faster firing frequency Smaller neuron cell body Lower DAT, VMAT expression Respond to opioid receptor activation (Ford et al., 2006)	
VTA^{DA} → NAc medial shell			Cocaine increases A:N ratio (Lammel et al., 2011)
VTA^{DA} → BLA			
VTA^{DA} → PFC	Medial posterior, in the PN and the most medial aspect of PBP (Lammel et al., 2008)	No I_h (sag) current Faster firing frequency Smaller neuron cell body Lack Girk2-coupled D2R autoreceptors (Lammel et al., 2008) Lower DAT, VMAT expression	Cocaine does not change A:N ratio Activated by formalin to hindpaw (Lammel et al., 2012)
VTA^{DA} → HPC (Scatton et al., 1980; Gasbarri et al., 1994)			Memory retention, novelty (McNamara et al., 2014; Duszkiewicz et al., 2018)
VTA^{DA}→ VP (Klitenick et al., 1992)			Reward, aversion (Wulff et al., 2018)
VTA^{DA} → LHb		Releases GABA (Stamatakis et al., 2013)	Rewarding (Stamatakis et al., 2013)

Table 1.2. Summary of input to VTA DA neurons.

CRF, corticotrophin releasing factor; NE, norepinephrine, NT, neurotransmitter; Ref., references. * indicates input has been described for the VTA, but has not been not confirmed to directly synapse onto VTA DA neurons.

Input	NT	Other details	Ref.
Local, *i.e.*, VTA			
Other DA neurons	DA	Inhibit other DA neurons via D_2R autoreceptors	(Beckstead et al., 2004)
GABAergic interneurons	GABA	Inhibit DA neurons, with apparent preference for $GABA_AR$	(Edwards et al., 2017)
Glutamatergic neurons	Glutamate		(Dobi et al., 2010)
Outside the VTA			
Bed nucleus of the stria terminalis	Glutamate CRF		(Georges and Aston-Jones, 2001)
Central amygdala	GABA* CRF		(Korotkova et al., 2006; Watabe-Uchida et al., 2012)
Dorsal raphe nucleus	Glutamate GABA	Glutamatergic input increases DA release in the NAc	(Qi et al., 2014; Beier et al., 2015)
Lateral habenula	Glutamate	Excites DA neurons projecting to PFC	(Lammel et al., 2012; Stamatakis and Stuber, 2012)
Lateral hypothalamus	Glutamate GABA Orexin	GABAergic input involved in driving feeding behavior	(Peyron et al., 1998; Fadel and Deutch, 2002; Korotkova et al., 2003; Watabe-Uchida et al., 2012; Nieh et al., 2015)
Laterodorsal tegmentum	Glutamate GABA Acetylcholine	Glutamatergic input to DA neurons projecting to lateral NAc shell; GABAergic input to DA neurons projecting to the PFC	(Carr and Sesack, 2000; Omelchenko and Sesack, 2005; Lammel et al., 2012)
Locus coeruleus	NE*	LC NE neurons also have other peptides, such as neuropeptide Y and galanin	(Mejias-Aponte et al., 2009)
Nucleus Accumbens	GABA	Inhibits DA neurons, with apparent preference for $GABA_BR$	(Edwards et al., 2017)
Pedunculopontine tegmental nucleus	Acetylcholine Glutamate GABA*		(Charara et al., 1996; Garzo´n et al., 1999; Mena-Segovia and Bolam, 2017)

Periaqueductal gray	Glutamate GABA		(Omelchenko and Sesack, 2009; Ntamati et al., 2018)
Prefrontal cortex	Glutamate	Excites DA neurons projecting to PFC	(Carr and Sesack, 2000)
Rostral medial tegmental nucleus	GABA	Inhibits DA neurons, with apparent preference for $GABA_AR$	(Lammel et al., 2012; Edwards et al., 2017)
Ventral pallidum	Glutamate GABA		(Hjelmstad et al., 2013)

GABA neurons

GABAergic neurons in the VTA function as local interneurons and projection neurons. Electrophysiological characteristics of VTA GABA neurons include small size, often a lack of I_h, and fast firing frequencies (Lammel et al., 2014; Morales and Margolis, 2017). Because these electrophysiological characteristics overlap with those of "non-classical" VTA DA neurons, GABA neuron specific reporter mice, such as vGATCre, GADCre, GAD-eGFP, are useful for identifying these neurons. Local GABAergic interneurons inhibit VTA DA neurons and *in vivo* stimulation of VTA GABA neurons is aversive (Tan et al., 2012) and disrupts the consumption of reward (van Zessen et al., 2012). Additionally, the inhibition of VTA GABA neurons excites VTA DA neurons, known as "disinhibition," which can be elicited by opioids in most, but not all, VTA GABA neurons (Johnson and North, 1992; Margolis et al., 2012). Projection VTA GABA neurons go to the NAc, where they inhibit cholinergic interneurons to enhance associative learning (Brown et al., 2012), and to the LHb, where they inhibit glutamatergic neurons (Root et al., 2014b).

VTA GABA neurons receive input from and are modulated by a number of reward-related regions. VTA GABA neurons receive glutamatergic input from the lateral habenula (Omelchenko et al., 2009), PFC (Carr and Sesack, 2000), PAG (Omelchenko and Sesack, 2009), DRN (Beier et al., 2015); lateral hypothalamus (Nieh et al., 2015), and BNST (Kudo et al., 2012). VTA GABA neurons receive GABAergic input from the PAG (Omelchenko and Sesack, 2009), DRN (Beier et al., 2015); lateral hypothalamus (Nieh et al., 2015), BNST (Kudo et al., 2012), and LDT (Faget et al., 2016). GABAergic and glutamatergic projections innervate VTA GABA neurons that inhibit DA neurons (Jennings et al., 2013). VTA GABA neurons appear to play a key role in tempering the

excitability of VTA DA neurons, with the activity of VTA GABA neurons decreasing reward-associated behaviors (Jennings et al., 2013).

Glutamatergic neurons

2-15% of neurons in the VTA are glutamatergic, *i.e.*, express VGLUT2, a vesicular glutamate transporter (Nair-Roberts et al., 2008). Glutamatergic neurons are predominantly found in the medial VTA (Nair-Roberts et al., 2008) receive input from the cortex (Faget et al., 2016), synapse onto local DA and non-DA neurons (Dobi et al., 2010), and project to several different brain areas including the NAc, glutamatergic neurons of the LHb, VP, amygdala, and PFC (Yamaguchi et al., 2007, 2015; Hnasko et al., 2012; Root et al., 2014a; Faget et al., 2016). VTA glutamatergic neurons have small to no I_h current and fast spontaneous firing rates (Hnasko et al., 2012). Glutamatergic projections from the VTA to NAc parvalbumin GABAergic interneurons and to the LHb to drive aversion (Root et al., 2014a; Qi et al., 2016). Conversely, stimulation of local VTA glutamatergic neurons is rewarding and reinforcing (Wang et al., 2015).

Hybrid neurons of the VTA

Interestingly, some VTA neurons contain and release more than one neurotransmitter (Root et al., 2014b; Zhang et al., 2015; Berrios et al., 2016). GABA/DA neurons target NAc MSNs (Kim et al., 2015) and the lateral habenula, where GABAergic signaling promotes reward (Stamatakis et al., 2013). GABA/glutamate neurons project to the lateral habenula as well (Root et al., 2014b). DA/glutamate neurons target NAc MSNs (Zhang et al., 2015), NAc cholinergic interneurons (Chuhma et al., 2014), and PFC parvalbumin GABAergic interneurons (Kabanova et al., 2015). More work is needed to understand the full extent of the behavioral roles of these hybrid VTA neurons.

Nucleus Accumbens

The NAc can be divided into several functional subregions: the core, the medial shell, and the lateral shell. The NAc core is thought to play a larger part in motor function related to reward, while the NAc shell is associated with positive reinforcement, motivation, and incentive salience. The NAc core receives the majority of its prefrontal input from the prelimbic PFC and lateral oribitofrontal cortex (OFC), and in turn projects to the SN (Saddoris et al., 2013). The NAc shell receives input from the infralimbic cortex and medial lateral OFC and in turn projects to the VTA (Saddoris et al., 2013). DA release in the NAc has classically been associated with reward or the anticipation of reward (Schultz, 1998; Phillips et al., 2003). Extensive work has implicated the NAc in the wanting and liking aspects of reward. Interestingly, opioid receptors expressed in the anterior and ventral to posterior and dorsal medial shell of the NAc appear to mediate a gradient of pleasure to aversion, respectively (Castro and Berridge, 2014; Al-Hasani et al., 2015).

In addition to regional diversity, the NAc has a number of cell types. Over 95% of neurons in the NAc are D_1R and D_2R medium-sized spiny neurons (MSNs). MSNs receive glutamatergic input from the BLA, PFC, and HPC (Saddoris et al., 2013). D_1R MSNs, also called direct pathway MSNs, express the neuropeptides dynorphin and substance P. They are called the “direct” pathway because they project directly to the globus pallidus internal and SN pars reticulata. D_1R MSNs connect to and inhibit VTA DA and GABA neurons (Bocklisch et al., 2013; Edwards et al., 2017). D_2R MSNs, also called indirect MSNs, express the neuropeptide encephalin and project to the globus pallidus external. Other cell types in the NAc are parvalbumin and cholinergic interneurons, the latter of which are reciprocally connected with the VTA (Brown et al., 2012; Cachope et al., 2012; Chuhma et al., 2014). Changes in glutamatergic signaling in

the NAc, particularly MSNs, have been observed following repeat exposure to drugs of abuse, and these adaptations may partly underlie behavioral adaptations elicited by repeated exposure to and withdrawal from drugs of abuse (Lüscher and Malenka, 2011).

Prefrontal Cortex

The PFC, which includes the prelimbic cortex (PL), infralimbic cortex (IL), and orbitofrontal cortex (OFC), is a layered cortical structure, with glutamatergic pyramidal neurons in layers 2/3 and 5/6 making up the majority of neurons (Hearing et al., 2012). Layer 5/6 pyramidal neurons project to other brain regions in the mesocorticolimbic system, while GABAergic interneurons temper the excitability of PFC pyramidal neurons. The glutamatergic pyramidal neurons in the PFC receive dopaminergic input from the VTA; these PFC neurons in turn project to the NAc and VTA (Carr and Sesack, 1999; Carr et al., 1999). VTA DA neurons and PFC glutamatergic neurons are reciprocally connected and associated with aversion (Carr and Sesack, 2000; Omelchenko and Sesack, 2005; Lammel et al., 2012; Watabe-Uchida et al., 2012). The IL is generally thought to drive drug seeking behaviors, while the PL is through to drive extinction. However, recent research suggests the role of PFC in drug addiction is more complex, tying into its complex cognitive role (Moorman et al., 2015).

1.2 Addiction in human patients and animal models

1.2.1 Addiction: the human disease

In the United States, approximately 20-22 million people are addicted to drugs (Volkow et al., 2016), and the lives of countless more people are affected indirectly by having a loved one struggle with addiction. Substance-use disorder (SUD) is a complex, chronic mental disorder characterized by compulsive, continued consumption of a

substance in spite of negative consequences and the desire to stop consuming the substance (Root et al., 2014a). The term “addiction” describes the most severe, chronic stage of SUD. Current treatment options for SUD and addiction are not numerous, nor are they completely effective. Awareness of individual and communal risk factors, such adolescence, novelty seeking, impulsive traits, and socioeconomic status can aid in the development and allocation of preventative treatments for addiction (Castellanos-Ryan and Conrod, 2011). After SUD and addiction has developed, the goal of treatment is to reduce withdrawal symptoms and prevent relapse. Generally, treatment consists of a combination of behavioral changes, *e.g.*, therapy and avoidance of drug-associated cues, and medication. Medications are specific for the type of substance consumed: opioid SUDs can be managed with methadone and buprenorphine (Bell, 2014); alcohol dependence can be treated with disulfiram and naltrexone (Kranzler and Soyka, 2018); and nicotine addiction can be managed with nicotine replacement products, bupropion, and varenicline (Jackson et al., 2019). There are no medications for addiction to psychostimulants, such as cocaine.

The pathological pattern of behaviors associated with SUD and addiction consist of four main criteria: impaired control, social impairment, risky use, and pharmacological criteria (American Psychiatric Association, 2013). Impaired control includes deficits in decision making and craving, the intense urge to consume the substance (American Psychiatric Association, 2013). Pharmacological criteria include “tolerance,” which is characterized by requiring a large amount of drug to achieve the desired effect or experiencing a smaller effect when a typical amount of drug is consumed. Another pharmacologic criteria is “withdrawal,” which occurs when blood and tissue concentrations of the substance decrease in a person who has maintained prolonged heavy use and the accompanying negative emotional state and physical symptoms

(American Psychiatric Association, 2013; Koob and Volkow, 2016). There is a great deal of individual variability in SUD and addiction, as not all individuals who consume addictive substances transition to becoming habitual users. SUD and addiction can occur alongside other mental illnesses, such as anxiety, depression, or post-traumatic stress disorder, and these illnesses can be worsened by environmental stimuli associated with the consumed substance (Holly and Miczek, 2016).

Addiction can be conceptualized as three repeating stages, which incorporate the defining criteria of this disease: binge and intoxication, withdrawal and negative affect, and preoccupation and anticipation (*i.e.*, craving) (American Psychiatric Association, 2013; Volkow and Koob, 2015; Koob and Volkow, 2016; Volkow et al., 2016). These stages are characterized by different internal states, anatomical regions, and neurotransmitter systems.

"Binge and intoxication" describes the reorientation of priorities of a person with addiction toward the consumed substance, driven by the initial desire to feel good early in addiction and to escape dysphoria as the disease progresses. This phase is associated with a sharp increase in DA release in the ventral striatum, which corresponds to the euphoric, "high" feeling associated with drugs of abuse (Koob and Volkow, 2016). These feelings are initially associated with consumption of the substance, but shift to become associated with environmental stimuli that precede, or predict, the receipt of the substance through neuroplasticity within the mesocorticolimbic reward circuitry (Lüscher and Malenka, 2011; Schultz, 2013). These changes can lead to exposure to cues associated with the substance promoting drug seeking and relapse.

Withdrawal and negative affect. As SUD and addiction progress, the consumption of the same amount of substance leads to smaller increases in DA levels, *i.e.*, tolerance, making the brain less sensitive to substance and non-substance rewards

(Koob and Volkow, 2016; Volkow et al., 2016). This can increase negative affect, such as feelings of reduced energy, reduced excitement, depression, anxiety, and restlessness (Koob and Le Moal, 2005). Repeated exposure to DA can lead to adaptations in and increased activation of brain regions implicated in negative affect, *e.g.*, the extended amygdala, as well as in neurotransmitter systems involved in the stress response, *e.g.*, corticotrophin-releasing factor (CRF) and dynorphin (Polter and Kauer, 2014). These changes can lead to a dysphoric state when the direct effects of the consumed substance dissipate during withdrawal and generally due to the reduced responsiveness of DA neurons. These symptoms can drive compulsive consumption in an attempt to escape these negative feelings.

Preoccupation and anticipation. As addiction progresses, the PFC adapts and contributes to impaired executive function, including impaired self-regulation, decision making, flexibility choosing and completing actions, determining value, and monitoring error (Goldstein and Volkow, 2011). Initial alterations in dopaminergic signaling contribute to subsequent changes in glutamatergic signaling in prefrontal regions (Britt and Bonci, 2013), which contribute to impaired decision making and obsessive desire for the drug.

1.2.2 Preclinical models of addiction

The goal of preclinical (*i.e.*, animal) models of addiction is to recapitulate one or more of the hallmarks of human SUD and addiction. These features include craving, impaired decision making, increased negative affective symptoms (*i.e.*, withdrawal), the association of environmental cues with the drug, cue-induced drug-seeking behavior after a period without drug-seeking (*i.e.*, relapse), repeated exposure to drug changing the response to drug, and persistently taking drug despite negative consequences. Preclinical models assist with our understanding of basic mechanisms underling SUD

and addiction. This basic knowledge is especially needed in the context of psychostimulant addiction, where there is not yet an effective pharmacotherapy to pair with behavioral treatment approaches for human patients.

Self-administration

The gold standard for studying drug addiction using rodent models is self-administration, as it shares many features with human addiction. In this model, mice or rats are implanted with an intravenous catheter and are trained to take drug by pressing a lever or poking their nose into a port. This assay can allow one to observe the acquisition of self-administration behavior, which provides insight into the early "binge and intoxication" stage of addiction. Using different doses of drug to create dose response curves can yield insight into sensitivity to drug and tolerance. Escalating schedules of drug delivery can assess break point and provide a measure of motivation to work for drug, or craving. The requirement for animals to approach and work for drug resembles the pursuit feature of reward-related behaviors. Additionally, one can extinguish drug seeking behavior (*i.e.,* nose pokes, lever presses) akin to abstinence, and subsequently reinstate drug use with drug-associated environmental cues (*e.g.*, a light) or stress (such as restraint or an injection of yohimbine, an α2-adenergic receptor antagonist, which increases norepinephrine) to model relapse. Thus, this behavioral paradigm aligns well with many features of human SUD and addiction. Recent iterations of the self-administration task have incorporated foot shocks and other aversive stimuli as a model of drug taking in the face of negative consequences, another hallmark of addiction.

Conditioned place preference

Conditioned place preference (CPP) relies upon the rewarding valence of a substance becoming associated with the environment in which the substance is consumed. In CPP, rodents are exposed to a behavioral chamber with two distinct contexts, often distinguished by visual (*e.g.*, stripes on the wall), tactile (*e.g.*, bar or wire mesh flooring), and odorant (*e.g.*, different bedding) cues. After a baseline preference test, rodents are injected with vehicle and confined to one side of the chamber. Later in the day or the next day, subjects are injected with drug and confined to the other side of the chamber. After several pairings, rodents have free access to the entire chamber, and the time spent in each side is recorded. Increased time in the drug-paired chamber, compared with the initial preference, is indicative of the rewarding valence of the drug. An optogenetic variant of this task is real time place preference, in which light pulses are delivered on one chamber side.

CPP behavior engages the association of drug with environment, and is a way to indirectly assess a substance's hedonic component. While the administration of the substance is non-contingent (*i.e.*, the experiment administers a specific amount of drug, rather than the subject choosing to take drug), the ability of mice to physically move to indicate their preference models an aspect of drug seeking and approach in human patients with SUDs. Additionally, this association can be extinguished through repeated exposure to the drug-paired side without drug, and this preference can be reinstated by exposure to drug or stress, which models relapse, similar to self-administration reinstatement studies.

Locomotor activity and behavioral sensitization

When rodents are exposed to different classes of drugs of abuse, *i.e*., psychostimulants like cocaine or methamphetamine and opioids like morphine, they increase their locomotor activity due to the increase of DA in the striatum. Subsequent exposures to the substance leads to an enhancement of the locomotor response; this phenomenon is termed “sensitization.” While humans do not have an explicit behavioral correlate of this increased locomotor behavior following drug exposure (*i.e.*, people with SUD or addiction do not run around the room in which they take drug), the concept of sensitization shares the same premise as tolerance, in which repeated drug exposure causes a behavioral change in response to the drug. While this test lacks the volitional aspect of drug taking, best modeled by self-administration, the ability to control the amount of drug exposure allows for improved experimenter control and the straightforward measurement of locomotor activity makes this a reliable, high-throughput approach for assessing behavioral sensitivity to drugs of abuse.

1.2.3 Mechanisms of action of drugs of abuse

Drugs of abuse exert their behavioral effects via brain regions and neurotransmitter systems that mediate natural reward. In general, the initial positive effects of drug exposure are associated with increased DA, which can reinforce the association of drug taking with cues, while later developing behaviors, result from adaptations in glutamatergic signaling.

Psychostimulants, including cocaine, methamphetamine, and amphetamine, increase DA by altering the function of DAT. Cocaine blocks the dopamine transporter (DAT), which is necessary for the rewarding properties of cocaine; cocaine also blocks the serotonin transporter (SERT) and the norepinephrine transporter (NET) (Rocha, 2003; Hall et al., 2004; Chen et al., 2006). As a result of blocking DAT, DA increases in

brain regions receiving dopaminergic projections (*e.g.*, NAc), and locally within the VTA (Di Chiara and Imperato, 1988; Aragona et al., 2008). Human users consume cocaine through multiple routes of administration, including intravenously, intranasally, and by smoking “crack” cocaine. Cocaine metabolism differs among these routes of administration. The duration and intensity of drug effects depends on the method of use; injecting or smoking cocaine produces a quicker and stronger, but shorter-lasting, high than snorting.

Opioids, including morphine, heroin, and fentanyl, act by binding to opioid receptors, *i.e.*, mu opioid receptors (MORs), kappa opioid receptors, and delta opioid receptors, and opioid receptors in the NAc and VTA are critical for the rewarding effects of opioids (Fields and Margolis, 2015). Opioids are thought to increase DA release in the NAc through the disinhibition of VTA DA neurons, wherein GABA neurons expressing MORs and synapsing onto VTA DA neurons are inhibited (Johnson and North, 1992). MORs on GABAergic input from the RMTg, VP, and VTA provide this disinhibition (Xia et al., 2011; Hjelmstad et al., 2013; Matsui et al., 2014).

1.3 Inhibitory G protein receptor signaling

Reward behavior is orchestrated by chemical communication between the brain regions and neuron types outlined in **Section 1.1.2**. Communication between neurons is generally mediated by activity- and calcium-dependent release of neurotransmitters usually from the presynaptic neuron axon terminal. Neurotransmitters are ligands for and bind to channels or receptors, located on the dendrites and soma of the postsynaptic neuron. Channels are ionotropic, directly opening when a ligand is bound to the channel allowing for fast excitation or inhibition. Receptors are metabotropic, acting through G protein signaling cascades to modulate cellular excitability over a longer time scale.

These receptors can presynaptic, allowing for the modulation of neurotransmitter release, as changing the potential of a neuron changes the activation of voltage-gated channels that regulate neurotransmitter release. While all of these cellular mechanisms work in concert to regulate the excitability of neurons and thus control behavior, the present thesis focuses on the contribution of inhibitory G protein signaling to behavior.

1.3.1 Inhibitory G protein coupled receptors

G protein coupled receptors (GPCRs) are a large family of 7 transmembrane domain proteins play a vital role in regulating physiology, demonstrated by ~34% of all drugs approved by the US Food and Drug Administration acting on GPCRs (Hauser et al., 2017). GPCRs have an extracellular amino (N) terminus and an intracellular carboxyl (C) terminus, and are activated by the extracellular binding of ligands, which can include neurotransmitters, proteins, hormones, and lipids. GPCRs share the ability to transduce the extracellular binding of ligands to intracellular responses through the activity of the heterotrimeric G proteins Gα, Gβ, and Gγ. The binding of ligands to the extracellular portion of the GPCR promotes the exchange of GTP for GDP and the dissociation of the Gα and Gβγ (**Figure 1.2**). Activated Gα and Gβγ interact with and modulate a wide range of intracellular effectors, including ion channels, cyclases and lipases. Several different Gα, Gβ, and Gγ subunits have been identified in the nervous system, further contributing to the functional diversity of different receptor populations. GPCRs are classified by sequence homology and functional similarity, as well as by the subfamily of their associated Gα subunit. Gα subunit families include Gαs, Gαi/o, Gαq/11, and Gα12/13, which differ in sequence and in their modulatory effect on cellular excitability. Gαs and Gαi/o both act on adenylyl cyclase (AC) to increase or decrease its function,

respectively. Gαq/11 acts on phospholipase C, which alters internal calcium stores, among other effects.

GPCRs provide “gain control” for neuronal excitability, altering the likelihood of an action potential, rather than producing a signal itself. GPCRs located presynaptically influence neurotransmitter release liklihood, while postsynaptically located GPCRs influence the liklihood of producing an action potential. The focus of the present thesis is on signaling mediated by inhibitory $GABA_BR$ and D_2R GPCRs present in VTA DA neurons.

1.3.2 Downstream effectors of inhibitory GPCRs

The activation of inhibitory GPCRs associated with Gαi/o proteins generally leads to the hyperpolarization of neurons. The function of these inhibitory GPCRs is blocked by pertussis toxin (PTX), produced by the bacterium *Bordetella pertussis*, which keeps the Gαi/o protein in the GDP-bound state (Fields and Casey, 1997). Following activation of inhibitory GPCRs, GDP on the Gαi/o protein is exchanged for GTP, and Gαi/o and Gβγ dissociate and act on different downstream effectors (**Figure 1.2**). Gαi/o-GTP reduces the activity of AC, decreasing the amount of the kinase cyclic adenosine monophosphate (cAMP), a second messenger that activates protein kinase A (PKA), which then interacts with phosphorylation dependent mechanism. Gβγ blocks voltage gated calcium channels (Ye et al., 1999; Kamp and Hell, 2000), which prevents depolarization. Gβγ also binds to and open G protein-gated inwardly rectifying potassium (K^+; GIRK) channels, hyperpolarizing the neuron as K^+ leaves. Inhibitory GPCR function is also mediated by blockade of the sodium leak channel, NALCN (Philippart and Khaliq, 2018). G protein signaling is terminated when GTP on Gαi/o is hydrolyzed to GDP and re-associates with Gβγ, a process hastened by regulator of G protein signaling (RGS)

proteins. The function GPCRs is also modulated by G protein coupled receptor kinases (GRKs), which phosphorylate GPCRs allowing for the binding of β–arrestin (βARR), which blocks G protein signaling through internalization.

The focus of this thesis is on one of these downstream effectors of inhibitory G protein signaling, the GIRK channel.

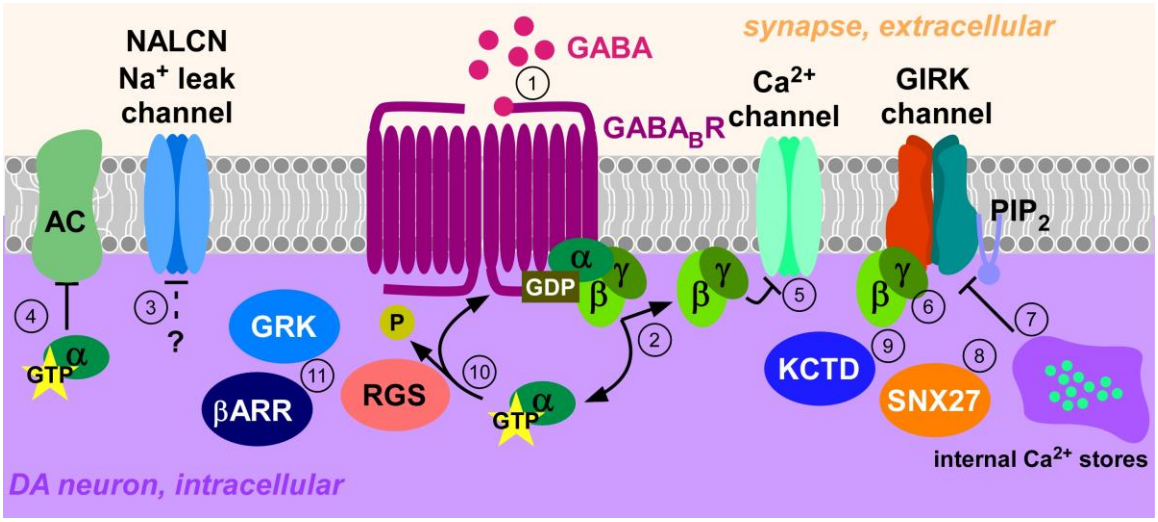

Figure 1.3. Schematic depicting some of the mechanisms regulating inhibitory G protein signaling in a VTA DA neuron.

In this example, when 1) the neurotransmitter GABA binds to $GABA_BR$, 2) GDP is exchanged for GTP on Gαi/o, and Gαi/o and Gβγ dissociate. 3) Activation of inhibitory GPCRs block the function of a Na^+ leak channel. 4) Gαi/o blocks the function of AC, while 5) Gβγ blocks the function of Ca^{2+} channels. 6) Gβγ binds to and opens GIRK channels, which is PIP_2 dependent. 7) Internal Ca^{2+} stores, 8) SNX27, and 9) KCTD proteins negatively modulate GIRK channel activity. 10) The endogenous GTPase activity of Gαi/o hydrolyzes GTP, allowing Gαi/o and Gβγ to re-associate. This process can be hastened by the activity of RGS proteins 11) GRK can phosphorylate GPCRs, allowing βARR to internalize these receptors, thereby negatively modulate G protein signaling.

1.3.3 GIRK channels

G protein-gated inwardly-rectifying potassium (K^+; GIRK/Kir3) channels are functionally coupled to PTX sensitive inhibitory GPCRs, including $GABA_BRs$; dopamine D_2Rs, D_3Rs and D_4Rs; muscarinic acetylcholine receptors (mAChRs); group II metabotropic glutamate receptors (mGluR2 and mGluR3); kappa, delta, and mu opioid receptors (KORs; DORs; and MORs); serotonin receptors ($5\text{-}HT_1Rs$, $5\text{-}HT_{2B}R$, $5\text{-}HT_{5A}R$); somatostatin receptors (SSTRs, 1-5); neuropeptide Y receptors (Y1R, Y2R); and adenosine receptor A_1R. GIRK channels hyperpolarize and decrease the excitability of neurons, similar to other K^+ channels under physiological conditions. G protein-gated refers to the role of $G\beta\gamma$ in opening GIRK channels (Lüscher and Slesinger, 2010). However, GDP-bound $G\alpha i/o$ subunits can bind to sites on the C and N terminal domains of GIRK1 and GIRK2, inhibiting the baseline activation of GIRK channels and GPCR-GIRK channel coupling (Logothetis et al., 1987; Reuveny et al., 1994; Wickman et al., 1994; Kofuji et al., 1995). Inward rectification refers to the presence of a more dramatic slope in the current-voltage (I-V) relationship below the reversal potential (or equilibrium) of K^+ where K^+ enters the neuron, than above the reversal potential of K^+ where K^+ leaves the neuron. Inward rectification is due to the occlusion of the GIRK channel's central pore by intracellular Mg^{2+} and polyamines above the equilibrium potential of K^+ (Leaney and Tinker, 2000; Peleg et al., 2002; Clancy et al., 2005; Rubinstein et al., 2009). Under physiological conditions, the resting membrane of a typical neuron, including VTA DA neurons, is above the equilibrium potential for K^+, making inwardly rectification an interesting quality, but not a practical consideration when considering the contribution of this channel to neuronal excitability.

GIRK channel subunits

There are four GIRK channels subunits: GIRK1, GIRK2, GIRK3, and GIRK4 (Yamada et al., 1998; Hibino et al., 2010). They are encoded by the following genes, respectively: Kcnj3, Kcnj6, Kcnj9, and Kncj5. These subunits have distinct structural elements and domains, which influence expression patterns and channel function. GIRK1, GIRK2, and GIRK3 are widely expressed in the central nervous system while GIRK4 is generally lacking in the brain, with some exceptions (Karschin et al., 1996; Wickman et al., 2000).

GIRK1

GIRK1 is thought to be part of the prototypical neuronal GIRK channel, as the loss of GIRK1 decreases GIRK channel function in most neuron types tested, and GIRK1 interacts with Gβγ (Huang et al., 1997; Hearing et al., 2013). However, GIRK1 cannot form homotetramers *in vivo or in vitro* (Lüscher and Slesinger, 2010). GIRK1 has splice variants (Karschin et al., 1996), but they have not been significantly investigated. The C- and N-terminal domains of GIRK1 are able to associate with Gαi/o, negatively modulating the activity of GIRK channels at baseline (Nelson et al., 1997). GIRK1-containing channels have ~5-fold higher sensitivity to activation by Gβγ, compared with GIRK2/GIRK3 channels (Leaney and Tinker, 2000; Peleg et al., 2002; Clancy et al., 2005; Rubinstein et al., 2009).

GIRK2

GIRK2 is also considered part of the prototypical neuronal GIRK channel, as mice lacking GIRK2 have profoundly decreased inhibitory GPCR currents in all cell types that have been measured (Lüscher et al., 1997; Slesinger et al., 1997; Jelacic et al., 2000; Torrecilla et al., 2013, 2002, 2008; Cruz et al., 2004; Koyrakh et al., 2005; Marker

et al., 2006; Kotecki et al., 2015; McCall et al., 2017). GIRK2 has an endoplasmic reticulum export signal allowing GIRK2 to be able to form homotetramers (Ma et al., 2002). Additionally, GIRK2 also has an internalization VL motif (Kofuji et al., 1995), so GIRK2 could also play a more general role in channel activity. There are three splice variants of GIRK2: GIRK2a, GIRK2b, and GIRK2c. GIRK2c has a postsynaptic density-95, discs large, zona occludens (PDZ) binding motif, which interacts with PDZ-containing trafficking motifs of sorting nexin 27 (SNX27) (Ma et al., 2002). This interaction between GIRK2c and SNX27 could facilitate both forward trafficking and internalization (Lunn et al., 2007). GIRK2c displays an even distribution from soma to distal dendrites, while GIRK2a is more localized to dendrites proximal to the cell body, suggesting a difference in subcellular trafficking (Marron Fernandez de Velasco et al., 2017b). Additionally, a Leu in the C-terminal domain of GIRK1 (L333) and GIRK2 (L344) channels appears to have a critical role in the G$\beta\gamma$-dependent activation of GIRK channels (He et al., 1999).

GIRK3

Interestingly, the loss of GIRK3 does not overtly impact the function of GIRK channels, as the loss of GIRK3 does not usually alter the maximal $GABA_BR$-GIRK current (Finley et al., 2004; Ivanina et al., 2004; Arora et al., 2010). However, the loss of GIRK3 in VTA DA neurons, which lack GIRK1, decreases the EC_{50} for the $GABA_BR$ agonist baclofen, suggesting that GIRK3 has a subtle, negative modulatory role (Labouèbe et al., 2007; Hearing et al., 2013). RGS2 decreases $GABA_BR$-GIRK coupling in a GIRK3-dependent manner (Labouèbe et al., 2007). GIRK3 has a PDZ binding domain (Lesage et al., 1995), and a lysosomal targeting sequence YWSI (Lunn et al., 2007); these features can promote the internalization of GIRK channels. There are no reported splice variants for GIRK3, and GIRK3 is unable to form homoteramers.

GIRK4

GIRK4, like GIRK2, contains an endoplasmic reticulum export motif that allows for forward trafficking and the potential formation of functional homotetrameric channels (Ma et al., 2002). GIRK4 is expressed in cardiac pacemaker cells, where GIRK channels (I_{KACh}) are functionally linked to muscarinic and adenosine receptors and regulate heart rate (Kofuji et al., 1995; Slesinger et al., 1996; Wickman et al., 1998; Kennedy et al., 1999; Ma et al., 2002). GIRK4 is sparsely expressed in the central nervous system, but appears to have some a role in behavior. A notable exception is the population of $GIRK4^+$ neurons in the hypothalamus, which links GIRK4-containing channels to energy balance, as *Girk4*$^{-/-}$ mice display increased late-onset obesity (Perry et al., 2008). GIRK4 is also expressed in the hippocampus (Perry et al., 2008), and *Girk4*$^{-/-}$ mice have impaired performance in the Morris water maze (Wickman et al., 2000).

Neuronal GIRK channel expression

GIRK channels are expressed widely throughout the brain (Karschin et al., 1996), including VTA DA neurons (Kotecki et al., 2015; McCall et al., 2017), VTA GABA neurons (Cruz et al., 2004; Kotecki et al., 2015), PFC pyramidal neurons (Hearing et al., 2013), HPC pyramidal neurons (Lüscher et al., 1997), substantia nigra DA neurons (Koyrakh et al., 2005), cerebellar granular neurons (Slesinger et al., 1997), locus coeruleus neurons (Torrecilla et al., 2002, 2008, 2013), and spinal cord lamina II neurons (Marker et al., 2006). Interestingly, GIRK channels are not widely expressed in the striatum, as evidenced by *in situ* hybridization studies (Karschin et al., 1996) and electrophysiological characterization (Marcott et al., 2014). However, GIRK channels do appear to be present in approximately 10% of MSNs neurons in the striatum (Marron Fernandez de Velasco et al., 2017a).

The prototypical neuronal GIRK channel likely consists of GIRK1 and GIRK2, as the genetic ablation of either of these subunits significantly decreases the size of somatodendritic GIRK currents in many neuron types, including pyramidal neurons of the PFC (Hearing et al., 2013) and HPC (Lüscher et al., 1997). Additionally, GIRK1 and GIRK2 can be co-immunoprecipitated, and in regions where these subunits are co-expressed, the disruption of GIRK2 expression significantly diminishes GIRK1 expression (Luján et al., 2014). This suggests the expression of GIRK1 and GIRK2 are linked, supporting the idea that the prototypical neuronal GIRK channel consists of GIRK1 and GIRK2.

The cellular expression pattern of GIRK channels suggests they are predominantly a postsynaptic inhibitory mechanism. Indeed, electroimmunomicroscopy studies have found that GIRK channels are most prominently expressed in the postsynaptic dendrite and cell body regions in many brain regions (Luján et al., 2014). These postsynaptic GIRK channels are usually located in extrasynaptic, also called perisynaptic, regions outside of the postsynaptic density, suggesting their function mediates the effects of inhibitory GPCRs activated by neurotransmitters overflowing from the synapse. However, there do appear to be some instances in which GIRK channels are found presynaptically (Koyrakh et al., 2005).

VTA DA neurons have a unique GIRK channel

While the prototypical neuronal GIRK channel is thought to contain GIRK1 and GIRK2, the GIRK channel present in VTA DA neurons appears to be GIRK1-lacking (Liao et al., 1996). Indeed, $GABA_BR$-GIRK somatodendritic currents in putative VTA DA neurons are not altered in *Girk1*$^{-/-}$ mice (Cruz et al., 2004; Labouèbe et al., 2007; Arora et al., 2010), and single cell multiplexed RT-PCR found that TH-expressing (DA) neurons

of the VTA expressed GIRK2 and GIRK3, but not GIRK1 (Arora et al., 2010). GIRK2c (Arora et al., 2010), the splice variant expressed in VTA DA neurons, appears to be vital for GIRK channel function, as genetically ablating *Girk2* causes a profound decrease in $GABA_BR$-GIRK somatodendritic currents (Cruz et al., 2004). This is congruent with GIRK2 being necessary for a functional GIRK channel, due to its endoplasmic reticulum export signal (Ma et al., 2002). While putative DA neurons of the VTA in *Girk3*$^{-/-}$ mice have normal maximal $GABA_BR$-GIRK somatodendritic currents (Arora et al., 2010), their EC_{50} for baclofen is significantly reduced (Labouèbe et al., 2007). This suggests that GIRK3 has a subtle negative affect on the function of VTA DA neuron GIRK channels, and that GIRK2 homotetramers are more sensitive to $GABA_BR$ activation. Interestingly, another prominent dopaminergic population, SN DA neurons, only expresses GIRK2a and GIRK2c (Inanobe et al., 1999).

Regulators of GIRK channel activity

The activity of GIRK channels is most profoundly regulated by the $G\beta\gamma$ subunits, as their direct binding to GIRK channels opens GIRK channels (Slesinger et al., 1995). Additionally, the interaction of PIP_2 with GIRK channels can activate GIRK channels and is required for $G\beta\gamma$ binding to activate GIRK channels (Wickman et al., 1994; Huang et al., 1995, 1997, 1998; Krapivinsky et al., 1995; Chan et al., 1997; Sui et al., 1998; Zhang et al., 1999; Hibino et al., 2010; Whorton and MacKinnon, 2011, 2013). Ethanol can directly activate GIRK1/GIRK2 and GIRK1/GIRK4 channels, via the hydrophobic pocket formed by the N-terminal domain and βD-βE loop of one GIRK channel subunit and the βL-βM loop of a neighboring subunit (Kobayashi et al., 1999; Lewohl et al., 1999; Aryal et al., 2009). Sodium also activates GIRK channels (Sui et al., 1996; Ho and Murrell-

Lagnado, 1999). Basal GIRK channel activity is suppressed by the binding of the Gαi/o-GDP subunit (Müllner et al., 2000).

The strength of GIRK channel signaling is modulated by a number of mechanisms. Phosphorylation mediated by PKA appears to increase channel function (Leaney and Tinker, 2000; Peleg et al., 2002; Clancy et al., 2005; Rubinstein et al., 2009), while the dephosphorylation of GIRK channels by protein phosphatase 2A (PP2A) reduces G protein-mediated activation (Medina et al., 2000; Rusinova et al., 2009). Conversely, GIRK channel currents are decreased by protein kinase C (PKC) phosphorylation of GIRK1 (Leaney et al., 2001; Müllner et al., 2003; Mao et al., 2004; Brown et al., 2005). The release of internal calcium stores via the activation of group I mGluRs also decreases $GABA_BR$- and D_2R-GIRK currents (Kramer and Williams, 2016). GIRK channels and inhibitory GPCRs form macrocomplexes, allowing for phosphorylation-dependent trafficking of receptors to influence GIRK channel function (Lavine et al., 2002; Lober et al., 2006; Ciruela et al., 2010; Terunuma et al., 2010; Padgett et al., 2012; Fajardo-Serrano et al., 2013; Hearing et al., 2013).

Potassium channel tetramerization domain-containing (KCTD) proteins 8, 12, 12b, and 16 associate with the C-terminal domain of $GABA_{B2}R$ (Guetg et al., 2010) and regulate GIRK currents in a subtype-specific manner. KCTD12 reduces constitutive receptor internalization and increases signaling at the cell surface (Schwenk et al., 2010). However, GIRK currents induced by receptors associated with KCTD12 and 12b have very pronounced desensitization, while KCTD8 and KCTD16 show very little desensitization (Ivankova et al., 2013), possibly due to differences in specific homology domains in the various KCTD subtypes (Schwenk et al., 2010; Adelfinger et al., 2014; Turecek et al., 2014). KCTD12 causes fast, reversible desensitization by binding to

activated Gβγ subunits and preventing their interaction with GIRK channels (Seddik et al., 2012).

SNX27, expressed throughout the brain, modulates GIRK channel activity in a complex manner (Rifkin et al., 2017). Coexpression of SNX27 and GIRK channels in HEK cells and hippocampal culture reduces inhibitory GPCR-GIRK currents (Lunn et al., 2007; Balana et al., 2011). However, the genetic ablation of SNX27 from DA neurons also reduces $GABA_BR$-GIRK currents (Munoz and Slesinger, 2014; Rifkin et al., 2018). This suggests SNX27 is involved in both the internalization and forward trafficking of GIRK channels, suggesting that SNX27 could function as an adapter between GIRK channels and a retromer complex (Munoz and Slesinger, 2014; Rifkin et al., 2017, 2018). Interestingly, GIRK2c and GIRK3 both contain a class I PDZ-binding motif in their C-terminus (ESKV). This facilitates their interaction with the N-terminal PDZ domain on SNX27 (Lunn et al., 2007). In addition to this PDZ domain, SNX27 contains two other notable functional domains, a Phox homology (PX) domain and a 4.1/ezrin/radixin/moesin (FERM)-like domain. The PX domain binds phosphatidylinositol-3-phosphate, which is enriched in early endosomes, targeting SNX27 to early endosomes (Kajii et al., 2003; Joubert et al., 2004). The FERM-like domain contains a Ras-association domain, that is necessary for SNX27 regulation of GIRK channels (Lunn et al., 2007; Balana et al., 2013).

RGS proteins negatively regulate G protein signaling through the interaction of the “RGS box” or RH homology domain motif with Gα-GTP proteins. This interaction increases the endogenous GTPase activity of the Gα subunit, accelerating its inactivation, caused by GTP hydrolyzing to GDP (Neubig and Siderovski, 2002). Thus, RGS proteins regulate cellular excitability by indirectly modulating the activation of GIRK channels and inhibition of voltage-gated calcium channels (Doupnik et al., 1997; Chuang

et al., 1998; Ross and Wilkie, 2000; Hollinger and Hepler, 2002; Traynor, 2010). RGS2 decreases coupling efficiency between $GABA_BR$ and GIRK channels in VTA DA neurons, due to the interaction between RGS2 and GIRK3 in the unique GIRK2/GIRK3 channel (Labouèbe et al., 2007). R7 family RGS proteins, which include RGS6, RGS7, RGS9, and RGS11, contain the Gγ-like domain allowing for an interaction with the atypical member of the Gβ protein family, Gβ5, to make a complex similar to the Gβγ dimer (Anderson et al., 2009, 2010). The RGS7/Gβ5 complex interacts with GIRK channels in CA1 pyramidal neurons of the hippocampus (Anderson et al., 2009, 2010), modulating GIRK channel function and spatial learning and memory (Fajardo-Serrano et al., 2013; Ostrovskaya et al., 2014).

Finally, neuronal activity can bi-directionally modulate the strength of GIRK channel activity. These adaptations are mediated by protein trafficking dependent upon the PDZ domain present on GIRK2c and GIRK3 subunits (Lalive et al., 2014). The potentiation of GIRK channel activity caused by increased neuronal activity requires NMDAR activation, intracellular calcium, and CaMKII activation (Lalive et al., 2014). Additionally, activity-dependent dephosphorylation of GIRK2 at Ser-9 increases GIRK channel activity through increased forward trafficking (Lalive et al., 2014). Drugs of abuse likely usurp these mechanisms, leading to drug-dependent plasticity of GIRK channel activity (**Section 1.4.1**).

1.3.4 GIRK channels in behavior

Inhibitory GPCRs are expressed throughout the brain and modulate a large variety of behaviors. As a major downstream effector of inhibitory GPCRs, GIRK channels are poised to influence behavior. The loss of GIRK channels globally and in specific cell types leads to a variety of changes in behavior, including locomotion, anxiety, depression, learning, memory, analgesia, and obesity (**Table 1.3**). Behavioral

sensitivity to drugs of abuse is also altered by the loss of GIRK channels, a topic explored in depth in this thesis.

Table 1.3. Behavioral alterations in GIRK channel knockout mice.

Knockout	Behavior	Ref.
***Girk1*$^{-/-}$**	Hyperactivity ↓anxiety (↓time in open arm of EPM) Increased operant responding for food	(Pravetoni and Wickman, 2008; Arora et al., 2010)
***Girk2*$^{-/-}$**	Increased propensity for seizures Hyperactivity Hyperalgesia ↓analgesia ↓anxiety (↓time in open arm of EPM) Increased operant responding for food Do not phase advance wheel-running behavior in response to melatonin Fear conditioning deficit	(Signorini et al., 1997; Ikeda et al., 2000; Blednov et al., 2002, 2003, Marker et al., 2002, 2004, 2005; Pravetoni and Wickman, 2008; Arora et al., 2010; Hablitz et al., 2015; Victoria et al., 2016)
***Girk3*$^{-/-}$**	Regular locomotor activity Regular anxiety	(Pravetoni and Wickman, 2008)
***Girk4*$^{-/-}$**	Impaired performance in Morris water maze Late onset obesity	(Wickman et al., 1998; Perry et al., 2008)
***Girk2*$^{-/-}$/*Girk3*$^{-/-}$**	Increased propensity for seizures	(Jelacic et al., 2000)
CamKIICre:*Girk1*$^{fl/fl}$	Impaired chemogenetic induction of associative learning	(Tipps et al., 2018)
CamKIICre:*Girk2*$^{fl/fl}$	Impaired contextual associative learning	(Victoria et al., 2016)
GADCre:*Girk2*$^{fl/fl}$	Regular cue and contextual associative learning	(Victoria et al., 2016)
DATCre:*Girk2*$^{fl/fl}$	↓depressive-like behavior (↓immobility in FST)	(Honda et al., 2018)

1.4 Inhibitory G protein signaling in addiction

Experience-based plasticity of excitatory signaling, *e.g.*, long term potentiation of glutamatergic signaling, is a key feature of learning and other behavioral adaptations in response to environmental stimuli. Interestingly, inhibitory G protein signaling mediated by GIRK channel activity also changes following exposure to a variety of environmental stimuli (**Table 1.4**). Indeed, stressful stimuli, such as footshock exposure or forced swim stress, elicit adaptations in inhibitory G protein signaling mediated by GIRK channel in LHb neurons and serotonin DRNs (Lemos et al., 2012; Lecca et al., 2016). Additionally, changes in VTA DA neuron activity elicits adaptations in GIRK channel signaling (Lalive et al., 2014). Thus, it follows that drugs of abuse, which alter the activity of VTA DA neurons also elicit adaptations in GIRK channel activity which persist beyond acute drug exposure.

1.4.1 Drugs of abuse alter inhibitory G protein signaling mediated by GIRK channels

Psychostimulants and ethanol have been shown to alter GIRK channel activity (**Table 1.4**), and the majority of these studies have focused on VTA DA neurons. Putative DA neurons of the VTA have decreased $GABA_BR$ and D_2R signaling 1 to 5 days following the injection of 15 mg/kg cocaine (Arora et al., 2011). This adaptation is dependent on D_2R activation and appears to be mediated by the internalization of GIRK channels (Arora et al., 2011). Interestingly, this effect was not observed in putative DA neurons of the neighboring SN (Arora et al., 2011). However in a similar study GIRK channel activity in VTA DA neurons identified with the DA neuron marker line Pitx3-eGFP did not change following cocaine exposure (Padgett et al., 2012). These findings suggest a subpopulation of DA neurons experienced adaptation described in putative

DA neurons, most likely the laterally located NAc lateral shell projecting population (Lammel et al., 2008, 2012). Similarly, GIRK channel activity in VTA DA neurons is decreased by exposure to methamphetamine (Padgett et al., 2012; Sharpe et al., 2015; Munoz et al., 2016). Perhaps the psychostimulants cocaine and methamphetamine share a common mechanism for decreasing GIRK channel activity. Since both drugs increase extracellular DA concentrations which activate D_2R to inhibit DA neurons (Beckstead et al., 2004), they could work via an activity-dependent mechanism to internalize GIRK channels (Lalive et al., 2014). In contrast to acute cocaine exposure, prolonged exposure to methamphetamine reduces GIRK channel activity in SN DA neurons as well (Sharpe et al., 2015). Interestingly, repeated exposure to EtOH increases D_2R-GIRK currents, but does not alter $GABA_BR$-GIRK currents (Perra et al., 2011). This adaptation can be mimicked by the attenuation of intracellular calcium (Perra et al., 2011), congruent with the NMDAR- and CaMKII-dependent burst firing-induced increase in GIRK channel activity in the same neuron population (Lalive et al., 2014), as these mechanisms involve an increase in calcium. This suggests calcium-mediated signaling could be a shared mechanism underlying adaptations in GIRK channel activity.

In addition to VTA DA neurons, GIRK channel activity is also reduced following exposure to psychostimulants in other neuron populations. A single injection of cocaine or methamphetamine decreases GIRK channel activity in VTA GABA neurons (Padgett et al., 2012). $GABA_BR$-GIRK signaling in prelimbic layer 5/6 PFC pyramidal neurons is decreased following repeated exposure to cocaine (Hearing et al., 2013). GIRK channel trafficking in these neurons appears to be mediated by a phosphorylation dependent mechanism, as a protein phosphatase inhibitor rapidly reverses the effects of psychostimulants on GIRK channel activity in PFC pyramidal neurons and VTA GABA neurons (Padgett et al., 2012; Hearing et al., 2013).

Table 1.4. Experience-based plasticity of GIRK channel activity.

Experience	Cell population	Effect on GIRK channel activity	Ref.
***Ex vivo* manipulations**			
ex vivo depolarization/burst firing protocol	VTA DA neurons	↑	(Lalive et al., 2014)
ex vivo tonic firing protocol	VTA DA neurons	↓	
Estrogen (E2)	Hypothalamic POMC and DA neurons	↓ uncouples μORs and $GABA_BRs$ from GIRK channels	(Kelly et al., 2003)
ex vivo morphine, ~20 h	Cultured hippocampal neurons	↑ 5-HT, ↓ $GABA_BR$	(Nassirpour et al., 2010)
Non-drug experiences			
Footshock exposure	Lateral habenula	↓	(Lecca et al., 2016)
Repeated forced swim stress	Dorsal raphe nucleus serotonergic neurons	↑	(Lemos et al., 2012)
Circadian cycle, during the light cycle	Suprachiasmatic nucleus	↑ GIRK2 protein and function	(Hablitz et al., 2014)
Cocaine			
5 d 15 mg/kg, i.p.	Prelimbic PFC layer 5/6 pyramidal neurons	↓	(Hearing et al., 2013)
1 d 15 mg/kg, i.p.	VTA, putative DA neurons	↓, lasted up to 5d	(Arora et al., 2011)
	SN, putative DA neurons	n.c.	
1 d 15 mg/kg, i.p.	VTA DA neurons	n.c.	(Padgett et al., 2012)
	VTA GABA neurons	↓	
Methamphetamine			
1 d 2 mg/kg	VTA DA neurons	↓, observed at 1d, did not last to 7d	(Padgett et al., 2012)
3 d 2 mg/kg	lateral VTA DA neurons	↓	(Sharpe et al., 2015)
14 d 2 mg/kg	lateral VTA DA neurons	↓	(Sharpe et al., 2015)
5 d 2 mg/kg, i.p., in a novel environment	lateral VTA DA neurons	↓	(Sharpe et al., 2015)
1d 2 mg/kg, i.p.	VTA GABA neurons	↓, lasted through 7d	(Padgett et al., 2012)

Self-administration for 20 – 44 d,	VTA DA neurons	↓	(Sharpe et al., 2015)
	SN DA neurons	↓	
Ethanol			
2 g/kg, 3 times per day, for 7 d	VTA, putative DA neurons	↑ D_2R currents n.c. $GABA_BR$ currents	(Rahman et al., 2003)

1.4.2 Inhibitory G protein signaling influences behavioral sensitivity to drugs of abuse

Just as exposure to drugs of abuse can shift GIRK channel activity, genetic manipulations of inhibitory signaling G protein signaling, $GABA_BRs$, and D_2Rs and GIRK channels alter behavioral sensitivity to drugs of abuse (**Table 1.5**).

$GABA_BR$ appears to play a role in mediating the behavioral sensitivity to a range of drugs of abuse. Behavioral, neurochemical, biochemical, and molecular alterations induced by nicotine were prevented by the $GABA_BR$ agonist, while these alterations by nicotine were potentiated by pretreatment with a $GABA_BR$ antagonist and in $GABA_{B1}R^{-/-}$ knockout mice (Varani et al., 2018). Intra-VTA $GABA_BR$ agonist suppresses alcohol self-administration in alcohol-preferring rats (Maccioni et al., 2018), decreases EtOH-induced CPP (Bechtholt and Cunningham, 2005), reduces heroin self-administration (Xi and Stein, 1999, 2000), blocks cocaine self-administration (Backes and Hemby, 2008), and reduces amphetamine- or morphine-enhanced locomotion (Leite-Morris et al., 2004; Zhou et al., 2005). Pretreatment with a novel positive allosteric modulators of $GABA_BRs$ decrease cocaine self-administration and ethanol drinking (de Miguel et al., 2018). The loss of $GABA_{B1}R$ from dopamine neurons induces cocaine sensitivity in a mouse strain that is unresponsive to cocaine, but does not appear to have altered behavioral sensitivity to morphine (Edwards et al., 2017). Together, this suggests $GABA_BRs$ in the VTA temper behavioral responses to drugs of abuse.

D_2R has also been implicated in behavioral sensitivity to drugs of abuse. A significant reduction in locomotor activity, likely due to the importance of D_2R signaling in the striatum, makes data from *Drd2*$^{-/-}$ mice challenging to interpret (Yamaguchi et al., 1996). However, the loss of D_2Rs from DA neurons increases behavioral sensitivity to

cocaine, in both CPP and locomotor behavior, and increases the acquisition of cocaine self-administration and cue-induced reinstatement (Bäckman et al., 2006; Bello et al., 2011; Holroyd et al., 2015). Additionally, the knockdown of D_2R in the VTA, where DA neurons are the most prominent cell type, increase cocaine-induced locomotion and enhanced cue-induced reinstatement (de Jong et al., 2015). DATCre(+):*Drd2*$^{fl/fl}$ mice are slower to reach a learning criterion and had difficulty sustaining a prolonged nose poke response, phenotypes congruent with impaired behavioral inhibition (Linden et al., 2018). These findings suggest D_2R also decrease behavioral sensitivity to cocaine.

GIRK channels have also been implicated in behavioral sensitivity to drugs of abuse. *Girk2*$^{-/-}$ mice display increased behavioral sensitivity to cocaine and morphine, as measured in the acute locomotor activity assay (Arora et al., 2010; Kotecki et al., 2015). *Girk2*$^{-/-}$,*Girk3*$^{-/-}$, and *Girk2*$^{-/-}$/*Girk3*$^{-/-}$ mice also have altered cocaine self-administration (Morgan et al., 2003). *Girk3*$^{-/-}$ have increased EtOH binge behavior (Herman et al., 2015). GIRK channels expressed in the medulla, which functionally couple to MORs, have been implicated in the respiratory depression aspect of the opioid fentanyl (Montandon et al., 2016). Additionally, a recently developed GIRK1 channel activator ML297 does not appear to have rewarding effects, measured with conditioned place preference (Wydeven et al., 2014), possibly implicating neuronal populations lacking GIRK1, *i.e.*, VTA and SN DA neurons (Koyrakh et al., 2005; Arora et al., 2010), in mediating these drug-related behaviors.

Other inhibitory G protein signaling modulators, such as SNX27 and RGS9-2 have been implicated in mediating behavioral sensitivity to drugs of abuse. The loss of SNX27 from DA neurons, which decreases $GABA_BR$ and D_2R function, results in increased behavioral sensitivity to cocaine (Munoz and Slesinger, 2014; Rifkin et al., 2018). RGS9-2 is highly expressed in the striatum (Anderson et al., 2010), and appears

to accelerate the on and off kinetics of D_2R-GIRK responses (Gold et al., 1997). *Rgs9-2*$^{-/-}$ mice display enhanced behavioral responses to acute and chronic morphine related to reward, analgesia, tolerance, and withdrawal, as well as increased locomotor responding to psychostimulants (Rahman et al., 2003; Zachariou et al., 2003; Psigfogeorgou et al., 2011; Gaspari et al., 2014).

Overall, inhibitory G protein signaling, particularly in VTA DA neurons, appears to temper behavioral responding to cocaine.

Table 1.5. Behaviors linked to drugs of abuse in knockout mice with altered inhibitory GPCR signaling.

Drug	Knockout	Effect	Ref.
Morphine	*Girk1*$^{-/-}$	↑ locomotor activity at 30 mg/kg	(Kotecki et al., 2015)
Cocaine		↑ locomotor activity at 15 mg/kg	(Arora et al., 2010)
Morphine	*Girk2*$^{-/-}$	↑ locomotor activity at 10 and 30 mg/kg	(Kotecki et al., 2015)
Fentanyl		↓ respiratory depression	(Montandon et al., 2016)
Cocaine		↑ locomotor activity at 15 mg/kg ↓ self-administration	(Kotecki et al., 2015) (Morgan et al., 2003)
EtOH		↓ behavioral effects of EtOH	(Blednov et al., 2001; Hill et al., 2003)
Morphine	*Girk3*$^{-/-}$	↓ locomotor activity at 10 mg/kg morphine	(Kotecki et al., 2015)
Cocaine		n.c. locomotor activity ↓ self-administration	(Arora et al., 2010) (Morgan et al., 2003)
EtOH		↑ binge-like drinking	(Herman et al., 2015)
Morphine	*Girk2*$^{-/-}$:*Girk3*$^{-/-}$	↓ morphine withdrawal	(Cruz et al., 2008)
Cocaine		↓ self-administration	(Morgan et al., 2003)
Nicotine	$GABA_{B1}R^{-/-}$	↑ CPP activity	(Varani et al., 2018)
Cocaine	Rgs9-2$^{-/-}$	↑ locomotor activity ↑ CPP activity	(Rahman et al., 2003)
Amphetamine	Rgs9-2$^{-/-}$	↑ locomotor activity	(Rahman et al., 2003)
Morphine	Rgs9-2$^{-/-}$	↑ CPP activity	(Rahman et al., 2003)
Morphine	DATCre:*Girk2*$^{fl/fl}$	↑ locomotor activity	(Kotecki et al., 2015)
Morphine	GADCre:*Girk2*$^{fl/fl}$	n.c. locomotor activity	
Cocaine	DATCre:SNX27$^{fl/fl}$	↑ ratio of locomotor activity	(Padgett et al., 2012)
Cocaine	THCre:SNX27$^{fl/fl}$	↑ locomotor activity	(Rifkin et al., 2018)
Cocaine	THCre:$GABA_{B1}R^{fl/fl}$	↑ locomotor activity	(Edwards et al., 2017)
Morphine		n.c. locomotor activity	
Cocaine	DATCre:*Drd2*$^{fl/fl}$	↑ locomotor activity ↑ conditioned place preference ↑ self-administration	(Bello et al., 2011; Holroyd et al., 2015; Linden et al., 2018)

1.4.3 GIRK channels in DA neurons temper opioid-induced motor activity

Section 1.4.3 summarizes work on which I am a co-author previously published in J Neurosci. 2015 May 6;35(18):7131-42. doi: 10.1523/JNEUROSCI.5051-14.2015. "GIRK Channels Modulate Opioid-Induced Motor Activity in a Cell Type- and Subunit-Dependent Manner." Kotecki L, Hearing M, McCall NM, Marron Fernandez de Velasco E, Pravetoni M, Arora D, Victoria NC, Munoz MB, Xia Z, Slesinger PA, Weaver CD, Wickman K.

VTA GABA neurons are thought to be primary mediators of the increase in DA by opioids, *e.g.*, morphine, through disinhibition. The activation MORs causes an inhibitory GPCR-dependent inhibition of VTA GABA neurons, disinhibiting DA neurons that receive this GABAergic input (Johnson and North, 1992). As GIRK channels functionally couple to MORs, one might expect the genetic ablation of GIRK channels or the genetic ablation of MORs to produce similar effects on behavioral sensitivity to morphine. However, the genetic loss of MORs prevents the locomotor stimulatory effect of opioids (Tian et al., 1997; Contarino et al., 2002; Yoo et al., 2003), while *Girk2*$^{-/-}$, and to a more limited extend *Girk1*$^{-/-}$, mice have increased behavioral sensitivity to morphine, as determined in an acute locomotor assay (Kotecki et al., 2015). This suggests that GIRK channels act as an inhibitory barrier to the locomotor stimulatory effects of morphine. However, it is unclear which brain region and cell type mediates this behavioral effect.

To ascertain whether GIRK channels in GABA neurons are mediate this effect, the GADCre line was crossed with *Girk2*$^{fl/fl}$ mice to ablate GIRK channels from GABA neurons (Kotecki et al., 2015). Cre- and Cre+ mice did not display any difference in

morphine locomotor activity (Kotecki et al., 2015), suggesting that GIRK channels in GABA neurons do not influence morphine locomotor activity. This suggests that the inhibitory effects of VTA GABA neuron MORs are not largely influenced by GIRK channels.

To determine if GIRK channels in VTA DA neurons, a cell population involved in drug-related reward, contribute to increased morphine sensitivity, the DATCre line was crossed with *Girk2*$^{fl/fl}$ mice to ablate GIRK channels from DA neurons (Kotecki et al., 2015). DATCre:*Girk2*$^{fl/fl}$ mice display a significant decrease in $GABA_BR$ currents in VTA DA neurons (**Figure 1.4 A,B**), but $GABA_BR$ currents in putative GABA neurons were unaltered (**Figure 1.4 C,D**). This indicates the selectivity of this manipulation for DA neurons. The loss of GIRK channels from DA neurons yielded an increase in the locomotor response to morphine, similar to our observations in *Girk2*$^{-/-}$ mice (Kotecki et al., 2015).

There are a number of potential mechanisms that could account for this behavioral phenotype. One possible mechanism for this observation could be the presence of GIRK channel-coupled MORs on DA neurons. In this scenario, the loss of MOR-GIRK-mediated inhibition of DA neurons allows leads to the release of additional DA in the presence of morphine, increasing the locomotor stimulatory effect. Another possible mechanism is that the loss of GIRK channels from VTA DA neurons reduces the ability of other GPCRs, such as $GABA_BRs$ (**Figure 1.4 A,B**) or D_2Rs engaged following morphine administration to temper DA release. The expression of MORs on DA neurons goes against classical thinking about MOR expression being primarily in GABA neurons in the VTA, recent evidence suggests that a subset of VTA DA neurons are directly inhibited by MOR agonists (Kotecki et al., 2015). Indeed, the MOR agonist DAMGO elicited outward currents in 20-25% of VTA DA neurons, and these currents

were significantly smaller in DATCre(+):*Girk2*$^{fl/fl}$ mice (Kotecki et al., 2015). This finding supports the possibility that MORs expressed on VTA DA neurons could contribute to this morphine locomotor phenotype, but it is not resounding evidence for this explanation. This suggests the reduction of the strength of other, more robust inhibitory GPCRs mechanisms in VTA DA neurons, such as $GABA_B$Rs or D_2Rs, likely underlies this behavior. Together, this data suggests that the GIRK channel present in VTA DA neurons is important for mediating behavioral sensitivity to morphine, and might mediate behavioral sensitivity to other classes of addictive drugs.

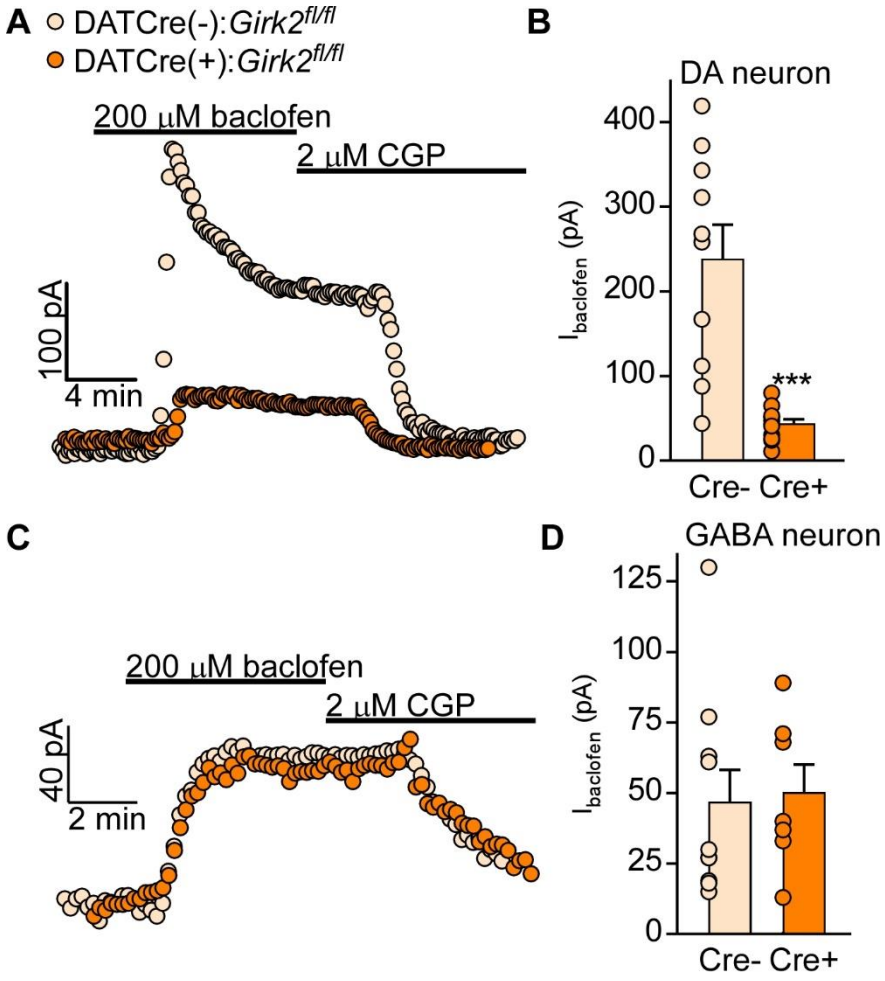

Figure 1.4. $GABA_BR$-GIRK currents in DA and GABA neurons of DATCre (-):*Girk2*$^{fl/fl}$ and DATCre(+):*Girk2*$^{fl/fl}$ mice.

A) Representative somatodendritic currents elicited by baclofen (200 μM) in Pitx3eGFP+ neurons (DA neurons) in the VTA of DATCre(-):*Girk2*$^{fl/fl}$ and DATCre(+):*Girk2*$^{fl/fl}$ mice and reversed by CGP (2 μM). **B**) Summary of baclofen-induced currents in DA neurons of DATCre(-):*Girk2*$^{fl/fl}$ (n = 10 cells, 238 ± 41 pA) and DATCre(+):*Girk2*$^{fl/fl}$ mice (n = 12 cells, 44 ± 5 pA; Mann-Whitney test, U = 6, p = 0.0004). **C**) Representative somatodendritic baclofen currents in Pitx3eGFP- neurons (putative GABA neurons) in the VTA of DATCre(-):*Girk2*$^{fl/fl}$ and DATCre(+):*Girk2*$^{fl/fl}$ mice, reversed by CGP. **D**) Summary of baclofen-induced currents in putative GABA neurons of DATCre(-):*Girk2*$^{fl/fl}$ (n = 10 cells, 47 ± 12 pA) and DATCre(+):*Girk2*$^{fl/fl}$ mice (n = 7 cells, 50 ± 10 pA; t test, t_{15} = 0.21, p = 0.83). Error bars: mean ± SEM. ***p<0.001.

Data in this figure was previously published in Kotecki et al., 2015 *J Neurosci*, and was collected by NMM.

1.5 Purpose of studies

The goal of my thesis work is to understand the contribution of VTA DA neuron GIRK channels to behavioral sensitivity to the psychostimulant cocaine, and to better understand the mechanism of plasticity of VTA DA neuron GIRK channels. In **Chapter 2**, I investigate whether stimuli known to modulate excitatory signaling in VTA DA neurons, *i.e.*, morphine and stress (Saal et al., 2003), alter $GABA_BR$-GIRK inhibitory signaling. Additionally, I assess the ability of systemic D_2R agonism to suppress GIRK channel activity in VTA DA neurons, building upon a previous finding that D_2R signaling is necessary for a cocaine-induced decrease in GIRK channel activity (Arora et al., 2011). In **Chapter 3**, I characterize the contribution of the GIRK channel in DA neurons to acute and repeated cocaine locomotion, cocaine CPP, and cocaine self-administration using the DATCre(+):*Girk2*$^{fl/fl}$ mouse line (Kotecki et al., 2015). In **Chapter 4**, I employ a viral chemogenetic approach to determine if engaging inhibitory G protein signaling in DA neurons of the VTA decreases the locomotor behavioral response to cocaine and morphine, a logical outcome based on our findings with the DATCre(+):*Girk2*$^{fl/fl}$ mouse line. Finally, in **Chapter 5**, I used viral approaches to bi-directionally manipulate the strength of GIRK channel activity in VTA DA neurons. With these tools, I test the ability of the unique VTA DA neuron GIRK channel to influence negative affective behaviors and behavioral sensitivity to cocaine. Overall, my thesis research provides insight into the behavioral role of the unique VTA DA neuron GIRK channel, and suggest this channel may be a good target for future pharmacotherapies to treat SUD and addiction.

Chapter 2

VTA DA neuron GIRK channel activity adaptations are induced by stress and D_2R activation but not morphine

2.1 Introduction

2.1.1 Do cocaine, stress, and morphine share the ability to decrease GIRK channel activity?

Psychostimulants, stress, and opioids share the ability to increase excitatory signaling mediated by AMPA receptors and decrease inhibitory signaling mediated by $GABA_A$ receptors in VTA DA neurons (Ungless et al., 2001; Saal et al., 2003; Polter and Kauer, 2014). While cocaine decreases inhibitory G protein signaling mediated by GIRK channels in VTA DA neurons (Arora et al., 2011), the effect of stress or morphine exposure on GIRK channel activity is unknown.

Adaptations in GIRK channel activity following stress have been characterized in brain regions outside of VTA DA neurons. In LHb neurons, footshock stress decreases GIRK channel activity (Lecca et al., 2016, 2017). Similarly, forced swim stress (FSS) or KOR agonist exposure decreases GIRK channel activity in DRN serotonergic neurons (Lemos et al., 2012). This data suggests stress-inducing stimuli can influence GIRK channel activity in VTA DA neurons. Chronic restraint and social defeat increase the spontaneous and burst firing of VTA DA neurons (Kobayashi et al., 2004), suggesting stressful stimuli could decrease inhibitory signaling in VTA DA neurons, including GIRK channel activity.

While the effect of morphine exposure on inhibitory G protein signaling in VTA DA neurons is unknown, there is some evidence to suggest it might induce an adaptation in GIRK channel activity. Indeed, morphine and other opioids activate GIRK channels through MORs. *Ex vivo* morphine exposure increases 5-HT-GIRK currents, but decreases $GABA_BR$-GIRK currents in hippocampal cultures (Ikeda et al., 2000; Marker et al., 2004, 2005; Kanbara et al., 2014; Nakamura et al., 2014; Abney et al., 2018), suggesting morphine can elicit adaptations in GIRK channel activity. Additionally, genetic ablation of GIRK2 from DA neurons increases behavioral sensitivity to morphine (Nassirpour et al., 2010), which could indicate that a reduction of GIRK channel activity in VTA DA neurons could be a contributing mechanism to morphine sensitization (Kotecki et al., 2015).

A goal of this chapter was to determine if GIRK channel activity could be altered by exposure to stress or morphine. I hypothesized that stress and morphine exposure would hypothesized to illicit decreases in GIRK channel activity in VTA DA neurons. Such adaptations could increase the excitability of DA neurons, complementing increases in excitatory signaling that are also elicited by stress and morphine exposure (Saal et al., 2003). To test this hypothesis, mice were exposed to stress or morphine, and GIRK channel activity in VTA DA neurons was measured 24 hours later. Footshock, but not morphine or FSS, were found to decrease $GABA_BR$-GIRK currents.

2.1.2 Can D_2R activation mimic cocaine-induced adaptations in VTA DA neuron GIRK channel activity?

Exposure to cocaine decreases GIRK channel activity in VTA DA neurons, and pretreatment with a D_2R antagonist prevents this adaptation (Arora et al., 2011). This suggests D_2R activity is necessary for this adaptation. This adaptation could depend on

activity-dependent plasticity, which has been described in VTA DA neurons (Lalive et al., 2014). In this model, the large increase in extracellular DA elicited by cocaine would lead to the activation of the D_2 autoreceptor on VTA DA neurons (Beckstead et al., 2004). This inhibition of DA neurons could elicit a PDZ-domain dependent internalization of GIRK channels (Lalive et al., 2014). To determine if the activation of VTA DA neuron D_2Rs is sufficient to induce adaptations in GIRK channel activity, Pitx3eGFP mice were given the D_2R agonist quinpirole i.p. and 24 hours later, D_2R- and $GABA_B$R-GIRK currents were assessed. Interestingly, $GABA_B$R, but not D_2R, currents were diminished by systemic quinpirole treatment.

2.2 Methods

2.2.1 Animals

All studies were approved by the Institutional Animal Care and Use Committees at the University of Minnesota. Male C57BL6/J mice were purchased from The Jackson Laboratory (Bar Harbor, ME). Male and female Pitx3eGFP(+) mice were bred in-house. Mice were group housed and maintained on a 12 h light/dark cycle (lights on at 0700 hours), with food and water available *ad libitum.*

2.2.2 Reagents

Morphine was obtained through Boynton Health Pharmacy at the University of Minnesota. 0.9% saline was purchased from Baxter Healthcare Corporation (Deerfield, IL). Yohimbine, baclofen, CGP54626, quinpirole, sulpiride, and tetrodotoxin (TTX) were purchased from Sigma (St. Louis, MO).

2.2.3 Stress paradigms

Controls. All controls were habituated to the testing room for an hour, handled by the experimenter, and returned to the housing room prior to the test mice were stressed.

Forced swim stress (FSS). I used two methods of forced swim stress in this study. For blood collection, mice were placed in 1.5 L of cold (~6 °C) water in a 4 L beaker for 5 min (Saal et al., 2003). For slice electrophysiology, I used a 2 day method based on another publication which found stress-induced adaptations in GIRK channel activity (Lemos et al., 2012), where mice swam for 15 min on day one, and for four 6 min bouts, separated by 6 min in 29.0 – 31.0 °C water on day 2.

Footshock. Mice were exposed to two foot shocks for 2 s at 1.5 mA, based on previous studies using a footshock stress (Polta et al., 2013; Kao et al., 2015).

Yohimbine injection. Mice were administered 5mg/kg yohimbine via i.p. injection (Aghajanian and VanderMaelen, 1982; Conrad et al., 2012).

2.2.4 Blood collection

Mice were brought into the testing room and habituated for 1 hour. Baseline blood samples were collected via the retroorbital vein, and mice recovered for 1 hour. Mice were then stressed (FSS, footshock, or yohimbine injection), and blood was collected at the following time points after stress: 0 min, 30 min, 75 min, 24 hr. Blood was spun down in heparin-coated tubes and plasma was stored at -80 °C prior to the corticosterone radio immunoassay.

2.2.5 Corticosterone radioimmunoassay

Corticosterone in plasma was measured using an I^{125} radioimmunoassay with a commercially available kit (MP Biomedical, Solon, OH). Corticosterone values were determined using a corticosterone standard curve run in parallel with blood samples.

2.2.6 Morphine administration

For single morphine exposure studies, locomotor activity was assessed in open field activity chambers (Med-Associates, St Albans, VT), as described (Pravetoni and

Wickman, 2008). Subjects were acclimated over 4 days, during which the animals were handled (2 days) and exposed to i.p. injection (saline; 2 days) and the open field for 1 hour. On the test day, subjects were given either a third i.p. saline injection or a 10 mg/kg dose of morphine. For repeated morphine exposure, mice were brought to a separate room, left to acclimate for approximately 1 hour, administered 10 mg/kg morphine in their home cage. After approximately 1 hour, the mice were brought back to the housing room. Mice received morphine once per day for 5 consecutive days.

2.2.7 Quinpirole administration

For quinpirole exposure, locomotor activity was assessed in open field activity chambers (Med-Associates, St Albans, VT), as described (Pravetoni and Wickman, 2008). Subjects were acclimated over 4 days, during which the animals were handled (2 days) and exposed to i.p. injection (saline; 2 days) and the open field for 1 hour. On the test day, subjects were given either a third i.p. saline injection or a 1 mg/kg dose of quinpirole.

2.2.8 Slice electrophysiology

Horizontal slices (225 μm) of the mouse VTA (5–9 weeks) were prepared as described (Kotecki et al., 2015). Neurons medial to the medial terminal nucleus of the accessory optic tract and identified via GFP expression driven by the *Pitx3* promoter were targeted for analysis in studies using Pitx3eGFP mice. In studies using wild-type C57BL6/J mice, putative DA neurons were identified by I_h (> 100 pA). Whole-cell data were acquired using a Multiclamp 700 A amplifier and the pCLAMPv.9.2 software (Molecular Devices; Sunnyvale, CA). I_h amplitude was assessed using a 1-s voltage ramp (−60 to −120 mV). Spontaneous activity was measured in current-clamp mode (I=0) for 1 min. Rheobase was measured by injecting currents from −60 pA, increasing in 20 pA increments

(1 s/step). Rheobase was not measured in footshock or quinpirole studies, when TTX was included in the bath solution. Rheobase was defined as the minimum current evoking one or more action potentials. To assess the effect of $GABA_BR$ activation on excitability, neurons were voltage-clamped (V_{hold}=−60 mV) while baclofen (200 μM) was applied to the bath. Command potentials factored in a junction potential of −15 mV. Series and membrane resistances were tracked throughout the experiment. If series resistance was high (>20 MΩ) or unstable (>20% variation), the experiment was excluded from analysis.

2.2.9 Statistical Analysis

Data are presented throughout as the mean ± SEM. Statistical analyses were performed using Prism 5 (GraphPad Software, La Jolla, CA). Studies with Pitx3eGFP mice used male and female mice; studies using wild-type C57BL6/J mice used males. Data were analyzed first for effects of sex and treatment using a two-way ANOVA. When sex differences were observed, male and female data were pooled. For studies where there was a possible effect of sex, I also show the data separated by males and females. Pairwise comparisons were performed using t tests or Mann–Whitney *U* tests, or Bonferroni *post-hoc* test, as appropriate. Differences were considered significant if $p < 0.05$.

2.3 Results

2.3.1 Acute stress paradigms increase plasma corticosterone

To ensure that acute footshock and FSS paradigms were adequately stressful, the ability of these paradigms to increase serum levels of corticosterone was compared against the α2-adenergic receptor antagonist yohimbine, which blocks presynaptic receptors on norepinephrine neurons to increase norepinephrine release and has been

used to pharmacologically mimic stress (Aghajanian and VanderMaelen, 1982). Blood was collected from mice prior to stress, and 0 min, 30 min, 75 min, and 24 hours following stress (**Figure 2.1A**). Blood samples were then analyzed for corticosterone using a radioimmunoassay. In all paradigms, corticosterone increased significantly from baseline 0, 30, and 75 min following stress, and returned to baseline levels 24 hours later (**Figure 2.1B**). Interestingly, corticosterone in mice that experienced the FSS paradigm began to decline faster at 75 min (**Figure 2.1B**), suggesting that the FSS paradigm was not as stressful as footshock.

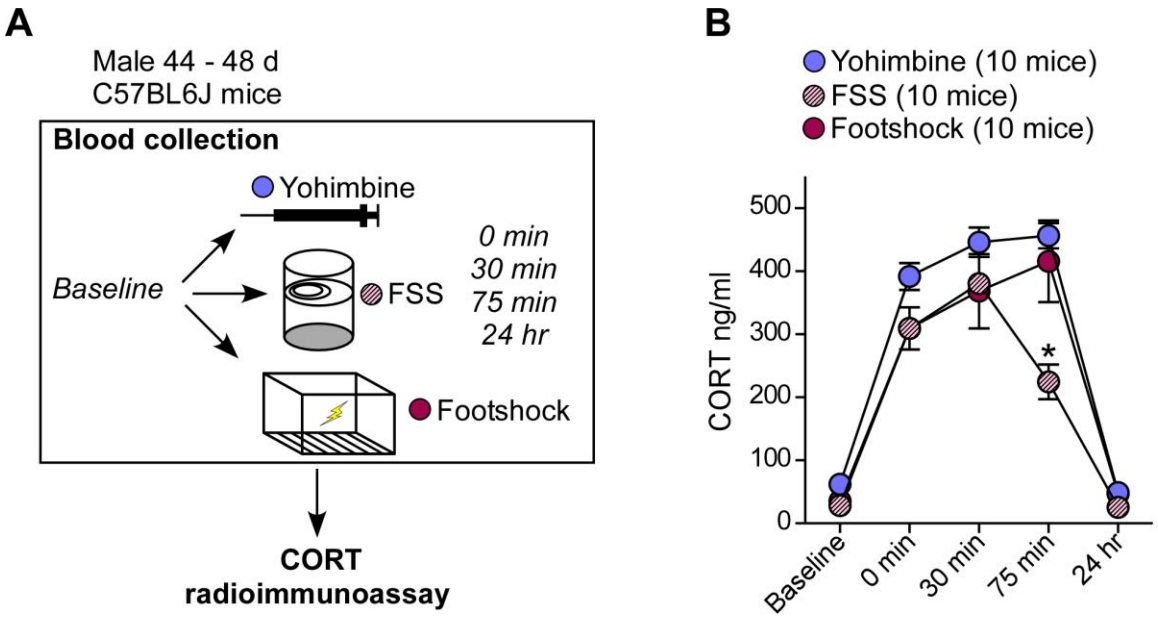

Figure 2.1. Yohimbine injection, FSS, and footshock acutely increase corticosterone.

A) Schematic depicting corticosterone (CORT) radioimmunoassay experimental design. **B**) Serum corticosterone (CORT) levels in mice following exposure to the acute stress induced by yohimbine (5 mg/kg, i.p.), FSS, or footshock (two-way ANOVA, interaction of stress type and sample collection time, $F_{8,108} = 5.59$, $p < 0.0001$; post hoc Bonferroni tests: footshock versus FSS at 75 min, $t = 4.865$, $p < 0.001$; yohimbine versus FSS at 75 min, $t = 5.892$, $p < 0.001$)

2.3.2 Footshock, but not FSS, reduces $GABA_BR$-GIRK currents in VTA DA neurons

Next, I wanted to determine if stress was able to elicit adaptations in $GABA_BR$-GIRK signaling. Because the shorter FSS paradigm appeared to be less stressful than footshock, which had a very similar CORT profile as yohimbine (**Figure 2.1B**), I employed a 2 day FSS protocol, which elicited adaptations in GIRK channel activity in DRN serotonin neurons (Lemos et al., 2012), for electrophysiological studies, along with footshock stress. 1-2 days following exposure to handling (control condition) or stress, somatodendritic $GABA_BR$-GIRK currents were measured in VTA DA neurons (**Figure 2.2A**). While there was no difference in $GABA_BR$-GIRK signaling between FSS and control conditions, there was a significant decrease in $GABA_BR$-GIRK currents following footshock (**Figure 2.2B**). There were no differences in baseline electrophysiological parameters (**Table 2.1**).

2.3.3 Morphine exposure does not alter $GABA_BR$-GIRK currents in VTA DA neurons

To determine if GIRK channel activity is altered in VTA DA neurons following exposure to morphine, Pitx3eGFP+ mice were injected with 10 mg/kg morphine and 24 hours later $GABA_BR$-GIRK currents were measured (**Figure 2.3A**). Morphine injection increased locomotor activity (**Figure 2.3B**), and elicited the stereotypical straub tail phenotype (Nath et al., 1994). However, there was no significant difference in somatodendritic $GABA_BR$-GIRK currents in VTA DA neurons (**Figure 2.3C**).

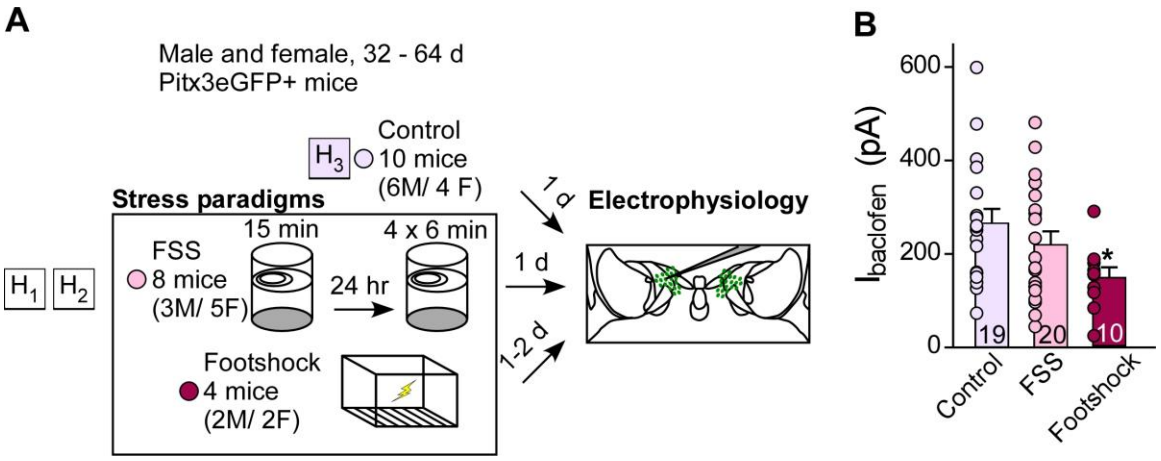

Figure 2.2. Footshock, but not FSS, reduces $GABA_BR$-GIRK currents in VTA DA neurons.

A) Schematic depicting stress study experimental design. **B**) Summary of baclofen-elicited responses for control (n = 19 cells from 10 mice, 266 ± 30 pA), FSS n = 20 cells from 8 mice, 221 ± 28 pA), and footshock (n = 10 cells from 4 mice, 146 ± 22; One-way ANOVA, $F = 3.345$, $p = 0.044$; Bonferroni post test: control vs. FSS, $t = 1.181$, $p > 0.05$; control vs. footshock, $t = 2.584$, $p < 0.05$).

Table 2.1. Baseline electrophysiology parameters in VTA DA neurons following control, FSS, or footshock.
From data included in **Figure 2.2B**. In footshock study, TTX was included in all solutions; 2 cells in the control condition were from the footshock study.

Condition	n	Cm (pF)	Rm (MΩ)	I_h (pA)	RMP (mV)	Rheobase (pA)	Active neurons	Freq (Hz)
Control	19	52 ± 3	357 ± 65	249 ± 61	-35 ± 0 (2)	-20 ± 4 (16)	14/17	2.76 ± 0.33
FSS	20	52 ± 3	364 ± 55	203 ± 52	N/A	-13 ± 5	18/20	2.08 ± 0.26
Footshock	13	41 ± 5	339 ± 75	103 ± 37	-40 ± 2	N/A	N/A	N/A

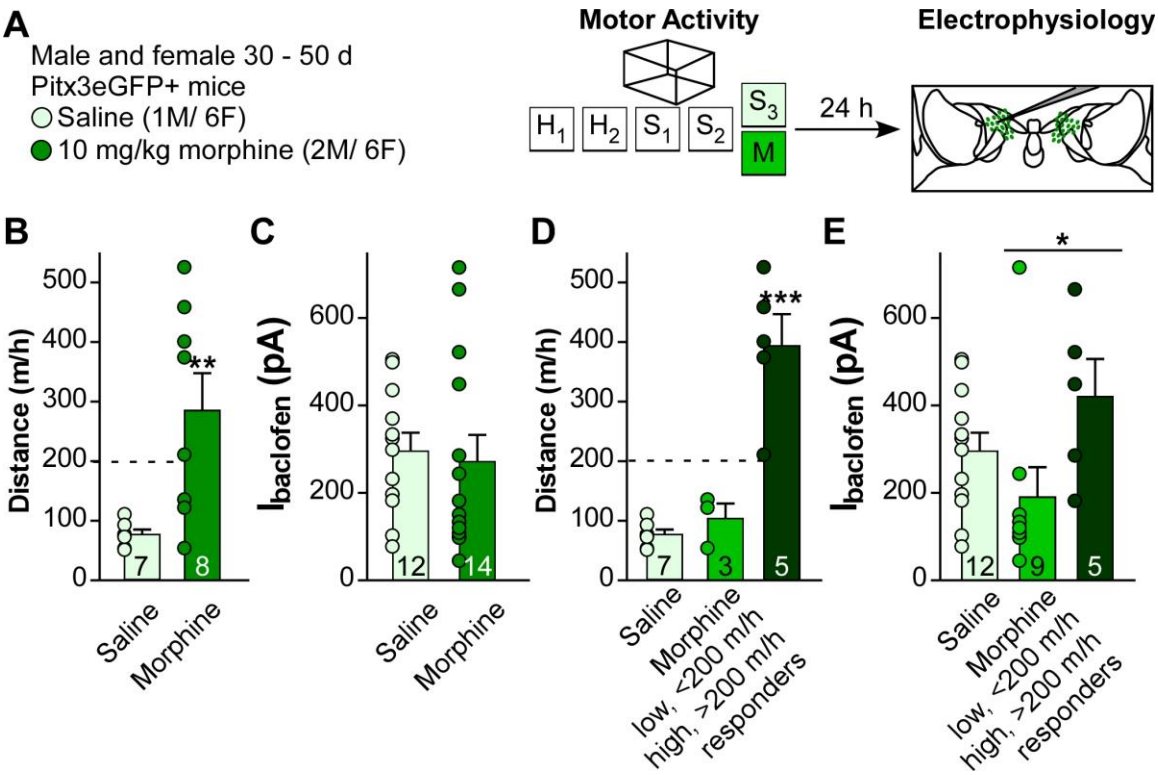

Figure 2.3. A single exposure to morphine does not alter $GABA_BR$-GIRK currents in VTA DA neurons.

A) Schematic of acute morphine exposure experimental design. **B**) 1 h locomotor activity following injection of saline (n = 7 mice, 71 ± 9 m) or 10 mg/kg morphine (n = 8 mice, 285 ± 62 m; Mann-Whitney test, U = 5.0, p = 0.003). **C**) Summary of baclofen-elicited responses in saline (n = 12 cells from 7 mice; 297 ± 41 pA) and morphine (n = 14 cells from 8 mice, 273 ± 60 pA; t test, t_{24} = 0.316, p = 0.755). **D**) 1 h locomotor activity following injection of saline or 10 mg/kg morphine, separated into groups of low (n = 3 mice, 104 ± 25 m) and high responders (n = 5 mice, 394 ± 53 m; One-way ANOVA, F = 34.92, p < 0.0001; saline vs. high morphine responders, t = 8.105, p < 0.0001). **E**) Summary of baclofen-elicited responses in saline (same as panel B), low morphine responders (n = 9 cells from 3 mice, 191 ± 68 pA), and high morphine responders (n = 5 cells from 5 mice, 421 ± 86 pA; Kruskal-Wallis test, K-W = 6.544, p = 0.038; low vs. high responders, Dunn's multiple comparison test, p < 0.05).

Table 2.2. Baseline electrophysiology parameters in VTA DA neurons following a single injection of saline or morphine.
From data included in **Figure 2.3C**. There was an effect of sex in excitability measures.

Condition	n	Cm (pF)	Rm (MΩ)	I_h (pA)		Rheobase (pA)	Active neurons	Freq (Hz)
Saline	12	67 ± 6	258 ± 25	367 ± 93	male female	-20 ± 0 0 ± 7	3/3 8/9	2.90 ± 0.49 2.21 ± 0.38
Morphine	14	64 ± 7	270 ± 30	295 ± 72	male female	-28 ± 5 18 ± 16	5/5 6/8	3.18 ± 0.44 2.02 ± 0.62

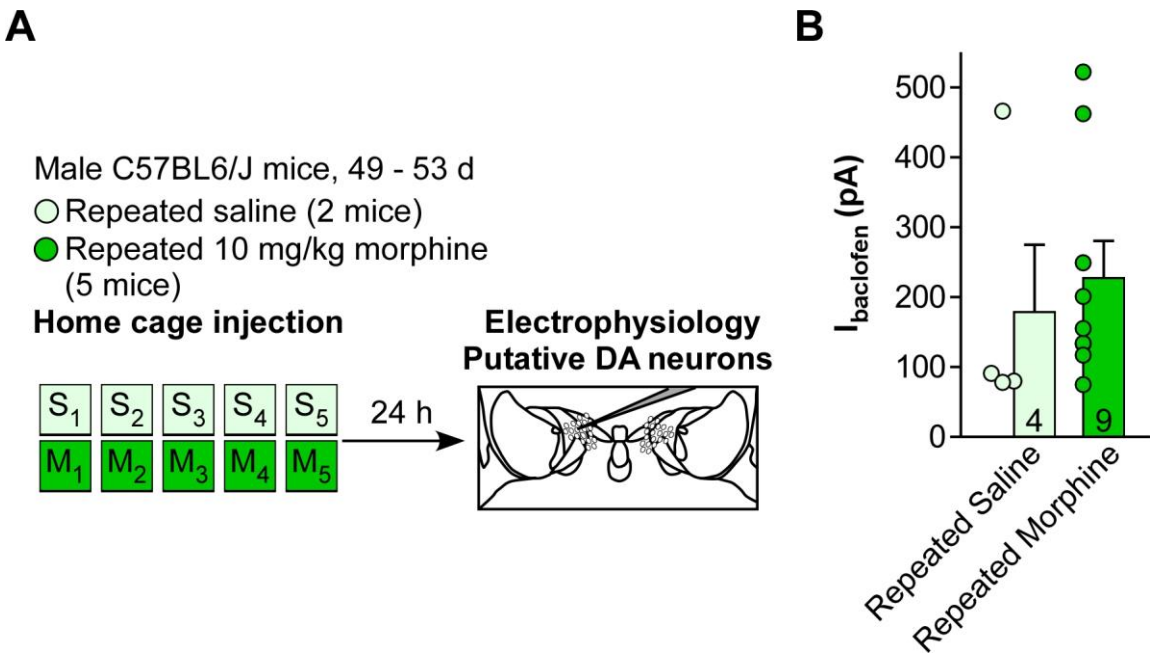

Figure 2.4. Repeated exposure to morphine does not alter $GABA_BR$-GIRK currents in putative DA neurons of the VTA.

A) Schematic of repeated morphine experimental design. **B**) Summary of baclofen-elicited responses in saline (n = 4 cells from 2 mice; 179 ± 96 pA) and repeated morphine (n= 9 cells from 5 mice, 228 ± 53 pA; t test, t_{11} = 0.483, p = 0.639).

Table 2.3. Baseline electrophysiology parameters in putative DA neurons of the VTA following a repeated injection of saline or morphine.
From data included in **Figure 2.4B**.

Condition	n	Cm (pF)	Rm (MΩ)	I_h (pA)	Rheobase (pA)	Active neurons	Freq (Hz)
Saline	4	62 ± 17	136 ± 32	306 ± 140	-30 ± 6	4/4	1.52 ± 0.49
Morphine	9	43 ± 3	158 ± 13	118 ± 45	-2 ± 18	6/9	1.01 ± 0.19

Looking carefully at the spread of the locomotor data, it appeared that while all mice receiving morphine displayed the straub tail phenotype, not all mice displayed a robust increase in locomotor activity, compared with controls (**Figure 2.3D**). Mice administered morphine were separated by their locomotor response: low responders, which moved less than 200 m/h and were not significantly different from controls, and high responders, which moved more than 200 m/h (**Figure 2.3D**). When assessing $GABA_BR$-GIRK currents from high and low responders separately, high responders had increased $GABA_BR$-GIRK currents compared with low responders (**Figure 2.3E**). This observation is contrary to my expectation that morphine would decrease GIRK channel activity. Additionally, there were no morphine-dependent alterations in baseline electrophysiological properties, but neurons from females displayed increased excitability (**Table 2.2**).

After failing to observe a clear impact of a single injection of morphine, I next asked whether repeated morphine could influence GIRK channel activity in putative DA neurons of the VTA. To test this, adult male C57BL6/J mice were injected with saline or morphine (10 mg/kg) for 5 days (**Figure 2.4.A**). Similar to my findings with a single exposure to morphine (**Figure 2.3C**), repeated morphine did not alter on $GABA_BR$-GIRK currents in putative DA neurons of the VTA (**Figure 2.4B**), nor did it alter baseline electrophysiological properties (**Table 2.3**).

2.3.4 Systemic activation of D_2Rs decreases $GABA_BR$-GIRK currents in VTA DA neurons

Cocaine decreases GIRK channel activity in VTA DA neurons, an adaptation dependent on D_2R activation (Arora et al., 2011). However, it is unknown whether the stimulation of D_2Rs alone is sufficient reduce GIRK channel activity in VTA DA neurons.

To test this, mice were injected with saline or 1 mg/kg quinpirole (Thompson et al., 2010), and somatodendritic $GABA_BR$-GIRK currents were recorded in VTA DA neurons 24 hours later (**Figure 2.5A**). Systemic quinpirole significantly decreased locomotor activity (**Figure 2.5B**). While systemic quinpirole did not alter the strength of D_2R-GIRK currents in VTA DA neurons (**Figure 2.5D**), $GABA_BR$-GIRK currents were significantly decreased (**Figure 2.5F**). Baseline electrophysiological properties were not altered by systemic quinpirole (**Table 2.4**). While there were no significant effects of sex in this study, sex differences in the strength of GIRK channel activity have been previously described in other regions of the mesocorticolimbic system (Marron Fernandez de Velasco et al., 2015a). When the locomotor and electrophysiological data was separated by sex (**Figure 2.5C, E, G**), females appeared to be primary drivers of the decrease in $GABA_BR$-GIRK currents (**Figure 2.5F**).

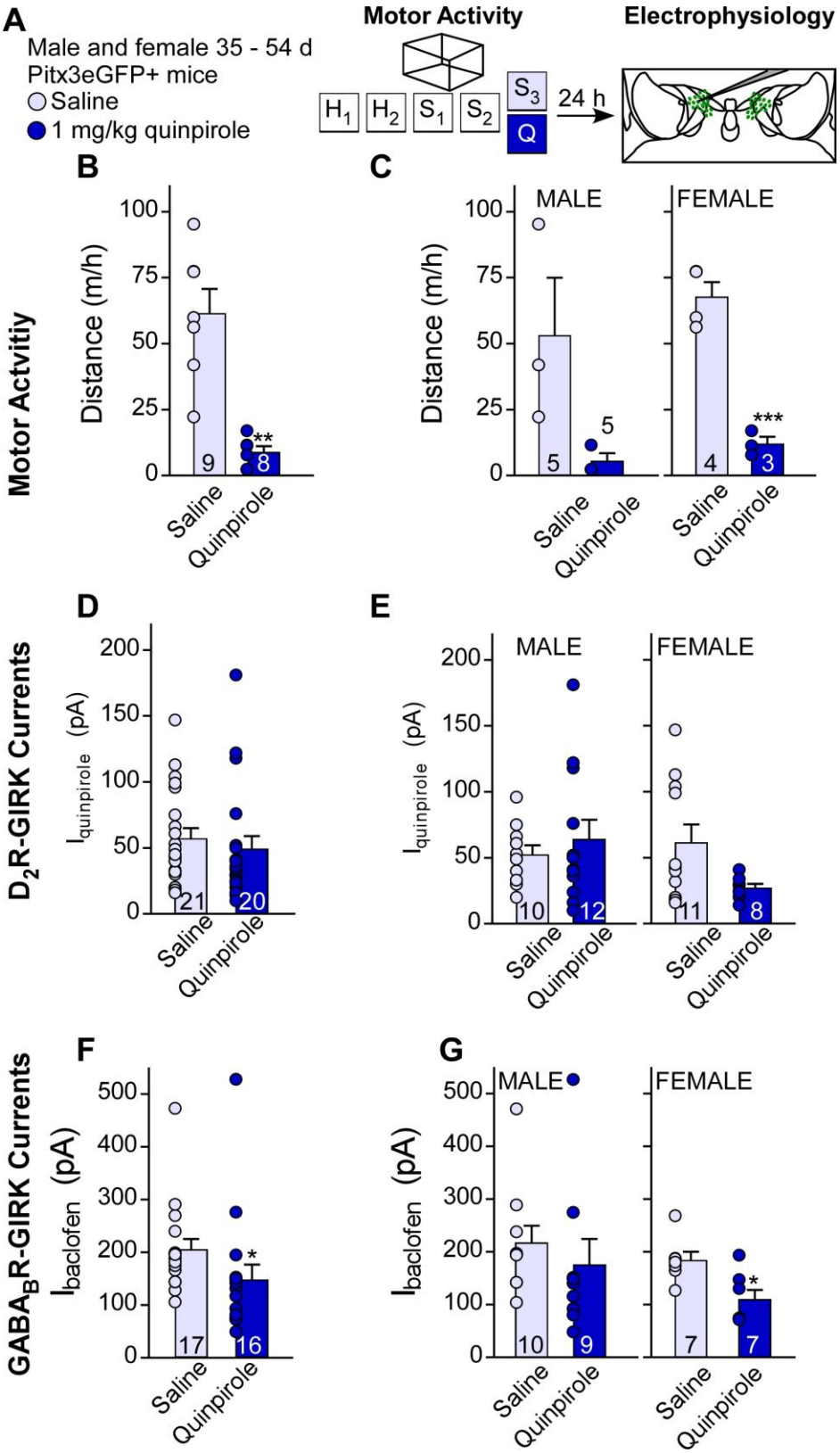
A
Male and female 35 - 54 d
Pitx3eGFP+ mice
Saline
1 mg/kg quinpirole
Motor Activity
Electrophysiology
H1
H2
S1
S2
S3
Q
24 h
B
C
Motor Actvitiy
Distance (m/h)
MALE
FEMALE
Saline
Quinpirole
D
E
D2R-GIRK Currents
Iquinpirole (pA)
F
G
GABABR-GIRK Currents
Ibaclofen (pA)

Figure 2.5. Systemically administered quinpirole decreases $GABA_BR$-GIRK currents in VTA DA neurons.

A) Schematic of systemic quinpirole electrophysiology experiment. **B**) Motor activity following injection of saline (n = 9 mice, 7 included in analysis, 61 ± 9 m) or quinpirole (n = 8 mice, 6 included in analysis, 9 ± 2 m; Mann-Whitney test, U = 0.00, p = 0.001). **C**) Motor activity in male mice that received saline (n = 5 mice, 3 included in analysis, 53 ± 22 m) or quinpirole (n = 5 mice, 3 included in analysis, 5 ± 3 m; Mann-Whitney test, U = 0.0, p = 0.1) and in female mice that received saline (n = 4 mice, 68 ± 6 m) or quinpirole (n = 3 mice, 12 ± 3 m; t test, t_5 = 7.96, p = 0.0005). **D**) D_2R-GIRK currents in VTA DA neurons of mice treated with saline (n = 21 cells from 9 mice, 57 ± 8 pA) or quinpirole (n = 20 cells from 8 mice, 49 ± 10 pA; Mann-Whitney test, U = 165, p = 0.246). **E**) D_2R-GIRK currents in VTA DA neurons of male mice that received saline (n = 10 cells from 5 mice, 52 ± 7 pA) or quinpirole (n = 12 cells from 5 mice, 64 ± 15 pA; Mann-Whitney test, U = 59.5, p = 1.00) and in female mice that received saline (n = 11 cells from 4 mice, 62 ± 14 pA) or quinpirole (n = 8 cells from 3 mice, 27 ± 3 pA; Mann-Whitney test, U = 23.5, p = 0.10). **F**) $GABA_BR$-GIRK currents in VTA DA neurons of mice treated with saline (n = 17 cells from 9 mice, 204 ± 20 pA) or quinpirole (n = 16 cells from 8 mice, 147 ± 29 pA; Mann-Whitney test, U = 58, p = 0.005). **G**). $GABA_BR$-GIRK currents in VTA DA neurons of male mice that received saline (n = 10 cells from 5 mice, 218 ± 33 pA) or quinpirole (n = 9 cells from 5 mice, 176 ± 49 pA; Mann-Whitney test, U = 26.0, p = 0.131) and in female mice that received saline (n = 7 cells from 4 mice, 184 ± 16 pA) or quinpirole (n = 7 cells from 3 mice, 110 ± 18 pA; Mann-Whitney test, U = 8.00, p = 0.038).

Table 2.4. Baseline electrophysiology parameters in VTA DA neurons following injection of saline or quinpirole.
From data included in **Figure 2.5D**.

Condition	n	Cm (pF)	Rm (MΩ)	I_h (pA)	RMP (mV)
Saline	21	55 ± 4	193 ± 11	110 ± 25	-40 ± 2
Quinpirole	20	45 ± 3	255 ± 29	109 ± 46	-40 ± 1

2.4 Discussion

The studies in this chapter revealed that only some of the stimuli that elicit adaptations in excitatory signaling in VTA DA neurons, *i.e.*, stress and morphine exposure, alter GIRK channel activity. Additionally, D_2R activation was sufficient to elicit a reduction in the GIRK channel activity in VTA DA neurons, similar to cocaine (Arora et al., 2011).

2.4.1 Footshock, but not FSS, decreases GIRK channel activity in VTA DA neurons

I found that only one of the two stress paradigms influence GIRK channel activity. Indeed, $GABA_BR$-GIRK currents in VTA DA neurons were decreased by footshock, but were not altered by FSS. Footshock is likely a more severe stressor than FSS, supported by FSS's slightly quicker recovery of corticosterone. The influence of DA neuron activity on GIRK channel activity (Lalive et al., 2014) could be an underlying mechanism for this observation. Perhaps footshock, but not FSS, induces a robust decrease in VTA DA neuron activity, eliciting adaptations in in GIRK channel trafficking. Indeed, aversive, painful stimuli can elicit a robust decrease in VTA DA neuron activity through the activation of GABAergic neurons in the RMTg (Jhou et al., 2009). Other inhibitory signaling in the VTA engaged by stress, including that mediated by dynorphin or neuropeptide Y (Korotkova et al., 2003, 2006), could contribute to the decrease in $GABA_BR$-GIRK currents following footshock. Interestingly, CRF inputs to VTA DA are generally glutamatergic and excite VTA DA neurons (Korotkova et al., 2006; Tagliaferro and Morales, 2008), and a number of noxious stimuli are able to increase VTA DA neuron activity and DA release (Holly and Miczek, 2016). Thus, the mechanisms by which GIRK channel activity is decreased by footshock might go beyond VTA DA

neuron activity, or might be specific to a specific projection target-defined subpopulation of DA neurons (Lammel et al., 2014).

2.4.2 Morphine does not alter VTA DA neuron GIRK channel activity

While cocaine decreases GIRK channel activity in VTA DA neurons through a D_2R- and perhaps excitability-dependent mechanism (Arora et al., 2011; Lalive et al., 2014), morphine exposure did not alter GIRK channel activity. Morphine and other opioids are thought to increase DA release indirectly, “disinhibiting” DA neurons, by acting on MOR on the GABA neurons (Johnson and North, 1992) of the VTA and RMTg. Thus, morphine exposure increases DA neuron activity. While there are MOR on VTA DA neurons (Margolis et al., 2014; Kotecki et al., 2015), these receptors might not impact the excitability of enough VTA DA neurons to significantly decrease the strength of GIRK channel activity, at least when generally surveying VTA DA neurons. Interestingly, phasic firing increases GIRK channel activity (Lalive et al., 2014). When looking at low and high locomotor responders to morphine, the high responders appear to have enhanced GIRK channel activity. This is consistent with increased DA neuron excitability leading to increased GIRK channel activity.

2.4.3 D_2R activation is sufficient to reduce $GABA_B$R-GIRK currents in VTA DA neurons

Activation of D_2Rs is necessary for the cocaine-induced decrease in GIRK channel activity in VTA DA neurons. In this study, I found that D_2R activation was sufficient to reduce $GABA_B$R-GIRK currents, but did alter D_2R-GIRK currents. The difference between $GABA_B$R-GIRK and D_2R-GIRK signaling might be due differences in how these receptors are trafficked or due to the heterogeneity of the D_2R response (observed in **Chapters 3 and 5** as well). Sex is also a potential contributor to this

heterogeneity, as sex differences have been observed in GIRK-related physiology and behavior (Marron Fernandez de Velasco et al., 2015a; McCall et al., 2017). Indeed, when the electrophysiology data is assessed by sex, females appear to drive the decrease in $GABA_BR$-GIRK currents, as well as possible decrease in D_2R-GIRK currents. Additionally, because the $GABA_BR$ response is larger than the D_2R response (~250 pA versus ~60 pA for control D_2R responses), it might be easier to statistically detect a decrease in these responses.

Interestingly, activating D_2Rs caused a significant decrease in locomotor activity. This result is consistent with some previous findings with quinpirole (Hofford et al., 2012; Pértile et al., 2017), though other experiments found systemic quinpirole increased locomotor behavior and induced locomotor sensitization (Szechtman et al., 1993; Thompson et al., 2010; Johnson and Szechtman, 2016; Jung et al., 2017). This difference in behavior following D_2R agonist administration is thought to be mediated by differences in the activities of presynaptic and postsynaptic D_2Rs, which can mediate hypo- and hyper-locomotion (Hofford et al., 2012).

2.4.4 Overall conclusions

GIRK channel activity in VTA DA neurons adapts following exposure to psychostimulants and changes in neuronal activity (Arora et al., 2011; Padgett et al., 2012; Lalive et al., 2014). The findings in this chapter further demonstrate that decreased neuronal activity, in this case mediated by D_2R activation, is able to reduce GIRK channel activity in this cell type. Additionally, this chapter found that some, perhaps more severe, forms of stress to induce similar changes in GIRK channel activity as cocaine. This chapter also identified a notable divergence in the ability of psychostimulants and opioids to alter GIRK channel activity in DA neurons, despite the

loss of GIRK channels from DA neurons influencing behavioral sensitivity to psychostimulants and opioids.

Author Contributions for Chapter 3

NM McCall*	Nora McCall designed, performed, and analyzed the ventral tegmental area electrophysiology studies (Fig 1, Fig 2, Table 1, Table 2). Nora performed a control motor activity study (Fig S2). Nora performed some conditioned place preference studies, and designed follow-up conditioned place preference studies (Fig 4b, Fig 4c). Nora analyzed all motor activity data and conditioned place preference data (Fig 3, Fig 4). Nora wrote a complete initial draft of the paper and worked with Dr. Wickman in an iterative process to produce the final manuscript prior to submission. Nora wrote the initial response to reviewer comments, and worked with Dr. Wickman in an iterative process to write the final responses to reviewers submitted to the journal editor.
L Kotecki*	Lydia Kotecki designed motor activity studies (Fig 3) and initial conditioned place preference studies (Fig 3, Fig 4a). Lydia supervised the efforts of Nicholas Carlblom, who conducted the motor activity and conditioned place preference studies.
S Dominguez-Lopez	Sergio Dominguez-Lopez designed, performed, and analyzed the self-administration study (Fig 5, Fig S3, Fig S4).
E Marron Fernandez de Velasco	Ezequiel Marron Fernandez de Velasco performed and analyzed the nucleus accumbens electrophysiology study (Fig S1).
N Carlblom	Nicholas Carlblom performed motor activity and conditioned place preference studies (Fig 3, Fig 4). Nicholas managed the transgenic mouse colony.
AL Sharpe	Amanda Sharpe helped design and analyze the self-administration study (Fig 5, Fig S3, Fig S4) and answered pertinent reviewer questions.
MJ Beckstead	Michael Beckstead helped design and analyze the self-administration study (Fig 5, Fig S3, Fig S4) and answered pertinent reviewer questions. Michael offered general comments about the manuscript.
K Wickman	Kevin Wickman provided funding and supervision for the project supervision, and edited the manuscript and responses to reviewers in an iterative fashion with Nora McCall.

*indicates co-first authors

Chapter 3

Selective ablation of GIRK channels in dopamine neurons alters behavioral effects of cocaine in mice

Chapter 2 contains works was previously published in Neuropsychopharmacology *2017 Feb; 42(3): 707–715. Published online 2016 Aug 24. Prepublished online 2016 Jul 29.*

"Selective Ablation of GIRK Channels in Dopamine Neurons Alters Behavioral Effects of Cocaine in Mice." ***Nora M McCall****,[1,5] Lydia Kotecki,[2,5] Sergio Dominguez-Lopez,[3] Ezequiel Marron Fernandez de Velasco,[2] Nicholas Carlblom,[2] Amanda L Sharpe,[3,4] Michael J Beckstead,[3] and Kevin Wickman[2]*

[1]Graduate Program in Neuroscience, [2]Department of Pharmacology, University of Minnesota; [3]Department of Physiology, The University of Texas Health Science Center at San Antonio; [4]Feik School of Pharmacy, University of the Incarnate Word; [5]These authors contributed equally to this work.

3.1 Abstract

The increase in dopamine (DA) neurotransmission stimulated by *in vivo* cocaine exposure is tempered by G protein-dependent inhibitory feedback mechanisms in DA neurons of the ventral tegmental area (VTA). G protein-gated inwardly rectifying

K^+ (GIRK/Kir3) channels mediate the direct inhibitory effect of $GABA_B$ receptor ($GABA_BR$) and D_2 DA receptor (D_2R) activation in VTA DA neurons. Here we examined the effect of the DA neuron-specific loss of GIRK channels on D_2R-dependent regulation of VTA DA neuron excitability and on cocaine-induced, reward-related behaviors. Selective ablation of *Girk2* in DA neurons did not alter the baseline excitability of VTA DA neurons but significantly reduced the magnitude of D_2R-dependent inhibitory somatodendritic currents and blunted the impact of D_2R activation on spontaneous activity and neuronal excitability. Mice lacking GIRK channels in DA neurons exhibited increased locomotor activation in response to acute cocaine administration and an altered locomotor sensitization profile, as well as increased responding for and intake of cocaine in an intravenous self-administration test. These mice, however, showed unaltered cocaine-induced conditioned place preference. Collectively, our data suggest that feedback inhibition to VTA DA neurons, mediated by GIRK channel activation, tempers the locomotor stimulatory effect of cocaine while also modulating the reinforcing effect of cocaine in an operant-based self-administration task.

3.2 Introduction

Dopamine (DA) neurons of the ventral tegmental area (VTA) are an integral part of the mesocorticolimbic system, a network of brain regions involved in reward-related behavior. Most drugs of abuse share the ability to increase extracellular levels of DA within this circuit (Nestler, 2005). Cocaine enhances DA neurotransmission by inhibiting transporters that remove DA from the extracellular space, allowing levels of DA to rise in downstream targets of DA neurons (Di Chiara and Imperato, 1988). Elevated DA signaling triggered by cocaine is implicated in behavioral effects, including locomotor stimulation and sensitization, and conditioned place preference (CPP) (Pierce and Kalivas, 1997; Zweifel et al., 2008).

In addition to enhancing DA levels in downstream targets of VTA DA neurons, cocaine also increases DA within the VTA (Groves et al., 1975; Beart et al., 1979). The cocaine-induced increase in VTA DA levels activates autoreceptors (D_2R) that, together with $GABA_BR$-dependent feedback (Waddington and Cross, 1978; Wolf et al., 1978), temper VTA DA neuron excitability (Einhorn et al., 1988). Pharmacological blockade or genetic suppression of G protein-dependent inhibitory feedback pathways in midbrain DA neurons alters behavioral effects of cocaine, including locomotor activation and self-administration (Steketee and Kalivas, 1991; Bello et al., 2011; de Jong et al., 2015; Holroyd et al., 2015). Moreover, inhibitory G protein signaling mediated by $GABA_BR$ and D_2R is decreased following cocaine administration (Ackerman and White, 1990; Kushner and Unterwald, 2001; Arora et al., 2011), highlighting the reciprocal relationship between cocaine and inhibitory G protein signaling in DA neurons.

The direct inhibitory influence of $GABA_BR$ and D_2R activation on VTA DA neurons is mediated primarily by activation of G protein-gated inwardly rectifying K^+ (GIRK/Kir3) channels found in the somatodendritic compartment (Beckstead et al., 2004; Cruz et al., 2004). Although GIRK1/GIRK2 heterotetramers are considered to be the prototypical neuronal GIRK channel (Luján et al., 2014), VTA DA neurons express a GIRK2/GIRK3 heteromer (Cruz et al., 2004). *Girk2* ablation eliminates all GIRK channel activity in VTA DA neurons (Beckstead et al., 2004; Cruz et al., 2004).

Multiple lines of evidence suggest that GIRK channels modulate DA-dependent behaviors. Constitutive *Girk2*$^{-/-}$ mice are hyperactive, a phenotype normalized by D_1 DA receptor (D_1R) blockade (Blednov et al., 2002). Moreover, *Girk2*$^{-/-}$ mice exhibit enhanced locomotor activation in response to morphine and cocaine (Arora et al., 2010; Kotecki et al., 2015). The many phenotypes and adaptations associated with global *Girk2* ablation, however, confound interpretation of these data (Luján et al., 2014).

For example, VTA DA neurons, NAc medium spiny neurons (MSNs), and layer 5/6 medial prefrontal cortex (mPFC) pyramidal neurons from *Girk2*$^{-/-}$ mice exhibit elevated AMPA receptor-mediated neurotransmission (Arora et al., 2010; Hearing et al., 2013). The recent availability of mice lacking GIRK2 in DA neurons permits a more precise evaluation of the role of GIRK-dependent signaling in modulating DA neuron excitability and cocaine-induced behaviors (Kotecki et al., 2015). Here we report that GIRK channel ablation in DA neurons reduces the autoreceptor-mediated inhibition of VTA DA neurons and alters behavioral sensitivity to cocaine.

3.3 Materials and methods

3.3.1 Animals

All studies were approved by the Institutional Animal Care and Use Committees at the University of Minnesota and University of Texas Health Science Center, San Antonio. The generation of *Girk2*$^{flox/flox}$, DATCre(+/−):*Girk2*$^{flox/flox}$, and Pitx3-eGFP(+)/DATCre(+/−):*Girk2*$^{flox/flox}$ mice was described previously (Kotecki et al., 2015). DATCre (B6.SJL-Slc6a3$^{tm1.1(cre)Bkmn}$) and Drd1a-tdTomato (B6.Cg-Tg(Drd1a-tdTomato)6Calak/J) lines were purchased from The Jackson Laboratory (Bar Harbor, ME), and the Drd2-eGFP strain (Tg(Drd2-EGFP)S118Gsat) was obtained from the Mutant Mouse Regional Resource Center. Mice were maintained on a 12 h light/dark cycle (lights on at 0700 hours), with food and water available *ad libitum.*

3.3.2 Drugs

Quinpirole, sulpiride, tetrodotoxin (TTX), and picrotoxin were purchased from Sigma (St Louis, MO). Cocaine hydrochloride was purchased from Sigma or provided by the National Institute on Drug Abuse drug supply program (RTI International, Research Triangle Park, NC).

3.3.4 Slice electrophysiology

Horizontal slices (225 µm) of the mouse VTA (5–7 weeks) were prepared as described (Kotecki et al., 2015). Neurons medial to the medial terminal nucleus of the accessory optic tract, and identified via GFP expression driven by the *Pitx3* promoter, were targeted for analysis. DA neurons in the most medial aspect of the VTA were avoided as they were reported to exhibit low GIRK2 and D_2R expression (Lammel et al., 2008). Whole-cell data were acquired using a Multiclamp 700 A amplifier and the pCLAMPv.9.2 software (Molecular Devices; Sunnyvale, CA). I_h amplitude was assessed using a 1-s voltage ramp (−60 to −120 mV). Somatodendritic currents (V_{hold}=−60 mV) were measured in the presence of TTX (0.5 µM). Spontaneous activity was measured in current-clamp mode (I=0) for 1 min. Neurons exhibiting no or irregular spontaneous activities were not evaluated. Rheobase and current/spike relationships were measured by injecting currents from −60 to 220 pA, increasing in 20 pA increments (1 s/step). Rheobase was defined as the minimum current evoking one or more action potentials. To assess the effect of $D_{2/3}R$ activation on excitability, neurons were voltage-clamped (V_{hold}=−60 mV) while quinpirole was applied to the bath. At the peak of the quinpirole response, spontaneous activity and excitability were reassessed. All command potentials factored in a junction potential of −15 mV. Series and membrane resistances were tracked throughout the experiment. If series resistance was high (>20 MΩ) or unstable (>20% variation), the experiment was excluded from analysis.

3.3.5 Locomotor activity

Cocaine-induced activity was assessed in open field activity chambers (Med-Associates, St Albans, VT), as described (Pravetoni and Wickman, 2008). Subjects (7–10 weeks) were acclimated over 3 days, during which the animals were handled and exposed to i.p.

injection (saline) and the open field. Distance traveled during the 60-min period following saline injection on the last acclimation day was taken as baseline activity. For acute cocaine-induced activity studies, subjects were given 1 of the 3 cocaine doses (3, 15, or 30 mg/kg i.p.). For cocaine sensitization, subjects received cocaine (15 mg/kg i.p.) for 5 days, followed by cocaine challenge (15 mg/kg i.p.) 10–11 days later.

3.3.6 Conditioned place preference

CPP testing was performed in two-compartment chambers (Med Associates) housed within sound-attenuating cubicles. One cohort was evaluated with 0 (saline) or 15 mg/kg cocaine using a three conditioning session design (Mirkovic et al., 2012). A second cohort was evaluated using a modified design involving lower cocaine doses (0.5 and 3 mg/kg) (Wydeven et al., 2014). Side preference in this study was evaluated twice, after the second and fourth cocaine conditioning sessions. CPP was calculated as the difference in time spent in drug- and saline-paired chamber during the posttest.

3.3.7 Self-administration

Male mice (15–20 weeks) were group-housed (3–5/cage) on a 12/12 h reverse light–dark cycle (lights off at 0900 hours), with *ad libitum* access to food and water throughout the study. Following jugular catheterization, mice were housed individually and allowed $\geqslant$7 days to recover. Operant sessions (2 h) were conducted as described (Sharpe et al., 2015), with minor modifications. During training, responses in the correct nose poke hole were rewarded on a fixed ratio 1 (FR1) schedule of reinforcement for infusions 1–5, an FR2 for infusions 6–8, and FR3 thereafter. Upon completing the response requirement, a green stimulus light in the correct nose poke hole was turned off, a 30-s time out was initiated, and cocaine was delivered (0.5 mg/kg/infusion over 2 s), accompanied by a sound stimulus of 2 kHz. After the timeout, the correct nose poke hole was re-

illuminated. Although responding in both holes was recorded during the timeout, no responses were reinforced. Self-administration was considered acquired when infusion number was $\geqslant$8 in two consecutive sessions and the number of nose pokes in the correct hole represented 70% of the total. Mice then advanced to 7 days of training on an FR3 schedule (0.5 mg/kg/infusion) to ensure stable responding prior to the dose-response assessment. For the dose–response study, cocaine dose per infusion was increased daily (0.03, 0.1, 0.3, 1.0, and 3.0 mg/kg/infusion). Self-administration across this dose range was evaluated over three rounds, with the first round considered training. The average of data for each subject over the last two rounds was used for analysis. Although all doses were calculated based on a typical weight of a young adult mouse (28 g), final intake values were corrected for actual bodyweight. Catheters were flushed before and after sessions to assess patency. Two $GIRK2_{DA}$WT and four $GIRK2_{DA}$KO subjects were excluded from the study owing to inconsistent self-administration or failed catheter patency.

3.3.8 Statistical analysis

Data are presented throughout as the mean±SEM. Statistical analyses were performed using Prism (GraphPad Software, La Jolla, CA) and SigmaPlot (Systat Software, San Jose, CA). With the exception of mEPSC and self-administration studies, which included males only, all studies involved balanced groups of male and female mice. Data were analyzed first for effects of sex and genotype using two-way ANOVA when those were the only variables. For studies with additional variables (*e.g.*, multiple testing days), the interaction of sex and genotype was assessed using two-way ANOVAs at each level; the effect of sex within each genotype was determined using a repeated-measures two-way ANOVA. When an effect of sex or a sex interaction was observed, data from each sex were analyzed separately. When sex differences were not observed, male and female

data were pooled. Pairwise comparisons were performed using Student's *t*or Mann–Whitney *U* tests, or Bonferroni *post-hoc* test, as appropriate. Differences were considered significant if $P<0.05$.

3.3.9 Supplementary methods

For mEPSC recordings in NAc medium spiny neurons (MSNs), coronal slices (250 µm) containing NAc core and shell from adolescent (5-7 wk) male $GIRK2_{DA}WT$ and $GIRK2_{DA}KO$ mice, crossed with either Drd1a-tdTomato or Drd2-eGFP lines to identify D1 or D2 MSNs, respectively, were prepared an ice-cold solution containing (in mM): 229 mM sucrose, 1.9 KCl, 1.2 Na_2HPO_4, 33 $NaHCO_3$, 6 $MgCl_2$, 0.5 $CaCl_2$, 10 glucose, 0.4 ascorbic acid (pH 7.4), constantly bubbled with 95% O_2/5% CO_2. Prior to recordings, slices were allowed to recover for at least 1 h in pre-warmed (32 °C) ACSF (in mM): 125 NaCl, 2.5 KCl, 1.25 Na_2HPO_4, 25 $NaHCO_3$, 4 $MgCl_2$, 1 $CaCl_2$, 10 glucose, 0.4 ascorbic acid (pH 7.4), saturated with 95% O_2/5% CO_2.

Slices were transferred to a recording chamber and superfused with oxygenated ACSF (in mM): 125 NaCl, 2.5 KCl, 25 $NaHCO_3$, 1.3 $MgCl_2$, 2.0 $CaCl_2$, 10 glucose, 0.4 ascorbic acid (pH 7.4), at a flow rate of 2–2.5 mL/min. TTX (0.5 µM) and picrotoxin (50 µM) were included in the bath solution throughout the recording to prevent action potentials and $GABA_AR$-mediated currents, respectively. Subsequent bath application of 2 mM kynurenic acid was used to verify that observed mEPSC activity was specific to ionotropic glutamate receptors. mEPSCs (Vhold= -70 mV) were recorded using borosilicate electrodes (2.7-3.5 MΩ), filtered at 2 kHz, and digitized at 10 kHz using an EPC10 HEKA amplifier and Patchmaster 2x73.2 software (HEKA Elektronic; Bellmore, NY). Amplitude and frequency values were extracted with Mini Analysis (Synaptosoft) software. All command potentials factored in a junction potential of -15 mV, and series resistance, membrane resistance, and apparent cell capacitance were tracked

throughout the experiment. If series resistance was unstable (>20% variation), the experiment was excluded from the final dataset.

3.4 Results

3.4.1 $D_{2/3}$R-dependent signaling and excitability in VTA DA neurons from GIRK2$_{DA}$KO mice

We recently demonstrated that VTA DA neurons in DATCre(+):*Girk2*$^{flox/flox}$ mice (GIRK2$_{DA}$KO mice) exhibited diminished inhibitory somatodendritic current responses to GABA$_B$R activation (Kotecki et al., 2015). To test whether autoreceptor-mediated signaling in VTA DA neurons from GIRK2$_{DA}$KO mice was similarly blunted, we measured currents evoked by a saturating concentration (20 µM) of the $D_{2/3}$R agonist quinpirole. GIRK2$_{DA}$KO mice were crossed with mice expressing GFP under the control of a DA neuron-specific promoter (Pitx3) to permit targeted characterization of VTA DA neurons. VTA DA neurons from DATCre(−):*Girk2*$^{flox/flox}$ mice (GIRK2$_{DA}$WT mice) exhibited outward currents that were reversed by the $D_{2/3}$R antagonist sulpiride (5 µM; **Figure 3.1A**). Although DA neurons from GIRK2$_{DA}$KO mice also showed quinpirole-induced responses, amplitudes were smaller than their wild-type counterparts (**Figure 3.1A, B**; Mann–Whitney U=85.5, ***P<0.001). There was no effect of genotype on other properties of VTA DA neurons (**Table 3.1**).

We next measured spontaneous activity and rheobase in the absence or presence of quinpirole (20 µM). At baseline, VTA DA neurons from GIRK2$_{DA}$WT and GIRK2$_{DA}$KO mice exhibited no difference in spontaneous activity (**Figure 3.2A, B**), rheobase (**Figure 3.2C, D**), current–spike relationship (**Figure 3.2E**), or other properties (**Table 3.2**). In the presence of quinpirole, spontaneous activity of VTA DA neurons from GIRK2$_{DA}$WT mice was completely eliminated (16/16 neurons; **Figure 3.2A, B**). In

contrast, quinpirole eliminated spontaneous activity in only 6/12 neurons GIRK2$_{DA}$KO VTA DA neurons, with the remainder showing an incomplete suppression of activity (Mann–Whitney U=48.0, $^{**}P$<0.01). Quinpirole markedly decreased excitability (increased rheobase) in GIRK2$_{DA}$WT VTA DA neurons but had less of an effect on GIRK2$_{DA}$KO VTA DA neurons (**Figure 3.2C, D**; Mann–Whitney U=17.5, $^{***}P$<0.001). Finally, the current/spike relationship was more prominently suppressed by quinpirole in VTA DA neurons from GIRK2$_{DA}$WT as compared with GIRK2$_{DA}$KO mice (**Figure 3.2E**; $F_{14,336}$=24.5, P<0.001, current × genotype interaction). These data indicate that, while loss of GIRK-dependent signaling does not impact baseline excitability of VTA DA neurons, it does dampen the inhibitory influence of autoreceptor-dependent signaling on these neurons.

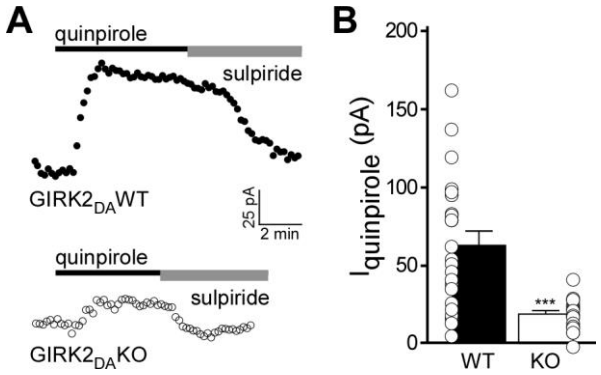

Figure 3.1. $D_{2/3}R$-dependent somatodendritic currents in VTA DA neurons from $GIRK2_{DA}WT$ and $GIRK2_{DA}KO$ mice.

A) Representative currents evoked by quinpirole (20 µM) and reversed by sulpiride (5 µM) in VTA DA neurons from $GIRK2_{DA}WT$ and $GIRK2_{DA}KO$ mice. Currents were recorded with TTX (0.5 µM) in the bath to prevent synaptic activity. **B**) Summary of quinpirole-induced currents in VTA DA neurons from $GIRK2_{DA}WT$ (*n*=23) and $GIRK2_{DA}KO$ (*n*=19) mice. Circles represent individual data points. ***P<0.001 *vs* $GIRK2_{DA}WT$.

Table 3.1. Summary of data for VTA DA neurons evaluated in Figure 3.1

Parameter	$GIRK2_{DA}WT$	$GIRK2_{DA}KO$	Test	Test statistic	P value
Group size (n)	23	19	n/a	n/a	n/a
Age (d)	40 ± 1	40 ± 1	n/a	n/a	n/a
Capacitance (pF)	49 ± 4	44 ± 3	M-W	U = 187	0.43
I_h amplitude (pA)	-165 ± 49	-68 ± 20	M-W	U = 148	0.08

Electrophysiological parameters obtained for experiments assessing quinpirole-induced somatodendritic currents in the presence of 0.5 µM TTX, shown in **Figure 3.1**. The impact of genotype was assessed using the Mann-Whitney (M-W) *U*-test.

Table 3.2. Summary data for VTA DA neurons evaluated in Figure 3.2

Parameter	$GIRK2_{DA}WT$	$GIRK2_{DA}KO$	Test	Test statistic	P value
Group size (n)	16	12	n/a	n/a	n/a
Age (d)	37 ± 1	39 ± 1	n/a	n/a	n/a
Capacitance (pF)	49 ± 3	53 ± 4	t	t_{26} = -0.81	0.43
I_h amplitude (pA)	-126 ± 27	-126 ± 36	M-W	U = 89	0.75
Action potential					
amplitude (mV)	64 ± 2	60 ± 2	t	t_{26} = 1.25	0.22
half-width (ms)	1.53 ± 0.05	1.56 ± 0.06	t	t_{26} = -0.44	0.66
threshold (mV)	-51.6 ± 0.7	-51.2 ± 0.3	M-W	U = 90	0.80

Baseline electrophysiological parameters obtained for excitability experiments shown in **Figure 3.2**. The impact of genotype was assessed using the Student's t-test (t) or Mann-Whitney (M-W) *U*-test, as appropriate.

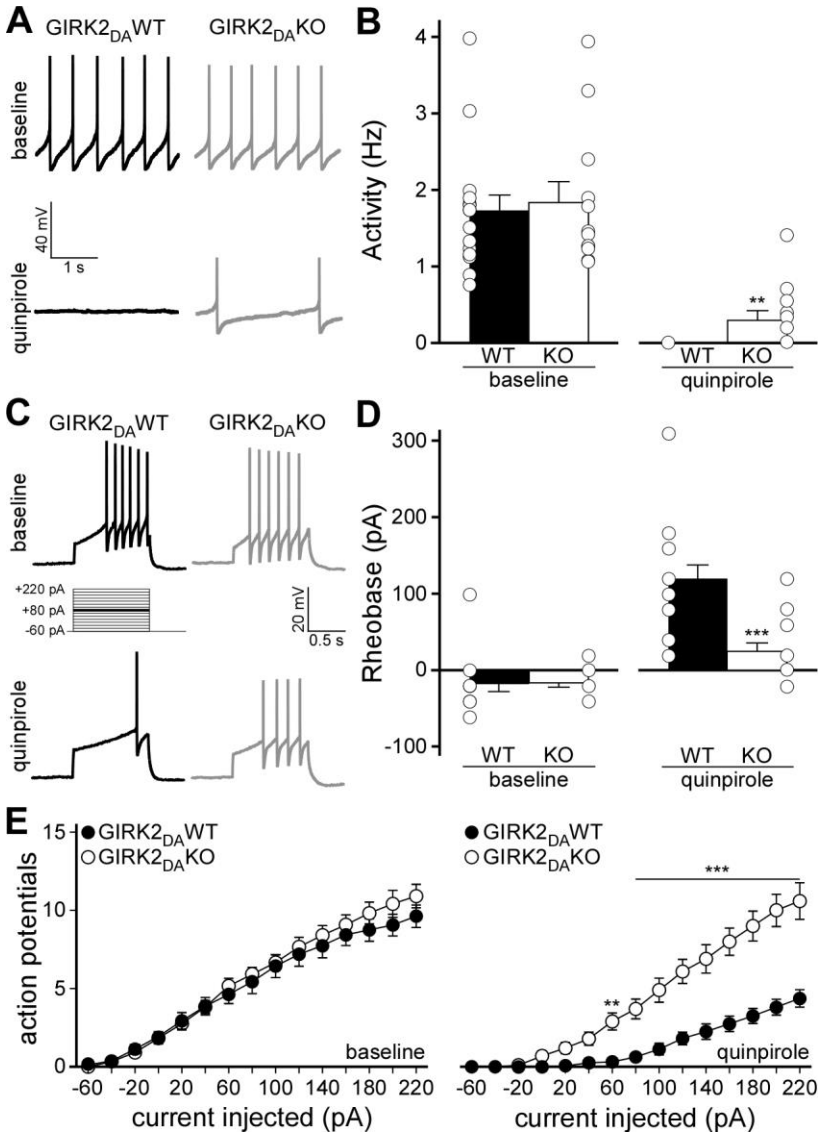

Figure 3.2. Excitability of GIRK2$_{DA}$WT and GIRK2$_{DA}$KO VTA DA neurons in the absence and presence of quinpirole.

A) Representative traces showing spontaneous activity in GIRK2$_{DA}$WT and GIRK2$_{DA}$KO VTA DA neurons at baseline and in the presence of quinpirole (20 µM). **B**) Summary of spontaneous activity in GIRK2$_{DA}$WT (*n*=16) and GIRK2$_{DA}$KO (*n*=12) VTA DA neurons. **C**) Typical responses of GIRK2$_{DA}$WT and GIRK2$_{DA}$KO VTA DA neurons to depolarizing current injection (80 pA), at baseline, and in the presence of quinpirole (20 µM). **D**) Rheobase summary for GIRK2$_{DA}$WT (*n*=16) and GIRK2$_{DA}$KO (*n*=12) VTA DA neurons at baseline and in the presence of quinpirole (20 µM). **E**) Plots showing the number of action potentials elicited by a 1-s current injection (−60 to 220 pA) in GIRK2$_{DA}$WT (*n*=16) and GIRK2$_{DA}$KO (*n*=12) VTA DA neurons at baseline and in the presence of quinpirole (20 µM). ***P*<0.01 and ****P*<0.001 *vs* GIRK2$_{DA}$WT (within current step).

3.4.2 Excitatory neurotransmission in the NAc of GIRK2$_{DA}$KO mice

The amplitude and frequency of miniature excitatory postsynaptic currents (mEPSCs) were elevated in MSNs of the nucleus accumbens (NAc) shell from constitutive *Girk2*$^{-/-}$ mice, observations paralleling an increase in AMPA receptor levels at excitatory synapses in these neurons (Arora et al., 2010). To discern whether this adaptation is driven by loss of GIRK-dependent signaling in VTA DA neurons, we compared mEPSCs in NAc core and shell MSNs from GIRK2$_{DA}$WT and GIRK2$_{DA}$KO mice. To facilitate the targeted evaluation of neuron subpopulations in the NAc, we crossed GIRK2$_{DA}$KO mice with transgenic mice expressing fluorescent proteins in D_1R-expressing (Drd1a-tdTomato) or D_2R-expressing (Drd2-GFP) MSNs. No genotype difference in mEPSC amplitude or frequency was observed in D_1R- or D_2R-expressing MSNs in the NAc core or shell (**Supplementary Figure 3.S1**). Thus the increased excitatory neurotransmission observed in NAc MSNs in *Girk2*$^{-/-}$ mice is driven by loss of GIRK2 in a non-DA neuron population(s).

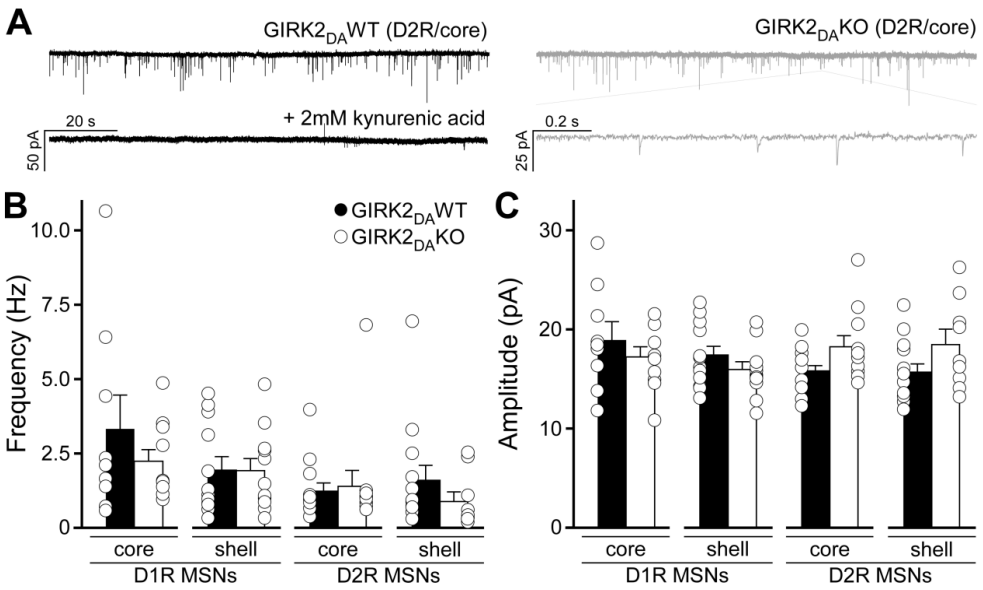

Supplementary Figure 3.S1. Excitatory neurotransmission in NAc MSNs of GIRK2$_{DA}$WT and GIRK2$_{DA}$KO mice.

A) Representative traces of mEPSCs in D_2R-expressing MSNs in the NAc core of male GIRK2$_{DA}$WT and GIRK2$_{DA}$KO mice; observed events were blocked by 2 mM kynurenic acid. **B**) mEPSC frequency in D_1R-expressing MSNs in the NAc core (n=9-10) and shell (n=11-12), and D_2R-expressing MSNs in the NAc core (n=11-13) and shell (n=9-13). **C**) Summary of mEPSC amplitude in D_1R-expressing MSNs in the NAc core (n=9-10) and shell (n=11-12), and D2R-expressing MSNs in the NAc core (n=11-13) and shell (n=9-13).

3.4.3 Cocaine-induced locomotor activity in GIRK2$_{DA}$KO mice

We next evaluated GIRK2$_{DA}$WT and GIRK2$_{DA}$KO mice in an open field activity test (**Figure 3.3**). We observed a significant effect of sex ($F_{1,99}$=7.7, P<0.01) and genotype ($F_{1,99}$=15.0, P<0.001) on baseline activity (saline day 2, S_2), with GIRK2$_{DA}$KO mice exhibiting a small but significantly higher level of activity than GIRK2$_{DA}$WT mice, and females showing higher activity than males. Significant main effects of genotype (male $F_{1,42}$=30.8, P<0.001; female $F_{1,49}$=8.2, P<0.01) and dose (male $F_{2,42}$=74.0, P<0.001; female $F_{2,49}$=43.8, P<0.001), as well as genotype × dose interactions (male $F_{2,42}$=4.6, P<0.05; female $F_{2,49}$=6.7, P<0.01), were observed in both sexes. Notably, mice of both genotypes and sexes increased locomotor activity in response to cocaine, with the 15 mg/kg dose revealing elevated responses in male (**Figure 3.3A**) and female (**Figure 3.3B**) GIRK2$_{DA}$KO mice. Interestingly, there was no difference between female GIRK2$_{DA}$WT and GIRK2$_{DA}$KO at the 30 mg/kg dose. No difference in baseline activity or the locomotor-stimulatory effect of 15 mg/kg cocaine was observed between DATCre(+) and DATCre(−) littermates (**Supplementary Figure 3.S2**), arguing that activity differences between GIRK2$_{DA}$WT and GIRK2$_{DA}$KO mice are attributable to the loss of GIRK channels from DA neurons.

Repeated cocaine leads to locomotor sensitization, the enhanced response to subsequent cocaine exposures that persists after prolonged withdrawal (Robinson and Berridge, 2001). To test whether locomotor sensitization differed between GIRK2$_{DA}$WT and GIRK2$_{DA}$KO mice, we used a repeated dosing procedure involving 5 days of cocaine injections (15 mg/kg) and a cocaine challenge test. We observed a significant interaction of sex and injection number in GIRK2$_{DA}$WT mice ($F_{8,136}$=2.5; P<0.05), and thus male (**Figure 3.3C**) and female (**Figure 3.3D**) subjects were analyzed separately. Significant

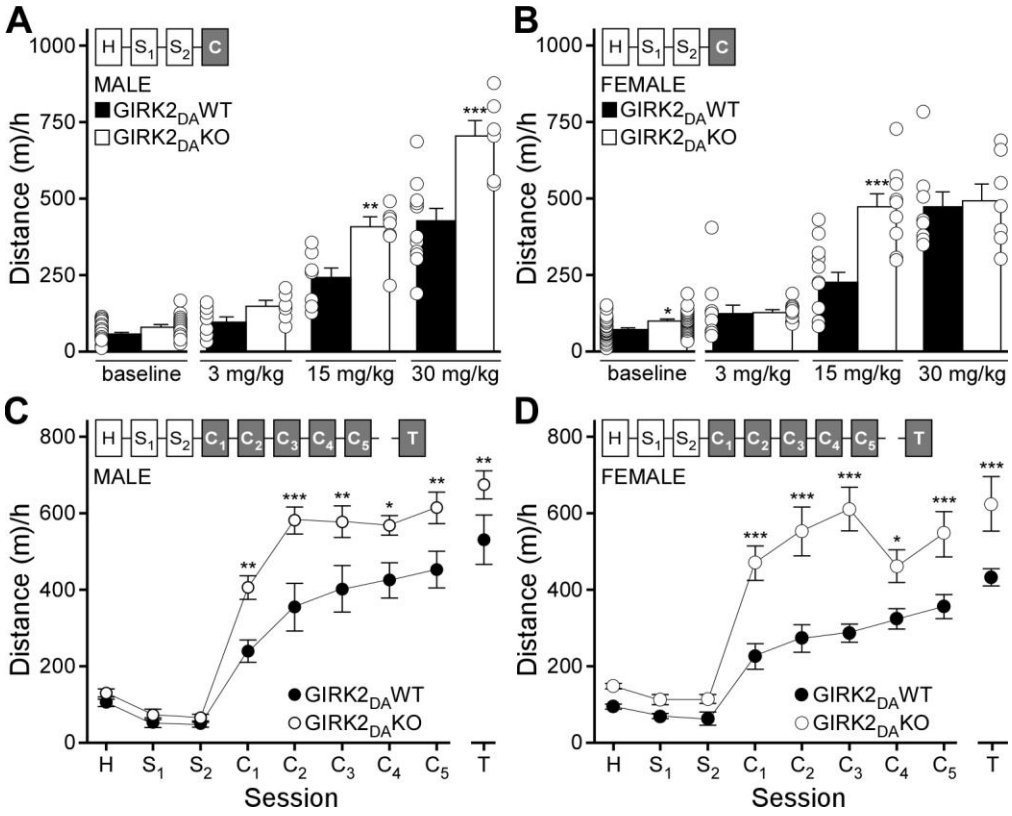

Figure 3.3. Cocaine-induced locomotor activity and sensitization in GIRK2$_{DA}$WT and GIRK2$_{DA}$KO mice.

Distance traveled (in m) by GIRK2$_{DA}$WT and GIRK2$_{DA}$KO mice in an open field test. The test included a handling day (H), followed by 2 days of saline injections (S_1 and S_2), and then a final day with injection of 3, 15, or 30 mg/kg cocaine. Distance traveled on S_2 was taken as baseline activity. **A**) Baseline (*n*=20–28 per genotype) and acute cocaine-induced locomotor activity (*n*=6–12 per genotype and dose) in male GIRK2$_{DA}$WT and GIRK2$_{DA}$KO mice. ***P*<0.01 and ****P* 0.001 *vs* GIRK2$_{DA}$WT (within dose). **B**) Baseline (*n*=25–30 per genotype) and acute cocaine-induced locomotor activity (*n*=7–11 per genotype and dose) in female GIRK2$_{DA}$WT and GIRK2$_{DA}$KO mice. Symbols: ****P*<0.001 *vs* GIRK2$_{DA}$WT (within dose). **C**) Total distance traveled by male GIRK2$_{DA}$WT (*n*=8) and GIRK2$_{DA}$KO (*n*=8) mice during the locomotor sensitization test. The repeated dosing protocol included a handling day (H) followed by 2 days of saline injections (S_1 and S_2), and then 5 days of cocaine injections ($C_{1–5}$; 15 mg/kg); mice were challenged again with 15 mg/kg cocaine test (T) 10–11 days after the fifth cocaine injection. Symbols: **P*<0.05, ***P*<0.01, and ****P*<0.001 *vs* GIRK2$_{DA}$WT (within injection). **D**) Distance traveled by female GIRK2$_{DA}$WT (*n*=11) and GIRK2$_{DA}$KO (*n*=9) mice during the locomotor sensitization test. **P*<0.05 and ****P*<0.001 *vs* GIRK2$_{DA}$WT (within injection).

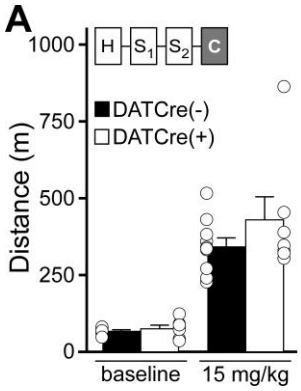

Supplementary Figure 3.S2. Cocaine-induced locomotor activity in DATCre(-) and DATCre(+) mice.

A) Baseline (S2) and acute cocaine-induced locomotor activity (15mg/kg) in male and female DATCre(-) (n=10) and DATCre(+) (n=7) littermate mice.

main effects of genotype (male $F_{1,112}$=10.6, P<0.01; female $F_{1,144}$=20.2, P<0.001) and injection number (male $F_{8,112}$=110.2, P<0.001; female $F_{8,144}$=89.0, P<0.001), as well as genotype × injection number interactions (male $F_{8,112}$=3.8, P<0.001; female $F_{8,144}$=8.3, P<0.001), were observed for male and female subjects. Male and female GIRK2$_{DA}$KO mice exhibited enhanced locomotor activity relative to GIRK2$_{DA}$WT counterparts in response to cocaine on all days (**Figure 3.3C, D**). Moreover, all groups exhibited significantly greater locomotor activity on the challenge test relative to activity measured after the initial cocaine exposure (not shown). Notably, while the activity of GIRK2$_{DA}$WT mice increased with each cocaine injection, the activity of GIRK2$_{DA}$KO mice plateaued between the first and third injections. These findings suggest that GIRK2$_{DA}$KO mice exhibit a 'presensitized' phenotype similar to that induced by genetic suppression of GIRK-dependent signaling in the mPFC (Hearing et al., 2013).

3.4.4 Cocaine-induced CPP in GIRK2$_{DA}$KO mice

We next assessed cocaine reward in GIRK2$_{DA}$KO mice using a CPP test. As male and female GIRK2$_{DA}$KO mice exhibited increased locomotor-stimulatory effect of 15 mg/kg cocaine relative to GIRK2$_{DA}$WT counterparts, we used this dose with three drug/side pairings. A separate group of mice was conditioned with saline (0 mg/kg). Surprisingly, cocaine CPP was indistinguishable in GIRK2$_{DA}$WT and GIRK2$_{DA}$KO mice (**Figure 3.4A**). Previous CPP studies have shown a shallow or non-existent dose–response relationship for cocaine in the 4–12 mg/kg dose range in mice and a significant effect of conditioning session number on CPP magnitude (Brabant et al., 2005). Thus we also evaluated CPP utilizing lower cocaine doses (0.5 or 3 mg/kg) and after both two and four conditioning sessions. Again, no significant difference in cocaine CPP was detected between genotypes (**Figure 3.4B, C**).

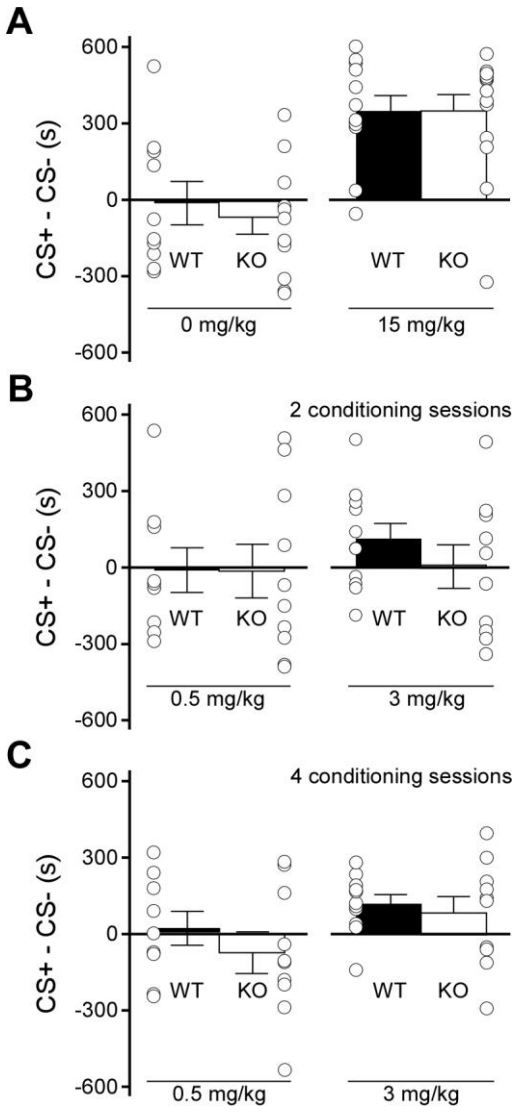

Figure 3.4. Cocaine-induced CPP in GIRK2$_{DA}$WT and GIRK2$_{DA}$KO mice.

A) Cocaine-induced CPP in GIRK2$_{DA}$WT (*n*=10–12 per dose) and GIRK2$_{DA}$KO (*n*=12–14 per dose) mice, measured as the difference in time spent in the drug (CS+) and saline (CS−) paired sides on test day. **B**) Cocaine-induced CPP in a separate cohort of GIRK2$_{DA}$WT (*n*=9–11 per dose) and GIRK2$_{DA}$KO (*n*=10 per dose) mice, measured after two drug conditioning sessions. **C**) Cocaine-induced CPP in the same mice as in panel B, measured after four drug conditioning sessions.

3.4.5 Cocaine self-administration in GIRK2$_{DA}$KO mice

Finally, we asked whether intravenous cocaine self-administration was impacted by the loss of GIRK channels in DA neurons. No difference between GIRK2$_{DA}$WT and GIRK2$_{DA}$KO mice was observed with respect to acquisition of self-administration (**Figure 3.5A-C**), defined as earning eight infusions during two consecutive sessions, with nose pokes at the correct hole accounting for >70% of the total (**Supplementary Figure 3.S3A, B**). After meeting acquisition criteria, mice were transitioned to an FR3 schedule of reinforcement (0.5 mg/kg/infusion), during which GIRK2$_{DA}$WT (14.3±1.2) and GIRK2$_{DA}$KO (12.8±0.8; t_{138}=1.1, P=0.29) earned comparable infusions per session.

After completing baseline FR3 training, self-administration behavior as a function of cocaine dose was assessed using an FR3 schedule of reinforcement. Although patterns of responding were comparable within and across subjects at the various cocaine doses (**Supplementary Figure 3.S4**), an interaction between genotype and dose with respect to infusions earned was observed ($F_{4,72}$=3.0, P<0.05); GIRK2$_{DA}$KO mice earned more infusions of cocaine than GIRK2$_{DA}$WT controls, most evident during sessions involving the lowest three cocaine doses (**Figure 3.5D**). Importantly, a strong preference for responding in the correct nose poke hole was observed both GIRK2$_{DA}$WT and GIRK2$_{DA}$KO throughout the dose–response study (**Supplementary Figure 3.S3C, D**). Furthermore, a main effect of genotype was detected for total cocaine intake ($F_{1,72}$=6.1, P<0.05), with higher levels observed for GIRK2$_{DA}$KO mice relative to littermate controls (**Figure 3.5E**).

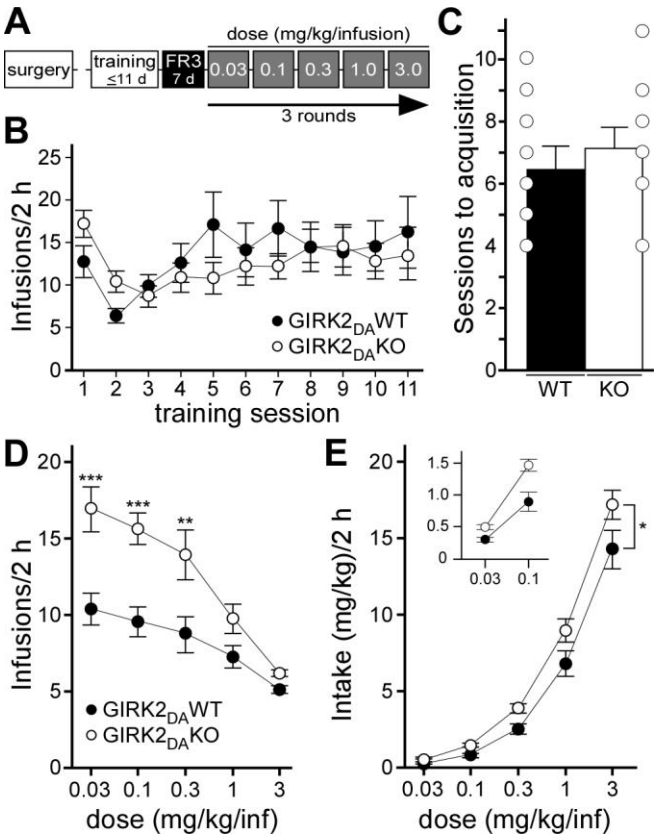

Figure 3.5. Cocaine self-administration in male $GIRK2_{DA}WT$ and $GIRK2_{DA}KO$ mice.

A) Depiction of the self-administration procedure, beginning with jugular catheterization surgery and a ⩾7-day recovery period. Acquisition of cocaine self-administration was achieved in daily 2-h sessions where the response requirement was raised from an FR1 to an FR3 (0.5 mg/kg/infusion). $GIRK2_{DA}WT$ (n=9) and $GIRK2_{DA}KO$ (n=11) meeting acquisition criteria were maintained at an FR3 schedule for 7 days (baseline) prior to assessing intake and infusions as a function of cocaine dose. **B**) The number of infusions earned during the first 11 days of cocaine self-administration (training). **C**) Number of training sessions needed to meet acquisition criteria (t_{18}=0.65, P=0.54). **D**) Number of infusions, with FR3 schedule of reinforcement, earned as a function of unit dose of cocaine (0.03–3.0 mg/kg/infusion). **P<0.01 and ***P<0.001 *vs* $GIRK2_{DA}WT$ (within dose). **E**) Cocaine intake as a function of unit dose, with the two lowest doses expanded in the inset. *P<0.05 (main effect of genotype).

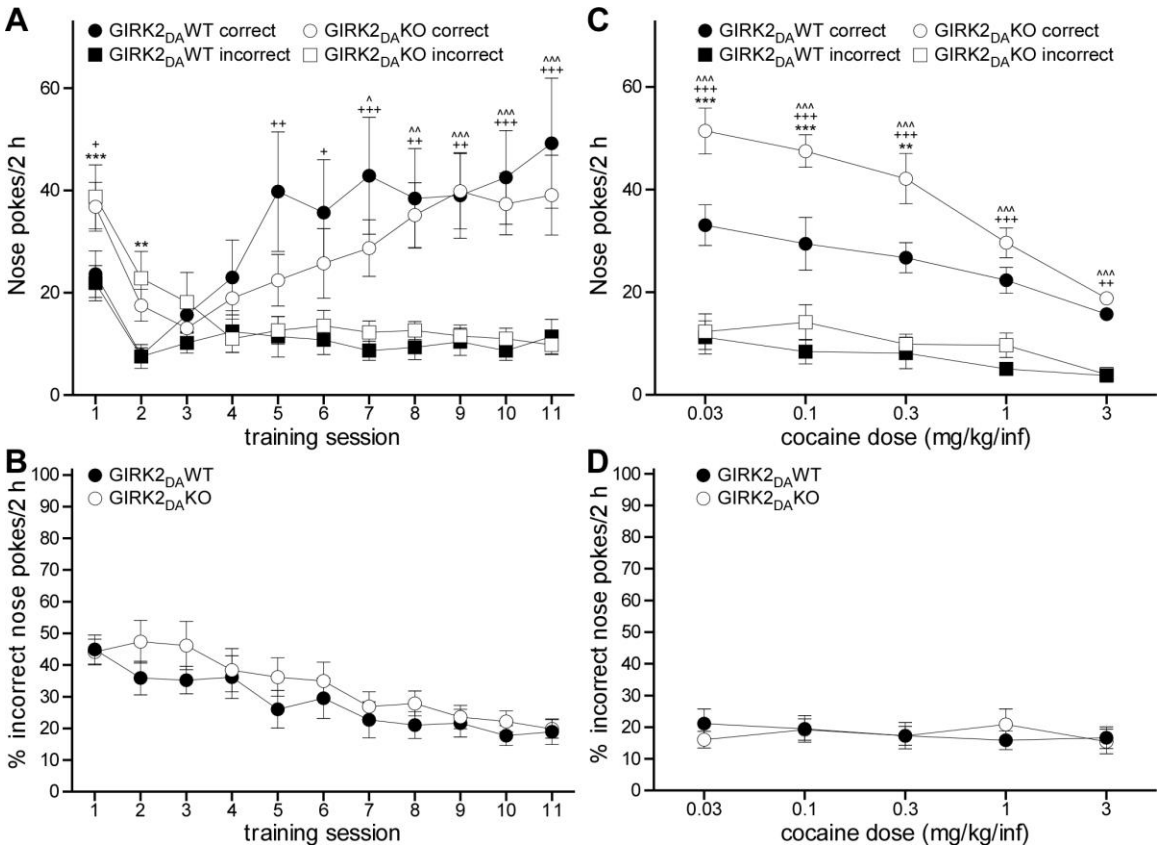

Supplementary Figure 3.S3. Operant responding in GIRK2$_{DA}$WT and GIRK2$_{DA}$KO mice.

A) Nose pokes at the correct/active and incorrect holes during acquisition. An interaction of session and genotype on incorrect side nose pokes ($F_{10,180}$=2.2, P<0.05) was seen, along with an effect of session on correct side nose pokes ($F_{10,180}$=7.2, P<0.001). GIRK2$_{DA}$WT ($F_{10,80}$=4.9,P<0.001) and GIRK2$_{DA}$KO mice ($F_{10,100}$=6.7, P<0.001) exhibited more correct than incorrect nose pokes in the latter sessions. Symbols: **,***P<0.01 and 0.001 (GIRK2$_{DA}$WT vs. GIRK2$_{DA}$KO, incorrect nose pokes); $^{+}$,$^{++}$,$^{+++}$$P$<0.05, 0.01, and 0.001 (correct/active vs. incorrect nose pokes; GIRK2$_{DA}$WT mice). ^,^^,^^^P<0.05, 0.01, and 0.001 (active vs. inactive nose pokes; GIRK2$_{DA}$KO mice). **B**) Percentage of total nose pokes made on the incorrect side during acquisition. A significant effect of training session was observed ($F_{10,180}$=10.7, P<0.001). **C**) Correct/active and incorrect nose pokes during the dose-response study. A significant interaction between genotype and dose was seen for correct/active nose pokes ($F_{4,72}$=2.7, P<0.05). A significant effect of dose ($F_{4,72}$=7.9, P<0.001) but not genotype on incorrect nose pokes was found. Both GIRK2$_{DA}$WT ($F_{4,32}$=3.0, P<0.05) and GIRK2$_{DA}$KO ($F_{4,40}$=11.5, P<0.001) mice exhibited more correct/active than incorrect nose pokes. Symbols: **,***P<0.01 and 0.001 (GIRK2$_{DA}$WT vs. GIRK2$_{DA}$KO; correct/active nose pokes). $^{+}$,$^{++}$,$^{+++}$$P$<0.05, 0.01, and 0.001 (correct/active vs. incorrect nose pokes; GIRK2$_{DA}$WT mice). ^,^^,^^^P<0.05, 0.01, and 0.001 (correct/active vs. incorrect nose pokes; GIRK2$_{DA}$KO mice). **D**) Percentage of total nose pokes made on the incorrect side during the dose-response assessment.

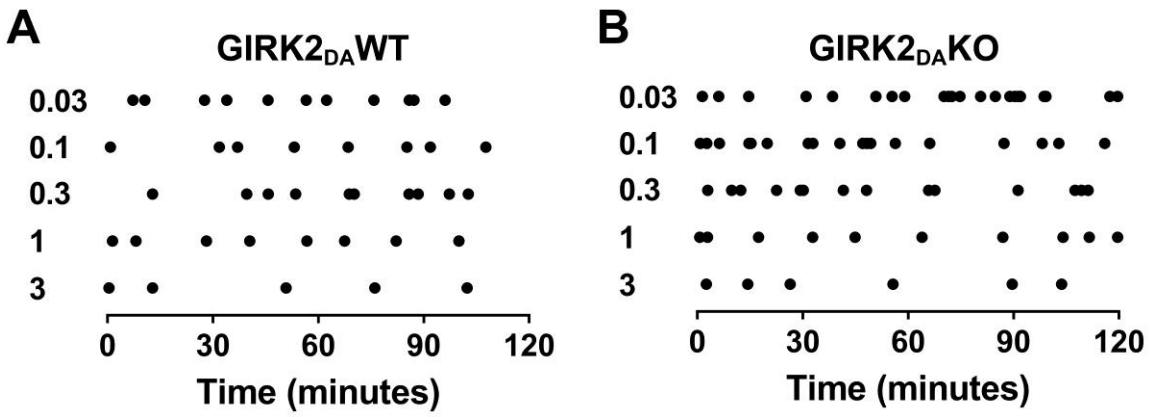

Supplementary Figure 3.S4.

Representative raster plots for GIRK2$_{DA}$WT **A**) and GIRK2$_{DA}$KO **B**) mice depicting their patterns of responding during the daily 2-h cocaine self-administration sessions at specified doses (0.03-3 mg/kg/infusion). Each dot indicates delivery of a cocaine infusion with an FR3 schedule of reinforcement.

3.5 Discussion

We reported previously that $GABA_BR$-GIRK signaling was diminished in VTA DA neurons, but not in VTA GABA neurons, from $GIRK2_{DA}KO$ mice (Kotecki et al., 2015). Here we show that autoreceptor-mediated signaling is also diminished in $GIRK2_{DA}KO$ mice, while baseline measures of neuronal excitability are unchanged. Thus the $GIRK2_{DA}KO$ mouse is a selective model of decreased inhibitory feedback (both $GABA_BR$ and autoreceptor mediated) to DA neurons. Behavioral analysis of these mice revealed the critical influence of inhibitory feedback to DA neurons in both non-contingent (locomotor activity) and response-contingent (self-administration) cocaine-related behaviors.

3.5.1 GIRK-dependent inhibitory feedback and cocaine-induced locomotor activity

$GIRK2_{DA}KO$ mice, similar to constitutive *Girk2*$^{-/-}$ mice (Arora et al., 2010), are more sensitive to the locomotor-stimulatory effect of cocaine. This unconditioned behavioral response to cocaine is DA dependent and tempered by $GABA_BR$- and autoreceptor-mediated inhibitory feedback to VTA DA neurons. Indeed, cocaine-induced locomotor activity was enhanced by intra-VTA infusion of pertussis toxin (Steketee and Kalivas, 1991), which inhibits the G proteins that mediate $GABA_BR$ and autoreceptor-dependent signaling. In addition, intra-VTA infusion of the $GABA_BR$ agonist baclofen or the $D_{2/3}R$-antagonist sulpiride blocked and potentiated, respectively, the locomotor-stimulatory effect of cocaine (Steketee and Kalivas, 1991; Chen and Reith, 1994). In terms of cocaine-induced locomotor activity, $GIRK2_{DA}KO$ mice behave comparably to mice lacking D_2R in DA neurons (Bello et al., 2011). RNAi-dependent suppression of D_2R in VTA in rats also yielded enhanced cocaine-induced locomotor activity (de Jong et

al., 2015). As GIRK2-containing channels mediate most of the direct inhibitory effect of $GABA_BR$ and autoreceptor activation on VTA DA neurons (Beckstead et al., 2004; Cruz et al., 2004), these behavioral insights highlight the key influence of the GIRK component of the inhibitory G protein-mediated feedback pathways on acute cocaine-induced locomotor stimulation. Our data further show that while GIRK-dependent signaling in DA neurons is not required for the development of locomotor sensitization, they do provide an opposing influence on this addiction-related phenomenon.

3.5.2 GIRK-dependent inhibitory feedback and cocaine reinforcement

Although available evidence shows that inhibitory G protein-dependent feedback to VTA DA neurons modulates the reinforcing effect of cocaine, the nature of this influence differs across studies. For example, we show here that $GIRK2_{DA}KO$ mice display normal acquisition of cocaine-induced self-administration but an overall higher intake of cocaine and, specifically, enhanced responding when presented with low cocaine doses per infusion. Constitutive *Girk2*$^{-/-}$ mice were also able to acquire cocaine self-administration but displayed decreased responding at lower cocaine doses (Morgan et al., 2003). The divergent phenotypes of constitutive *Girk2*$^{-/-}$ and $GIRK2_{DA}KO$ mice are likely attributable to widespread deficits in GIRK-dependent signaling and alterations in both excitatory and inhibitory ionotropic neurotransmission in the former model (Luján et al., 2014). Interestingly, $GIRK2_{DA}WT$ and $GIRK2_{DA}KO$ mice exhibited different responding for cocaine at a dose (0.3 mg/kg/infusion) comparable to that used during training, wherein no genotype difference was detected. This may reflect an impact of the order of cocaine dose presentation on self-administration behavior or a manifestation of differential adaptations triggered by cumulative cocaine exposure between the groups.

$GIRK2_{DA}KO$ mice also differ from other genetic models of autoreceptor ablation in terms of cocaine reinforcement. For example, the RNAi-mediated suppression of D_2R

in the rat VTA enhanced motivation to work for cocaine as assessed using progressive ratio scheduling, whereas not altering acquisition of cocaine self-administration or fixed ratio responding (de Jong et al., 2015). Moreover, mice lacking D_2R in DA neurons acquired cocaine self-administration more quickly than control subjects, while other parameters, including intake, motivation, and sensitivity, were normal (Holroyd et al., 2015). Interestingly, these mice also exhibited enhanced cocaine CPP at low doses (Bello et al., 2011), whereas we detected no CPP phenotype in $GIRK2_{DA}KO$ mice. Apparent behavioral discrepancies across these genetic models could reflect procedural and/or species differences or point to the overlapping but distinct impact of the genetic lesions. With respect to the latter point, it is noteworthy that $GIRK2_{DA}KO$ mice exhibit deficits in both $GABA_BR$- and autoreceptor-mediated inhibitory feedback to DA neurons. $GABA_BR$ activation in the VTA decreases cocaine self-administration in rats (Brebner et al., 2000; Backes and Hemby, 2008), suggesting that $GABA_BR$-GIRK signaling in VTA DA neurons may also influence sensitivity to cocaine in a response-contingent procedure. In addition, whereas GIRK channels contribute to the somatodendritic inhibitory impact of autoreceptor activation on VTA DA neurons, D_2R are also expressed on axon terminals of DA neurons in terminal regions where they can modulate neurotransmitter release (Sesack et al., 1994). Finally, the residual quinpirole-induced current seen in VTA DA neurons from $GIRK2_{DA}KO$ mice shows that the inhibitory influence of autoreceptor activation on these neurons is mediated by multiple effectors.

Notably, our self-administration studies involving $GIRK2_{DA}KO$ mice did not attempt to dissociate motivation to gain access to cocaine from intake, and thus we cannot speak of the potential impact of GIRK ablation in DA neurons on motivation separate from intake. Furthermore, it is important to note that increased levels of responding may reflect a decreased sensitivity to the reinforcing effect of the drug. Given

that GIRK2$_{DA}$KO mice exhibit increased sensitivity to the locomotor-stimulatory effect of cocaine, however, our current working hypothesis is that GIRK2$_{DA}$KO mice are more sensitive to cocaine.

3.5.3 The unique GIRK channel in VTA DA neurons

The VTA DA neuron GIRK channel (GIRK2/GIRK3) is unique, as most neuronal GIRK channels contain GIRK1 (Cruz et al., 2004; Koyrakh et al., 2005; Labouèbe et al., 2007). Interestingly, *Girk2* ablation yields a complete loss of VTA DA neuron GIRK channel activity (Beckstead et al., 2004; Cruz et al., 2004), whereas *Girk3* ablation yields increased sensitivity of the residual channel (GIRK2 homomer) to receptor activation (Labouèbe et al., 2007; Lunn et al., 2007). The opposing contributions of GIRK2 and GIRK3 are also sensed at the behavioral level, where loss of GIRK2 in DA neurons correlates with increased locomotor effects of cocaine and morphine, while constitutive *Girk3* ablation correlates with decreased locomotor-stimulatory effect of morphine (Arora et al., 2010; Kotecki et al., 2015). The GIRK channel in VTA DA neurons undergoes activity-dependent bidirectional modulation; burst firing increases GIRK-dependent signaling in VTA DA neurons, whereas tonic firing suppresses channel activity (Lalive et al., 2014). The latter phenomenon is reminiscent of the cocaine-induced suppression of GIRK-dependent signaling in VTA DA neurons, attributable to a subcellular redistribution of GIRK2-containing channels (Arora et al., 2011). The plasticity of GIRK channels provides a plausible explanation for how experience could impact the sensitivity of the mesocorticolimbic system to subsequent experiences, drug or otherwise.

3.6 Concluding remarks

The unique subunit composition of the VTA DA neuron GIRK channel, and its importance in modulating sensitivity to cocaine and other drugs of abuse, suggests that direct modulation of this target could be useful for treating aspects of addiction. Indeed, $GABA_BR$ activation reduced self-administration and addiction-related behaviors linked to cocaine and other drugs of abuse in rodents (Brebner et al., 2000; Xi and Stein, 2000; Ranaldi and Poeggel, 2002; Leite-Morris et al., 2004; Liang et al., 2006; Filip et al., 2007). As most GIRK channels contain GIRK1, a GIRK2/GIRK3-selective activator should selectively enhance GIRK-dependent signaling in VTA DA neurons. Although GIRK2/GIRK3 channel activators have not yet been reported, the development of potent modulators of GIRK1-containing GIRK channels suggests that other channel subtype-selective modulators will be forthcoming (Kaufmann et al., 2013; Wydeven et al., 2014).

3.7 Funding and disclosure

This work was supported by National Institute of Health grants to NMM (DA007234 and DA041767), LK (DA007097), MJB (DA032701), and KW (DA034696 and MH061933). The authors declare no conflict of interest.

3.8 Acknowledgments

We thank Zhilian Xia for exceptional care of the mouse colony at the University of Minnesota and Dr. Ramaswamy Sharma for genotyping mice bred in San Antonio.

Chapter 4

Chemogenetic activation of inhibitory G protein signaling in VTA DA neurons decreases neuronal excitability and locomotor behavior

4.1 Introduction

GIRK channel activity in VTA DA neurons tempers behavioral sensitivity to morphine and cocaine (Kotecki et al., 2015; McCall et al., 2017) (**Chapter 1 and Chapter 3**), and exposure to cocaine decreases in GIRK channel activity in VTA DA neurons (Arora et al., 2011). These observations support the hypothesis that the strength of GIRK channel activity in VTA DA neurons is inversely related to behavioral sensitivity to drugs of abuse. A prediction of this hypothesis is that generally increasing inhibitory G protein signaling, which is mediated in part by GIRK channels, in VTA DA neurons will result in decreased behavioral sensitivity to cocaine and morphine. In the chapter, I tested this prediction using a chemogenetic approach to inhibit VTA DA neurons prior to cocaine- or morphine-enhanced locomotion. I employed inhibitory hM4Di designer receptors exclusively activated by designer drugs (DREADDs), which are based upon the muscarinic 4 receptor. The activity of DREADDs is mediated in part by GIRK channels (Armbruster et al., 2007), though inhibitory hM4Di DREADDs function in brain regions that generally lack GIRK channels, such as the striatum (Karschin et al., 1996; Ferguson et al., 2011).

In this chapter, I assessed the ability of on-demand inhibitory G protein signaling in VTA DA neurons to mitigate the behavioral effects of drugs of abuse. I predicted that engaging inhibitory G protein signaling in VTA DA neurons would decrease the locomotor behavioral response to cocaine and morphine. I also assessed the GIRK channel contribution to the inhibitory effect of hM4Di DREADDs in VTA DA neurons. I found the activation of inhibitory hM4Di DREADDs in VTA DA neurons elicits an outward current mediated in part by GIRK channels. Interestingly, I also found engaging hM4Di DREADDs in VTA DA neurons causes a profound, general decrease in locomotor activity.

4.2 Methods

4.2.1 Animals

All studies were approved by the Institutional Animal Care and Use Committee at the University of Minnesota. B6.SJL-*Slc6a3*$^{tm1.1(cre)Bkmn}$/J (stock #006660, The Jackson Laboratory), hereafter referred to as DATCre(+) mice, heterozygous for Cre, were used in all viral manipulation studies. This DATCre line has been extensively used for the selective viral manipulation of DA neurons, offers improved dopaminergic targeting over other available DA neuron-targeting Cre lines, and does not alter DAT expression in heterozygotes(Bäckman et al., 2006; Lammel et al., 2015; Stuber et al., 2015). All mice for this study were bred in-house at the University of Minnesota. Male and female mice were used for all studies, with groups balanced by sex. Mice were maintained on a 12 h light/dark cycle, and were provided *ad libitum* access to food and water.

4.2.2 Reagents

Cocaine and morphine were obtained through Boynton Health Pharmacy at the University of Minnesota. 0.9% saline was purchased from Baxter Healthcare Corporation

(Deerfield, IL). Clozapine-N-oxide (CNO) was obtained from Tocris Bioscience (Bristol, UK). Barium chloride was obtained from Sigma-Aldrich (St. Louis, MO). In behavioral studies CNO was dissolved in saline and DMSO (Sigma-Aldrich; St. Louis, MO), for a final dose of 10 mg/kg in 1 mg/ml. All viruses were produced by the University of Minnesota Viral Vector and Cloning Core (Minneapolis, MN). AAV8-DIO-hSyn-hM4Di-mCherry was used to express hM4Di inhibitory DREADD in a Cre-dependent manner. A Cre-dependent virus expressing mCherry (AAV8-DIO-hSyn-mCherry) served as the control.

4.2.3 Intracranial viral manipulations

Mice (≥45 d) were placed in a stereotaxic frame (David Kopf Instruments; Tujunga, CA) under isoflurane anesthesia. Microinjectors, made by affixing a 33-gauge stainless steel hypodermic tube within a shorter 26-gauge stainless steel hypodermic tube, were attached to polyethylene-20 tubing affixed to 10 μL Hamilton syringes, and were lowered through burr holes in the skull to the VTA (from bregma: -2.6 mm A/P, ±0.6-0.7 mm M/L, -4.7 mm D/V). 500 nL (2.16×10^{13} – 3.26×10^{14} genocopies/mL) of virus per side was injected over 5 min. Microinjectors left in place for 10 min following infusion to reduce backflow along the infusion track. Immunohistochemistry, slice electrophysiology, and behavioral experiments were performed 3 weeks after surgery to allow for full recovery and viral expression.

4.2.4 Slice electrophysiology

Somatodendritic currents were evaluated in both behaviorally naïve mice (4 weeks following viral injection). Horizontal slices (225 μm) containing the VTA were prepared in ice-cold sucrose ACSF, as described (Kotecki et al., 2015; McCall et al., 2017). Neurons medial to the medial terminal nucleus of the accessory optic tract (MT) and identified via

the Cre-dependent viral-mediated fluorescence were targeted for analysis. Whole-cell data were acquired using a Multiclamp 700A amplifier and pCLAMPv.9.2 software (Molecular Devices; Sunnyvale, CA). I_h amplitude was assessed using a 1-s voltage ramp (-60 to -120 mV). Spontaneous activity was measured in current-clamp mode (I=0) for 1 min. For rheobase assessments, cells were held in current-clamp mode and given 1-s current pulses, beginning at -80 pA and progressing in 20 pA increments until spiking was elicited. Rheobase was defined as the minimum current step evoking one or more action potentials. CNO-induced somatodendritic currents were measured at a holding potential (V_{hold}) of -60 mV. For CNO rheobase measures, after an outward current was detected in voltage clamp, we returned to current clamp and ran the rheobase protocol again. All command potentials factored in a junction potential of -15 mV predicted using JPCalc software (Molecular Devices, LLC; Sunnyvale, CA). Series and membrane resistances were tracked throughout the experiment. If series resistance was unstable, the experiment was excluded from analysis.

4.2.5 Locomotor behavior

Locomotor activity was assessed in open field activity chambers (Med-Associates, St. Albans, VT), as described (Pravetoni and Wickman, 2008). In brief, subjects were acclimated over 3 d, during which the animals were handled on one day and exposed to i.p. injection (saline) on two days, and then placed in the open field. On the fourth (test) day, mice were injected with 2 mg/kg CNO, placed back in their home cage for 30 minutes, and then injected with saline, cocaine (15 mg/kg, i.p.), or morphine (10 mg/kg, i.p.). Distance traveled during the following 60 minute period was recorded.

4.2.6 Tissue processing

Viral targeting accuracy was assessed in all behavioral subjects using fluorescence microscopy following behavior. Brains were drop-fixed in 4% paraformaldehyde (PFA) in phosphate buffered saline (PBS). After fixing overnight, brains were placed in 10% sucrose in PBS for 24 h, followed by 30 % sucrose until tissue suck. Brains were sliced on a Thermo Scientific HM525 NX cryostat at 40 μm thickness. To assess and summarize the expression pattern and spread of virus, 2x images of bright field and fluorescent viral expression were taken with a IX81ZDC2 Olympus microscope, overlaid, and matched to the horizontal mouse brain atlas (Franklin and Paxinos, 2008). Only data from mice in which the majority (>80%) of expression was confined to the VTA, with limited or no diffusion to adjacent structures (*i.e.*, SN pars compacta), was included in the analysis of behavioral studies.

4.2.7 Statistical Analysis

Data are presented throughout as the mean ± SEM. Statistical analyses were performed using Prism 5 (GraphPad Software, La Jolla, CA). All studies involved balanced groups of male and female mice. Data were analyzed first for effects of sex and virus using two-way ANOVA. No sex differences were observed; therefore, male and female data were pooled. Pairwise comparisons were performed using t tests or Mann–Whitney *U* tests, one way ANOVA, or two way ANOVA, with Bonferroni *post-hoc* test, as appropriate. Differences were considered significant if $p < 0.05$.

4.3 Results

4.3.1 Chemogenetic-activated inhibitory G protein signaling in VTA DA neurons decreases neuronal excitability and is partially mediated by GIRK channels

My first goal was to use inhibitory hM4Di DREADDs to reduce VTA DA neuron excitability by engaging inhibitory G protein signaling. First, I wanted to confirm that GIRK channels mediated part of hM4Di DREADD inhibition in VTA DA neurons. To achieve this, I virally the VTA of DATCre(+) (Bäckman et al., 2006) or DATCre(+):*Girk2*$^{fl/fl}$ mice (Kotecki et al., 2015) with a Cre-dependent viruses expressing inhibitory hM4Di DREADDs or a control mCherry-expressing Cre-dependent virus in (**Figure 4.1A**). After allowing 4 weeks for recovery from surgery and viral expression, mice were prepared for brain slice electrophysiology (**Figure 4.1A**). I assessed the ability of inhibitory hM4Di DREADDs in VTA DA neurons to decrease excitability by assessing rheobase at baseline and following the bath application of the DREADD agonist clozapine-N-oxide (CNO; 10 μM). The bath application of CNO significantly increased the rheobase of DREADD-expressing VTA DA neurons in DATCre(+) mice (**Figure 4.1B**), confirming the ability of inhibitory DREADDs to inhibit DA neurons of the VTA.

I also assessed the contribution of GIRK channels to the inhibitory outward currents elicited by CNO. Bath application of CNO elicited outward currents that were reversed by the bath application of a low dose of Ba^{2+} (0.3 mM), a K^+ channel blocker (**Figure 4.1C, D**). This reversal by Ba^{2+} suggests that GIRK channels are involved in the inhibitory effect of DREADDs. To further assess the involvement of GIRK channels in mediating the inhibitory effect of hM4Di DREADDs, CNO currents were assessed in DA neurons lacking GIRK channels (*i.e.*, DATCre(+):*Girk2*$^{fl/fl}$ mice). The CNO current was

significantly smaller in mCherry+ VTA neurons in DATCre(+):*Girk2*$^{fl/fl}$ mice than in DATCre(+) mice (**Figure 4.1C, D,** dark purple), lending further support that GIRK channels contribute to the function of hM4Di DREADDs. Importantly, the bath application of CNO does not elicit significant outward currents in VTA DA neurons expressing a mCherry control viral construct (**Figure 4.1C, D,** light purple). This suggests the CNO-induced change in rheobase and outward currents are mediated by inhibitory hM4Di DREADDs rather than an "off target" effect of CNO. Baseline electrophysiological parameters were largely unaltered in our viral manipulations (**Table 4.1**). Overall, the inhibitory hM4Di DREADD decreases the excitability of VTA DA neurons partially GIRK-dependent manner.

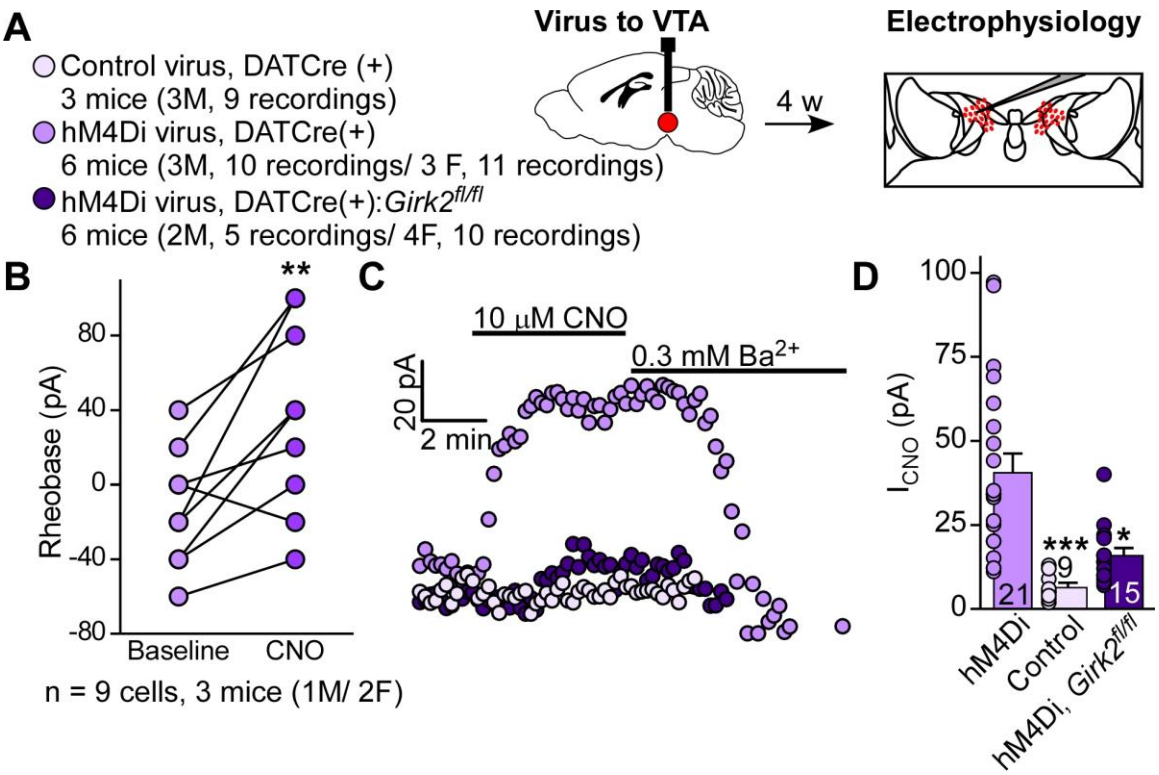

Figure 4.1. CNO inhibits VTA DA neurons expressing inhibitory DREADD viral construct and reduces locomotor behavior.

A) Schematic of electrophysiology study. **B**) CNO application increases rheobase in VTA DA neurons expressing inhibitory DREADD (n = 9 cells from 3 mice, 1M/2F; paired t test, t_8 = 3.55, p = 0.008). **C**) Representative somatodendritic CNO currents (10 μM) in DATCre(+) mice expressing control and DREADD viruses, and DATCre(+):*Girk2*$^{fl/fl}$ mice expressing DREADD virus. **D**) Summary of somatodentric CNO currents in hM4Di (n = 21 cells, 41 ± 6 pA), control (n = 9, 7 ± 1 pA), hM4Di in *Girk2*$^{fl/fl}$ (n = 15, 16 ± 2 pA) DATCre(+) mice (Kruskal-Wallis test, *K-W* = 24.8, p < 0.0001).

Table 4.1 Baseline electrophysiology parameters in VTA DA neurons expressing inhibitory hM4Di DREADD or control virus.
From data included in **Figure 4.1C, D**. Difference is from the DATCre(+)-hM4Di condition.

Condition	n	Cm (pF)	Rm (MΩ)	I_h (pA)	Rheobase (pA)	Active neurons	Freq (Hz)
DATCre(+) hM4Di	21	33 ± 3	507 ± 103	56 ± 19	-11 ± 6	14/21	3.85 ± 0.69
DATCre(+) Control	9	44 ± 5	181 ± 30	147 ± 43* t test t_{28} = 2.22 p = 0.03	-22 ± 14	8/9	2.51 ± 0.47
DATCre(+):*Girk2*$^{fl/fl}$ hM4Di	13	45 ± 5* t-test t_{32} = 2.32 p = 0.027	315 ± 85	103 ± 28	-6 ± 16	10/13	2.14 ± 0.36

4.3.2 Chemogenetic inhibition in VTA DA neurons decreases locomotor activity

The loss of GIRK channels from VTA DA neurons increased the behavioral locomotor response to cocaine (**Chapter 3**) (McCall et al., 2017) and morphine (**Chapter 1**) (Kotecki et al., 2015). Thus, I hypothesized that increasing inhibitory G protein signaling in VTA DA neurons using a chemogenetic approach would decrease behavioral sensitivity to these drugs. Control or hM4Di inhibitory DREADD Cre-dependent viruses were infused to the VTA of DATCre(+) mice (**Figure 4.2A**). On test day, all mice received CNO (2 mg/kg, i.p.) 30 minutes prior to an i.p. injection of saline, cocaine (15 mg/kg), or morphine (10 mg/kg). The activation of hM4Di inhibitory DREADD significantly reduced locomotor activity, whether following the injection of saline, cocaine, or morphine (**Figure 4.2B**).

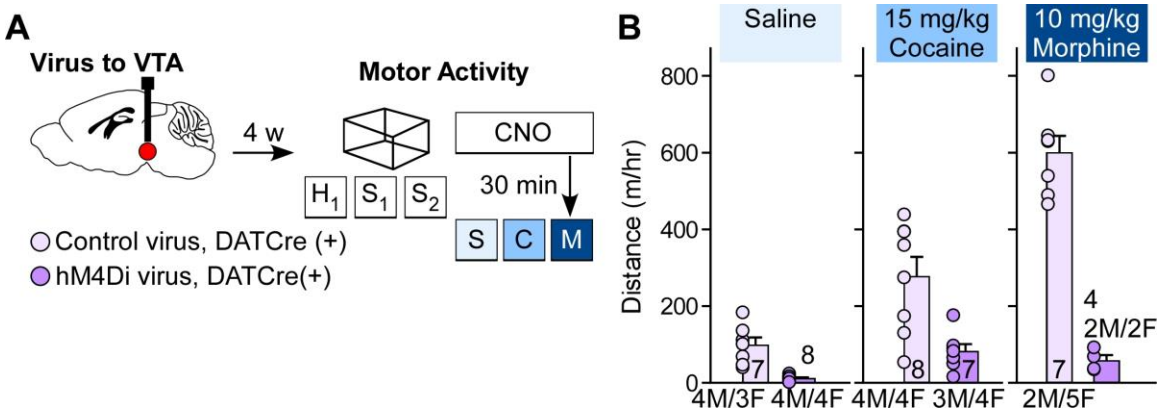

Figure 4.2. hM4Di inhibitory DREADD-mediated inhibition of VTA DA neurons reduces locomotion.

A) Schematic of behavioral study assessing the impact of inhibiting VTA DA neurons on drug-potentiated locomotor activity. **B**) 1h locomotor activity following saline (control, n = 7, 99 ± 19 m/h; hM4Di, n = 8, 12 ± 3 m/h), 15 mg/kg cocaine (control, n = 8, 278 ± 50 m/h; hM4Di, n = 7, 83 ± 19 m/h), or 10 mg/kg morphine (control, n = 7, 601 ± 43 m/h; hM4Di, n = 4, 59 ± 14 m/h) 30 min following an i.p. injection of 2 mg/kg CNO.

4.4 Discussion

The goal of this chapter was to test the hypothesis that the strength of inhibitory G protein signaling in VTA DA neurons is inversely related to a behavioral sensitivity to drugs of abuse. Inhibitory hM4Di DREADDs decreased the excitability of DA neurons in a partially GIRK-dependent manner. Interestingly, engaging inhibitory hM4Di DREADDs elicited a general decease in locomotor activity, rather than selectivity for cocaine or morphine. This suggests that inhibitory G protein signaling in VTA DA neurons contributes generally to locomotor activity, rather than specifically for sensitivity to drugs of abuse. Interestingly, another research group performed a very similar experiment using an AAV-hSyn-DIO-hM4Di-mCherry virus in adult male THCre(+) mice (Runegaard et al., 2018b), another mouse line commonly used to target DA neurons (Lammel et al., 2015; Stuber et al., 2015). This group also found that CNO alone decreased locomotor activity in the open similar to the present findings for the saline control group. This group attributes this finding to novelty-induced exploratory activity, rather than a general locomotor effect, as DA has been implicated in novelty-related behavior (Redgrave and Gurney, 2006). To reduce the confound of exploratory activity, Runegaard et al. allowed mice to habituate to the open field for 90 min prior to CNO and subsequent cocaine or saline administration (Runegaard et al., 2018b). With this approach, engaging inhibitory hM4Di DREADD in VTA DA neurons, and in NAc projecting DA neurons, was able to selectively decrease cocaine-induced locomotion (Runegaard et al., 2018b). While the mice in the present study were habituated to the locomotor chambers for 3 d in an attempt to remove the confound of novelty-induced exploratory activity, habituation to the chambers just prior to the administration of cocaine appears to be needed to fully dissociate this effect. Another possible explanation for the general locomotor effect is that the VTA was not selectively targeted enough. Indeed, a study targeting the VTA and

SN with a KOR-inspired DREADD (Vardy et al., 2015) found a decrease in locomotor activity (Marchant et al., 2016), similar to the present study. Because it is challenging to be entirely selective for the VTA, the locomotor results in the present study could be confounded by some expression of hM4Di inhibitory DREADD in the SN.

Intriguingly, chemogenetic activation of inhibitory G protein signaling in VTA DA neurons is able to reduce some, but not all, types of drug-related behavior. Engaging inhibitory hM4DI DREADDs does not prevent behavioral sensitization to cocaine, nor does it prevent cocaine CPP or alter preference for or free consumption of a sweetened milk reward (Runegaard et al., 2018b). Another study found that engaging inhibitory hM4Di DREADDs in VTA DA neurons caused male THCre(+) rats decreased motivation for cocaine and attenuated drug seeking induced by yohimbine, a chemical stand-in for stress, or cocaine (Mahler et al., 2018). Furthermore, inhibiting VTA DA neurons with hM4Di DREADDs blocks heroin self-administration (Corre et al., 2018).

Overall, the hypothesis tested in this chapter, that engaging inhibitory G protein signaling in VTA DA neurons decreases behavioral sensitivity to drugs of abuse, was not supported by the findings presented in this chapter, but is supported by similar work from other groups. This suggests that inhibitory G protein signaling in VTA DA neurons is important for tempering the early behavioral aspects of reward seeking, particularly those with a motor component. Thus, engaging inhibitory G protein signaling in VTA DA neurons through pharmacotherapy could be useful as a prophylactic approach for preventing addiction or for a treatment to reduce stress or drug exposure-induced relapse.

Author Contributions for Chapter 5

NM McCall	Nora McCall designed research, performed research, analyzed data, and wrote the paper.
E Marron Fernandez de Velasco	Ezequiel Marron Fernandez de Velasco designed research and produced all viral vectors as part of his work with the University of Minnesota Viral Vector and Cloning Core.
K Wickman	Kevin Wickman helped design research and edit the paper.

Conflict of interest
The authors declare no competing financial interests or conflicts of interest.

Acknowledgements
This work was supported by NIH grants to KW (DA034696) and NMM (DA041767). The authors thank Nicholas Carlblom, Hannah Oberle, Zhilian Xia, and JingYing Zhang for their care of the mouse colony, Dr. Megan Tipps for providing training in intracranial surgeries and discussing the manuscript, Dr. Yasushi Nakagawa for assistance with the immunohistochemistry studies, Nihan Gencerliler for helping with the design and initial testing of the GIRK3 expression vector, and Dr. Mark Sanders and Yung Kim of the University of Minnesota University Imaging Centers for microscopy support.

Author Contributions
NMM designed research, performed research, analyzed data, and wrote the paper. EM designed research and produced all viral vectors as part of his work with the University of Minnesota Viral Vector and Cloning Core. KW helped design research and edit the paper.

Chapter 5

GIRK channel activity in dopamine neurons of the ventral tegmental area bi-directionally regulates behavioral sensitivity to cocaine

Chapter 5 was submitted for review at The Journal of Neuroscience *on 11 December 2018 and accepted for publication 22 February 2019.*

Abstract

Dopamine (DA) neurons of the ventral tegmental area (VTA) have been widely implicated in the cellular and behavioral responses to drugs of abuse. Inhibitory G protein signaling mediated by $GABA_B$ receptors ($GABA_BRs$) and D_2 DA receptors (D_2Rs) regulates the excitability of VTA DA neurons, DA neurotransmission, and behaviors modulated by DA. Most of the somatodendritic inhibitory effect of $GABA_BR$ and D_2R activation on DA neurons reflects the activation of G protein-gated inwardly rectifying K^+ (GIRK) channels. Furthermore, GIRK-dependent signaling in VTA DA neurons can be weakened by exposure to psychostimulants and strengthened by phasic DA neuron firing. The objective of this study was to determine how the strength of GIRK channel activity in VTA DA neurons influences sensitivity to cocaine. We employed a Cre-dependent viral strategy to overexpress the individual GIRK channel subunits in VTA DA neurons of male and female adult mice, leading to enhancement (GIRK2) or suppression (GIRK3) of GIRK channel activity. Overexpression of GIRK3 decreased somatodendritic $GABA_BR$- and D_2R-dependent signaling and increased cocaine-induced locomotor activity, while overexpression of GIRK2 increased $GABA_BR$-dependent signaling and decreased cocaine-induced locomotion. Neither manipulation impacted anxiety- or

depression-related behavior, despite the link between such behaviors and DA signaling. Together, these data show that behavioral sensitivity to cocaine in mice is inversely proportional to the strength of GIRK channel activity in VTA DA neurons and suggest that direct activators of the unique VTA DA neuron GIRK channel subtype (GIRK2/GIRK3 heteromer) could represent a promising therapeutic target for treatment of addiction.

Significance Statement

Inhibitory G protein signaling in dopamine (DA) neurons, including that mediated by G protein-gated inwardly rectifying K^+ (GIRK) channels, has been implicated in behavioral sensitivity to cocaine. Here, we used a viral approach to bi-directionally manipulate GIRK channel activity in DA neurons of the ventral tegmental area (VTA). We found that decreasing GIRK channel activity in VTA DA neurons increased behavioral sensitivity to cocaine, while increasing GIRK channel activity decreased behavioral sensitivity to cocaine. These manipulations did not alter anxiety- or depression-related behaviors. These data highlight the unique GIRK channel subtype in VTA DA neurons as a possible therapeutic target for addiction.

5.1 Introduction

Dopamine (DA) neurons of the ventral tegmental area (VTA) are an integral part of the mesocorticolimbic system, a network of brain regions that mediates behavioral responses to reward and drugs of abuse, including cocaine (Juarez and Han, 2016). Cocaine inhibits membrane monoamine transporters, including the dopamine transporter (DAT) (Rocha, 2003; Hall et al., 2004). As a result, cocaine increases DA levels in brain regions receiving dopaminergic projections (*e.g.*, nucleus accumbens/NAc), and locally within the VTA (Di Chiara and Imperato, 1988; Aragona et al., 2008). Cocaine exposure engages inhibitory G protein signaling in VTA DA neurons, including that mediated by somatodendritic D_2 DA autoreceptors (D_2Rs) and $GABA_B$R receptors ($GABA_B$Rs). Elevated VTA DA levels stimulate D_2Rs (Brodie and Dunwiddie, 1990; Ford, 2014), while GABAergic inputs activate $GABA_B$Rs on VTA DA neurons (Edwards et al., 2017). The direct inhibitory effect of D_2R and $GABA_B$R activation on VTA DA neurons is mediated largely by activation of G protein-gated inwardly rectifying K^+ (GIRK/Kir3) channels (Cruz et al., 2004; Labouèbe et al., 2007; Arora et al., 2010). While most neuronal GIRK channels contain GIRK1 and GIRK2 subunits (Luján et al., 2014), VTA DA neurons express a GIRK2/GIRK3 heteromeric channel (Cruz et al., 2004).

Work with knockout mice suggests that behavioral sensitivity to cocaine is inversely proportional to the strength of GIRK-dependent signaling in DA neurons. *Girk2*$^{-/-}$ mice exhibit increased locomotor responses to cocaine and morphine (Arora et al., 2010; Kotecki et al., 2015) and altered cocaine self-administration (Morgan et al., 2003), as do mice lacking GIRK channels in DA neurons (DATCre(+):*Girk2*$^{fl/fl}$ mice) (Kotecki et al., 2015; McCall et al., 2017). However, *Girk2*$^{-/-}$ mice exhibit an array of other behavioral phenotypes (Signorini et al., 1997; Blednov et al., 2001, 2003; Marker et al., 2004, 2005; Costa et al., 2005; Pravetoni and Wickman, 2008), as well as adaptations in

excitatory and inhibitory neurotransmission in multiple reward-associated neuron populations (Arora et al., 2010; Hearing et al., 2013), making it challenging to attribute changes in cocaine-related behavior to a specific population. While DATCre(+):*Girk2*$^{fl/fl}$ mice afford increased cell specificity over *Girk2*$^{-/-}$ mice, GIRK-dependent signaling in all DA neurons, including those in the VTA, substantia nigra, and hypothalamus (Meister and Elde, 1993; Lorang et al., 1994; DeMaria et al., 2000), is likely altered in this model.

Suppression of inhibitory G protein signaling in the VTA by pertussis toxin enhances the behavioral effects of cocaine (Steketee and Kalivas, 1991), suggesting that this signaling tempers behavioral sensitivity to cocaine. Notably, GIRK-dependent signaling in VTA DA neurons following psychostimulant exposure is decreased through channel internalization (Arora et al., 2011; Munoz et al., 2016). The strength of GIRK channel activity in VTA DA neurons is also modulated by neuronal excitability, with large depolarization events (*e.g.*, phasic DA neuron firing) potentiating GIRK-dependent signaling, and hyperpolarization or tonic DA neuron firing reducing GIRK-dependent signaling (Lalive et al., 2014). These observations converge on a working model wherein *in vivo* psychostimulant exposure inhibits DA neurons via $GABA_BR$ and D_2R activation, leading to decreased strength of inhibitory G protein signaling mediated by GIRK channel activation and, consequently, increased behavioral sensitivity to cocaine (Hearing et al., 2012; Marron Fernandez de Velasco et al., 2015b; Rifkin et al., 2017).

Here, we used viral and genetic approaches to determine how the strength of GIRK channel activity in VTA DA neurons influences behavioral sensitivity to cocaine in mice. Since VTA DA neurons project to a number of brain regions implicated in anxiety and depression, including the hippocampus, amygdala, and prefrontal cortex, and activation of DA receptors in these brain regions influences anxiety- and depression-like behaviors (Zarrindast and Khakpai, 2015; Belujon and Grace, 2017), we also asked

whether manipulation of GIRK channel activity in VTA DA neurons impacted negative affective behavior. We found that while anxiety and depression-related behaviors were unaltered by our manipulations, behavioral sensitivity to cocaine was inversely related to the strength of GIRK-dependent signaling in VTA DA neurons.

5.2 Materials and Methods

5.2.1 Mice

All studies were approved by the Institutional Animal Care and Use Committee at the University of Minnesota. B6.SJL-*Slc6a3*$^{tm1.1(cre)Bkmn}$/J (stock #006660, The Jackson Laboratory, RRID:IMSR_JAX:006660), hereafter referred to as DATCre(+) mice, heterozygous for Cre, were used in all viral manipulation studies. This DATCre line has been widely used for the selective viral manipulation of DA neurons, offers improved selective targeting of dopaminergic over other available DA neuron-targeting Cre lines, and does not exhibit altered DAT expression in heterozygotes (Bäckman et al., 2006; Lammel et al., 2015; Stuber et al., 2015). The generation of DATCre:*Girk2*$^{fl/fl}$ mice was described previously (Kotecki et al., 2015). All mice for this study were bred in-house. Male and female mice were used for all studies, with groups balanced by sex. All mice were maintained on a 12 h light/dark cycle, and were provided *ad libitum* access to food and water.

5.2.2 Reagents

Baclofen, CGP54626, quinpirole, sulpiride, triton-X, and DPX were purchased from Sigma (St. Louis, MO). Cocaine was obtained through Boynton Health Pharmacy at the University of Minnesota. Saline (0.9%) was purchased from Baxter Healthcare Corporation (Deerfield, IL). Normal donkey serum was purchased from Gemini Bio-Products (West Sacramento, CA). The anti-tyrosine hydroxylase antibody, made in

sheep was purchased from PelFreez (Cat# P60101-0, RRID:AB_461070) and the anti-GFP antibody, made in chicken, was purchased from abcam (Cat# ab13970, RRID:AB_300798). Donkey anti-sheep Cy5 (Cat# 703-225-155, RRID:AB_2340370) and donkey anti-chicken Cy2 (Cat# 713-175-147, RRID:AB_2340730) secondary antibodies were purchased from Jackson ImmunoResearch. All viruses were produced by the University of Minnesota Viral Vector and Cloning Core (Minneapolis, MN). AAV8-DIO-hSyn-GIRK2c-IRES-GFP and AAV8-DIO-hSyn-GIRK3-IRES-GFP vectors were used to overexpress GIRK2 and GIRK3, respectively, in a Cre-dependent manner. Cre-dependent viruses expressing GFP (AAV8-DIO-hSyn-GFP) or mCherry (AAV8-DIO-hSyn-mCherry) served as controls.

5.2.3 Intracranial viral manipulations

Mice (≥45 d) were placed in a stereotaxic frame (David Kopf Instruments; Tujunga, CA) under isoflurane anesthesia. Microinjectors, made by affixing a 33-gauge stainless steel hypodermic tube within a shorter 26-gauge stainless steel hypodermic tube, were attached to polyethylene-20 tubing affixed to 10 μL Hamilton syringes, and were lowered through burr holes in the skull to the VTA (from bregma: -2.6 mm A/P, ±0.6-0.7 mm M/L, -4.7 mm D/V); 500 nL (2.16×10^{13} – 3.26×10^{14} genocopies/mL) of virus per side was injected over 5 min. Microinjectors were left in place for 10 min following infusion to reduce solution backflow along the infusion track. Immunohistochemistry, slice electrophysiology, and behavioral experiments were performed 3 wk after surgery to allow for full recovery and viral expression.

5.2.4 Immunohistochemistry

Mice were anesthetized with ketamine/xylazine and transcardially perfused with phosphate buffer (PB), followed by 4% PFA in 0.1M PB. Brains were extracted and post-

fixed overnight in 4% PFA in PB at 4˚C. Brains were then rinsed with PB and transferred to 30% sucrose in PB. Horizontal slices of VTA (50 μm) were prepared using a sliding microtome (Leica SM 2000R) and stored in PB at 4˚C. Three slices, separated by ~350 μm, were stained for each mouse; 3 separate mice per viral condition were analyzed. All steps were performed at room temperature, with free-floating slices, in a 24-well plate on a rocker. Slices were rinsed in phosphate buffered saline (PBS; 3x10 min) and incubated in blocking solution (0.3% triton-X and 3% normal donkey serum in PBS) for 2 h. Slices were then incubated overnight in blocking solution containing a sheep anti-tyrosine hydroxylase antibody (1:500) and chicken anti-GFP antibody (1:500). Slides were rinsed with PBS (3x10 min) and then incubated in secondary antibodies diluted in PBS (1:500 donkey anti-sheep Cy5; 1:200 donkey anti-chicken Cy2) for 2 h, after which slices were rinsed with PBS (6x10 min). Slices were mounted on glass slides and allowed to fully dry before being dehydrated with 3 min incubations in: 70% EtOH, 80% EtOH, 95% EtOH, 100% EtOH, and xylene. Slides were mounted using DPX and allowed to dry. Slides were imaged by the University Imaging Center at the University of Minnesota on a Nikon A1R confocal microscope (Nikon USA, Melville, NY) imaged with the galvano scanner using 488 nm and 567 nm lines and filters. The images were collected using a 10x, 0.45na plan apo objective at 1024x1024 pixels, with a zoom of 1x using the Scan Large Area feature utilizing Perfect Focus. Four 15-μm z-steps were collected and images were generated in Nikon Nis-Elements AR (Nikon USA, Melville, NY) using Extended Depth of Focus (EDF). To assess the fidelity and penetrance of the viruses, the Cy2 and Cy5 channels were merged using Fiji (imagej.nih.gov), with Cy2 as green and Cy5 as magenta. In the region of viral expression with in the VTA, the number of Cy2+ neurons, Cy5+ neurons, and Cy2+/Cy5+ neurons were quantified using the cell counter plugin in

Fiji. Representative images in **Figure 5.1** were taken with an IX81ZDC2 Olympus microscope (Shinjuku, Tokyo, Japan) at 20x.

5.2.5 Slice electrophysiology

Somatodendritic currents were evaluated in both behaviorally naïve mice (3 wk following viral injection; 66-73 d), and at the conclusion of behavioral testing (5-6 wk following viral injection; 80-110 d). Horizontal slices (225 μm) containing the VTA were prepared in ice-cold sucrose ACSF, as described (Kotecki et al., 2015; McCall et al., 2017). Neurons medial to the medial terminal nucleus of the accessory optic tract (MT), and identified via Cre-dependent viral-mediated fluorescence, were targeted for analysis. Whole-cell data were acquired using a Multiclamp 700A amplifier and pCLAMPv.9.2 software (Molecular Devices; Sunnyvale, CA). I_h amplitude was assessed using a 1-s voltage ramp (-60 to -120 mV). Spontaneous activity was measured in current-clamp mode (I=0) for 1 min. For rheobase assessments, cells were held in current-clamp mode and given 1-s current pulses, beginning at -80 pA and progressing in 20 pA increments until spiking was elicited. Rheobase was defined as the minimum current step evoking one or more action potentials. Agonist-induced somatodendritic currents were measured at a holding potential (V_{hold}) of -60 mV. All command potentials factored in a junction potential of -15 mV predicted using JPCalc software (Molecular Devices, LLC; Sunnyvale, CA). Series and membrane resistances were tracked throughout the experiment. If series resistance was unstable, the experiment was excluded from analysis.

5.2.6 Behavior

All mice in this study were evaluated in elevated plus maze (EPM), forced swim test (FST), and open field cocaine-induced locomotor activity assays in the light cycle, in this order, with at least 1 d separating each test. For the EPM test, mice were transferred to the testing room 1 h prior to evaluation. Mice were placed in the middle of the maze, facing a corner between an open and closed arm. Video was recorded using ANY-Maze Maze 5.2 (Wood Dale, IL) software and a STC-TB83USB-AS camera (Sensor Technologies America, Inc; Carrollton, TX). Mice were allowed to freely explore the maze for 5 min. Between tests, the maze was wiped down with 70% EtOH. Time in arms, number of arm entries, and total distance traveled were analyzed using ANY-Maze software. For the FST study, mice were transferred to the testing room 1 h prior to evaluation. Mice were placed in a 4 L beaker filled with ~1.5 L of 23˚C water, for 6 min. Video was recorded using ANY-Maze software and a C615 camera (Logitech; Newark, NJ), and the latency to first immobile bout and total immobility time during the final 4 min of testing was analyzed by hand using ANY-Maze software. Cocaine-induced activity was assessed in open field activity chambers (Med-Associates, St. Albans, VT), as described (Pravetoni and Wickman, 2008). In brief, subjects were acclimated over 3 d, during which the animals were handled on one day and exposed to i.p. injection (saline) on two days, and then placed in the open field. Distance traveled during the 60-min period following saline injection on the last acclimation day was taken as baseline activity. Cocaine-induced activity was then assessed following administration of 3 cocaine doses (3, 15, and 30 mg/ kg i.p.), with each dose separated by 3 d, as described (Kotecki et al., 2015).

Viral targeting accuracy was assessed in all subjects using fluorescence microscopy prior to *post hoc* slice electrophysiology experiments. To assess and

summarize the expression pattern and spread of virus, 2x images of bright field and fluorescent viral expression were taken with a IX81ZDC2 Olympus microscope, overlaid, and matched to figures in the horizontal atlas of the mouse brain (Franklin and Paxinos, 2008), and spread patterns were summarized. The pattern of viral spread pattern for each mouse was overlaid on a simplified version of the atlas, with each spread pattern at 10% transparency to provide a sense of viral spread for individual subjects, and cumulatively for the study. Only data from mice in which the majority (>80%) of expression was confined to the VTA, with limited or no diffusion to adjacent structures (*i.e.*, SN pars compacta), were analyzed in behavioral studies.

5.2.7 Experimental design and statistical analyses

Data are presented throughout as the mean ± SEM. Statistical analyses were performed using Prism 5 (GraphPad Software, Inc.; La Jolla, CA) and SigmaPlot 11.0 (Systat Software, Inc.; San Jose, CA). All studies involved balanced groups of male and female mice. Data were analyzed first for effects of sex and viral condition, or sex and genotype, using two-way ANOVA when those were the only variables. For cocaine locomotor activity data with multiple testing days, the interaction of sex for each virus or genotype group was assessed using two-way repeated measure ANOVA. When there was no effect of sex, male and female data were pooled. When there was an effect of sex or an interaction of sex with another factor, male and female data were analyzed and presented separately. Data were analyzed by t test, Mann-Whitney *U* test, two-way ANOVA, or repeated measures ANOVA, with Bonferroni or *post hoc* tests, as appropriate. Differences were considered significant if $p < 0.05$.

5.3 Results

5.3.1 Viral manipulation of GIRK channel activity in VTA DA neurons

To manipulate the strength of GIRK channel activity in VTA DA neurons, we employed a Cre-dependent viral strategy to overexpress GIRK2 or GIRK3 in adult DATCre(+) mice. We predicted that the overexpression of GIRK2 in VTA DA neurons would enhance GIRK channel activity, as GIRK2 can form functional homomeric channels and it mediates the forward trafficking of GIRK channels (Lesage et al., 1995; Ma et al., 2002). Conversely, we predicted that the overexpression of GIRK3 would suppress GIRK channel activity, as GIRK3 is unable to form functional homomeric channels, it harbors a lysosomal targeting sequence that can promote GIRK channel internalization, and its presence correlates with decreased sensitivity of the VTA DA GIRK channel to $GABA_BR$-induced activation (Labouèbe et al., 2007; Lesage et al., 1995; Ma et al., 2002; Lunn et al., 2007).

We infused Cre-dependent control, GIRK2, or GIRK3 expression vectors into the VTA of DATCre(+) mice (**Figure 5.1A**). Following viral infusion (3 wk), we performed immunohistochemistry with horizontal sections containing the VTA, to assess the fidelity of our viral manipulations (**Figure 5.1B-E**). Similar to published reports involving DATCre(+) mice (Lammel et al., 2015), we found that the vast majority of GFP-positive neurons examined in slices from mice treated with control (96%), GIRK2 (93%), or GIRK3 (92%) vectors expressed tyrosine hydroxylase (TH+; **Figure 5.1C, D, E**). Moreover, 75% of TH+ neurons in the region of viral expression were also GFP+, as measured in sections from DATCre(+) mice treated with control vector. Thus, our approach yielded a selective manipulation of VTA DA neurons in adult mice.

To assess the functional consequences of overexpressing GIRK2 or GIRK3 in VTA DA neurons, we measured somatodendritic currents in acutely isolated brain slices evoked by a maximal concentration of the $GABA_BR$ agonist baclofen (200 μM), as GIRK channels mediate ~80% of this inhibitory current in VTA DA neurons (Labouèbe et al., 2007; Arora et al., 2010; Kotecki et al., 2015). As predicted, overexpression of GIRK2 in VTA DA neurons yielded enhanced $GABA_BR$-dependent currents, as compared with currents from control VTA DA neurons (**Figure 5.1F***)*. Overexpression of GIRK2 did not, however, yield significant differences in apparent capacitance, membrane resistance, I_h, or spontaneous activity (**Table 5.1**). There was a significant increase in rheobase (**Table 5.1**), however, suggesting that GIRK2 overexpression decreased baseline neuronal excitability. Conversely, GIRK3 overexpression in VTA DA neurons suppressed $GABA_BR$-dependent currents (**Figure 5.1G**). There were no significant differences in apparent capacitance, membrane resistance, I_h, rheobase, or spontaneous activity following GIRK3 overexpression (**Table 5.1**). Thus, the overexpression of GIRK2 or GIRK3 in VTA DA neurons bi-directionally alters the strength of GIRK-dependent signaling.

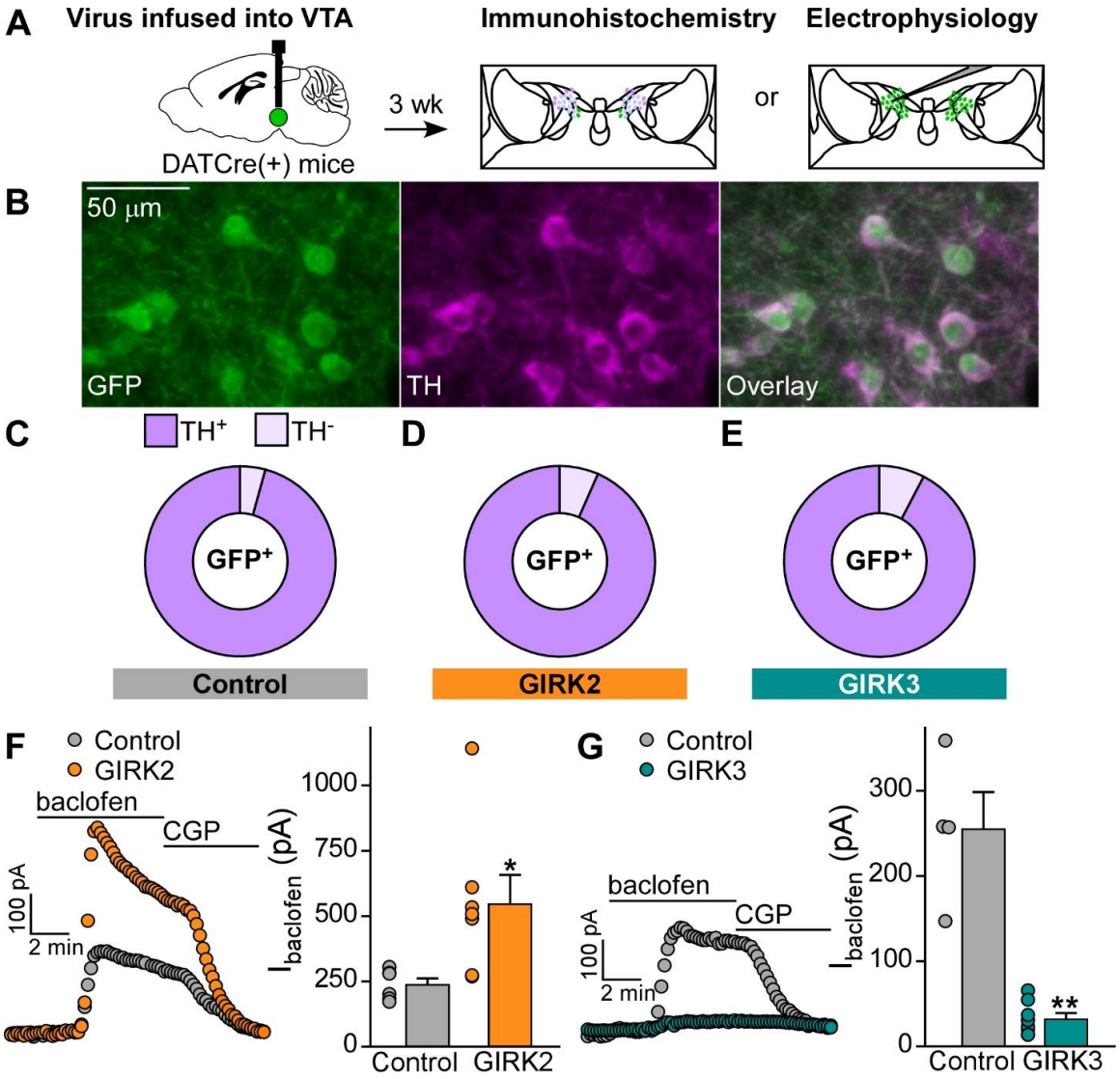

Figure 5.1. Viral overexpression of GIRK channel subunits in VTA DA neurons.

A) DATCre(+) mice were given intra-VTA infusion of Cre-dependent control, GIRK2, or GIRK3 vector. Following viral injection (3 w), mice were either processed for immunohistochemistry or slice electrophysiology. **B**) Control virus expression in the VTA of DATCre(+) mice. In the region of viral infusion, the percent of GFP+ neurons that were also dopaminergic (TH+) was calculated to determine viral fidelity in control (**C**), GIRK2 (**D**), and GIRK3 (**E**) viral conditions. **F**) The overexpression of GIRK2 (n = 7 cells from 3 mice, 547 + 111 pA) enhanced $GABA_BR$ currents compared with cells expressing a control virus (n = 6 cells from 2 mice, 238 ± 24 pA; Mann-Whitney U test, $U = 6$, $p = 0.035$). **G**) The overexpression of GIRK3 (n = 8 cells from 5 mice, 33 ± 7 pA) diminished $GABA_BR$ currents compared with cells expressing a control virus (n = 4 cells from 3 mice, 255 ± 44 pA; Mann-Whitney U test, $U = 0$, $p = 0.004$). *,** $p < 0.05, 0.01$.

Table 5.1. Baseline electrophysiological parameters for neurons in Figure 5.1.

	n	Cm (pF)	Rm (MΩ)	I_h (pA)	Rheobase (pA)	Active neurons	Frequency (Hz)
Control	6	47 ± 4	367 ± 70	99 ± 38	-27 ± 11	4/6	1.85 ± 0.51
GIRK2	7	48 ± 7	230 ± 55	32 ± 12	43 ± 22*****	4/7	1.17 ± 0.27
		t_{11} = 0.290	*t_{11} = 1.547*	*U = 12*	*t_{11}= 2.671*		*t_6 = 1.187*
		p = 0.778	*p = 0.150*	*p = 0.234*	*p = 0.022*		*p = 0.280*
Control	4	48 ± 1	243 ± 119	191 ± 85	-15 ± 25	4/4	2.12 ± 0.49
GIRK3	8	40 ± 6	383 ± 136	58 ± 13	-8 ± 14	7^+/8	2.40 ± 0.66
		U = 6.5	*t_{10} = 0.659*	*U = 7*	*t_{10} = 0.284*		*t_8 = 0.316*
		p = 0.125	*p = 0.523*	*p = 0.154*	*p = 0.783*		*p = 0.760*

$^+$One burst firing neuron was included in the count of neurons spontaneously active for the GIRK3 condition, but was not included in firing frequency analysis

**p* < 0.05.

5.3.2 Negative affective behaviors and cocaine sensitivity in DATCre:Girk2$^{fl/fl}$ mice

Previously, we reported that the genetic ablation of *Girk2* in DA neurons correlated with an increased acute locomotor response to cocaine (McCall et al., 2017). Intriguingly, the excitability of VTA DA neurons has also been shown to influence negative affective behavior (Anstrom and Woodward, 2005; Nestler and Carlezon, 2006; Krishnan et al., 2007; Cao et al., 2010; Chaudhury et al., 2013; Russo and Nestler, 2013; Tye et al., 2013; Polter and Kauer, 2014). Thus, we sought to assess how manipulation of GIRK channel activity in VTA DA neurons altered performance in anxiety (elevated plus maze/EPM), depression (forced swim test/FST), and cocaine-induced motor activity tests (**Figure 5.2A**). Because this behavioral battery approach had not been previously employed by our lab, we evaluated DATCre(+):*Girk2*$^{fl/fl}$ and DATCre(-):*Girk2*$^{fl/fl}$ mice before testing the impact of VTA DA neuron-specific GIRK channel manipulations.

DATCre(+):*Girk2*$^{fl/fl}$ mice exhibited similar percent time in open arms of the EPM as compared with DATCre(-):*Girk2*$^{fl/fl}$ mice (**Figure 5.2B**), and there were no genotype differences in percent time spent in closed arms (Cre-, 63 ± 3 %; Cre+, 59 ± 4 %, t test, t_{36} = 0.820, p = 0.418), number of entries into open arms (Cre-, 10 ± 1 entries; Cre+ 10 ± 1 entries, Mann-Whitney test, U = 150.5, p = 0.393), and number of entries into closed arms (Cre-, 11 ± 1 entries; Cre+, 11 ± 1 entries; t test, t_{36} = 0.7710, p = 0.446). Thus, loss of GIRK channel activity in DA neurons does not appear to influence anxiety-like behavior.

In the FST, we did not observe a difference in time immobile for DATCre(-):*Girk2*$^{fl/fl}$ mice and DATCre(+):*Girk2*$^{fl/fl}$ mice (**Figure 5.2C**). We did observe a main effect

of sex in the latency to immobility measure (ANOVA, $F_{1,34}$ = 12.67, p = 0.001), however, and as such, these data were analyzed separately by sex (**Figure 5.2D**). While female mice did not display an effect of genotype on latency to immobility (**Figure 5.2D**), male DATCre(+):*Girk2*$^{fl/fl}$ mice exhibited a longer latency than male DATCre(-):*Girk2*$^{fl/fl}$ mice, suggesting an anti-depressive behavioral phenotype. Notably, the reduced time to immobility in male DATCre(+):*Girk2*$^{fl/fl}$ mice (**Figure 5.2D**) is consistent with a previous report which found that male Cre+ mice from a separately developed DATCre:*Girk2*$^{fl/fl}$ mouse line displayed an anti-depressive behavioral phenotype (Honda et al., 2018). Thus, GIRK channel activity in DA neurons appears to enhance depression-related behavior in male mice.

Finally, we assessed cocaine-induced motor activity in DATCre(+):*Girk2*$^{fl/fl}$ mice (**Figure 5.2A, E**). Similar to our previous study (McCall et al., 2017), we observed a significant interaction of sex and cocaine dose in DATCre(+):*Girk2*$^{fl/fl}$ mice ($F_{3,54}$ = 4.133, p = 0.010); as such, males and females were analyzed separately. We did not observe a difference in total distance traveled by males on the first day (handling, H) of exposure to the open field (**Figure 5.2E**); however, female Cre+ mice traveled further than Cre- mice (**Figure 5.2E**), an observation that aligns with our previous report (McCall et al., 2017). This genotype difference in female mice is not observed on saline day 2 (S_2; 0 mg/kg cocaine in **Figure 5.2F**), suggesting the significant effect on handling day may be driven by a difference in exploration, rather than purely motor activity. Similar to our previous findings with acute cocaine administration (McCall et al., 2017), male and female DATCre(+):*Girk2*$^{fl/fl}$ mice exhibit increased locomotor activity at 15 mg/kg cocaine, and female Cre+ mice do not respond to 30 mg/kg cocaine as much as male Cre+ mice (**Figure 5.2F**). Overall, our findings support the hypothesis that reduced GIRK channel activity in DA neurons increases behavioral sensitivity to cocaine.

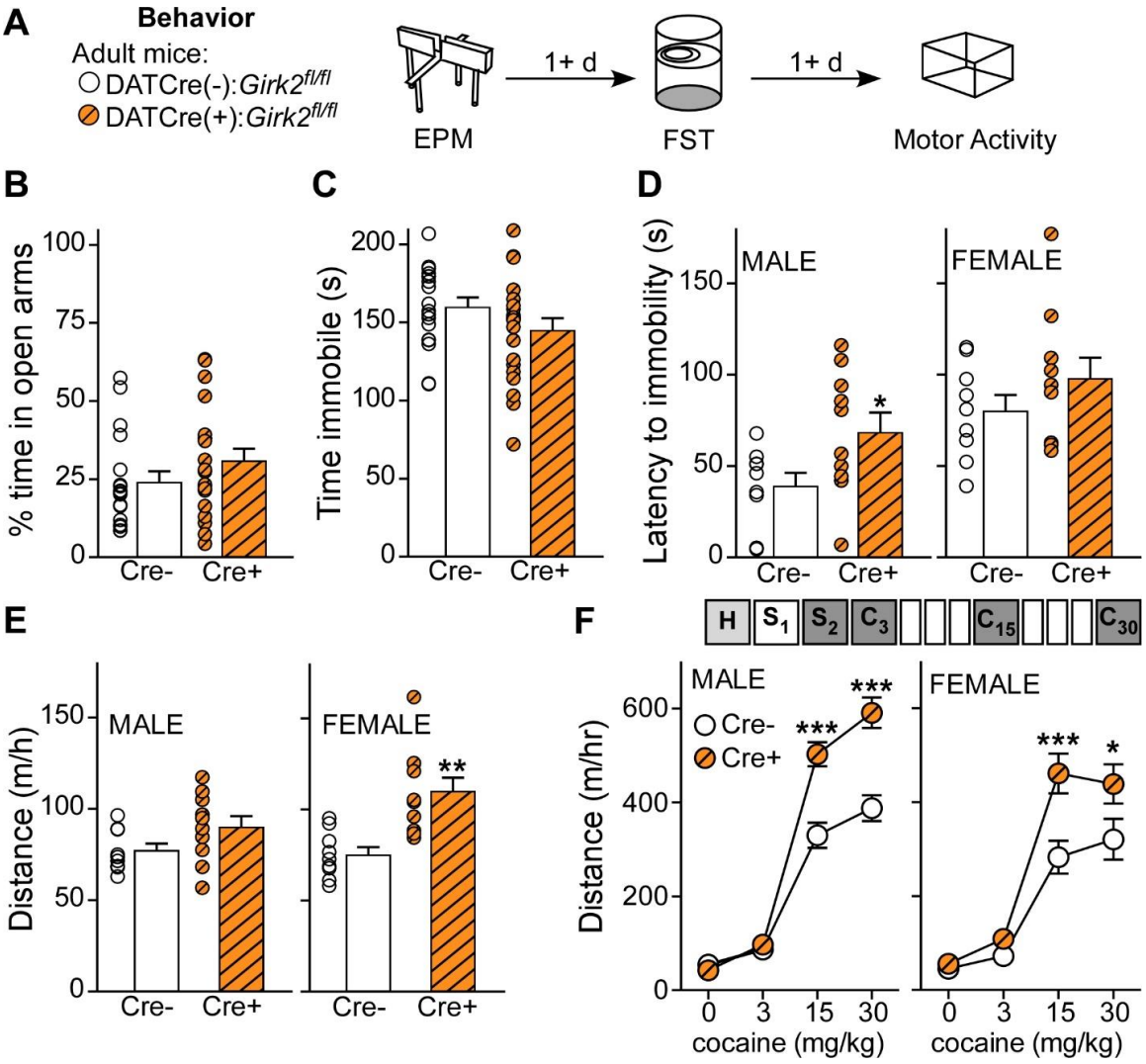

Figure 5.2. Negative affective and cocaine locomotor behavior in DATCre(+):*Girk2*$^{fl/fl}$ mice.

A) Adult male and female DATCre(-):Girk2$^{fl/fl}$ and DATCre(+):*Girk2*$^{fl/fl}$ mice were tested in EPM, FST, and cocaine locomotor activity tests, with each task separated by at least 1 d. **B**) Percent time in open arms in the EPM is not different in Cre- (n = 18, 24 ± 4 %) and Cre+ (n = 20, 31 ± 4 %; Mann-Whitney U test, U = 132, p = 0.165). **C**) Time immobile for Cre- (n = 18, 160 ± 6 s) and Cre+ (n= 20, 145 ± 8 s) mice in the FST does not differ (t test, t_{36} = 1.499, p = 0.143). **D**) Latency to immobility in male Cre+ (n = 10, 68 ± 11 s) mice is greater than in Cre- mice (n = 9, 39 ± 7 s; t test, t_{17} = 2.210, p = 0.041), while there is no difference in latency to immobility between Cre- (n = 9, 80 ± 9 s) and Cre+ (n = 10, 98 ± 11 s; t test, t_{17} = 1.213, p = 0.242) mice. **E**) There is no significant difference in distance moved on the handling habituation day between male Cre- (n = 9, 77 ± 4 m/h) and Cre+ (n = 10, 90 ± 6 m/h; t test, t_{17} = 1.774, p = 0.094) mice. However, female Cre+ mice (n = 10, 110 ± 8 m/h) moved significantly more than Cre- mice (n = 9, 75 ± 4m/h; t test, t_{17} = 3.876, p = 0.001). **F**) In male and female mice, distance traveled

following injection of 0, 3, 15, and 30 mg/kg cocaine resulted in an interaction between cocaine dose and genotype (males, two-way repeated measure ANOVA, interaction between cocaine dose and virus, $F_{3,51}$ = 13.557, p < 0.001; females, two-way repeated measure ANOVA, interaction between cocaine dose and virus, $F_{3,51}$ = 3.213, p = 0.030). Male Cre+ mice moved significantly more than Cre- mice at 15 mg/kg (Bonferroni post-hoc test, t = 5.863, p < 0.001) and 30 mg/kg (Bonferroni post-hoc test, t = 6.907, p < 0.001) cocaine. Similarly, female Cre+ mice moved significantly more than Cre- mice at 15 mg/kg (Bonferroni *post hoc* test, t = 4.249, p < 0.001) and 30 mg/kg (Bonferroni post-hoc test, t = 2.809, p = 0.006) cocaine. *,**,*** p < 0.05, 0.01, 0.001.

5.3.3 Reduced GIRK channel activity in VTA DA neurons increases cocaine sensitivity

Having recapitulated findings related to depression-like behavior (Honda et al., 2018) and cocaine sensitivity (McCall et al., 2017) for DATCre:*Girk2*$^{fl/fl}$ mice using this behavioral test battery, we next assessed the behavioral impact of viral suppression of GIRK channel activity in adult VTA DA neurons. To do this, we compared the behavioral performance of DATCre(+) mice treated with control or GIRK3 overexpression vectors (**Figure 5.3A**). No difference was detected between control and GIRK3 overexpression groups in percent time spent in open arms in the EPM (**Figure 5.3B**). Additionally, there was no difference in percent time spent in closed arms (control 53 ± 5 %; GIRK3 57 ± 3 %; Mann-Whitney test, $U = 109$, $p = 0.706$), number of entries into open arms (control 10 ± 1 entries; GIRK3 9 ± 1 entries; t test, $t_{29} = 0.711$, $p = 0.483$), or number of entries into closed arms (control 10 ± 1 entries; GIRK3 11 ± 1 entries; t test, $t_{29} = 0.367$, $p = 0.716$). Similarly, no group differences were observed in total immobility time (**Figure 5.3C**), or latency to immobility (control, 70 ± 8 s; GIRK3, 76 ± 10 s; t test, $t_{21} = 0.476$, $p = 0.639$) in the FST. No difference was observed in locomotor activity on the handling day or saline day 2 between control and GIRK3 overexpression conditions (**Figure 5.3D, E**). We did, however, observe a significant interaction between cocaine dose and viral treatment, with DATCre(+) mice treated with the GIRK3 virus exhibiting significantly enhanced locomotor activity at the 15 mg/kg cocaine dose (**Figure 5.3E**). Thus, viral suppression of GIRK channel activity in adult VTA DA neurons elicits a selective and dose-dependent enhancement of cocaine-induced motor activity, without impacting anxiety- or depression-like behaviors.

Following behavioral testing, mice were prepared for slice electrophysiological evaluation, and the extent of viral spread was summarized for control and GIRK3 overexpression conditions (**Figure 5.3F**). As we found in behaviorally naïve subjects (**Figure 5.1G**), $GABA_BR$-dependent somatodendritic currents were significantly smaller in fluorescent VTA neurons in the GIRK3 overexpression group, as compared with controls (**Figure 5.3G**). Similarly, somatodendritic currents evoked by a maximal concentration of the D_2R agonist quinpirole (20 μM) were significantly decreased in the GIRK3 overexpression group (**Figure 5.3H**). Thus, results from our initial viral validation and *post hoc* analysis suggest that GIRK3 overexpression suppresses GIRK channel activity evoked by $GABA_BR$ and D_2R in VTA DA neurons throughout the entire duration of behavioral testing.

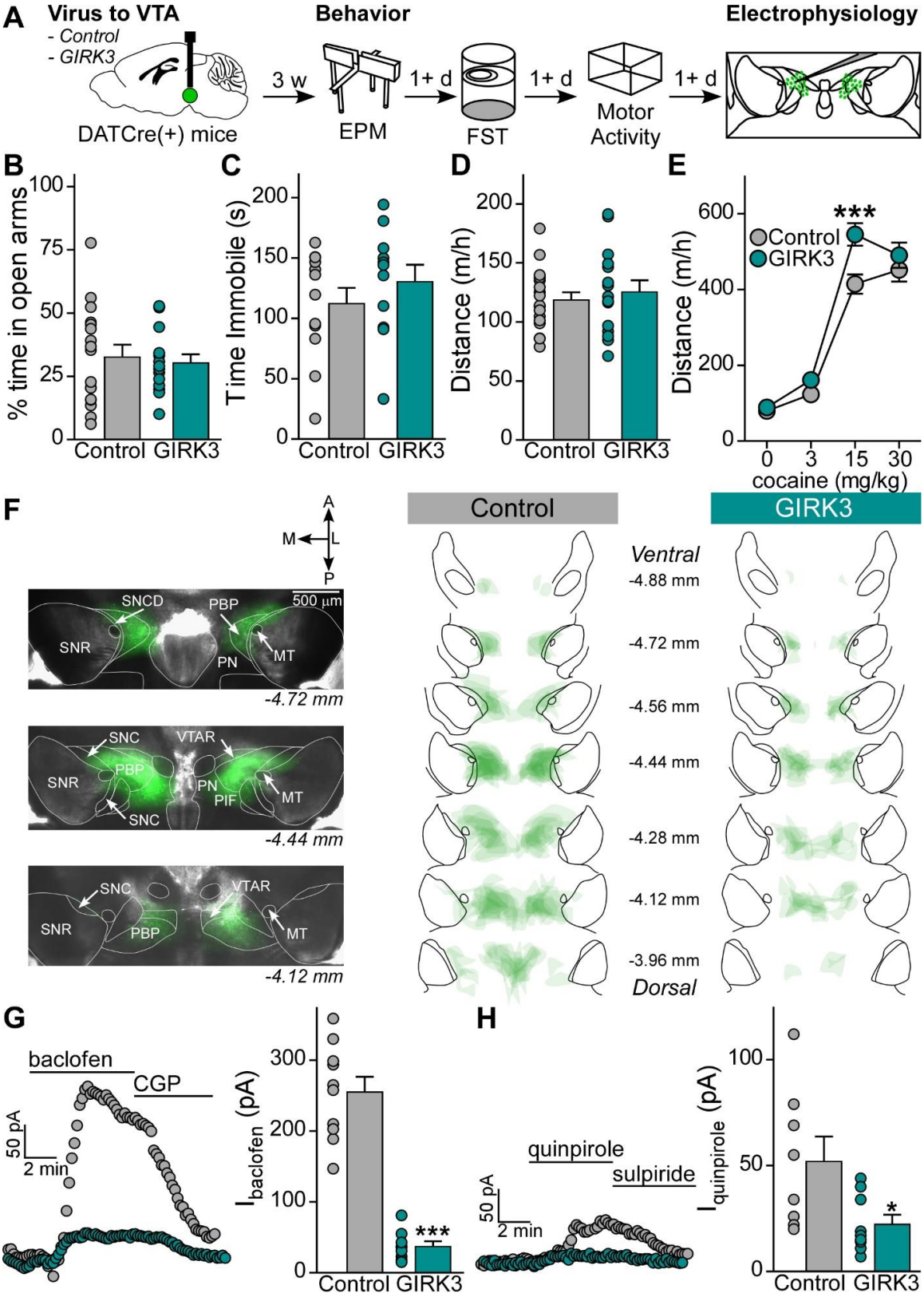
A
Virus to VTA
- Control
- GIRK3
DATCre(+) mice
3 w
Behavior
EPM
1+ d
FST
1+ d
Motor Activity
1+ d
Electrophysiology
B
% time in open arms
Control
GIRK3
C
Time Immobile (s)
D
Distance (m/h)
E
Distance (m/h)
***
Control
GIRK3
cocaine (mg/kg)
F
A
M
L
P
SNCD
PBP
500 µm
SNR
PN
MT
-4.72 mm
SNC
VTAR
PBP
SNR
PN
PIF
MT
SNC
-4.44 mm
SNC
VTAR
SNR
PBP
MT
-4.12 mm
Control
GIRK3
Ventral
-4.88 mm
-4.72 mm
-4.56 mm
-4.44 mm
-4.28 mm
-4.12 mm
-3.96 mm
Dorsal
G
baclofen
CGP
50 pA
2 min
I baclofen (pA)
***
Control
GIRK3
H
quinpirole
sulpiride
50 pA
2 min
I quinpirole (pA)
*
Control
GIRK3

Figure 5.3. Viral suppression of GIRK channel activity in VTA DA neurons increases behavioral sensitivity to cocaine.

A) DATCre(+) mice were injected with control or GIRK3 virus. Mice were tested for EPM, FST, and cocaine locomotor activity 3 wk after surgery, with each task separated by at least 1 d. Following behavior, mice were processed for placement and electrophysiology validation. **B**) EPM percent time in open arms is not different in control mice (n = 17, 33 ± 5 %) and GIRK3 mice (n = 14, 30 ± 3 %; t test, t_{29} = 0.396, p = 0.695). **C**) FST time immobile during the final 4 min of the task does not differ between control mice (n = 12, 112 ± 13 s) and GIRK3 mice (n = 11, 131 ± 14 s; t test, t_{21} = 0.957, p = 0.350). **D**) Distance moved on the handling habituation day was not different between control mice (n = 17, 119 ± 6 m/h) and GIRK3 (n = 15, 126 ± 9 m/h; t test, t_{30} = 0.630, p = 0.534). **E**) Distanced traveled following injection of 0, 3, 15, and 30 mg/kg cocaine resulted in interaction between cocaine dose and virus (two-way repeated measures ANOVA, $F_{3,90}$ = 3.438, p = 0.020; Bonferroni post-hoc test at 15 mg/kg cocaine, t = 4.111, p < 0.001). **F**) Representative images of viral spread in horizontal slices from a mouse in the control condition, imaged at 2x just prior to electrophysiology, and summary of viral spread for all mice in control and GIRK3 conditions. Abbreviations: MT, medial terminal nucleus of the accessory optic tract; SNC, substantia nigra, compact part; SNCD, substantia nigra, compact part, dorsal tier; SNR, substantia nigra, reticular part; PBP, parabrachial pigmented nucleus of the VTA; PIF, parainterfasicular nucleus of the VTA; PN, paranigral nucleus of the VTA; VTAR, ventral tegmental area, rostral part. **G**) $GABA_BR$-GIRK currents in the GIRK3 group (n = 9 cells from 8 mice, 38 ± 7 pA) are significantly smaller than those in the control virus condition (n = 10 cells from 6 mice, 255 ± 21 pA; Mann-Whitney U test, U = 0.0, p < 0.0001). **H**) D_2R-GIRK currents in the GIRK3 group (n = 9 cells from 7 mice, 22 ± 4 pA) are significantly smaller than those in the control virus condition (n = 8 cells from 6 mice, 52 ± 12 pA; Mann-Whitney U test, U = 11.50, p = 0.021). *,*** p < 0.05, 0.001.

5.3.4 Increased GIRK channel activity in VTA DA neurons decreases cocaine sensitivity

We next assessed the behavioral effect of enhancing GIRK channel activity in VTA DA neurons (**Figure 5.4A**). There was no difference between control and GIRK2 overexpression groups in percent time spent in open arms of the EPM (**Figure 5.4B**). Additionally, there was no difference in percent time spent in closed arms (control 53 ± 4 %; GIRK2 57 ± 5 %; t test, t_{31} = 0.692, p = 0.494), number of entries into open arms (control 11 ± 1 entries; GIRK2 9 ± 1 entries; t test, t_{31} = 1.107, p = 0.277), or number of entries into closed arms (control 10 ± 1 entries; GIRK2 10 ± 1 entries; t test, t_{31} = 0.254, p = 0.801). We did not observe a significant difference in time immobile during the FST (**Figure 5.4C**), nor did we observe any difference in latency to immobility between control (61 ± 6 s) and GIRK2 (69 ± 11 s; Mann-Whitney test, U = 83, p = 0.519) viral conditions. We also found no difference in locomotor activity on the handling day or saline day 2 (**Figure 5.4D, E**). There was a significant interaction of viral condition and cocaine dose, with mice in the GIRK2 overexpression group responding significantly less at the 15 and 30 mg/kg cocaine doses (**Figure 5.4E**). Thus, increasing the strength of GIRK channel activity in VTA DA neurons decreases behavioral sensitivity to cocaine, without impacting anxiety- or depression-like behaviors.

Following behavioral testing, control and GIRK2 overexpression mice were prepared for slice electrophysiological evaluation and the extent of viral spread was summarized for control and GIRK2 overexpression conditions (**Figure 5.4F**). Similar to our electrophysiological findings prior to behavioral testing (**Figure 5.1F**), $GABA_BR$-dependent currents were significantly enhanced following GIRK2 overexpression, compared with control virus (**Figure 5.4G**). However, D_2R-GIRK currents in the GIRK2

overexpression condition were not significantly different from controls (**Figure 5.4H**). The D_2R-dependent response was heterogeneous, however, and the range of data in the GIRK2 overexpression group was substantially larger than that of the control condition (F test to compare variances, $F_{7,7}$ = 6.774, p = 0.022 **Figure 5.4H**). This suggests that the overexpression of GIRK2 could alter the strength of D_2R-GIRK channel mediated signaling in some, but not all, DA neurons.

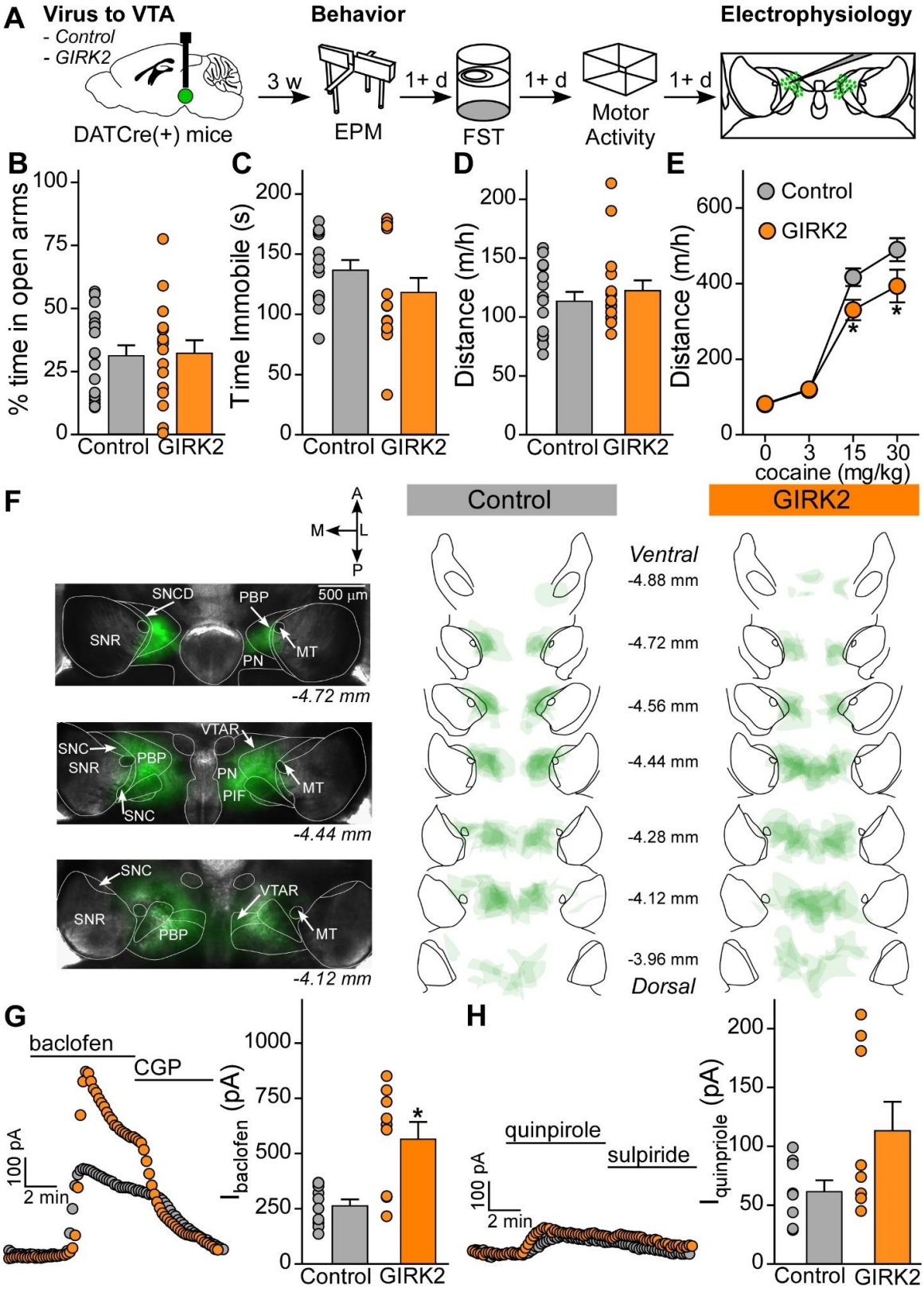
A
Virus to VTA
- Control
- GIRK2
DATCre(+) mice
3 w
Behavior
EPM
1+ d
FST
1+ d
Motor Activity
1+ d
Electrophysiology
B
% time in open arms
Control GIRK2
C
Time Immobile (s)
Control GIRK2
D
Distance (m/h)
Control GIRK2
E
Distance (m/h)
Control
GIRK2
cocaine (mg/kg)
F
A
M
L
P
SNCD
PBP
500 µm
SNR
PN
MT
-4.72 mm
VTAR
SNC
SNR
PBP
PN
PIF
MT
SNC
-4.44 mm
SNC
VTAR
SNR
PBP
MT
-4.12 mm
Control
GIRK2
Ventral
-4.88 mm
-4.72 mm
-4.56 mm
-4.44 mm
-4.28 mm
-4.12 mm
-3.96 mm
Dorsal
G
baclofen
CGP
100 pA
2 min
I baclofen (pA)
Control GIRK2
H
quinpirole
sulpiride
100 pA
2 min
I quinpriole (pA)
Control GIRK2

Figure 5.4. Viral enhancement of GIRK channel activity in VTA DA neurons decreases behavioral sensitivity to cocaine.

A) Schematic of experiment, in which DATCre(+) mice were injected with control of GIRK2 virus. 3 wk following surgery, mice were tested for EPM, FST, and cocaine locomotor activity, with each task separated by at least 1 d. Following behavior, mice were processed for placement and electrophysiology validation. **B**) EPM percent time in open arms is not different in control mice (n = 17, 31 ± 4 %) and GIRK2 mice (n = 16, 32 ± 5 %; t test, t_{31} = 0.1446, p = 0.8860). **C**) FST time immobile during the final 4 min of the task does not differ between control mice (n = 13, 137 ± 8 s) and GIRK2 mice (n = 15, 119 ± 12 s; Mann-Whitney U test, U = 76, p = 0.3334). **D**) Distance moved on the handling habituation day was not different between control mice (n = 16, 114 ± 8 m/h) and GIRK2 mice (n = 16, 123 ± 9 m/h; Mann-Whitney U test, U = 119, p = 0.7487). **E**) Distanced traveled following injection of 0, 3, 15, and 30 mg/kg cocaine resulted in interaction between cocaine dose and virus (two-way repeated measures ANOVA, $F_{3,90}$ = 3.054, p = 0.032; Bonferroni post-hoc test for 15 mg/kg, t = 2.548, p = 0.012, for 30 mg/kg, t = 2.824, p = 0.006). **F**) Representative images of viral spread in horizontal slices from a mouse in the control condition, imaged at 2x just prior to electrophysiology, and summary of viral spread for all mice in control and GIRK2 conditions. Abbreviations: MT, medial terminal nucleus of the accessory optic tract; SNC, substantia nigra, compact part; SNCD, substantia nigra, compact part, dorsal tier; SNR, substantia nigra, reticular part; PBP, parabrachial pigmented nucleus of the VTA; PIF, parainterfasicular nucleus of the VTA; PN, paranigral nucleus of the VTA; VTAR, ventral tegmental area, rostral part. **G**) $GABA_BR$-GIRK currents in the GIRK2 condition (n = 9 cells from 7 mice, 566 ± 77 pA) are significantly higher than those in the control condition (n = 10 cells from 7 mice, 265 ± 28 pA; Mann-Whitney U test, U = 14, p = 0.010). **H**) D_2R-GIRK currents are not significantly different in control (n = 8 cells from 5 mice, 62 ± 9 pA) and GIRK2 conditions (n = 8 cells from 7 mice, 113 ± 25 pA; Mann-Whitney U test, U = 19.50, p = 0.207). * $p < 0.05$.

5.4 Discussion

Here, we used a viral approach to bi-directionally manipulate the strength of GIRK channel activity in VTA DA neurons of adult mice. We found that behavioral sensitivity to cocaine was inversely proportional to the strength of GIRK channel activity in VTA DA neurons, while negative affective behaviors were unaltered by VTA DA neuron-specific GIRK channel manipulations. These findings show that GIRK channel activity in VTA DA neurons can influence behavioral sensitivity to cocaine and suggest that manipulation of these channels could represent a new therapeutic approach to treating certain aspects of addiction. This prospect is enhanced by the fact that the GIRK2/GIRK3 channel subtype expressed in DA neurons is unique (Cruz et al., 2004; Labouèbe et al., 2007; Arora et al., 2010). Given that VTA DA neurons appear to be most influential in the early phase of addiction (*i.e.*, binge/intoxication; Volkow et al., 2012), an agonist selective for GIRK2/GIRK3 channels might be expected to suppress drug reward and acquisition of self-administration, without altering negative affective behavior.

5.4.1 GIRK channel activity in VTA DA neurons shapes behavioral sensitivity to cocaine

Our previous work demonstrated genetic ablation of GIRK channels globally or in DA neurons increased behavioral sensitivity to cocaine (Arora et al., 2010; McCall et al., 2017). Similarly, the DA neuron-specific ablation of sorting nexin 27 (SNX27), a cytoplasmic protein that interacts with the PDZ-binding motifs of GIRK2c and GIRK3 to regulate channel trafficking, decreased $GABA_BR$- and D_2R-GIRK signaling and increased behavioral responding to cocaine (Lunn et al., 2007; Munoz and Slesinger, 2014; Rifkin et al., 2018). D_2Rs in DA neurons have also been implicated in modulating

behavioral sensitivity to cocaine. Indeed, mice lacking D_2R in DA neurons display increased cocaine-induced locomotor activity, increased preference for a low dose of cocaine in the conditioned place preference test, and accelerated acquisition of self-administration (Bello et al., 2011; Holroyd et al., 2015). The interpretation of these DA neuron-specific genetic manipulations is limited by their congenital nature and lack of regional selectivity, which makes it challenging to dissociate them from developmental alterations and to attribute behavioral phenotypes to a specific dopaminergic population. Here, we report that genetic enhancement or suppression of GIRK-dependent signaling in adult mouse VTA DA neurons decreased or increased, respectively, behavioral sensitivity to cocaine.

The impact of VTA DA neuron GIRK channels on behavioral sensitivity to cocaine is likely attributable in large part to the engagement of $GABA_BR$- and/or D_2R-dependent signaling by cocaine. Indeed, increased synaptic DA levels evoked by cocaine activates both terminal and somatodendritic D_2Rs (Brodie and Dunwiddie, 1990; Beckstead et al., 2004). In addition, cocaine enhances GABAergic ("long-loop") feedback to VTA DA neurons by increasing DA in the NAc (Edwards et al., 2017). While VTA DA neurons receive GABAergic input from local interneurons and several regions (Morales and Margolis, 2017), NAc-derived input from D_1R-expressing medium spiny neurons appears to selectively activate $GABA_BRs$ in VTA DA neurons (Edwards et al., 2017; Yang et al., 2018). Notably, recent studies targeting D_2R in VTA DA neurons have yielded outcomes of comparable magnitude as those reported herein following viral suppression of GIRK channel activity. For example, RNAi-dependent suppression of D_2R in the rat VTA correlates with increased cocaine locomotor activity, as well as increased responding for cocaine and sucrose in a self-administration progressive ratio task (de Jong et al., 2015). Similarly, $GABA_BR$ ablation in VTA DA neurons correlated with

increased cocaine-induced locomotor activity in mice (Edwards et al., 2017). It is important to note, however, that GIRK channels may mediate the effects of other inhibitory G protein-coupled receptors on VTA DA neurons, such as kappa opioid and nociceptin receptors (Di Giannuario and Pieretti, 2000; Lutfy et al., 2001; Margolis et al., 2003; Ford et al., 2006). As such, the behavioral impact of VTA DA neuron-specific manipulations on GIRK channel activity may reflect in part the modulation of signaling via these receptors as well.

5.4.2 Suppression of VTA DA neuron GIRK channel activity by GIRK3

Similar to other published results (Kofuji et al., 1995; Lesage et al., 1995; Ma et al., 2002), we found that overexpression of GIRK3 neurons yielded a robust suppression of GIRK channel activity in VTA DA neurons. The molecular mechanisms underlying this dominant negative influence of ectopic GIRK3 are unclear. Overexpression of GIRK3 may enhance trafficking of GIRK channels to internal sites, a prospect supported by the presence of a lysosomal targeting motif in the GIRK3 carboxyl-terminal domain (Ma et al., 2002). GIRK3 might promote an interaction between the VTA DA neuron GIRK channel and SNX27, which can bi-directionally regulate channel trafficking (Lunn et al., 2007; Munoz and Slesinger, 2014). The presence of GIRK3 could also increase the negative regulatory influence of regulator of G protein signaling 2 (RGS2) on GIRK-dependent signaling in VTA DA neurons (Jelacic et al., 2000; Labouèbe et al., 2007). Interestingly, activity-dependent and psychostimulant-induced plasticity of GIRK channel activity in VTA DA neurons is dependent upon GIRK3 (Lalive et al., 2014; Munoz et al., 2016). Given these observations, it is tempting to speculate that GIRK3 titrates the strength of GIRK channel activity in VTA DA neurons via the extent to which it incorporates into the GIRK2/GIRK3 heterotetromeric channel.

5.4.3 GIRK channels and negative affective behavior

Girk2$^{-/-}$ mice display reduced anxiety- and depression-related behaviors, which are modulated by DA (Pravetoni and Wickman, 2008; Llamosas et al., 2015; Zarrindast and Khakpai, 2015; Belujon and Grace, 2017). While viral manipulation of GIRK channel activity in VTA DA neurons did not alter these behaviors, male DATCre(+):*Girk2*$^{fl/fl}$ mice displayed decreased depression-related behavior, congruent with findings from another DATCre:*Girk2*$^{fl/fl}$ line (Honda et al., 2018). The apparent discrepancy in depression-related behavior in DATCre(+):*Girk2*$^{fl/fl}$ mice and the viral loss-of-function model could reflect a lack of penetrance in the viral manipulation, developmental compensation in DATCre(+):*Girk2*$^{fl/fl}$ mice, or the influence of a different, non-VTA population of DA neurons on this behavior.

The lack of anxiolytic phenotype in DATCre(+):*Girk2*$^{fl/fl}$ and viral gain- and loss-of-function models suggests GIRK-dependent signaling in VTA DA neurons does not contribute to baseline anxiety-related behavior. The anxiolytic phenotype observed in both *Girk1*$^{-/-}$ and *Girk2*$^{-/-}$ mice, and the anxiolytic efficacy of a direct-acting agonist of GIRK1-containing channels (ML297), support the contention that neuron populations expressing GIRK1-containing channels impact baseline anxiety in mice, not the GIRK1-lacking midbrain DA neurons (Cruz et al., 2004; Pravetoni and Wickman, 2008; Wydeven et al., 2014).

Overall, the outcomes of our viral manipulations suggest that GIRK-dependent signaling in VTA DA neurons exerts a minimal influence on negative affective behavior at baseline. However, the prior experience of subjects in our study is meaningfully distinct from that of mice in studies in which VTA DA neuron excitability was shown to correlate with altered negative affective behavior. Indeed, mice subjected to social defeat stress that subsequently displayed depressive-like behavior (“susceptible” mice)

also displayed increased VTA DA neuron excitability (Cao et al., 2010; Chaudhury et al., 2013; Friedman et al., 2014, 2016). In this context, it is noteworthy that while our viral manipulations did alter the amplitude of GIRK-dependent somatodendritic currents in VTA DA neurons, they exerted little or no impact on the excitability of VTA DA neurons (**Table 5.1**).

5.4.4 Future directions

A rich body of recent work has demonstrated that separate dopaminergic projections emanating from the VTA participate in distinct behaviors (Lammel et al., 2014; Holly and Miczek, 2016; Juarez and Han, 2016; Morales and Margolis, 2017). For example, DA neurons in the lateral VTA, which project to the lateral NAc shell, are responsive to rewarding stimuli (Lammel et al., 2011, 2012). In contrast, more medial VTA DA neurons projecting to the PFC and the core and medial shell of the NAc have been implicated in responding to aversive stimuli (Lammel et al., 2008, 2012; Vander Weele et al., 2018; de Jong et al., 2019). Interestingly, while overexpression of GIRK2 enhanced $GABA_BR$-GIRK signaling in VTA DA neurons, we did not observe a significant increase in D_2R-GIRK signaling with this manipulation (**Figure 5.4H**). Rather, there appeared to be two distinct populations of VTA DA neurons in our study: one with unaltered D_2R-GIRK responses and one with enhanced responses. It is possible that D_2Rs and GIRK channels are maximally coupled in the former population (*e.g.*, D_2R level is the factor limiting D_2R-GIRK signaling strength), which renders over-expression of GIRK2 functionally inert. In the latter population, the GIRK channel level may limit the strength of D_2R-GIRK signaling at baseline. It is possible this diversity of D_2R-GIRK signaling aligns with distinct, projection-defined subpopulations of VTA DA neurons (Lammel et al., 2008). Further investigation will be needed to determine if GIRK-dependent signaling in discrete VTA DA neuron projections mediates behavioral

sensitivity to cocaine, and if selective strengthening of GIRK channel activity in these projections might suppress other cocaine-related behaviors, including acquisition of self-administration or reinstatement.

Chapter 6

Discussion

6.1 Summary and synthesis of findings

My thesis research has contributed to the field's understanding of the role of VTA DA neuron GIRK channel activity in behavioral sensitivity to cocaine. The underlying premise driving my thesis research is the idea that the strength of GIRK channel activity in VTA DA neurons is inversely proportional to behavioral sensitivity to cocaine. This premise is grounded in the observation that GIRK channel activity in VTA DA neurons is decreased following exposure to psychostimulants (Arora et al., 2011; Sharpe et al., 2015; Munoz et al., 2016). These findings suggest VTA DA neuron GIRK channels serve as an inhibitory "barrier" to addiction, one that is eroded as substance use progresses from initial exposure to habitual use. Because this adaptation in GIRK channel activity in VTA DA neurons occurs after a single exposure to cocaine (Arora et al., 2011), it is tempting to speculate that this change is one of the initial adaptations that ultimately leads to the development of addiction. Overall, my thesis work highlights the importance of inhibitory G protein signaling mediated by GIRK channels in regulating behavioral sensitivity to cocaine.

6.1.1 VTA DA neuron GIRK channel activity decreases behavioral sensitivity to cocaine

My thesis research elucidated the role of the unique GIRK channel present in VTA DA neurons on behavioral sensitivity to cocaine. This was explored by knocking out GIRK2 from DA neurons and overexpressing GIRK channels in VTA DA neurons. These studies revealed the role GIRK channel activity in VTA DA neurons plays in behavioral

sensitivity to cocaine and provided further insight into the roles of GIRK2 and GIRK3 in inhibitory GPCR signaling in VTA DA neurons.

Impact of GIRK channels in VTA DA neurons on inhibitory GPCR physiology

My GIRK channel knockout and overexpression studies that have yielded further insight into the role of DA neuron GIRK channels in mediating the magnitude of inhibitory G protein signaling. The loss of GIRK2 from DA neurons in the DATCre(+):*Girk2*$^{fl/fl}$ mouse model significantly decreased $GABA_BR$- and D_2R-GIRK currents in mice (Kotecki et al., 2015; McCall et al., 2017) (**Figures 1.3 and 2.1**), similar to what has been described in putative DA neurons in the VTA of *Girk2*$^{-/-}$ mice (Arora et al., 2010). This is consistent with the hypothesis that GIRK2 is necessary for functional GIRK channels due the presence of an endoplasmic reticulum export signal on GIRK2 (Ma et al., 2002). The necessity of GIRK2 for GIRK channel activity is supported by similar profound decreases in $GABA_BR$-GIRK currents in other neuronal populations in *Girk2*$^{-/-}$, such as PFC and HPC pyramidal neurons (Lüscher et al., 1997; Hearing et al., 2013). Conversely, overexpression of GIRK2c in VTA DA neurons on $GABA_BR$-GIRK channel signaling (**Figures 5.1 and 5.4**). The presence of the endoplasmic reticulum export signal allows GIRK2 to form functional homotetramers, likely the mechanism underlying this observation (Ma et al., 2002). Together, these knockout and overexpression studies provide evidence for the positive influence of GIRK2 on the strength of GIRK channel activity.

In contrast to GIRK2, the GIRK3 subunit appears to have a negative regulatory effect on GIRK channel activity in VTA DA neurons. Indeed, the overexpression of GIRK3 decreases $GABA_BR$ and D_2R somatodendritic currents. In heterologous systems, the expression of GIRK3 strongly inhibits the surface expression of GIRK channels,

suggesting that GIRK3 can negatively influence GIRK channel activity through a trafficking-dependent mechanism (Ma et al., 2002). This trafficking mechanism could be mediated by an interaction with SNX27 or with a lysosomal targeting motif (Ma et al., 2002; Lunn et al., 2007). Putative DA neurons of the VTA in *Girk3*$^{-/-}$ mice display increased sensitivity to baclofen (*i.e.*, removal of GIRK3 lowers EC_{50} for baclofen) due to an interaction with RGS2 (Labouèbe et al., 2007), further suggesting that GIRK3 decreases GIRK channel function. Consistent with this, the overexpression of GIRK3 in VTA DA neurons decreases $GABA_BR$- and D_2R-GIRK currents (**Figures 5.1 and 5.3**). Another possible explanation for the negative modulatory GIRK3 overexpression electrophysiological finding is that the overexpression of GIRK3 causes a dominant negative-like effect, as GIRK3, unlike GIRK2, lacks an endoplasmic reticulum export domain (Ma et al., 2002). This could cause the overexpression of GIRK3 to block the ability of GIRK2 to traffic channels to the cell surface.

Overall, my electrophysiological studies highlight the opposing roles of the GIRK2c and GIRK3 on GIRK channel activity in VTA DA neurons, with GIRK2c enhancing and GIRK3 decreasing this inhibitory signaling strength.

GIRK channels in VTA DA neurons decrease behavioral sensitivity to cocaine

A complement of knockout and overexpression strategies specific to DA neurons strongly suggests the unique GIRK channel expressed in VTA DA neurons provides a negative influence on behavioral sensitivity to cocaine. The underlying premise for this hypothesis was inspired by the ability of acute exposure to cocaine to decrease GIRK channel activity in VTA DA neurons (Arora et al., 2011). This adaptation could imply that lessening this inhibitory signaling is a key cellular mechanism of addiction, perhaps in part underlying the process of behavioral sensitization. Thus, the loss of GIRK channels

from DA neurons was expected to increase behavioral sensitivity to cocaine in multiple assays.

Indeed, my study with DATCre(+):*Girk2*$^{fl/fl}$ mice suggests GIRK channels in DA neurons can temper some aspects of the behavioral response to cocaine (McCall et al., 2017). DATCre(+):*Girk2*$^{fl/fl}$ mice displayed increased locomotor responses to acute and repeated cocaine (**Figure 3.3**) (McCall et al., 2017). DATCre(+):*Girk2*$^{fl/fl}$ mice also appear to reach a plateau in their locomotor activity faster than Cre(-) littermates in the behavioral sensitization paradigm, suggesting the loss of GIRK channel activity in DA neurons causes cause a presensitization-like phenotype (**Figure 3.3**) (McCall et al., 2017). DATCre(+):*Girk2*$^{fl/fl}$ mice display increased cocaine self-administration, especially at low doses, but display no difference in the acquisition of self-administration from Cre(-) littermates (**Figure 3.5**) (McCall et al., 2017). Interestingly, we did not observe a difference in cocaine CPP (**Figure 3.4**) (McCall et al., 2017) in DATCre(+):*Girk2*$^{fl/fl}$ mice, suggesting that DA neuron GIRK channels do not contribute to the rewarding valence of cocaine.

Together, these behavioral data suggest that GIRK channel activity in DA neurons influence the sensitivity of cocaine in tasks that incorporate the motor activity and approach aspect of reward, rather than the positive valence aspect of cocaine reward. Interestingly, these findings differ from those for DATCre(+):*Drd2*$^{fl/fl}$ mice, which also display increased acute locomotor activity following cocaine exposure but also acquire cocaine self-administration faster than DATCre(-):*Drd2*$^{fl/fl}$ and have enhanced cocaine CPP at a typically subthreshold dose (Bello et al., 2011; Holroyd et al., 2015). Behavioral differences between mice lacking D_2Rs and those lacking GIRK channels from DA neurons suggests these elements of inhibitory G protein signaling differentially influence behavioral sensitivity to cocaine. While GIRK channels are engaged by D_2Rs,

they are only one of several downstream effectors and are predominantly located in postsynaptic compartments. Non-GIRK downstream effectors of D_2R signaling, such as calcium channels, NALCN channels, and AC activity (Ye et al., 1999; Kamp and Hell, 2000; Philippart and Khaliq, 2018), could underlie the valence-related behavioral effects of D_2R that GIRK channels do not mediate. Additionally, these valence-related behavioral effects could be mediated by presynaptic D_2Rs on DA neuron axonal terminals, which could play a more direct role in controlling the release of DA in downstream targets.

To gain insight into how broadly engaging inhibitory G protein signaling in VTA DA neurons could impact cocaine-enhanced locomotor behavior, inhibitory DREADDs were virally expressed in VTA DA neurons. Engaging inhibitory G protein signaling in VTA DA neurons decreased cocaine- and morphine-enhanced locomotor activity (**Figure 4.2**). However, a similar effect was observed in control mice administered saline vehicle (**Figure 4.2**), suggesting that engaging inhibitory GPCRs on VTA DA neurons generally diminishes locomotion. Indeed, another research group found a similar reduction in locomotor activity the activation of hM4Di is engaged in VTA THCre(+) neurons (Runegaard et al., 2018b). However, this hM4Di-induced decrease in motor activity is eliminated when mice are habituated to the testing chamber directly prior to the administration of CNO, and the subsequent administration of cocaine (Runegaard et al., 2018b). This suggests that the decrease in locomotor activity in my study (**Figure 4.2**) could also reflect a suppression of novelty-induced, exploratory locomotor activity rather than a general locomotor effect. Indeed, following habituation to the testing chamber, engaging hM4Di in VTA THCre(+) neurons decreases cocaine-increased locomotor activity (Runegaard et al., 2018b). This finding further implicates inhibitory G

protein signaling in VTA DA neurons in mediating the motor effects of cocaine, in accordance with my DATCre:*Girk2*$^{fl/fl}$ study (McCall et al., 2017).

Finally, the role of GIRK channel activity in DA neurons of the VTA in behavioral sensitivity to cocaine was further demonstrated using a viral GIRK overexpression approach to bi-directionally modulate the strength of GIRK channel activity. Indeed, decreasing GIRK channel activity in VTA DA neurons by overexpressing GIRK3 increased the acute motor response to cocaine (**Figure 5.3**), recapitulating the behavioral effect described in DATCre(+):*Girk2*$^{fl/fl}$ mice (McCall et al., 2017). Conversely, increasing GIRK channel activity in VTA DA neurons by overexpressing GIRK2c decreased the acute motor response to cocaine (**Figure 5.4**). Together, these behavioral findings implicate GIRK channel activity in VTA DA neurons in mediating the locomotor and approach aspects of cocaine-related reward, and suggest a GIRK2/GIRK3 channel activator might be able to decrease the behavioral response to cocaine and other psychostimulants.

6.1.2 VTA DA neuron GIRK channel activity impacts behavioral sensitivity to morphine, but is not altered by morphine

Increased DA release in the NAc occurs following exposure to different types of drugs, including cocaine and morphine, and could be a shared means of exerting their positively reinforcing behavioral effects (Nestler, 2005). While cocaine increases extracellular DA by blocking the activity of DATs (Di Chiara and Imperato, 1988), morphine is thought to elicit this effect through the disinhibition of DA neurons, in which morphine activates MORs on VTA GABA neurons, thereby decreasing GABAergic input to VTA DA neurons (Johnson and North, 1992). Interestingly, while cocaine exposure decreases GIRK channel activity (Arora et al., 2011) and both cocaine and morphine

administration increase excitatory signaling (Saal et al., 2003), the effect of acute morphine exposure on GIRK channel activity in VTA DA neurons had not been established.

To address this gap in the literature, morphine was administered to mice and GIRK channel activity in VTA DA neurons was subsequently measured. Neither acute nor repeated (5 d) i.p. morphine induced plasticity in $GABA_BR$-GIRK channel signaling (**Figures 2.3 and 2.4**), in contrast to the decrease in GIRK channel activity observed following exposure to the psychostimulants cocaine or methamphetamine (Arora et al., 2011; Padgett et al., 2012). Because GIRK channel adaptations can be driven by changes in DA neuron excitability (Lalive et al., 2014), this difference in GIRK channel adaptations following morphine versus cocaine exposure could be due to differences how these drugs alter the excitability of DA neurons. While cocaine acutely inhibits DA neurons by engaging D_2Rs (Beckstead et al., 2004), morphine increases the activity of VTA DA neurons through disinhibition (Johnson and North, 1992). As phasic firing protocols can increase GIRK channel activity (Lalive et al., 2014), it makes sense that morphine exposure does not decrease GIRK channel activity (**Figures 2.3 and 2.4**). Rather, one might expect morphine exposure to increase GIRK channel activity, which may be the case in higher responders to morphine (**Figure 2.3**).

Importantly, even though morphine does not significantly alter GIRK channel activity in VTA DA neurons, changing the strength of GIRK channel activity in VTA DA neurons is able to impact behavioral sensitivity to morphine. Indeed, DATCre(+):*Girk2*$^{fl/fl}$ mice display an increased locomotor response to morphine, while *Girk3*$^{-/-}$ mice have a diminished response to morphine (Kotecki et al., 2015). This data suggests GIRK channel activity in DA neurons negatively influences the behavioral response to morphine, similar to its effect on cocaine (Arora et al., 2010; McCall et al., 2017). This

could be due to the loss of GIRK channels from DA neurons reducing the inhibitory influence of long-loop GABAergic feedback from the NAc, which is engaged by the increase in NAc DA following morphine exposure. GIRK channel signaling in VTA DA neurons could temper the behavioral response to morphine.

6.1.3 VTA DA neuron GIRK channel activity and negative affect

In addition to reward behavior and the behavioral response to drugs of abuse, VTA DA neurons have also been implicated in negative affective behavior (Tye et al., 2013), particularly in a post-stress context (Lammel et al., 2014). Indeed, stressful stimuli can alter the excitability of VTA DA neurons as well as DA release. Mice and rats exposed to social defeat stress, forced swim stress, restraint stress, and pain exhibit increased DA release in the NAc and PFC as well as increased VTA DA neuron firing; however, other types of stressors elicit a decrease or no change in DA release (Holly and Miczek, 2016). These discrepancies suggest that the type and severity of stressor is important in defining how DA neurons are effected (Holly and Miczek, 2016), and also points to heterogeneity in the responses of individual subjects and DA neuron subpopulations to stress. Indeed, a study that separated mice into susceptible and resilient individuals based on behavioral phenotypes following chronic social defeat found susceptible mice have increased phasic firing in NAc-projecting VTA DA neurons (Chaudhury et al., 2013). Given the preponderance of data showing that stress can impact VTA DA neuron excitability. I pursued two relevant research questions: 1) does stress impact the strength of GIRK channel activity, and 2) does manipulation of GIRK channel activity in VTA DA neurons impact negative affective behavior.

To determine if stress modulates GIRK channel activity, we employed a negative stimuli, *i.e.*, footshock and forced swim stress, similar to those that have modulated excitatory signaling (Saal et al., 2003). Footshock decreased $GABA_BR$-GIRK currents in

VTA DA neurons, but forced swim stress did not alter GIRK channel activity (**Figure 2.2**). This suggests that only certain types of stress, perhaps more severe forms, are capable of inducing adaptations in GIRK channel signaling. This heterogeneous effect could be attributable to the ability of these stressors to activate brain regions which provide input to the VTA and are modulated by stress, such as the amygdala or locus coeruleus. A difference in the modulation of VTA DA neuron activity can in turn affect GIRK channel activity adaptations (Lalive et al., 2014).

To assess how GIRK channel activity in VTA DA neurons impacts negative affective behavior, DATCre(+):*Girk2*$^{fl/fl}$ mice and VTA DA neuron specific GIRK channel overexpression mice were assessed in tests of anxiety-like and depressive-like behavior. There were no changes in anxiety in any of these manipulations, suggesting that GIRK channels in VTA DA neurons do not impact anxiety at baseline (*i.e.*, non-stress) conditions (**Figures 5.2-5.4**). The loss of GIRK channels from DA neurons, but not the decrease of GIRK channel activity in VTA DA neurons, causes reduced depressive-like behavior in males (**Figures 5.2 and 5.3**). These findings are consistent with decreased depressive-like behavior observed in males of an independently developed DATCre(+):*Girk2*$^{fl/fl}$ line (Honda et al., 2018). Furthermore, enhancing GIRK channel activity does not impact depressive-like behavior (**Figure 5.4**). Together, this suggests that a non-VTA DA population could contribute to the DATCre(+):*Girk2*$^{fl/fl}$ behavioral phenotype, possibly SN DA neurons. Additionally, this phenotype and its sex-specific nature might be due developmental differences in reward related brain regions outside of the VTA DA neurons in males and females in the DATCre(+):*Girk2*$^{fl/fl}$ line, as there are no sex differences in DA neuron activity in the DATCre(+):*Girk2*$^{fl/fl}$ line. However, I only measured maximal GPCR-GIRK currents; perhaps a dose-response approach might yield different findings. The lack of effect on anxiety but on depression is congruent with

the preponderance of data linking DA neurons to depression, but relatively few studies linking them to anxiety (Nestler and Carlezon, 2006; Lammel et al., 2014). It is tempting to speculate that GIRK channels in VTA DA neurons might play a role on negative affective behavior following stress.

6.1.4 Summary

The findings presented in my thesis contribute to the field's understanding the experiences and pharmacologic agents that can elicit adaptations in VTA DA neurons, summarized in **Table 1.4** and continued in **Table 6.1**. It also expands our understanding of how the strength of GIRK channel activity in DA neurons contributes to sensitivity to cocaine, summarized in **Table 1.5** and continued in **Table 6.2**. The implications of this work likely extents to other psychostimulants as well. My electrophysiological studies following GIRK channel manipulation further demonstrate that GIRK channels are major downstream effectors of $GABA_BRs$ and D_2Rs. I also characterized how robust changes in VTA DA neuronal excitability, such as those induced D_2R activation, similar to cocaine, appear to be the most potent mediators of adaptations in GIRK channel activity (Arora et al., 2011; Lalive et al., 2014). Overall, the behavioral findings in this thesis strongly implicate GIRK channels in VTA DA neurons as a key mediator of behavioral sensitivity to cocaine, and suggest the unique VTA DA GIRK channel might be a promising target for the treatment of addiction.

Table 6.1 Experience-based plasticity of GIRK channel activity.
Continuation of **Table 1.4.** n.c. indicates no change.

Experience	Cell population	Effect on GIRK channel activity	Ref.
Non-drug experiences			
Foot shock exposure	VTA DA neurons	↓	Chapter 2
Repeated forced swim stress (Lemos et al., 2012)	VTA DA neurons	n.c.	Chapter 2
Quinpirole, 1 mg/kg	VTA DA neurons	↓ $GABA_BR$ n.c. D_2R	Chapter 2
Morphine			
10 mg/kg, 1 d	VTA DA neurons	n.c.	Chapter 2
10 mg/kg, 5 d	Putative DA neurons, VTA	n.c.	Chapter 2

Table 6.2. Behaviors linked to drugs of abuse in knockout mice with altered inhibitory GPCR signaling.
Continued from **Table 1.5**.

Drug	Manipulation	Effect	Ref.
Cocaine	DATCre(+):*Girk2*$^{fl/fl}$	↑ locomotor activity at 15 mg/kg	Chapters 3 and 5
Cocaine	GIRK3 overexpression in VTA DA neurons	↑ locomotor activity at 15 mg/kg	Chapters 3
Cocaine	GIRK2 overexpression in VTA DA neurons	↓ locomotor activity at 15 mg/kg	Chapters 3

6.2 Future Directions

This thesis research identified the strength of VTA DA neuron GIRK channel activity as a key mediator of behavioral sensitivity to cocaine. Future studies can build on these findings by trying to better understand how manipulating DA neuron GIRK channel activity can influence neuronal activity and DA release. Additionally, further work should add to our understanding of the impact of GIRK channel activity on more reward-relevant behavior, and in subpopulations of VTA DA neurons.

6.2.1 Determine the functional consequences of manipulating DA neuron GIRK channel activity in vivo

Electrophysiological findings in DATCre(+):*Girk2*$^{fl/fl}$ and GIRK overexpression studies suggest GIRK channel activity could influence the regulation of DA release and DA neuron activity *in vivo*. This could be particularly true in situations where inhibitory G protein signaling in DA neurons is engaged, such as cocaine exposure. To determine how DA release is altered *in vivo* in VTA DA neurons when GIRK channel activity is decreased or increased, one could employ fast scan cyclic voltammetry (FSCV) (McElligott, 2015) or genetically encoded dopamine sensors (dLight) (Patriarchi et al., 2018). Due to the somatodendritic location of GIRK channels, the most profound influence of GIRK channel signaling on DA release parameters could be within the VTA, where D_2R activation influences somatodendritic DA release (Ford, 2014). DA release in terminal regions, such as the NAc, might also be altered by the manipulation of VTA DA neuron GIRK channels when inhibitory G protein signaling is engaged. To determine how GIRK channel activity influences *in vivo* DA neuron activity, *in vivo* imaging using genetically encoded calcium indicators, which act a proxy for neuronal activity, could be used (Siciliano and Tye, 2019). My electrophysiological studies of DATCre(+):*Girk2*$^{fl/fl}$

mice and GIRK3 overexpressing mice suggest that at baseline, manipulations of GIRK channel activity might not effect DA neuron activity. However, in instances when inhibitory G protein signaling in engaged, manipulating GIRK channel activity is likely to alter DA neuron activity. Such *in vivo* studies of DA release and DA neuron activity could help bridge the gap between the changes I have observed in *ex vivo* physiology and behavior in this thesis.

6.2.2 DA neuron subpopulation-specific manipulations

The present work utilized the DATCre mouse line (Bäckman et al., 2006) and represents a marked improvement over previous approaches that were not neuron-specific (Pravetoni and Wickman, 2008; Arora et al., 2010). However, VTA DA neurons have diverse projection targets and influences on behavior (Lammel et al., 2015; Juarez and Han, 2016; Morales and Margolis, 2017). Thus, it is likely that manipulations of all DA neurons (**Chapter 3**) and potentially all VTA DA neurons (**Chapters 4 and 5**) are not specific enough to thoroughly understand how GIRK channels contribute to behavioral sensitivity to drugs of abuse. Future studies manipulating the strength of GIRK channel activity in a DA neuron subpopulation-specific manner could address this gap in knowledge. Retrograde-traveling Cre-dependent viral strategies, such as rabies viruses (Wickersham et al., 2007), herpes simplex virus type 1 (HSV 1) (Ugolini et al., 1987), canine adenovirus type 2 (CAV-2) (Junyent and Kremer, 2015), and retroAAV2-retro (Tervo et al., 2016), in DATCre(+) mice could be used to overexpress GIRK2c or GIRK3. To better facilitate these viral approaches, changes could be made to improve upon the viruses used in this thesis (**Chapters 4 and 5**). IRES sequences are known to reduce the expression of subsequent proteins (Licursi et al., 2011); therefore, it is likely that the expression of GFP in the GIRK overexpression viruses is decreased, making it harder to

determine the full extent of viral expression. In the future, a P2A sequence might improve this (Kim et al., 2011). Additionally, based on personal conversations with others manipulating DA neurons with retrogradely traveling viruses, the EF1α promotor will likely perform better in DA neurons than the human synapsin (hSyn) (de Jong et al., 2019).

Future studies using these retrograde-expressing viruses in DATCre(+) mice can build on the work described in **Chapter 5**, overexpressing GIRK channel subunits to manipulate strength of GIRK channel signaling in a subpopulation-specific manner. The most logical subpopulations that contribute to cocaine behavioral sensitivity are the NAc lateral shell projecting dopaminergic population, which has been implicated in reward-related behaviors (Lammel et al., 2012) or the NAc core projecting dopaminergic population, which has been implicated in the approach-related effects of drugs of abuse. Indeed, this subpopulation-specific manipulation of inhibitory G protein signaling has already begun to be performed. In one such study, the expression of SNX27 in NAc-projecting VTA DA neurons restored $GABA_BR$-GIRK responses but not responding to cocaine (Rifkin et al., 2018). However, the NAc lateral shell, medial shell, and core were all targeted in these manipulations (Rifkin et al., 2018). Perhaps if the lateral shell NAc subregion was targeted, behavioral responses to cocaine could have been rescued. More work manipulating GIRK channel activity in VTA DA neurons should be done to fully assess this possibility.

To manipulate other inhibitory G protein signaling pathway elements in subpopulations of VTA DA neurons (Hsu et al., 2014), the recently popularized CRISPR approach could be used in conjunction with retrograde viral approaches. CRISPR allows for the knockout of genes of interest by taking advantage of the anti-DNA immune system in bacteria. CRISPR (clustered regularly interspaced short palindromic repeats)

refers to DNA sequences that can be used to identify and subsequently remove foreign DNA in bacteria, or in the case of experimental applications, genes of interest. The enzyme CRISPR-associated 9 (Cas9) uses CRISPR sequences to recognize and cleave specific strands of DNA that are complementary to the CRISPR sequence. Using RNA guides, Cas9 can generate targeted DNA double-strand breaks to stimulate genome editing, disrupting the expression and/or function of proteins of interest. To employ CRISPR-mediated gene knockout specifically in DA neurons, one would cross the Cas9-GFP mouse (Platt et al., 2014) (Cat. No. 026175, The Jackson Laboratory) with the DATCre line (Bäckman et al., 2006), allowing for the expression of Cas9 in Cre-expressing, *i.e.*, DA, neurons. Viruses expressing guide RNA probes specific for different elements of inhibitory signaling infused into the VTA would allow for the knockout a gene of interest, *e.g.*, *Girk2*, Indeed, preliminary findings indicate that the CRISPR approach is capable of disrupting GIRK2 function and thus likely expression (**Figure 6.1**).

There are a number of other downstream effectors it would be interesting to manipulate with the CRISPR approach. These include the knockout of GIRK3 from DA neurons, to verify the increase in $GABA_BR$-GIRK coupling observed in *Girk3*$^{-/-}$ mice and decreased behavioral sensitivity to morphine (Labouèbe et al., 2007). The knockout of SNX27 and $GABA_BR$ from DA neurons, which impacts behavioral sensitivity to cocaine (Munoz and Slesinger, 2014; Edwards et al., 2017; Rifkin et al., 2018), could be recapitulated selectively in the VTA. Removing D_2R from VTA DA neurons could help confirm that the behavioral phenotypes observed in DATCre(+):*Drd2*$^{fl/fl}$ mice, *i.e.*, increased cocaine locomotor, CPP, and self-administration (Bello et al., 2011; Holroyd et al., 2015), are conferred by VTA DA neurons. The behavioral contributions of the NALCN sodium leak channel (Philippart and Khaliq, 2018) in VTA DA neurons, which might be responsible for the non-GIRK component of the $GABA_BR$ and D_2R response

(Arora et al., 2010; Kotecki et al., 2015; McCall et al., 2017), could also be explored using the CRISPR approach.

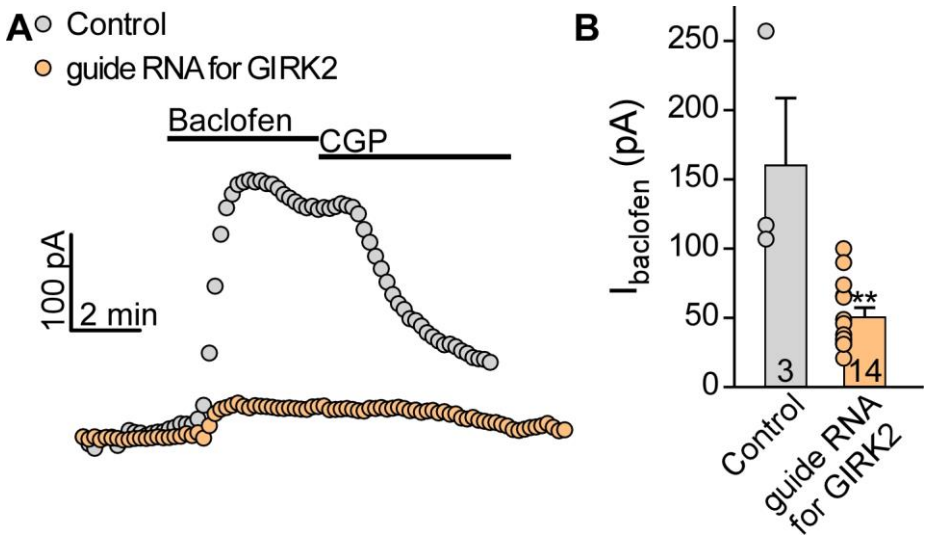

Figure 6.1. CRISPR to knockout GIRK2c from VTA DA neurons decreases $GABA_BR$-currents.

A) Summary of $GABA_BR$-GIRK currents elicited by the bath application of baclofen (200 μM) in DATCre(+):Cas9eGFP(+) mice injected with control virus (n = 3 cells from 1 mouse, 160 ± 48 pA) and virus expressing guide RNA for GIRK2 (n = 14 cells from 7 mice, 51 ± 6 pA; Mann-Whitney test, $U = 0.00$, $p = 0.01$) .

6.2.3 Subpopulation-specific studies of GIRK channel plasticity

Another future direction to explore is the possibility that adaptations GIRK channel activity caused by cocaine (Arora et al., 2011), methamphetamine (Padgett et al., 2012), or footshock (**Chapter 2**) might be specific to certain subpopulations. Indeed, work from our lab looked at putative DA neurons, which were most likely the NAc lateral shell projecting DA neurons based on their electrophysiological properties. Cocaine decreased GIRK channel activity in these VTA DA neurons (Arora et al., 2011); however, another lab performed a similar study Pitx3eGFP(+) mice and did not observe any changes in VTA DA neuron GIRK channel activity following acute cocaine exposure (Padgett et al., 2012). The use of Pitx3eGFP(+) mice to identify DA neurons, could have led to the assessment of a diverse population of DA neurons, making it challenging to detect the decrease in $GABA_BR$-GIRK currents in a subset of neurons. When designing future studies of inhibitory signaling plasticity of VTA DA neurons, it will be important to assess subpopulations of VTA DA neurons by projection target using retrobeads or a retrograde traveling virus expressing a fluorophore.

6.2.4 Improved behaviors

The work presented in **Chapters 3, 4, and 5**, as well as the work of others assessing the contributions of inhibitory G protein signaling in VTA DA neurons to the behavioral sensitivity to drugs of abuse has heavily relied on the acute and sensitized behavioral locomotor response to cocaine. While this assay is reliably run, easy to interpret, and captures some elements of drug addiction (*i.e.*, a response to drug that changes with repeated exposure), there are other behaviors that better model reward-related behavior.

One such behavior that could be measured in the GIRK overexpression manipulations (**Chapter 5**) is CPP. Indeed, DATCre(+):*Drd2*$^{fl/fl}$ mice showed increased preference for low dose of cocaine below detection for wild type mice. This suggests the strength of inhibitory G protein signaling in VTA DA neurons is important for regulating sensitivity to the rewarding effects of cocaine (Bello et al., 2011). However, I did not observe a difference in CPP in DATCre(+):*Girk2*$^{fl/fl}$ mice, suggesting GIRK channels might not mediate this conditioning-dependent means of measuring reward. A newly described variant of the CPP test, single exposure place preference (Runegaard et al., 2018a) represents a means of assessing the initial rewarding effects of psychostimulants, which may be more useful for VTA DA neuron manipulations. This test could be used to assess the effects of manipulating GIRK channel activity in VTA DA neuron on the initial behavioral effects of cocaine, similar to acute locomotor activity (**Chapters 3 and 5**).

It would also be useful to further characterize other aspects of self-administration in the DATCre(+):*Girk2*$^{fl/fl}$ mice, as well as in VTA DA neuron GIRK overexpression conditions. While acquisition of cocaine self-administration and dose response at a fixed ratio have been described, characterization of breakpoint, extinction, and reinstatement of self-administration by stress, drug cues, and drug exposure will allow for an improved understanding of the GIRK channel's therapeutic potential. This is especially important considering that GIRK channel signaling strength is decreased by acute exposure to psychostimulants (Arora et al., 2011), so there may not be sufficient GIRK channels to exert a therapeutic decrease in VTA DA neuron excitability.

Finally, it would be beneficial to assess how exposure to stress impacts negative affective behaviors and behavioral sensitivity to cocaine in DATCre(+):*Girk2*$^{fl/fl}$ and VTA DA neuron GIRK channel overexpression manipulations. Indeed, VTA DA neuron

excitability has been linked to depression and relapse (Nestler and Carlezon, 2006; Holly and Miczek, 2016), and severe stress, *i.e.* footshock, decreases GIRK channel activity in VTA DA neurons (**Chapter 2**). Thus, GIRK channel manipulation could influence negative affective behavior, but only following stressful experiences.

6.3 Concluding thoughts

This dissertation highlights the role the unique GIRK1-lacking (Cruz et al., 2004; Labouèbe et al., 2007) GIRK channel present in VTA DA neurons plays in tempering the behavioral effects of cocaine. It is tempting to speculate that preferentially engaging the VTA DA neuron GIRK channel with a GIRK2c/GIRK3 channel-specific activator might have therapeutic potential for treating addiction. While there are no such GIRK channel agonists available now, there are some in development. Indeed, the novel compound VU695 is able to reduce the firing rate of VTA DA neurons, but not in putative DA neurons of the VTA in mice lacking GIRK2 (**Figure 6.2**). While this compound is still under development, this is an exciting advance beyond previous GIRK activators, such as ML297 that were selective for GIRK1-containing channels (Wydeven et al., 2014; Kotecki et al., 2015).

There are a number of ways in which GIRK channel agonists could be incorporated into treatment for addiction. GIRK channels activators could potentially be used as a prophylactic to reduce the addictive liability of opioids given to manage pain. GIRK channel activators might also be able to be used to prevent relapse to psychostimulants. Indeed, increased GIRK channel activity decreased initial behavioral responding to cocaine. However, more relevant studies assessing GIRK channel activation on extinction and relapse will be needed before this approach could be tested in human patients with addiction. Overall, inhibitory G protein signaling, especially GIRK

channel activity, in VTA DA neurons represents a promising target for pharmacotherapy to treat addiction.

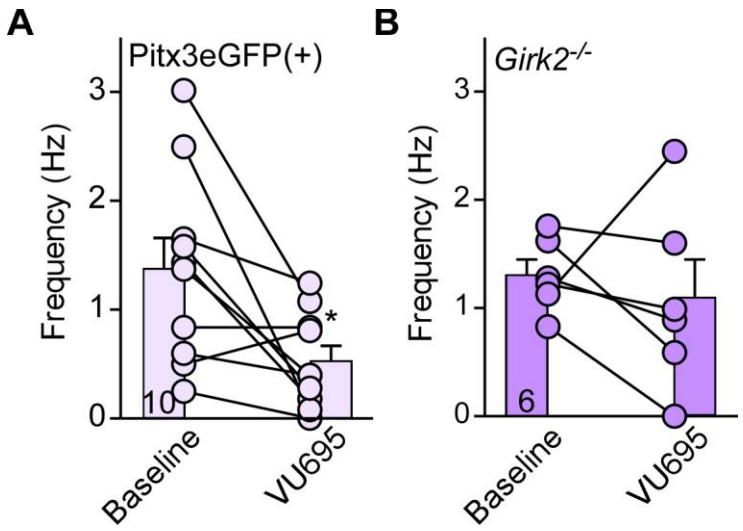

Figure 6.2. VU695 reduces the firing rate of VTA DA neurons in a GIRK2-dependent manner.

A) Spontaneous firing rate of wild type VTA Pitx3eGFP(+) (DA) neurons (n = 10 cells from 4 mice; baseline 1.38 ± 0.28 Hz, VU695 0.53 ± 0.14 Hz; paired t test, $t_9 = 3.01$, $p = 0.015$) following bath application of VU695 (30 μM). **B**) Spontaneous firing rate of putative DA neurons of the VTA in *Girk2*$^{-/-}$ mice (n = 6 cells from 3 mice; baseline 1.31 ± 0.14 Hz, VU695 1.09 ± 0.35 Hz; paired t test, $t_5 = 0.650$, $p = 0.544$).

Bibliography

Abney KK, Bubser M, Du Y, Kozek KA, Bridges TM, Linsdley CW, Daniels JS, Morrison RD, Wickman K, Hopkins CR, Jones CK, Weaver CD (2018) Analgesic effects of the GIRK activator, VU0466551, alone and in combination with morphine in acute and persistent pain models. *ACS Chem Neurosci*: acschemneuro.8b00370. doi 10.1021/acschemneuro.8b00370 pmid:30474955.

Ackerman JM, White FJ (1990) A10 somatodendritic dopamine autoreceptor sensitivity following withdrawal from repeated cocaine treatment. *Neurosci Lett* **117**: 181–187. pmid:2290614.

Adelfinger L, Turecek R, Ivankova K, Jensen AA, Moss SJ, Gassmann M, Bettler B (2014) GABAB receptor phosphorylation regulates KCTD12-induced K^+ current desensitization. *Biochem Pharmacol* **91**: 369–379. doi 10.1016/j.bcp.2014.07.013 pmid:25065880.

Aghajanian GK, VanderMaelen CP (1982) alpha 2-adrenoceptor-mediated hyperpolarization of locus coeruleus neurons: intracellular studies in vivo. *Science* **215**: 1394–1396. pmid:6278591.

Al-Hasani R, McCall JG, Shin G, Gomez AM, Schmitz GP, Bernardi JM, Pyo C-O, Park S Il, Marcinkiewcz CM, Crowley NA, Krashes MJ, Lowell BB, Kash TL, Rogers JA, Bruchas MR (2015) Distinct subpopulations of nucleus accumbens dynorphin neurons drive aversion and reward. *Neuron* **87**: 1063–1077. doi 10.1016/j.neuron.2015.08.019 pmid:26335648.

American Psychiatric Association (2013) Diagnostic and Statistical Manual of Mental Disorders. American Psychiatric Association. doi 10.1176/appi.books.9780890425596.

Anderson GR, Cao Y, Davidson S, Truong H V, Pravetoni M, Thomas MJ, Wickman K, Giesler GJ, Martemyanov KA (2010) R7BP complexes with RGS9-2 and RGS7 in the striatum differentially control motor learning and locomotor responses to cocaine. *Neuropsychopharmacology* **35**: 1040–1050. doi 10.1038/npp.2009.212 pmid:20043004.

Anderson GR, Lujan R, Martemyanov KA (2009) Changes in striatal signaling induce remodeling of RGS complexes containing G5 and R7BP subunits. *Mol Cell Biol* **29**: 3033–3044. doi 10.1128/MCB.01449-08 pmid:19332565.

Anstrom KK, Woodward DJ (2005) Restraint increases dopaminergic burst firing in awake rats. *Neuropsychopharmacology* **30**: 1832–1840. doi 10.1038/sj.npp.1300730.

Aragona BJ, Cleaveland NA, Stuber GD, Day JJ, Carelli RM, Wightman RM (2008) Preferential enhancement of dopamine transmission within the nucleus accumbens shell by cocaine is attributable to a direct increase in phasic dopamine release events. *J Neurosci* **28**: 8821–8831. doi 10.1523/JNEUROSCI.2225-08.2008 pmid:18753384.

Armbruster BN, Li X, Pausch MH, Herlitze S, Roth BL (2007) Evolving the lock to fit the key to create a family of G protein-coupled receptors potently activated by an inert ligand. *Proc Natl Acad Sci* **104**: 5163–5168. doi 10.1073/pnas.0700293104 pmid:17360345.

Arora D, Haluk DM, Kourrich S, Pravetoni M, Fernández-Alacid L, Nicolau JC, Luján R, Wickman K (2010) Altered neurotransmission in the mesolimbic reward system of Girk mice. *J Neurochem* **114**: 1487–1497. doi 10.1111/j.1471-4159.2010.06864.x

pmid:20557431.
Arora D, Hearing M, Haluk DM, Mirkovic K, Fajardo-Serrano A, Wessendorf MW, Watanabe M, Luján R, Wickman K (2011) Acute cocaine exposure weakens GABA(B) receptor-dependent G-protein-gated inwardly rectifying K+ signaling in dopamine neurons of the ventral tegmental area. *J Neurosci* **31**: 12251–12257. doi 10.1523/JNEUROSCI.0494-11.2011 pmid:21865468.
Aryal P, Dvir H, Choe S, Slesinger PA (2009) A discrete alcohol pocket involved in GIRK channel activation. *Nat Neurosci* **12**: 988–995. doi 10.1038/nn.2358 pmid:19561601.
Avery SN, Clauss JA, Blackford JU (2016) The human BNST: functional role in anxiety and addiction. *Neuropsychopharmacology* **41**: 126–141. doi 10.1038/npp.2015.185 pmid:26105138.
Backes EN, Hemby SE (2008) Contribution of ventral tegmental GABA receptors to cocaine self-administration in rats. *Neurochem Res* **33**: 459–467. doi 10.1007/s11064-007-9454-2 pmid:17943439.
Bäckman CM, Malik N, Zhang Y, Shan L, Grinberg A, Hoffer BJ, Westphal H, Tomac AC (2006) Characterization of a mouse strain expressing Cre recombinase from the 3′ untranslated region of the dopamine transporter locus. *genesis* **44**: 383–390. doi 10.1002/dvg.20228 pmid:16865686.
Balana B, Bahima L, Bodhinathan K, Taura JJ, Taylor NM, Nettleton MY, Ciruela F, Slesinger PA (2013) Ras-association domain of sorting nexin 27 Is critical for regulating expression of GIRK potassium channels Ikeda K, ed. *PLoS One* **8**: e59800. doi 10.1371/journal.pone.0059800 pmid:23536889.
Balana B, Maslennikov I, Kwiatkowski W, Stern KM, Bahima L, Choe S, Slesinger PA (2011) Mechanism underlying selective regulation of G protein-gated inwardly rectifying potassium channels by the psychostimulant-sensitive sorting nexin 27. *Proc Natl Acad Sci U S A* **108**: 5831–5836. doi 10.1073/pnas.1018645108 pmid:21422294.
Beart PM, McDonald D, Gundlach AL (1979) Mesolimbic dopaminergic neurones and somatodendritic mechanisms. *Neurosci Lett* **15**: 165–170. pmid:43496.
Bechtholt AJ, Cunningham CL (2005) Ethanol-induced conditioned place preference is expressed through a ventral tegmental area dependent mechanism. *Behav Neurosci* **119**: 213–223. doi 10.1037/0735-7044.119.1.213 pmid:15727526.
Beckstead MJ, Grandy DK, Wickman K, Williams JT (2004) Vesicular dopamine release elicits an inhibitory postsynaptic current in midbrain dopamine neurons. *Neuron* **42**: 939–946. doi 10.1016/j.neuron.2004.05.019 pmid:15207238.
Behbehani MM (1995) Functional characteristics of the midbrain periaqueductal gray. *Prog Neurobiol* **46**: 575–605. pmid:8545545.
Beier KT, Steinberg EE, DeLoach KE, Xie S, Miyamichi K, Schwarz L, Gao XJ, Kremer EJ, Malenka RC, Luo L (2015) Circuit Architecture of VTA Dopamine Neurons Revealed by Systematic Input-Output Mapping. *Cell* **162**: 622–634. doi 10.1016/j.cell.2015.07.015 pmid:26232228.
Bell J (2014) Pharmacological maintenance treatments of opiate addiction. *Br J Clin Pharmacol* **77**: 253–263. doi 10.1111/bcp.12051 pmid:23210630.
Bello EP, Mateo Y, Gelman DM, Noaín D, Shin JH, Low MJ, Alvarez VA, Lovinger DM, Rubinstein M (2011) Cocaine supersensitivity and enhanced motivation for reward in mice lacking dopamine D2 autoreceptors. *Nat Neurosci* **14**: 1033–1038. doi 10.1038/nn.2862 pmid:21743470.
Belujon P, Grace AA (2017) Dopamine system dysregulation in major depressive

disorders. *Int J Neuropsychopharmacol* **20**: 1036–1046. doi 10.1093/ijnp/pyx056 pmid:29106542.
Berridge KC (2007) The debate over dopamine's role in reward: the case for incentive salience. *Psychopharmacology (Berl)* **191**: 391–431. doi 10.1007/s00213-006-0578-x pmid:17072591.
Berridge KC, Robinson TE (1998) What is the role of dopamine in reward: hedonic impact, reward learning, or incentive salience? *Brain Res Brain Res Rev* **28**: 309–369. pmid:9858756.
Berridge KC, Robinson TE, Aldridge JW (2009) Dissecting components of reward: "liking", "wanting", and learning. *Curr Opin Pharmacol* **9**: 65–73. doi 10.1016/j.coph.2008.12.014 pmid:19162544.
Berrios J, Stamatakis AM, Kantak PA, McElligott ZA, Judson MC, Aita M, Rougie M, Stuber GD, Philpot BD (2016) Loss of UBE3A from TH-expressing neurons suppresses GABA co-release and enhances VTA-NAc optical self-stimulation. *Nat Commun* **7**: 10702. doi 10.1038/ncomms10702 pmid:26869263.
Blednov YA, Stoffel M, Alva H, Harris RA (2003) A pervasive mechanism for analgesia: activation of GIRK2 channels. *Proc Natl Acad Sci U S A* **100**: 277–282. doi 10.1073/pnas.012682399 pmid:12493843.
Blednov YA, Stoffel M, Chang SR, Harris RA (2001) Potassium channels as targets for ethanol: studies of G-protein-coupled inwardly rectifying potassium channel 2 (GIRK2) null mutant mice. *J Pharmacol Exp Ther* **298**: 521–530. pmid:11454913.
Blednov YA, Stoffel M, Cooper R, Wallace D, Mane N, Harris RA (2002) Hyperactivity and dopamine D1 receptor activation in mice lacking girk2 channels. *Psychopharmacology (Berl)* **159**: 370–378. doi 10.1007/s00213-001-0937-6 pmid:11823889.
Bocklisch C, Pascoli V, Wong JCY, House DRC, Yvon C, de Roo M, Tan KR, Luscher C, Lüscher C (2013) Cocaine disinhibits dopamine neurons by potentiation of GABA transmission in the ventral tegmental area. *Science* **341**: 1521–1525. doi 10.1126/science.1237059 pmid:24072923.
Brabant C, Quertemont E, Tirelli E (2005) Influence of the dose and the number of drug-context pairings on the magnitude and the long-lasting retention of cocaine-induced conditioned place preference in C57BL/6J mice. *Psychopharmacology (Berl)* **180**: 33–40. doi 10.1007/s00213-004-2138-6 pmid:15682299.
Brebner K, Phelan R, Roberts DC (2000) Intra-VTA baclofen attenuates cocaine self-administration on a progressive ratio schedule of reinforcement. *Pharmacol Biochem Behav* **66**: 857–862. pmid:10973526.
Brischoux F, Chakraborty S, Brierley DI, Ungless MA (2009) Phasic excitation of dopamine neurons in ventral VTA by noxious stimuli. *Proc Natl Acad Sci U S A* **106**: 4894–4899. doi 10.1073/pnas.0811507106 pmid:19261850.
Britt JP, Bonci A (2013) Optogenetic interrogations of the neural circuits underlying addiction. *Curr Opin Neurobiol* **23**: 539–545. doi 10.1016/j.conb.2013.01.010 pmid:23375167.
Brodie MS, Dunwiddie T V (1990) Cocaine effects in the ventral tegmental area: evidence for an indirect dopaminergic mechanism of action. *Naunyn Schmiedebergs Arch Pharmacol* **342**: 660–665. pmid:2096297.
Bromberg-Martin ES, Matsumoto M, Hikosaka O (2010) Dopamine in motivational control: rewarding, aversive, and alerting. *Neuron* **68**: 815–834. doi 10.1016/j.neuron.2010.11.022 pmid:21144997.
Brown MTC, Tan KR, O'Connor EC, Nikonenko I, Muller D, Lüscher C (2012) Ventral

tegmental area GABA projections pause accumbal cholinergic interneurons to enhance associative learning. *Nature* **492**: 452–456. doi 10.1038/nature11657 pmid:23178810.
Brown SG, Thomas A, Dekker L V, Tinker A, Leaney JL (2005) PKC-delta sensitizes Kir3.1/3.2 channels to changes in membrane phospholipid levels after M3 receptor activation in HEK-293 cells. *Am J Physiol Cell Physiol* **289**: C543-56. doi 10.1152/ajpcell.00025.2005 pmid:15857907.
Cachope R, Mateo Y, Mathur BN, Irving J, Wang H-L, Morales M, Lovinger DM, Cheer JF (2012) Selective activation of cholinergic interneurons enhances accumbal phasic dopamine release: setting the tone for reward processing. *Cell Rep* **2**: 33–41. doi 10.1016/j.celrep.2012.05.011 pmid:22840394.
Cao J-L, Covington HE, Friedman AK, Wilkinson MB, Walsh JJ, Cooper DC, Nestler EJ, Han M-H (2010) Mesolimbic dopamine neurons in the brain reward circuit mediate susceptibility to social defeat and antidepressant action. *J Neurosci* **30**: 16453–16458. doi 10.1523/JNEUROSCI.3177-10.2010 pmid:21147984.
Carr DB, O'Donnell P, Card JP, Sesack SR (1999) Dopamine terminals in the rat prefrontal cortex synapse on pyramidal cells that project to the nucleus accumbens. *J Neurosci* **19**: 11049–11060. pmid:10594085.
Carr DB, Sesack SR (1999) Terminals from the rat prefrontal cortex synapse on mesoaccumbens VTA neurons. *Ann N Y Acad Sci* **877**: 676–678. pmid:10415681.
Carr DB, Sesack SR (2000) Projections from the rat prefrontal cortex to the ventral tegmental area: target specificity in the synaptic associations with mesoaccumbens and mesocortical neurons. *J Neurosci* **20**: 3864–3873. pmid:10804226.
Castellanos-Ryan N, Conrod PJ (2011) Personality correlates of the common and unique variance across conduct disorder and substance misuse symptoms in adolescence. *J Abnorm Child Psychol* **39**: 563–576. doi 10.1007/s10802-010-9481-3 pmid:21181434.
Castro DC, Berridge KC (2014) Advances in the neurobiological bases for food "liking" versus "wanting". *Physiol Behav* **136**: 22–30. doi 10.1016/j.physbeh.2014.05.022 pmid:24874776.
Castro DC, Cole SL, Berridge KC (2015) Lateral hypothalamus, nucleus accumbens, and ventral pallidum roles in eating and hunger: interactions between homeostatic and reward circuitry. *Front Syst Neurosci* **9**: 90. doi 10.3389/fnsys.2015.00090.
Chan KW, Sui JL, Vivaudou M, Logothetis DE (1997) Specific regions of heteromeric subunits involved in enhancement of G protein-gated K+ channel activity. *J Biol Chem* **272**: 6548–6555. pmid:9045681.
Charara A, Smith Y, Parent A (1996) Glutamatergic inputs from the pedunculopontine nucleus to midbrain dopaminergic neurons in primates: Phaseolus vulgaris-leucoagglutinin anterograde labeling combined with postembedding glutamate and GABA immunohistochemistry. *J Comp Neurol* **364**: 254–266. doi 10.1002/(SICI)1096-9861(19960108)364:2<254::AID-CNE5>3.0.CO;2-4 pmid:8788248.
Chaudhury D et al. (2013) Rapid regulation of depression-related behaviours by control of midbrain dopamine neurons. *Nature* **493**: 532–536. doi 10.1038/nature11713 pmid:23235832.
Chen NH, Reith ME (1994) Autoregulation and monoamine interactions in the ventral tegmental area in the absence and presence of cocaine: a microdialysis study in freely moving rats. *J Pharmacol Exp Ther* **271**: 1597–1610. pmid:7996474.
Chen R, Tilley MR, Wei H, Zhou F, Zhou F-M, Ching S, Quan N, Stephens RL, Hill ER,

Nottoli T, Han DD, Gu HH (2006) Abolished cocaine reward in mice with a cocaine-insensitive dopamine transporter. *Proc Natl Acad Sci* **103**: 9333–9338. doi 10.1073/pnas.0600905103 pmid:16754872.
Chuang HH, Yu M, Jan YN, Jan LY (1998) Evidence that the nucleotide exchange and hydrolysis cycle of G proteins causes acute desensitization of G-protein gated inward rectifier K+ channels. *Proc Natl Acad Sci U S A* **95**: 11727–11732. pmid:9751733.
Chuhma N, Mingote S, Moore H, Rayport S (2014) Dopamine neurons control striatal cholinergic neurons via regionally heterogeneous dopamine and glutamate signaling. *Neuron* **81**: 901–912. doi 10.1016/j.neuron.2013.12.027 pmid:24559678.
Ciruela F, Fernández-Dueñas V, Sahlholm K, Fernández-Alacid L, Nicolau JC, Watanabe M, Luján R (2010) Evidence for oligomerization between GABAB receptors and GIRK channels containing the GIRK1 and GIRK3 subunits. *Eur J Neurosci* **32**: 1265–1277. doi 10.1111/j.1460-9568.2010.07356.x pmid:20846323.
Clancy SM, Fowler CE, Finley M, Suen KF, Arrabit C, Berton F, Kosaza T, Casey PJ, Slesinger PA (2005) Pertussis-toxin-sensitive Gα subunits selectively bind to C-terminal domain of neuronal GIRK channels: evidence for a heterotrimeric G-protein-channel complex. *Mol Cell Neurosci* **28**: 375–389. doi 10.1016/j.mcn.2004.10.009 pmid:15691717.
Cohen JY, Haesler S, Vong L, Lowell BB, Uchida N (2012) Neuron-type-specific signals for reward and punishment in the ventral tegmental area. *Nature* **482**: 85–88. doi 10.1038/nature10754 pmid:22258508.
Conrad KL, Davis AR, Silberman Y, Sheffler DJ, Shields AD, Saleh SA, Sen N, Matthies HJG, Javitch JA, Lindsley CW, Winder DG (2012) Yohimbine depresses excitatory transmission in BNST and impairs extinction of cocaine place preference through orexin-dependent, norepinephrine-independent processes. *Neuropsychopharmacology* **37**: 2253–2266. doi 10.1038/npp.2012.76 pmid:22617356.
Contarino A, Picetti R, Matthes HW, Koob GF, Kieffer BL, Gold LH (2002) Lack of reward and locomotor stimulation induced by heroin in mu-opioid receptor-deficient mice. *Eur J Pharmacol* **446**: 103–109. pmid:12098591.
Corre J, van Zessen R, Loureiro M, Patriarchi T, Tian L, Pascoli V, Lüscher C (2018) Dopamine neurons projecting to medial shell of the nucleus accumbens drive heroin reinforcement. *Elife* **7** doi 10.7554/eLife.39945 pmid:30373717.
Costa ACS, Stasko MR, Stoffel M, Scott-McKean JJ (2005) G-protein-gated potassium (GIRK) channels containing the GIRK2 subunit are control hubs for pharmacologically induced hypothermic responses. *J Neurosci* **25**: 7801–7804. doi 10.1523/JNEUROSCI.1699-05.2005 pmid:16120781.
Cruz HG, Berton F, Sollini M, Blanchet C, Pravetoni M, Wickman K, Lüscher C (2008) Absence and rescue of morphine withdrawal in GIRK/Kir3 knock-out mice. *J Neurosci* **28**: 4069–4077. doi 10.1523/JNEUROSCI.0267-08.2008 pmid:18400906.
Cruz HG, Ivanova T, Lunn M-L, Stoffel M, Slesinger PA, Lüscher C (2004) Bi-directional effects of GABA(B) receptor agonists on the mesolimbic dopamine system. *Nat Neurosci* **7**: 153–159. doi 10.1038/nn1181 pmid:14745451.
Daubner SC, Le T, Wang S (2011) Tyrosine hydroxylase and regulation of dopamine synthesis. *Arch Biochem Biophys* **508**: 1–12. doi 10.1016/j.abb.2010.12.017 pmid:21176768.
de Jong JW, Afjei SA, Pollak Dorocic I, Peck JR, Liu C, Kim CK, Tian L, Deisseroth K, Lammel S (2019) A neural circuit mechanism for encoding aversive stimuli in the

mesolimbic dopamine system. *Neuron* **0**: 133–151.e7. doi 10.1016/j.neuron.2018.11.005 pmid:30503173.

de Jong JW, Roelofs TJM, Mol FMU, Hillen AEJ, Meijboom KE, Luijendijk MCM, van der Eerden HAM, Garner KM, Vanderschuren LJMJ, Adan RAH (2015) Reducing ventral tegmental dopamine D2 receptor expression selectively boosts incentive motivation. *Neuropsychopharmacology* **40**: 2085–2095. doi 10.1038/npp.2015.60 pmid:25735756.

de Miguel E, Vekovischeva O, Kuokkanen K, Vesajoki M, Paasikoski N, Kaskinoro J, Myllymäki M, Lainiola M, Janhunen SK, Hyytiä P, Linden A-M, Korpi ER (2018) GABA B receptor positive allosteric modulators with different efficacies affect neuroadaptation to and self-administration of alcohol and cocaine. *Addict Biol* doi 10.1111/adb.12688 pmid:30421860.

DeMaria JE, Nagy GM, Lerant AA, Fekete MIE, Levenson CW, Freeman ME (2000) Dopamine transporters participate in the physiological regulation of prolactin. *Endocrinology* **141**: 366–374. doi 10.1210/endo.141.1.7281 pmid:10614659.

Di Chiara G, Imperato A (1988) Drugs abused by humans preferentially increase synaptic dopamine concentrations in the mesolimbic system of freely moving rats. *Proc Natl Acad Sci U S A* **85**: 5274–5278. pmid:2899326.

Di Giannuario A, Pieretti S (2000) Nociceptin differentially affects morphine-induced dopamine release from the nucleus accumbens and nucleus caudate in rats. *Peptides* **21**: 1125–1130. pmid:10998547.

Dobi A, Margolis EB, Wang H-L, Harvey BK, Morales M (2010) Glutamatergic and nonglutamatergic neurons of the ventral tegmental area establish local synaptic contacts with dopaminergic and nondopaminergic neurons. *J Neurosci* **30**: 218–229. doi 10.1523/JNEUROSCI.3884-09.2010 pmid:20053904.

Doupnik CA, Davidson N, Lester HA, Kofuji P (1997) RGS proteins reconstitute the rapid gating kinetics of gbetagamma-activated inwardly rectifying K+ channels. *Proc Natl Acad Sci U S A* **94**: 10461–10466. pmid:9294233.

Duszkiewicz AJ, McNamara CG, Takeuchi T, Genzel L (2018) Novelty and dopaminergic modulation of memory persistence: a tale of two systems. *Trends Neurosci* doi 10.1016/j.tins.2018.10.002 pmid:30455050.

Edwards NJ, Tejeda HA, Pignatelli M, Zhang S, McDevitt RA, Wu J, Bass CE, Bettler B, Morales M, Bonci A (2017) Circuit specificity in the inhibitory architecture of the VTA regulates cocaine-induced behavior. *Nat Neurosci* **20**: 438–448. doi 10.1038/nn.4482 pmid:28114294.

Einhorn LC, Johansen PA, White FJ (1988) Electrophysiological effects of cocaine in the mesoaccumbens dopamine system: studies in the ventral tegmental area. *J Neurosci* **8**: 100–112. pmid:3339402.

Fadel J, Deutch AY (2002) Anatomical substrates of orexin-dopamine interactions: lateral hypothalamic projections to the ventral tegmental area. *Neuroscience* **111**: 379–387. pmid:11983323.

Faget L, Osakada F, Duan J, Ressler R, Johnson AB, Proudfoot JA, Yoo JH, Callaway EM, Hnasko TS (2016) Afferent inputs to neurotransmitter-defined cell types in the ventral tegmental area. *Cell Rep* **15**: 2796–2808. doi 10.1016/j.celrep.2016.05.057 pmid:27292633.

Fajardo-Serrano A, Wydeven N, Young D, Watanabe M, Shigemoto R, Martemyanov KA, Wickman K, Luján R (2013) Association of Rgs7/Gβ5 complexes with GIRK channels and GABA B receptors in hippocampal CA1 pyramidal neurons. *Hippocampus* **23**: 1231–1245. doi 10.1002/hipo.22161 pmid:23804514.

Ferguson SM, Eskenazi D, Ishikawa M, Wanat MJ, Phillips PEM, Dong Y, Roth BL, Neumaier JF (2011) Transient neuronal inhibition reveals opposing roles of indirect and direct pathways in sensitization. *Nat Neurosci* **14**: 22–24. doi 10.1038/nn.2703 pmid:21131952.

Fields HL, Margolis EB (2015) Understanding opioid reward. *Trends Neurosci* **38**: 217–225. doi 10.1016/j.tins.2015.01.002 pmid:25637939.

Fields TA, Casey PJ (1997) Signalling functions and biochemical properties of pertussis toxin-resistant G-proteins. *Biochem J* **321 (Pt 3)**: 561–571. doi 10.1042/BJ3210561 pmid:9032437.

Filip M, Frankowska M, Przegaliński E (2007) Effects of GABAB receptor antagonist, agonists and allosteric positive modulator on the cocaine-induced self-administration and drug discrimination. *Eur J Pharmacol* **574**: 148–157. doi 10.1016/j.ejphar.2007.07.048 pmid:17698060.

Finley M, Arrabit C, Fowler C, Suen KF, Slesinger PA (2004) βL-βM loop in the C-terminal domain of G protein-activated inwardly rectifying K^+ channels is important for $G_{\beta\gamma}$ subunit activation. *J Physiol* **555**: 643–657. doi 10.1113/jphysiol.2003.056101 pmid:14724209.

Flagel SB, Akil H, Robinson TE (2009) Individual differences in the attribution of incentive salience to reward-related cues: Implications for addiction. *Neuropharmacology* **56**: 139–148. doi 10.1016/j.neuropharm.2008.06.027 pmid:18619474.

Ford CP (2014) The role of D2-autoreceptors in regulating dopamine neuron activity and transmission. *Neuroscience* **282**: 13–22. doi 10.1016/j.neuroscience.2014.01.025 pmid:24463000.

Ford CP, Mark GP, Williams JT (2006) Properties and opioid inhibition of mesolimbic dopamine neurons vary according to target location. *J Neurosci* **26**: 2788–2797. doi 10.1523/JNEUROSCI.4331-05.2006 pmid:16525058.

Franklin KBJ, Paxinos G (2008) The mouse brain in stereotaxic coordinates, 3rd ed. Academic Press.

Friedman AK, Juarez B, Ku SM, Zhang H, Calizo RC, Walsh JJ, Chaudhury D, Zhang S, Hawkins A, Dietz DM, Murrough JW, Ribadeneira M, Wong EH, Neve RL, Han M-H (2016) KCNQ channel openers reverse depressive symptoms via an active resilience mechanism. *Nat Commun* **7**: 11671. doi 10.1038/ncomms11671 pmid:27216573.

Friedman AK, Walsh JJ, Juarez B, Ku SM, Chaudhury D, Wang J, Li X, Dietz DM, Pan N, Vialou VF, Neve RL, Yue Z, Han M-H (2014) Enhancing depression mechanisms in midbrain dopamine neurons achieves homeostatic resilience. *Science (80-)* **344**: 313–319. doi 10.1126/science.1249240 pmid:24744379.

Garzo´n M, Garzo´n G, Vaughan RA, Uhl GR, Kuhar MJ, Pickel VM (1999) Cholinergic axon terminals in the ventral tegmental area target a subpopulation of neurons expressing low levels of the dopamine transporter. *J Comp Neurol* **410**: 197–210.

Gasbarri A, Packard MG, Campana E, Pacitti C (1994) Anterograde and retrograde tracing of projections from the ventral tegmental area to the hippocampal formation in the rat. *Brain Res Bull* **33**: 445–452. pmid:8124582.

Gaspari S, Papachatzaki MM, Koo JW, Carr FB, Tsimpanouli M-E, Stergiou E, Bagot RC, Ferguson D, Mouzon E, Chakravarty S, Deisseroth K, Lobo MK, Zachariou V (2014) Nucleus accumbens-specific interventions in RGS9-2 activity modulate responses to morphine. *Neuropsychopharmacology* **39**: 1968–1977. doi 10.1038/npp.2014.45 pmid:24561386.

Georges F, Aston-Jones G (2001) Potent regulation of midbrain dopamine neurons by the bed nucleus of the stria terminalis. *J Neurosci* **21**: RC160. pmid:11473131.
Gold SJ, Ni YG, Dohlman HG, Nestler EJ (1997) Regulators of G-protein signaling (RGS) proteins: region-specific expression of nine subtypes in rat brain. *J Neurosci* **17**: 8024–8037. pmid:9315921.
Goldstein RZ, Volkow ND (2011) Dysfunction of the prefrontal cortex in addiction: neuroimaging findings and clinical implications. *Nat Rev Neurosci* **12**: 652–669. doi 10.1038/nrn3119 pmid:22011681.
Groves PM, Wilson CJ, Young SJ, Rebec G V (1975) Self-inhibition by dopaminergic neurons. *Science* **190**: 522–528. pmid:242074.
Guetg N, Abdel Aziz S, Holbro N, Turecek R, Rose T, Seddik R, Gassmann M, Moes S, Jenoe P, Oertner TG, Casanova E, Bettler B (2010) NMDA receptor-dependent GABAB receptor internalization via CaMKII phosphorylation of serine 867 in GABAB1. *Proc Natl Acad Sci U S A* **107**: 13924–13929. doi 10.1073/pnas.1000909107 pmid:20643921.
Hablitz LM, Molzof HE, Abrahamsson KE, Cooper JM, Prosser RA, Gamble KL (2015) GIRK channels mediate the nonphotic effects of exogenous melatonin. *J Neurosci* **35**: 14957–14965. doi 10.1523/JNEUROSCI.1597-15.2015 pmid:26558769.
Hablitz LM, Molzof HE, Paul JR, Johnson RL, Gamble KL (2014) Suprachiasmatic nucleus function and circadian entrainment are modulated by G protein-coupled inwardly rectifying (GIRK) channels. *J Physiol* **592**: 5079–5092. doi 10.1113/jphysiol.2014.282079 pmid:25217379.
Hall F, Sora I, Drgonova J, Li X, Goeb M, Uhl G (2004) Molecular mechanisms underlying the rewarding effects of cocaine. *Ann N Y Acad Sci* **1025**: 47–56. doi 10.1196/annals.1316.006.
Hauser AS, Attwood MM, Rask-Andersen M, Schiöth HB, Gloriam DE (2017) Trends in GPCR drug discovery: new agents, targets and indications. *Nat Rev Drug Discov* **16**: 829–842. doi 10.1038/nrd.2017.178 pmid:29075003.
He C, Zhang H, Mirshahi T, Logothetis DE (1999) Identification of a potassium channel site that interacts with G protein beta gamma subunits to mediate agonist-induced signaling. *J Biol Chem* **274**: 12517–12524. pmid:10212228.
Hearing M, Kotecki L, Marron Fernandez de Velasco E, Fajardo-Serrano A, Chung HJ, Luján R, Wickman K (2013) Repeated cocaine weakens GABAB-GIRK signaling in layer 5/6 pyramidal neurons in the prelimbic cortex. *Neuron* **80**: 159–170. doi 10.1016/j.neuron.2013.07.019 pmid:24094109.
Hearing MC, Zink AN, Wickman K (2012) Cocaine-induced adaptations in metabotropic inhibitory signaling in the mesocorticolimbic system. *Rev Neurosci* **23**: 325–351. doi 10.1515/revneuro-2012-0045 pmid:22944653.
Herman MA, Sidhu H, Stouffer DG, Kreifeldt M, Le D, Cates-Gatto C, Munoz MB, Roberts AJ, Parsons LH, Roberto M, Wickman K, Slesinger PA, Contet C (2015) GIRK3 gates activation of the mesolimbic dopaminergic pathway by ethanol. *Proc Natl Acad Sci U S A* **112**: 7091–7096. doi 10.1073/pnas.1416146112 pmid:25964320.
Hibino H, Inanobe A, Furutani K, Murakami S, Findlay I, Kurachi Y (2010) Inwardly rectifying potassium channels: their structure, function, and physiological roles. *Physiol Rev* **90**: 291–366. doi 10.1152/physrev.00021.2009 pmid:20086079.
Hill KG, Alva H, Blednov YA, Cunningham CL (2003) Reduced ethanol-induced conditioned taste aversion and conditioned place preference in GIRK2 null mutant mice. *Psychopharmacology (Berl)* **169**: 108–114. doi 10.1007/s00213-003-1472-4

pmid:12721779.
Hjelmstad GO, Xia Y, Margolis EB, Fields HL (2013) Opioid modulation of ventral pallidal afferents to ventral tegmental area neurons. *J Neurosci* **33**: 6454–6459. doi 10.1523/JNEUROSCI.0178-13.2013 pmid:23575843.
Hnasko TS, Hjelmstad GO, Fields HL, Edwards RH (2012) Ventral tegmental area glutamate neurons: electrophysiological properties and projections. *J Neurosci* **32**: 15076–15085. doi 10.1523/JNEUROSCI.3128-12.2012 pmid:23100428.
Hnasko TS, Sotak BN, Palmiter RD (2005) Morphine reward in dopamine-deficient mice. *Nature* **438**: 854–857. doi 10.1038/nature04172 pmid:16341013.
Ho IH, Murrell-Lagnado RD (1999) Molecular determinants for sodium-dependent activation of G protein-gated K+ channels. *J Biol Chem* **274**: 8639–8648. pmid:10085101.
Hofford RS, Wellman PJ, Eitan S (2012) Morphine alters the locomotor responses to a D2/D3 dopamine receptor agonist differentially in adolescent and adult mice. *J Psychopharmacol* **26**: 1355–1365. doi 10.1177/0269881112443741 pmid:22522973.
Hollinger S, Hepler JR (2002) Cellular regulation of RGS proteins: modulators and integrators of G protein signaling. *Pharmacol Rev* **54**: 527–559. pmid:12223533.
Holly EN, Miczek KA (2016) Ventral tegmental area dopamine revisited: effects of acute and repeated stress. *Psychopharmacology (Berl)* **233**: 163–186. doi 10.1007/s00213-015-4151-3 pmid:26676983.
Holroyd KB, Adrover MF, Fuino RL, Bock R, Kaplan AR, Gremel CM, Rubinstein M, Alvarez VA (2015) Loss of feedback inhibition via D2 autoreceptors enhances acquisition of cocaine taking and reactivity to drug-paired cues. *Neuropsychopharmacology* **40**: 1495–1509. doi 10.1038/npp.2014.336 pmid:25547712.
Honda I, Araki K, Honda S, Soeda F, Shin M-C, Misumi S, Yamamura K-I, Takahama K (2018) Deletion of GIRK2 subunit containing GIRK channels of neurons expressing dopamine transporter decrease immobility time on forced swimming in mice. *Neurosci Lett* **665**: 140–146. doi 10.1016/j.neulet.2017.11.028 pmid:29180115.
Hsu PD, Lander ES, Zhang F (2014) Development and applications of CRISPR-Cas9 for genome engineering. *Cell* **157**: 1262–1278. doi 10.1016/j.cell.2014.05.010.
Huang CL, Feng S, Hilgemann DW (1998) Direct activation of inward rectifier potassium channels by PIP2 and its stabilization by Gbetagamma. *Nature* **391**: 803–806. doi 10.1038/35882 pmid:9486652.
Huang CL, Jan YN, Jan LY (1997) Binding of the G protein betagamma subunit to multiple regions of G protein-gated inward-rectifying K+ channels. *FEBS Lett* **405**: 291–298. pmid:9108307.
Huang CL, Slesinger PA, Casey PJ, Jan YN, Jan LY (1995) Evidence that direct binding of G beta gamma to the GIRK1 G protein-gated inwardly rectifying K+ channel is important for channel activation. *Neuron* **15**: 1133–1143. pmid:7576656.
Hurtubise JL, Howland JG (2017) Effects of stress on behavioral flexibility in rodents. *Neuroscience* **345**: 176–192. doi 10.1016/j.neuroscience.2016.04.007 pmid:27066767.
Hyman SE (2005) Addiction: a disease of learning and memory. *Am J Psychiatry* **162**: 1414–1422. doi 10.1176/appi.ajp.162.8.1414 pmid:16055762.
Ikeda K, Kobayashi T, Kumanishi T, Niki H, Yano R (2000) Involvement of G-protein-activated inwardly rectifying K (GIRK) channels in opioid-induced analgesia. *Neurosci Res* **38**: 113–116. pmid:10997585.

Inanobe A, Yoshimoto Y, Horio Y, Morishige KI, Hibino H, Matsumoto S, Tokunaga Y, Maeda T, Hata Y, Takai Y, Kurachi Y (1999) Characterization of G-protein-gated K+ channels composed of Kir3.2 subunits in dopaminergic neurons of the substantia nigra. *J Neurosci* **19**: 1006–1017. pmid:9920664.

Ivanina T, Varon D, Peleg S, Rishal I, Porozov Y, Dessauer CW, Keren-Raifman T, Dascal N (2004) Gαi1and Gαi3 differentially interact with, and regulate, the G protein-activated K+ channel. *J Biol Chem* **279**: 17260–17268. doi 10.1074/jbc.M313425200 pmid:14963032.

Ivankova K, Turecek R, Fritzius T, Seddik R, Prezeau L, Comps-Agrar L, Pin J-P, Fakler B, Besseyrias V, Gassmann M, Bettler B (2013) Up-regulation of GABA $_{B}$ Receptor Signaling by Constitutive Assembly with the K $^{+}$ Channel Tetramerization Domain-containing Protein 12 (KCTD12). *J Biol Chem* **288**: 24848–24856. doi 10.1074/jbc.M113.476770 pmid:23843457.

Jackson SE, McGowan JA, Ubhi HK, Proudfoot H, Shahab L, Brown J, West R (2019) Modelling continuous abstinence rates over time from clinical trials of pharmacological interventions for smoking cessation. *Addiction* doi 10.1111/add.14549 pmid:30614586.

Janak PH, Tye KM (2015) From circuits to behaviour in the amygdala. *Nature* **517**: 284–292. doi 10.1038/nature14188 pmid:25592533.

Jelacic TM, Kennedy ME, Wickman K, Clapham DE, Sims SM, Clapham DE (2000) Functional and biochemical evidence for G-protein-gated inwardly rectifying K+ (GIRK) channels composed of GIRK2 and GIRK3. *J Biol Chem* **275**: 36211–36216. doi 10.1074/jbc.M007087200 pmid:10956667.

Jennings JH, Sparta DR, Stamatakis AM, Ung RL, Pleil KE, Kash TL, Stuber GD (2013) Distinct extended amygdala circuits for divergent motivational states. *Nature* **496**: 224–228. doi 10.1038/nature12041 pmid:23515155.

Jhou TC, Fields HL, Baxter MG, Saper CB, Holland PC (2009) The rostromedial tegmental nucleus (RMTg), a GABAergic afferent to midbrain opamine neurons, encodes aversive stimuli and inhibits motor responses. *Neuron* **61**: 786–800. doi 10.1016/j.neuron.2009.02.001 pmid:19285474.

Johnson EF, Szechtman H (2016) A dose–response study of separate and combined effects of the serotonin agonist 8-OH-DPAT and the dopamine agonist quinpirole on locomotor sensitization, cross-sensitization, and conditioned activity. *Behav Pharmacol* **27**: 439–450. doi 10.1097/FBP.0000000000000219 pmid:26871406.

Johnson SW, North RA (1992) Opioids excite dopamine neurons by hyperpolarization of local interneurons. *J Neurosci* **12**: 483–488. pmid:1346804.

Joubert L, Hanson B, Barthet G, Sebben M, Claeysen S, Hong W, Marin P, Dumuis A, Bockaert J (2004) New sorting nexin (SNX27) and NHERF specifically interact with the 5-HT4a receptor splice variant: roles in receptor targeting. *J Cell Sci* **117**: 5367–5379. doi 10.1242/jcs.01379 pmid:15466885.

Juarez B, Han M-H (2016) Diversity of dopaminergic neural circuits in response to drug exposure. *Neuropsychopharmacology* **41**: 2424–2446. doi 10.1038/npp.2016.32.

Jung TD, Jung PS, Raveendran L, Farbod Y, Dvorkin-Gheva A, Sakic B, Surette MG, Szechtman H (2017) Changes in gut microbiota during development of compulsive checking and locomotor sensitization induced by chronic treatment with the dopamine agonist quinpirole. *Behav Pharmacol* **29**: 1. doi 10.1097/FBP.0000000000000363 pmid:29194070.

Junyent F, Kremer EJ (2015) CAV-2 — why a canine virus is a neurobiologist's best friend. *Curr Opin Pharmacol* **24**: 86–93. doi 10.1016/J.COPH.2015.08.004.

Kabanova A, Pabst M, Lorkowski M, Braganza O, Boehlen A, Nikbakht N, Pothmann L, Vaswani AR, Musgrove R, Di Monte DA, Sauvage M, Beck H, Blaess S (2015) Function and developmental origin of a mesocortical inhibitory circuit. *Nat Neurosci* **18**: 872–882. doi 10.1038/nn.4020 pmid:25961790.

Kajii Y, Muraoka S, Hiraoka S, Fujiyama K, Umino A, Nishikawa T (2003) A developmentally regulated and psychostimulant-inducible novel rat gene mrt1 encoding PDZ-PX proteins isolated in the neocortex. *Mol Psychiatry* **8**: 434–444. doi 10.1038/sj.mp.4001258.

Kamp TJ, Hell JW (2000) Regulation of cardiac L-type calcium channels by protein kinase A and protein kinase C. *Circ Res* **87**: 1095–1102. pmid:11110765.

Kanbara T, Nakamura A, Shibasaki M, Mori T, Suzuki T, Sakaguchi G, Kanemasa T (2014) Morphine and oxycodone, but not fentanyl, exhibit antinociceptive effects mediated by G-protein inwardly rectifying potassium (GIRK) channels in an oxaliplatin-induced neuropathy rat model. *Neurosci Lett* **580**: 119–124. doi 10.1016/j.neulet.2014.08.005 pmid:25128218.

Kao C-Y, Stalla G, Stalla J, Wotjak CT, Anderzhanova E (2015) Norepinephrine and corticosterone in the medial prefrontal cortex and hippocampus predict PTSD-like symptoms in mice. *Eur J Neurosci* **41**: 1139–1148. doi 10.1111/ejn.12860 pmid:25720329.

Karschin C, Dissmann E, Stühmer W, Karschin A, Averill S, Yan Q, McMahon S, Priestly J (1996) IRK(1-3) and GIRK(1-4) inwardly rectifying K+ channel mRNAs are differentially expressed in the adult rat brain. *J Neurosci* **16**: 3559–3570. doi 10.1523/jneurosci.3693-06.2006 pmid:8642402.

Kaufling J, Veinante P, Pawlowski SA, Freund-Mercier M-J, Barrot M (2010) γ-aminobutyric acid cells with cocaine-induced ΔFosB in the ventral tegmental area innervate mesolimbic neurons. *Biol Psychiatry* **67**: 88–92. doi 10.1016/j.biopsych.2009.08.001 pmid:19748079.

Kaufmann K, Romaine I, Days E, Pascual C, Malik A, Yang L, Zou B, Du Y, Sliwoski G, Morrison RD, Denton J, Niswender CM, Daniels JS, Sulikowski GA, Xie X (Simon), Lindsley CW, Weaver CD (2013) ML297 (VU0456810), the First Potent and Selective Activator of the GIRK Potassium Channel, Displays Antiepileptic Properties in Mice. *ACS Chem Neurosci* **4**: 1278–1286. doi 10.1021/cn400062a pmid:23730969.

Kelly MJ, Qiu J, Rønnekleiv OK (2003) Estrogen modulation of G-protein-coupled receptor activation of potassium channels in the central nervous system. *Ann N Y Acad Sci* **1007**: 6–16. pmid:14993035.

Kennedy ME, Nemec J, Corey S, Wickman K, Clapham DE (1999) GIRK4 confers appropriate processing and cell surface localization to G-protein-gated potassium channels. *J Biol Chem* **274**: 2571–2582. pmid:9891030.

Kim CK, Adhikari A, Deisseroth K (2017) Integration of optogenetics with complementary methodologies in systems neuroscience. *Nat Rev Neurosci* **18**: 222–235. doi 10.1038/nrn.2017.15 pmid:28303019.

Kim J-I, Ganesan S, Luo SX, Wu Y-W, Park E, Huang EJ, Chen L, Ding JB (2015) Aldehyde dehydrogenase 1a1 mediates a GABA synthesis pathway in midbrain dopaminergic neurons. *Science (80-)* **350**: 102–106. doi 10.1126/science.aac4690 pmid:26430123.

Kim JH, Lee S-R, Li L-H, Park H-J, Park J-H, Lee KY, Kim M-K, Shin BA, Choi S-Y (2011) High cleavage efficiency of a 2A peptide derived from porcine teschovirus-1 in human cell lines, zebrafish and mice Thiel V, ed. *PLoS One* **6**: e18556. doi

10.1371/journal.pone.0018556.
Klitenick MA, Deutch AY, Churchill L, Kalivas PW (1992) Topography and functional role of dopaminergic projections from the ventral mesencephalic tegmentum to the ventral pallidum. *Neuroscience* **50**: 371–386. doi 10.1016/0306-4522(92)90430-A.
Kobayashi T, Ikeda K, Kojima H, Niki H, Yano R, Yoshioka T, Kumanishi T (1999) Ethanol opens G-protein-activated inwardly rectifying K+channels. *Nat Neurosci* **2**: 1091–1097. doi 10.1038/16019 pmid:10570486.
Kobayashi T, Washiyama K, Ikeda K (2004) Modulators of G protein-activated inwardly rectifying K + channels: potentially therapeutic agents for addictive drug ssers. *Ann N Y Acad Sci* **1025**: 590–594. doi 10.1196/annals.1316.073 pmid:15542767.
Kofuji P, Davidson N, Lester HA (1995) Evidence that neuronal G-protein-gated inwardly rectifying K+ channels are activated by G beta gamma subunits and function as heteromultimers. *Proc Natl Acad Sci U S A* **92**: 6542–6546. pmid:7604029.
Koob GF, Le Moal M (2005) Plasticity of reward neurocircuitry and the “dark side” of drug addiction. *Nat Neurosci* **8**: 1442–1444. doi 10.1038/nn1105-1442 pmid:16251985.
Koob GF, Volkow ND (2016) Neurobiology of addiction: a neurocircuitry analysis. *Lancet* **3**: 760–773. doi 10.1016/S2215-0366(16)00104-8 pmid:27475769.
Korotkova TM, Brown RE, Sergeeva OA, Ponomarenko AA, Haas HL (2006) Effects of arousal- and feeding-related neuropeptides on dopaminergic and GABAergic neurons in the ventral tegmental area of the rat. *Eur J Neurosci* **23**: 2677–2685. doi 10.1111/j.1460-9568.2006.04792.x pmid:16817870.
Korotkova TM, Sergeeva OA, Eriksson KS, Haas HL, Brown RE (2003) Excitation of ventral tegmental area dopaminergic and nondopaminergic neurons by orexins/hypocretins. *J Neurosci* **23**: 7–11. pmid:12514194.
Kotecki L, Hearing M, McCall NM, Marron Fernandez de Velasco E, Pravetoni M, Arora D, Victoria NC, Munoz MB, Xia Z, Slesinger PA, Weaver CD, Wickman K (2015) GIRK channels modulate opioid-induced motor activity in a cell type- and subunit-dependent manner. *J Neurosci* **35**: 7131–7142. doi 10.1523/JNEUROSCI.5051-14.2015 pmid:25948263.
Koyrakh L, Luján R, Colón J, Karschin C, Kurachi Y, Karschin A, Wickman K (2005) Molecular and cellular diversity of neuronal G-protein-gated potassium channels. *J Neurosci* **25**: 11468–11478. doi 10.1523/JNEUROSCI.3484-05.2005 pmid:16339040.
Kramer PF, Williams JT (2016) Calcium release from stores inhibits GIRK. *Cell Rep* **17**: 3246–3255. doi 10.1016/j.celrep.2016.11.076 pmid:28009293.
Kranzler HR, Soyka M (2018) Diagnosis and pharmacotherapy of alcohol use disorder. *JAMA* **320**: 815. doi 10.1001/jama.2018.11406 pmid:30167705.
Krapivinsky G, Krapivinsky L, Wickman K, Clapham DE (1995) G beta gamma binds directly to the G protein-gated K+ channel, IKACh. *J Biol Chem* **270**: 29059–29062. pmid:7493925.
Krishnan V et al. (2007) Molecular adaptations underlying susceptibility and resistance to social defeat in brain reward regions. *Cell* **131**: 391–404. doi 10.1016/J.CELL.2007.09.018.
Kudo T, Uchigashima M, Miyazaki T, Konno K, Yamasaki M, Yanagawa Y, Minami M, Watanabe M (2012) Three types of neurochemical projection from the bed nucleus of the stria terminalis to the ventral tegmental area in adult mice. *J Neurosci* **32**: 18035–18046. doi 10.1523/JNEUROSCI.4057-12.2012 pmid:23238719.
Kushner SA, Unterwald EM (2001) Chronic cocaine administration decreases the

functional coupling of GABA(B) receptors in the rat ventral tegmental area as measured by baclofen-stimulated 35S-GTPgammaS binding. *Life Sci* **69**: 1093–1102. pmid:11508652.

Labouèbe G, Lomazzi M, Cruz HG, Creton C, Luján R, Li M, Yanagawa Y, Obata K, Watanabe M, Wickman K, Boyer SB, Slesinger PA, Lüscher C (2007) RGS2 modulates coupling between GABAB receptors and GIRK channels in dopamine neurons of the ventral tegmental area. *Nat Neurosci* **10**: 1559–1568. doi 10.1038/nn2006 pmid:17965710.

Lalive AL, Munoz MB, Bellone C, Slesinger PA, Lüscher C, Tan KR (2014) Firing modes of dopamine neurons drive bidirectional GIRK channel plasticity. *J Neurosci* **34**: 5107–5114. doi 10.1523/JNEUROSCI.5203-13.2014 pmid:24719090.

Lammel S, Hetzel A, Häckel O, Jones I, Liss B, Roeper J (2008) Unique properties of mesoprefrontal neurons within a dual mesocorticolimbic dopamine system. *Neuron* **57**: 760–773. doi 10.1016/j.neuron.2008.01.022 pmid:18341995.

Lammel S, Ion DI, Roeper J, Malenka RC (2011) Projection-specific modulation of dopamine neuron synapses by aversive and rewarding stimuli. *Neuron* **70**: 855–862. doi 10.1016/j.neuron.2011.03.025 pmid:21658580.

Lammel S, Lim BK, Malenka RC (2014) Reward and aversion in a heterogeneous midbrain dopamine system. *Neuropharmacology* **76**: 351–359. doi 10.1016/j.neuropharm.2013.03.019 pmid:23578393.

Lammel S, Lim BK, Ran C, Huang KW, Betley MJ, Tye KM, Deisseroth K, Malenka RC (2012) Input-specific control of reward and aversion in the ventral tegmental area. *Nature* **491**: 212–217. doi 10.1038/nature11527.

Lammel S, Steinberg EE, Földy C, Wall NR, Beier K, Luo L, Malenka RC (2015) Diversity of transgenic mouse models for selective targeting of midbrain dopamine neurons. *Neuron* **85**: 429–438. doi 10.1016/j.neuron.2014.12.036 pmid:25611513.

Lavine N, Ethier N, Oak JN, Pei L, Liu F, Trieu P, Rebois RV, Bouvier M, Hebert TE, Van Tol HHM (2002) G protein-coupled receptors form stable complexes with inwardly rectifying potassium channels and adenylyl cyclase. *J Biol Chem* **277**: 46010–46019. doi 10.1074/jbc.M205035200 pmid:12297500.

Leaney JL, Dekker L V, Tinker A (2001) Regulation of a G protein-gated inwardly rectifying K+ channel by a Ca(2+)-independent protein kinase C. *J Physiol* **534**: 367–379. pmid:11454957.

Leaney JL, Tinker A (2000) The role of members of the pertussis toxin-sensitive family of G proteins in coupling receptors to the activation of the G protein-gated inwardly rectifying potassium channel. *Proc Natl Acad Sci* **97**: 5651–5656. doi 10.1073/pnas.080572297 pmid:10779550.

Lecca S, Melis M, Luchicchi A, Muntoni AL, Pistis M (2012) Inhibitory inputs from rostromedial tegmental neurons regulate spontaneous activity of midbrain dopamine cells and their responses to drugs of abuse. *Neuropsychopharmacology* **37**: 1164–1176. doi 10.1038/npp.2011.302 pmid:22169942.

Lecca S, Pelosi A, Tchenio A, Moutkine I, Lujan R, Hervé D, Mameli M (2016) Rescue of GABAB and GIRK function in the lateral habenula by protein phosphatase 2A inhibition ameliorates depression-like phenotypes in mice. *Nat Med* **22**: 254–261. doi 10.1038/nm.4037 pmid:26808347.

Lecca S, Trusel M, Mameli M (2017) Footshock-induced plasticity of $GABA_B$ signalling in the lateral habenula requires dopamine and glucocorticoid receptors. *Synapse* **71**: e21948. doi 10.1002/syn.21948 pmid:27862283.

Leite-Morris KA, Fukudome EY, Shoeb MH, Kaplan GB (2004) GABA(B) receptor

activation in the ventral tegmental area inhibits the acquisition and expression of opiate-induced motor sensitization. *J Pharmacol Exp Ther* **308**: 667–678. doi 10.1124/jpet.103.058412 pmid:14610238.
Lemos JC, Roth CA, Messinger DI, Gill HK, Phillips PEM, Chavkin C (2012) Repeated stress dysregulates κ-opioid receptor signaling in the dorsal raphe through a p38α MAPK-dependent mechanism. *J Neurosci* **32**: 12325–12336. doi 10.1523/JNEUROSCI.2053-12.2012 pmid:22956823.
Lesage F, Guillemare E, Fink M, Duprat F, Heurteaux C, Fosset M, Romey G, Barhanin J, Lazdunski M (1995) Molecular properties of neuronal G-protein-activated inwardly rectifying K+ channels. *J Biol Chem* **270**: 28660–28667. doi 10.1074/JBC.270.48.28660 pmid:7499385.
Lewohl JM, Wilson WR, Mayfield RD, Brozowski SJ, Morrisett RA, Harris RA (1999) G-protein-coupled inwardly rectifying potassium channels are targets of alcohol action. *Nat Neurosci* **2**: 1084–1090. doi 10.1038/16012 pmid:10570485.
Liang J-H, Chen F, Krstew E, Cowen MS, Carroll FY, Crawford D, Beart PM, Lawrence AJ (2006) The GABAB receptor allosteric modulator CGP7930, like baclofen, reduces operant self-administration of ethanol in alcohol-preferring rats. *Neuropharmacology* **50**: 632–639. doi 10.1016/j.neuropharm.2005.11.011 pmid:16406445.
Liao YJ, Jan YN, Jan LY (1996) Heteromultimerization of G-protein-gated inwardly rectifying K+ channel proteins GIRK1 and GIRK2 and their altered expression in weaver brain. *J Neurosci* **16**: 7137–7150. pmid:8929423.
Licursi M, Christian SL, Pongnopparat T, Hirasawa K (2011) In vitro and in vivo comparison of viral and cellular internal ribosome entry sites for bicistronic vector expression. *Gene Ther* **18**: 631–636. doi 10.1038/gt.2011.11 pmid:21368899.
Linden J, James AS, McDaniel C, Jentsch JD (2018) Dopamine D2 receptors in dopaminergic neurons modulate performance in a reversal learning task in mice. *eneuro* **5**: ENEURO.0229-17.2018. doi 10.1523/ENEURO.0229-17.2018 pmid:29527566.
Lisman JE, Grace AA (2005) The hippocampal-VTA loop: controlling the entry of information into long-term memory. *Neuron* **46**: 703–713. doi 10.1016/j.neuron.2005.05.002 pmid:15924857.
Llamosas N, Bruzos-Cidón C, Rodríguez JJ, Ugedo L, Torrecilla M (2015) Deletion of GIRK2 subunit of GIRK channels alters the 5-HT 1A receptor-mediated signaling and results in a depression-resistant behavior. *Int J Neuropsychopharmacol* **18**: pyv051. doi 10.1093/ijnp/pyv051 pmid:25956878.
Lober RM, Pereira MA, Lambert NA (2006) Rapid activation of inwardly rectifying potassium channels by immobile G-protein-coupled receptors. *J Neurosci* **26**: 12602–12608. doi 10.1523/JNEUROSCI.4020-06.2006 pmid:17135422.
Logothetis DE, Kurachi Y, Galper J, Neer EJ, Clapham DE (1987) The βγ subunits of GTP-binding proteins activate the muscarinic K+ channel in heart. *Nature* **325**: 321–326. doi 10.1038/325321a0 pmid:2433589.
Lorang D, Amara SG, Simerly RB (1994) Cell-type-specific expression of catecholamine transporters in the rat brain. *J Neurosci* **14**: 4903–4914. pmid:8046459.
Luján R, Marron Fernandez de Velasco E, Aguado C, Wickman K (2014) New insights into the therapeutic potential of GIRK channels. *Trends Neurosci* **37**: 20–29. doi 10.1016/j.tins.2013.10.006 pmid:24268819.
Lunn M-L, Nassirpour R, Arrabit C, Tan J, McLeod I, Arias CM, Sawchenko PE, Yates JR, Slesinger PA (2007) A unique sorting nexin regulates trafficking of potassium

channels via a PDZ domain interaction. *Nat Neurosci* **10**: 1249–1259. doi 10.1038/nn1953 pmid:17828261.
Lüscher C, Jan LY, Stoffel M, Malenka RC, Nicoll RA (1997) G protein-coupled inwardly rectifying K+ channels (GIRKs) mediate postsynaptic but not presynaptic transmitter actions in hippocampal neurons. *Neuron* **19**: 687–695. pmid:9331358.
Lüscher C, Malenka RC (2011) Drug-evoked synaptic plasticity in addiction: from molecular changes to circuit remodeling. *Neuron* **69**: 650–663. doi 10.1016/j.neuron.2011.01.017 pmid:21338877.
Lüscher C, Slesinger PA (2010) Emerging roles for G protein-gated inwardly rectifying potassium (GIRK) channels in health and disease. *Nat Rev Neurosci* **11**: 301–315. doi 10.1038/nrn2834 pmid:20389305.
Lutfy K, Do T, Maidment NT (2001) Orphanin FQ/nociceptin attenuates motor stimulation and changes in nucleus accumbens extracellular dopamine induced by cocaine in rats. *Psychopharmacology (Berl)* **154**: 1–7. pmid:11291998.
Ma D, Zerangue N, Raab-Graham K, Fried SR, Jan YN, Jan LY (2002) Diverse trafficking patterns due to multiple traffic motifs in G protein-activated inwardly rectifying potassium channels from brain and heart. *Neuron* **33**: 715–729. pmid:11879649.
Maccioni P, Lorrai I, Contini A, Leite-Morris K, Colombo G (2018) Microinjection of baclofen and CGP7930 into the ventral tegmental area suppresses alcohol self-administration in alcohol-preferring rats. *Neuropharmacology* **136**: 146–158. doi 10.1016/j.neuropharm.2017.10.012 pmid:29050951.
Mahler S V, Brodnik ZD, Cox BM, Buchta WC, Bentzley BS, Quintanilla J, Cope ZA, Lin EC, Riedy MD, Scofield MD, Messinger J, Ruiz CM, Riegel AC, España RA, Aston-Jones G (2018) Chemogenetic Manipulations of Ventral Tegmental Area Dopamine Neurons Reveal Multifaceted Roles in Cocaine Abuse. *J Neurosci*: 0537-18. doi 10.1523/JNEUROSCI.0537-18.2018 pmid:30446532.
Mao J, Wang X, Chen F, Wang R, Rojas A, Shi Y, Piao H, Jiang C (2004) Molecular basis for the inhibition of G protein-coupled inward rectifier K(+) channels by protein kinase C. *Proc Natl Acad Sci U S A* **101**: 1087–1092. doi 10.1073/pnas.0304827101 pmid:14732702.
Marchant NJ, Whitaker LR, Bossert JM, Harvey BK, Hope BT, Kaganovsky K, Adhikary S, Prisinzano TE, Vardy E, Roth BL, Shaham Y (2016) Behavioral and Physiological Effects of a Novel Kappa-Opioid Receptor-Based DREADD in Rats. *Neuropsychopharmacology* **41**: 402–409. doi 10.1038/npp.2015.149 pmid:26019014.
Marcott PF, Mamaligas AA, Ford CP (2014) Phasic dopamine release drives rapid activation of striatal D2-receptors. *Neuron* **84**: 164–176. doi 10.1016/j.neuron.2014.08.058 pmid:25242218.
Margolis EB, Coker AR, Driscoll JR, Lemaître A-I, Fields HL (2010) Reliability in the identification of midbrain dopamine neurons Mansvelder HD, ed. *PLoS One* **5**: e15222. doi 10.1371/journal.pone.0015222 pmid:21151605.
Margolis EB, Hjelmstad GO, Bonci A, Fields HL (2003) Kappa-opioid agonists directly inhibit midbrain dopaminergic neurons. *J Neurosci* **23**: 9981–9986. pmid:14602811.
Margolis EB, Hjelmstad GO, Fujita W, Fields HL (2014) Direct bidirectional μ-opioid control of midbrain dopamine neurons. *J Neurosci* **34**: 14707–14716. doi 10.1523/JNEUROSCI.2144-14.2014 pmid:25355223.
Margolis EB, Lock H, Chefer VI, Shippenberg TS, Hjelmstad GO, Fields HL (2006a) Opioids selectively control dopaminergic neurons projecting to the prefrontal cortex.

Proc Natl Acad Sci **103**: 2938–2942. doi 10.1073/pnas.0511159103 pmid:16477003.
Margolis EB, Lock H, Hjelmstad GO, Fields HL (2006b) The ventral tegmental area revisited: is there an electrophysiological marker for dopaminergic neurons? *J Physiol* **577**: 907–924. doi 10.1113/jphysiol.2006.117069 pmid:16959856.
Margolis EB, Toy B, Himmels P, Morales M, Fields HL (2012) Identification of rat ventral tegmental area GABAergic neurons. *PLoS One* **7**: e42365. doi 10.1371/journal.pone.0042365 pmid:22860119.
Marker CL, Cintora SC, Roman MI, Stoffel M, Wickman K (2002) Hyperalgesia and blunted morphine analgesia in G protein-gated potassium channel subunit knockout mice. *Neuroreport* **13**: 2509–2513. doi 10.1097/01.wnr.0000048541.12213.bb pmid:12499858.
Marker CL, Lujan R, Colon J, Wickman K (2006) Distinct populations of spinal cord lamina II interneurons expressing G-protein-gated potassium channels. *J Neurosci* **26**: 12251–12259. doi 10.1523/JNEUROSCI.3693-06.2006 pmid:17122050.
Marker CL, Luján R, Loh HH, Wickman K (2005) Spinal G-protein-gated potassium channels contribute in a dose-dependent manner to the analgesic effect of mu- and delta- but not kappa-opioids. *J Neurosci* **25**: 3551–3559. doi 10.1523/JNEUROSCI.4899-04.2005 pmid:15814785.
Marker CL, Stoffel M, Wickman K (2004) Spinal G-protein-pated K+ channels formed by GIRK1 and GIRK2 subunits modulate thermal nociception and contribute to morphine analgesia. *J Neurosci* **24**: 2806–2812. doi 10.1523/JNEUROSCI.5251-03.2004 pmid:15028774.
Marron Fernandez de Velasco E, Carlblom N, Xia Z, Wickman K (2017a) Suppression of inhibitory G protein signaling in forebrain pyramidal neurons triggers plasticity of glutamatergic neurotransmission in the nucleus accumbens core. *Neuropharmacology* **117**: 33–40. doi 10.1016/j.neuropharm.2017.01.021 pmid:28131769.
Marron Fernandez de Velasco E, Hearing M, Xia Z, Victoria NC, Luján R, Wickman K (2015a) Sex differences in GABABR-GIRK signaling in layer 5/6 pyramidal neurons of the mouse prelimbic cortex. *Neuropharmacology* **95**: 353–360. doi 10.1016/j.neuropharm.2015.03.029 pmid:25843643.
Marron Fernandez de Velasco E, McCall N, Wickman K (2015b) GIRK channel plasticity and implications for drug addiction. In: International review of neurobiology, pp 201–238 doi 10.1016/bs.irn.2015.05.011 pmid:26422986.
Marron Fernandez de Velasco E, Zhang L, N Vo B, Tipps M, Farris S, Xia Z, Anderson A, Carlblom N, Weaver CD, Dudek SM, Wickman K (2017b) GIRK2 splice variants and neuronal G protein-gated K+ channels: implications for channel function and behavior. *Sci Rep* **7**: 1639. doi 10.1038/s41598-017-01820-2 pmid:28487514.
Matsui A, Jarvie BC, Robinson BG, Hentges ST, Williams JT (2014) Separate GABA afferents to dopamine neurons mediate acute action of opioids, development of tolerance, and expression of withdrawal. *Neuron* **82**: 1346–1356. doi 10.1016/j.neuron.2014.04.030 pmid:24857021.
McCall NM, Kotecki L, Dominguez-Lopez S, Marron Fernandez De Velasco E, Carlblom N, Sharpe AL, Beckstead MJ, Wickman K (2017) Selective ablation of GIRK channels in dopamine neurons alters behavioral effects of cocaine in mice. *Neuropsychopharmacology* **42** doi 10.1038/npp.2016.138.
McElligott Z (2015) Optogenetic and chemogenetic approaches to advance monitoring molecules. *ACS Chem Neurosci* **6**: 944–947. doi 10.1021/acschemneuro.5b00081

pmid:25791746.
McNamara CG, Tejero-Cantero Á, Trouche S, Campo-Urriza N, Dupret D (2014) Dopaminergic neurons promote hippocampal reactivation and spatial memory persistence. *Nat Neurosci* **17**: 1658–1660. doi 10.1038/nn.3843 pmid:25326690.
Medina I, Krapivinsky G, Arnold S, Kovoor P, Krapivinsky L, Clapham DE (2000) A switch mechanism for G beta gamma activation of I(KACh). *J Biol Chem* **275**: 29709–29716. doi 10.1074/jbc.M004989200 pmid:10900209.
Meister B, Elde R (1993) Dopamine transporter mRNA in neurons of the rat hypothalamus. *Neuroendocrinology* **58**: 388–395. doi 10.1159/000126568 pmid:8284024.
Mejias-Aponte CA, Drouin C, Aston-Jones G (2009) Adrenergic and noradrenergic innervation of the midbrain ventral tegmental area and retrorubral field: prominent inputs from medullary homeostatic centers. *J Neurosci* **29**: 3613–3626. doi 10.1523/JNEUROSCI.4632-08.2009 pmid:19295165.
Mena-Segovia J, Bolam JP (2017) Rethinking the pedunculopontine nucleus: from cellular organization to function. *Neuron* **94**: 7–18. doi 10.1016/j.neuron.2017.02.027 pmid:28384477.
Mirkovic K, Palmersheim J, Lesage F, Wickman K (2012) Behavioral characterization of mice lacking Trek channels. *Front Behav Neurosci* **6**: 60. doi 10.3389/fnbeh.2012.00060 pmid:22973213.
Montandon G, Ren J, Victoria NC, Liu H, Wickman K, Greer JJ, Horner RL (2016) G-protein–gated inwardly rectifying potassium channels modulate respiratory depression by opioids. *Anesthesiology* **124**: 641–650. doi 10.1097/ALN.0000000000000984 pmid:26675532.
Moorman DE, James MH, McGlinchey EM, Aston-Jones G (2015) Differential roles of medial prefrontal subregions in the regulation of drug seeking. *Brain Res* **1628**: 130–146. doi 10.1016/j.brainres.2014.12.024 pmid:25529632.
Morales M, Margolis EB (2017) Ventral tegmental area: cellular heterogeneity, connectivity and behaviour. *Nat Rev Neurosci* **18**: 73–85. doi 10.1038/nrn.2016.165 pmid:28053327.
Morgan AD, Carroll ME, Loth AK, Stoffel M, Wickman K (2003) Decreased cocaine self-administration in Kir3 potassium channel subunit knockout mice. *Neuropsychopharmacology* **28**: 932–938. doi 10.1038/sj.npp.1300100 pmid:12637950.
Müllner C, Vorobiov D, Bera AK, Uezono Y, Yakubovich D, Frohnwieser-Steinecker B, Dascal N, Schreibmayer W (2000) Heterologous facilitation of G protein-activated K(+) channels by beta-adrenergic stimulation via cAMP-dependent protein kinase. *J Gen Physiol* **115**: 547–558. pmid:10779313.
Müllner C, Yakubovich D, Dessauer CW, Platzer D, Schreibmayer W (2003) Single channel analysis of the regulation of GIRK1/GIRK4 channels by protein phosphorylation. *Biophys J* **84**: 1399–1409. doi 10.1016/S0006-3495(03)74954-6 pmid:12547819.
Munoz MB, Padgett CL, Rifkin R, Terunuma M, Wickman K, Contet C, Moss SJ, Slesinger PA (2016) A role for the GIRK3 subunit in methamphetamine-induced attenuation of GABAB receptor-activated GIRK currents in VTA dopamine neurons. *J Neurosci* **36**: 3106–3114. doi 10.1523/JNEUROSCI.1327-15.2016 pmid:26985023.
Munoz MB, Slesinger PA (2014) Sorting nexin 27 regulation of G protein-gated inwardly rectifying K+ channels attenuates in vivo cocaine response. *Neuron* **82**: 659–669.

doi 10.1016/j.neuron.2014.03.011 pmid:24811384.
Nair-Roberts RG, Chatelain-Badie SD, Benson E, White-Cooper H, Bolam JP, Ungless MA (2008) Stereological estimates of dopaminergic, GABAergic and glutamatergic neurons in the ventral tegmental area, substantia nigra and retrorubral field in the rat. *Neuroscience* **152**: 1024–1031. doi 10.1016/j.neuroscience.2008.01.046 pmid:18355970.
Nakamura A, Fujita M, Ono H, Hongo Y, Kanbara T, Ogawa K, Morioka Y, Nishiyori A, Shibasaki M, Mori T, Suzuki T, Sakaguchi G, Kato A, Hasegawa M (2014) G protein-gated inwardly rectifying potassium (K_{IR} 3) channels play a primary role in the antinociceptive effect of oxycodone, but not morphine, at supraspinal sites. *Br J Pharmacol* **171**: 253–264. doi 10.1111/bph.12441 pmid:24117458.
Nassirpour R, Bahima L, Lalive AL, Luscher C, Lujan R, Slesinger PA (2010) Morphine- and CaMKII-dependent enhancement of GIRK channel signaling in hippocampal neurons. *J Neurosci* **30**: 13419–13430. doi 10.1523/JNEUROSCI.2966-10.2010 pmid:20926668.
Nath C, Gupta MB, Patnaik GK, Dhawan KN (1994) Morphine-induced straub tail response: mediated by central mu2-opioid receptor. *Eur J Pharmacol* **263**: 203–205. pmid:7821354.
Nelson CS, Marino JL, Allen CN (1997) Cloning and characterization of Kir3.1 (GIRK1) C-terminal alternative splice variants. *Brain Res Mol Brain Res* **46**: 185–196. pmid:9191093.
Nestler EJ (2005) The neurobiology of cocaine addiction. *Sci Pract Perspect* **3**: 4–10. pmid:18552739.
Nestler EJ, Carlezon WA (2006) The mesolimbic dopamine reward circuit in depression. *Biol Psychiatry* **59**: 1151–1159. doi 10.1016/j.biopsych.2005.09.018 pmid:16566899.
Neubig RR, Siderovski DP (2002) Regulators of G-Protein signalling as new central nervous system drug targets. *Nat Rev Drug Discov* **1**: 187–197. doi 10.1038/nrd747 pmid:12120503.
Nieh EH, Matthews GA, Allsop SA, Presbrey KN, Leppla CA, Wichmann R, Neve R, Wildes CP, Tye KM (2015) Decoding neural circuits that control compulsive sucrose seeking. *Cell* **160**: 528–541. doi 10.1016/j.cell.2015.01.003 pmid:25635460.
Ntamati NR, Creed M, Achargui R, Lüscher C (2018) Periaqueductal efferents to dopamine and GABA neurons of the VTA Siegel A, ed. *PLoS One* **13**: e0190297. doi 10.1371/journal.pone.0190297 pmid:29304042.
Omelchenko N, Bell R, Sesack SR (2009) Lateral habenula projections to dopamine and GABA neurons in the rat ventral tegmental area. *Eur J Neurosci* **30**: 1239–1250. doi 10.1111/j.1460-9568.2009.06924.x pmid:19788571.
Omelchenko N, Sesack SR (2005) Laterodorsal tegmental projections to identified cell populations in the rat ventral tegmental area. *J Comp Neurol* **483**: 217–235. doi 10.1002/cne.20417 pmid:15678476.
Omelchenko N, Sesack SR (2009) Periaqueductal gray afferents synapse onto dopamine and GABA neurons in the rat ventral tegmental area. *J Neurosci Res* **88**: NA-NA. doi 10.1002/jnr.22265 pmid:19885830.
Ostrovskaya O, Xie K, Masuho I, Fajardo-Serrano A, Lujan R, Wickman K, Martemyanov KA (2014) RGS7/Gβ5/R7BP complex regulates synaptic plasticity and memory by modulating hippocampal GABABR-GIRK signaling. *Elife* **3**: e02053. doi 10.7554/eLife.02053 pmid:24755289.
Padgett CL, Lalive AL, Tan KR, Terunuma M, Munoz MB, Pangalos MN, Martínez-

Hernández J, Watanabe M, Moss SJ, Luján R, Lüscher C, Slesinger PA (2012) Methamphetamine-evoked depression of GABA(B) receptor signaling in GABA neurons of the VTA. *Neuron* **73**: 978–989. doi 10.1016/j.neuron.2011.12.031 pmid:22405207.

Patriarchi T, Cho JR, Merten K, Howe MW, Marley A, Xiong W-H, Folk RW, Broussard GJ, Liang R, Jang MJ, Zhong H, Dombeck D, von Zastrow M, Nimmerjahn A, Gradinaru V, Williams JT, Tian L (2018) Ultrafast neuronal imaging of dopamine dynamics with designed genetically encoded sensors. *Science (80-)* **360**: eaat4422. doi 10.1126/science.aat4422 pmid:29853555.

Peleg S, Varon D, Ivanina T, Dessauer CW, Dascal N (2002) G(alpha)(i) controls the gating of the G protein-activated K(+) channel, GIRK. *Neuron* **33**: 87–99. pmid:11779482.

Perra S, Clements MA, Bernier BE, Morikawa H (2011) In vivo ethanol experience increases D2 autoinhibition in the ventral tegmental area. *Neuropsychopharmacology* **36**: 993–1002. doi 10.1038/npp.2010.237 pmid:21248720.

Perry CA, Pravetoni M, Teske JA, Aguado C, Erickson DJ, Medrano JF, Lujan R, Kotz CM, Wickman K (2008) Predisposition to late-onset obesity in GIRK4 knockout mice. *Proc Natl Acad Sci* **105**: 8148–8153. doi 10.1073/pnas.0803261105 pmid:18523006.

Pértile RAN, Corvino ME, Marchette RCN, Pavesi E, Cavalli J, Ramos A, Izídio GS (2017) The quinpirole hypolocomotive effects are strain and route of administration dependent in SHR and SLA16 isogenic rats. *Behav Genet* **47**: 552–563. doi 10.1007/s10519-017-9865-z pmid:28822047.

Peyron C, Tighe DK, van den Pol AN, de Lecea L, Heller HC, Sutcliffe JG, Kilduff TS (1998) Neurons containing hypocretin (orexin) project to multiple neuronal systems. *J Neurosci* **18**: 9996–10015. pmid:9822755.

Philippart F, Khaliq ZM (2018) Gi/o protein-coupled receptors in dopamine neurons inhibit the sodium leak channel NALCN. *Elife* **7** doi 10.7554/eLife.40984.

Phillips PEM, Stuber GD, Heien MLA V., Wightman RM, Carelli RM (2003) Subsecond dopamine release promotes cocaine seeking. *Nature* **422**: 614–618. doi 10.1038/nature01476 pmid:12687000.

Pierce RC, Kalivas PW (1997) A circuitry model of the expression of behavioral sensitization to amphetamine-like psychostimulants. *Brain Res Brain Res Rev* **25**: 192–216. pmid:9403138.

Pignatelli M, Bonci A (2015) Role of dopamine neurons in reward and aversion: a synaptic plasticity perspective. *Neuron* **86**: 1145–1157. doi 10.1016/J.NEURON.2015.04.015.

Platt RJ et al. (2014) CRISPR-Cas9 knockin mice for genome editing and cancer modeling. *Cell* **159**: 440–455. doi 10.1016/j.cell.2014.09.014.

Polta SA, Fenzl T, Jakubcakova V, Kimura M, Yassouridis A, Wotjak CT (2013) Prognostic and symptomatic aspects of rapid eye movement sleep in a mouse model of posttraumatic stress disorder. *Front Behav Neurosci* **7**: 60. doi 10.3389/fnbeh.2013.00060 pmid:23750131.

Polter AM, Kauer JA (2014) Stress and VTA synapses: implications for addiction and depression. *Eur J Neurosci* **39**: 1179–1188. doi 10.1111/ejn.12490 pmid:24712997.

Pravetoni M, Wickman K (2008) Behavioral characterization of mice lacking GIRK/Kir3 channel subunits. *Genes, Brain Behav* **7**: 523–531. doi 10.1111/j.1601-183X.2008.00388.x pmid:18194467.

Psigfogeorgou K, Terzi D, Papachatzaki MM, Varidaki A, Ferguson D, Gold SJ, Zachariou V, Zachariou V (2011) A unique role of RGS9-2 in the striatum as a positive or negative regulator of opiate analgesia. *J Neurosci* **31**: 5617–5624. doi 10.1523/JNEUROSCI.4146-10.2011 pmid:21490202.

Qi J, Zhang S, Wang H-L, Barker DJ, Miranda-Barrientos J, Morales M (2016) VTA glutamatergic inputs to nucleus accumbens drive aversion by acting on GABAergic interneurons. *Nat Neurosci* **19**: 725–733. doi 10.1038/nn.4281 pmid:27019014.

Qi J, Zhang S, Wang H-L, Wang H, de Jesus Aceves Buendia J, Hoffman AF, Lupica CR, Seal RP, Morales M (2014) A glutamatergic reward input from the dorsal raphe to ventral tegmental area dopamine neurons. *Nat Commun* **5**: 5390. doi 10.1038/ncomms6390 pmid:25388237.

Rahman Z, Schwarz J, Gold SJ, Zachariou V, Wein MN, Choi KH, Kovoor A, Chen CK, DiLeone RJ, Schwarz SC, Selley DE, Sim-Selley LJ, Barrot M, Luedtke RR, Self D, Neve RL, Lester HA, Simon MI, Nestler EJ (2003) RGS9 modulates dopamine signaling in the basal ganglia. *Neuron* **38**: 941–952. pmid:12818179.

Ranaldi R, Poeggel K (2002) Baclofen decreases methamphetamine self-administration in rats. *Neuroreport* **13**: 1107–1110. pmid:12151750.

Redgrave P, Gurney K (2006) The short-latency dopamine signal: a role in discovering novel actions? *Nat Rev Neurosci* **7**: 967–975. doi 10.1038/nrn2022.

Reuveny E, Slesinger PA, Inglese J, Morales JM, Iñiguez-Lluhi JA, Lefkowitz RJ, Bourne HR, Jan YN, Jan LY (1994) Activation of the cloned muscarinic potassium channel by G protein βγ subunits. *Nature* **370**: 143–146. doi 10.1038/370143a0 pmid:8022483.

Rifkin RA, Huyghe D, Li X, Parakala M, Aisenberg E, Moss SJ, Slesinger PA (2018) GIRK currents in VTA dopamine neurons control the sensitivity of mice to cocaine-induced locomotor sensitization. *Proc Natl Acad Sci U S A* **115**: E9479–E9488. doi 10.1073/pnas.1807788115 pmid:30228121.

Rifkin RA, Moss SJ, Slesinger PA (2017) G protein-gated potassium channels: a link to drug addiction. *Trends Pharmacol Sci* **38**: 378–392. doi 10.1016/j.tips.2017.01.007 pmid:28188005.

Robinson TE, Berridge KC (2001) Incentive-sensitization and addiction. *Addiction* **96**: 103–114. doi 10.1080/09652140020016996 pmid:11177523.

Rocha BA (2003) Stimulant and reinforcing effects of cocaine in monoamine transporter knockout mice. *Eur J Pharmacol* **479**: 107–115. pmid:14612142.

Root DH, Mejias-Aponte CA, Qi J, Morales M (2014a) Role of glutamatergic projections from ventral tegmental area to lateral habenula in aversive conditioning. *J Neurosci* **34**: 13906–13910. doi 10.1523/JNEUROSCI.2029-14.2014 pmid:25319687.

Root DH, Mejias-Aponte CA, Zhang S, Wang H-L, Hoffman AF, Lupica CR, Morales M (2014b) Single rodent mesohabenular axons release glutamate and GABA. *Nat Neurosci* **17**: 1543–1551. doi 10.1038/nn.3823 pmid:25242304.

Root DH, Melendez RI, Zaborszky L, Napier TC (2015) The ventral pallidum: Subregion-specific functional anatomy and roles in motivated behaviors. *Prog Neurobiol* **130**: 29–70. doi 10.1016/j.pneurobio.2015.03.005 pmid:25857550.

Ross EM, Wilkie TM (2000) GTPase-activating proteins for heterotrimeric G proteins: regulators of G protein signaling (RGS) and RGS-like proteins. *Annu Rev Biochem* **69**: 795–827. doi 10.1146/annurev.biochem.69.1.795 pmid:10966476.

Roth BL (2016) DREADDs for Neuroscientists. *Neuron* **89**: 683–694. doi 10.1016/j.neuron.2016.01.040 pmid:26889809.

Rubinstein M, Peleg S, Berlin S, Brass D, Keren-Raifman T, Dessauer CW, Ivanina T,

Dascal N (2009) Divergent regulation of GIRK1 and GIRK2 subunits of the neuronal G protein gated K^+ channel by $G\alpha_i^{GDP}$ and Gβγ. *J Physiol* **587**: 3473–3491. doi 10.1113/jphysiol.2009.173229 pmid:19470775.
Runegaard AH, Jensen KL, Wörtwein G, Gether U (2018a) Initial rewarding effects of cocaine and amphetamine assessed in a day using the single-exposure place preference protocol. *Eur J Neurosci* doi 10.1111/ejn.14082 pmid:30044020.
Runegaard AH, Sørensen AT, Fitzpatrick CM, Jørgensen SH, Petersen A V., Hansen NW, Weikop P, Andreasen JT, Mikkelsen JD, Perrier J-F, Woldbye D, Rickhag M, Wortwein G, Gether U (2018b) Locomotor- and Reward-Enhancing Effects of Cocaine Are Differentially Regulated by Chemogenetic Stimulation of Gi-Signaling in Dopaminergic Neurons. *eneuro* **5**: ENEURO.0345-17.2018. doi 10.1523/ENEURO.0345-17.2018 pmid:29938215.
Rusinova R, Shen Y-MA, Dolios G, Padovan J, Yang H, Kirchberger M, Wang R, Logothetis DE (2009) Mass spectrometric analysis reveals a functionally important PKA phosphorylation site in a Kir3 channel subunit. *Pflugers Arch* **458**: 303–314. doi 10.1007/s00424-008-0628-9 pmid:19151997.
Russo SJ, Nestler EJ (2013) The brain reward circuitry in mood disorders. *Nat Rev Neurosci* **14**: 609–625. doi 10.1038/nrn3381 pmid:23942470.
Saal D, Dong Y, Bonci A, Malenka RC (2003) Drugs of abuse and stress trigger a common synaptic adaptation in dopamine neurons. *Neuron* **37**: 577–582. pmid:12597856.
Saddoris MP, Sugam JA, Cacciapaglia F, Carelli RM (2013) Rapid dopamine dynamics in the accumbens core and shell: learning and action. *Front Biosci* **5**: 273–288. pmid:23276989.
Salamone JD, Correa M (2012) The mysterious motivational functions of mesolimbic dopamine. *Neuron* **76**: 470–485. doi 10.1016/j.neuron.2012.10.021 pmid:23141060.
Scatton B, Simon H, Le Moal M, Bischoff S (1980) Origin of dopaminergic innervation of the rat hippocampal formation. *Neurosci Lett* **18**: 125–131. pmid:7052484.
Schultz W (1998) Predictive reward signal of dopamine neurons. *J Neurophysiol* **80**: 1–27. doi 10.1152/jn.1998.80.1.1 pmid:9658025.
Schultz W (2013) Updating dopamine reward signals. *Curr Opin Neurobiol* **23**: 229–238. doi 10.1016/j.conb.2012.11.012 pmid:23267662.
Schultz W, Dayan P, Montague PR (1997) A neural substrate of prediction and reward. *Science* **275**: 1593–1599. pmid:9054347.
Schwarz LA, Luo L (2015) Organization of the locus coeruleus-norepinephrine system. *Curr Biol* **25**: R1051–R1056. doi 10.1016/J.CUB.2015.09.039.
Schwenk J, Metz M, Zolles G, Turecek R, Fritzius T, Bildl W, Tarusawa E, Kulik A, Unger A, Ivankova K, Seddik R, Tiao JY, Rajalu M, Trojanova J, Rohde V, Gassmann M, Schulte U, Fakler B, Bettler B (2010) Native GABA(B) receptors are heteromultimers with a family of auxiliary subunits. *Nature* **465**: 231–235. doi 10.1038/nature08964 pmid:20400944.
Seddik R, Jungblut SP, Silander OK, Rajalu M, Fritzius T, Besseyrias V, Jacquier V, Fakler B, Gassmann M, Bettler B (2012) Opposite effects of KCTD subunit domains on GABA(B) receptor-mediated desensitization. *J Biol Chem* **287**: 39869–39877. doi 10.1074/jbc.M112.412767 pmid:23035119.
Sesack SR, Aoki C, Pickel VM (1994) Ultrastructural localization of D2 receptor-like immunoreactivity in midbrain dopamine neurons and their striatal targets. *J Neurosci* **14**: 88–106. pmid:7904306.
Sharpe AL, Varela E, Bettinger L, Beckstead MJ (2015) Methamphetamine self-

administration in mice decreases GIRK channel-mediated currents in midbrain dopamine neurons. *Int J Neuropsychopharmacol* **18**: pyu073-pyu073. doi 10.1093/ijnp/pyu073 pmid:25522412.
Siciliano CA, Tye KM (2019) Leveraging calcium imaging to illuminate circuit dysfunction in addiction. *Alcohol* **74**: 47–63. doi 10.1016/j.alcohol.2018.05.013 pmid:30470589.
Signorini S, Liao YJ, Duncan SA, Jan LY, Stoffel M (1997) Normal cerebellar development but susceptibility to seizures in mice lacking G protein-coupled, inwardly rectifying K+ channel GIRK2. *Proc Natl Acad Sci U S A* **94**: 923–927. pmid:9023358.
Slesinger PA, Patil N, Liao YJ, Jan YN, Jan LY, Cox DR (1996) Functional effects of the mouse weaver mutation on G protein-gated inwardly rectifying K+ channels. *Neuron* **16**: 321–331. pmid:8789947.
Slesinger PA, Reuveny E, Jan YN, Jan LY (1995) Identification of structural elements involved in G protein gating of the GIRK1 potassium channel. *Neuron* **15**: 1145–1156. pmid:7576657.
Slesinger PA, Stoffel M, Jan YN, Jan LY (1997) Defective gamma-aminobutyric acid type B receptor-activated inwardly rectifying K+ currents in cerebellar granule cells isolated from weaver and Girk2 null mutant mice. *Proc Natl Acad Sci U S A* **94**: 12210–12217. pmid:9342388.
Smidt MP, von Oerthel L, Hoekstra EJ, Schellevis RD, Hoekman MFM (2012) Spatial and temporal lineage analysis of a Pitx3-driven cre-recombinase knock-in mouse model Arenkiel B, ed. *PLoS One* **7**: e42641. doi 10.1371/journal.pone.0042641 pmid:22870339.
Stamatakis AM, Jennings JH, Ung RL, Blair GA, Weinberg RJ, Neve RL, Boyce F, Mattis J, Ramakrishnan C, Deisseroth K, Stuber GD (2013) A unique population of ventral tegmental area neurons inhibits the lateral habenula to promote reward. *Neuron* **80**: 1039–1053. doi 10.1016/j.neuron.2013.08.023 pmid:24267654.
Stamatakis AM, Stuber GD (2012) Activation of lateral habenula inputs to the ventral midbrain promotes behavioral avoidance. *Nat Neurosci* **15**: 1105–1107. doi 10.1038/nn.3145 pmid:22729176.
Steketee JD, Kalivas PW (1991) Sensitization to psychostimulants and stress after injection of pertussis toxin into the A10 dopamine region. *J Pharmacol Exp Ther* **259**: 916–924. pmid:1941636.
Stuber GD, Stamatakis AM, Kantak PA (2015) Considerations when using Cre-driver rodent lines for studying ventral tegmental area circuitry. *Neuron* **85**: 439–445. doi 10.1016/j.neuron.2014.12.034 pmid:25611514.
Sui JL, Chan KW, Logothetis DE (1996) Na+ activation of the muscarinic K+ channel by a G-protein-independent mechanism. *J Gen Physiol* **108**: 381–391. pmid:8923264.
Sui JL, Petit-Jacques J, Logothetis DE (1998) Activation of the atrial KACh channel by the betagamma subunits of G proteins or intracellular Na+ ions depends on the presence of phosphatidylinositol phosphates. *Proc Natl Acad Sci U S A* **95**: 1307–1312. pmid:9448327.
Szechtman H, Talangbayan H, Eilam D (1993) Environmental and behavioral components of sensitization induced by the dopamine agonist quinpirole. *Behav Pharmacol* **4**: 405–410. pmid:11224209.
Tagliaferro P, Morales M (2008) Synapses between corticotropin-releasing factor-containing axon terminals and dopaminergic neurons in the ventral tegmental area are predominantly glutamatergic. *J Comp Neurol* **506**: 616–626. doi 10.1002/cne.21576 pmid:18067140.

Tan KR, Yvon C, Turiault M, Mirzabekov JJ, Doehner J, Labouèbe G, Deisseroth K, Tye KM, Lüscher C (2012) GABA neurons of the VTA drive conditioned place aversion. *Neuron* **73**: 1173–1183. doi 10.1016/J.NEURON.2012.02.015.

Terunuma M, Pangalos MN, Moss SJ (2010) Functional modulation of GABAB receptors by protein kinases and receptor trafficking. In: Advances in pharmacology (San Diego, Calif.), pp 113–122 doi 10.1016/S1054-3589(10)58005-0 pmid:20655480.

Tervo DGR, Hwang B-Y, Viswanathan S, Gaj T, Lavzin M, Ritola KD, Lindo S, Michael S, Kuleshova E, Ojala D, Huang C-C, Gerfen CR, Schiller J, Dudman JT, Hantman AW, Looger LL, Schaffer D V., Karpova AY (2016) A designer AAV variant permits efficient retrograde access to projection neurons. *Neuron* **92**: 372–382. doi 10.1016/j.neuron.2016.09.021 pmid:27720486.

Thompson D, Martini L, Whistler JL (2010) Altered ratio of D1 and D2 dopamine receptors in mouse striatum is associated with behavioral sensitization to cocaine. *PLoS One* **5**: e11038. doi 10.1371/journal.pone.0011038 pmid:20543951.

Tian M, Broxmeyer HE, Fan Y, Lai Z, Zhang S, Aronica S, Cooper S, Bigsby RM, Steinmetz R, Engle SJ, Mestek A, Pollock JD, Lehman MN, Jansen HT, Ying M, Stambrook PJ, Tischfield JA, Yu L (1997) Altered hematopoiesis, behavior, and sexual function in mu opioid receptor-deficient mice. *J Exp Med* **185**: 1517–1522. pmid:9126934.

Tipps M, Marron Fernandez de Velasco E, Schaeffer A, Wickman K (2018) Inhibition of pyramidal neurons in the basal amygdala promotes fear learning. *eNeuro* **5** doi 10.1523/ENEURO.0272-18.2018 pmid:30406197.

Torrecilla M, Fernández-Aedo I, Arrue A, Zumarraga M, Ugedo L (2013) Role of GIRK channels on the noradrenergic transmission in vivo: an electrophysiological and neurochemical study on GIRK2 mutant mice. *Int J Neuropsychopharmacol* **16**: 1093–1104. doi 10.1017/S1461145712000971 pmid:23040084.

Torrecilla M, Marker CL, Cintora SC, Stoffel M, Williams JT, Wickman K (2002) G-protein-gated potassium channels containing Kir3.2 and Kir3.3 subunits mediate the acute inhibitory effects of opioids on locus ceruleus neurons. *J Neurosci* **22**: 4328–4334. doi 20026414 pmid:12040038.

Torrecilla M, Quillinan N, Williams JT, Wickman K (2008) Pre- and postsynaptic regulation of locus coeruleus neurons after chronic morphine treatment: a study of GIRK-knockout mice. *Eur J Neurosci* **28**: 618–624. doi 10.1111/j.1460-9568.2008.06348.x pmid:18702733.

Traynor J (2010) Regulator of G protein-signaling proteins and addictive drugs. *Ann N Y Acad Sci* **1187**: 341–352. doi 10.1111/j.1749-6632.2009.05150.x pmid:20201861.

Turecek R, Schwenk J, Fritzius T, Ivankova K, Zolles G, Adelfinger L, Jacquier V, Besseyrias V, Gassmann M, Schulte U, Fakler B, Bettler B (2014) Auxiliary GABAB receptor subunits uncouple G protein βγ subunits from effector channels to induce desensitization. *Neuron* **82**: 1032–1044. doi 10.1016/j.neuron.2014.04.015 pmid:24836506.

Tye KM, Mirzabekov JJ, Warden MR, Ferenczi EA, Tsai H-C, Finkelstein J, Kim S-Y, Adhikari A, Thompson KR, Andalman AS, Gunaydin LA, Witten IB, Deisseroth K (2013) Dopamine neurons modulate neural encoding and expression of depression-related behaviour. *Nature* **493**: 537–541. doi 10.1038/nature11740 pmid:23235822.

Ugolini G, Kuypers HGJM, Simmons A (1987) Retrograde transneuronal transfer of Herpes simplex virus type 1 (HSV 1) from motoneurones. *Brain Res* **422**: 242–256. doi 10.1016/0006-8993(87)90931-0.

Ungless MA, Whistler JL, Malenka RC, Bonci A (2001) Single cocaine exposure in vivo

induces long-term potentiation in dopamine neurons. *Nature* **411**: 583–587. doi 10.1038/35079077 pmid:11385572.
van Zessen R, Phillips JLL, Budygin EAA, Stuber GDD, van Zessen R, Phillips JLL, Budygin EAA, Stuber GDD (2012) Activation of VTA GABA neurons disrupts reward consumption. *Neuron* **73**: 1184–1194. doi 10.1016/J.NEURON.2012.02.016 pmid:22445345.
Vander Weele CM, Siciliano CA, Matthews GA, Namburi P, Izadmehr EM, Espinel IC, Nieh EH, Schut EHS, Padilla-Coreano N, Burgos-Robles A, Chang C-J, Kimchi EY, Beyeler A, Wichmann R, Wildes CP, Tye KM (2018) Dopamine enhances signal-to-noise ratio in cortical-brainstem encoding of aversive stimuli. *Nature* **563**: 397–401. doi 10.1038/s41586-018-0682-1 pmid:30405240.
Varani AP, Pedrón VT, Aon AJ, Höcht C, Acosta GB, Bettler B, Balerio GN (2018) Nicotine-induced molecular alterations are modulated by $GABA_B$ receptor activity. *Addict Biol* **23**: 230–246. doi 10.1111/adb.12506 pmid:28419642.
Vardy E et al. (2015) A New DREADD Facilitates the Multiplexed Chemogenetic Interrogation of Behavior. *Neuron* **86**: 936–946. doi 10.1016/j.neuron.2015.03.065 pmid:25937170.
Victoria NC, Marron Fernandez de Velasco E, Ostrovskaya O, Metzger S, Xia Z, Kotecki L, Benneyworth MA, Zink AN, Martemyanov KA, Wickman K (2016) G protein-gated K+ channel ablation in forebrain pyramidal neurons selectively impairs fear learning. *Biol Psychiatry* **80**: 796–806. doi 10.1016/j.biopsych.2015.10.004 pmid:26612516.
Volkow ND, Koob G (2015) Brain disease model of addiction: why is it so controversial? *Lancet* **2**: 677–679. doi 10.1016/S2215-0366(15)00236-9 pmid:26249284.
Volkow ND, Koob GF, McLellan AT (2016) Neurobiologic advances from the brain disease model of addiction Longo DL, ed. *N Engl J Med* **374**: 363–371. doi 10.1056/NEJMra1511480 pmid:26816013.
Volkow ND, Wang G-J, Fowler JS, Tomasi D (2012) Addiction circuitry in the human brain. *Annu Rev Pharmacol Toxicol* **52**: 321–336. doi 10.1146/annurev-pharmtox-010611-134625 pmid:21961707.
Volkow ND, Wise RA, Baler R (2017) The dopamine motive system: implications for drug and food addiction. *Nat Rev Neurosci* **18**: 741–752. doi 10.1038/nrn.2017.130 pmid:29142296.
Waddington JL, Cross AJ (1978) Neurochemical changes following kainic acid lesions of the nucleus accumbens: implications for a GABAergic accumbal-ventral tegmental pathway. *Life Sci* **22**: 1011–1014. pmid:25363.
Wang H-L, Qi J, Zhang S, Wang H, Morales M (2015) Rewarding effects of optical stimulation of ventral tegmental area glutamatergic neurons. *J Neurosci* **35**: 15948–15954. doi 10.1523/JNEUROSCI.3428-15.2015 pmid:26631475.
Watabe-Uchida M, Zhu L, Ogawa SK, Vamanrao A, Uchida N (2012) Whole-brain mapping of direct inputs to midbrain dopamine neurons. *Neuron* **74**: 858–873. doi 10.1016/j.neuron.2012.03.017 pmid:22681690.
Whorton MR, MacKinnon R (2011) Crystal structure of the mammalian GIRK2 K+ channel and gating regulation by G proteins, PIP2, and sodium. *Cell* **147**: 199–208. doi 10.1016/j.cell.2011.07.046 pmid:21962516.
Whorton MR, MacKinnon R (2013) X-ray structure of the mammalian GIRK2-βγ G-protein complex. *Nature* **498**: 190–197. doi 10.1038/nature12241 pmid:23739333.
Wickersham IR, Finke S, Conzelmann K-K, Callaway EM (2007) Retrograde neuronal tracing with a deletion-mutant rabies virus. *Nat Methods* **4**: 47–49. doi

10.1038/nmeth999 pmid:17179932.
Wickman K, Karschin C, Karschin A, Picciotto MR, Clapham DE (2000) Brain localization and behavioral impact of the G-protein-gated K+ channel subunit GIRK4. *J Neurosci* **20**: 5608–5615. pmid:10908597.
Wickman K, Nemec J, Gendler SJ, Clapham DE (1998) Abnormal heart rate regulation in GIRK4 knockout mice. *Neuron* **20**: 103–114. pmid:9459446.
Wickman KD, Iñiguez-Lluhi JA, Davenport PA, Taussig R, Krapivinsky GB, Linder ME, Gilman AG, Clapham DE (1994) Recombinant G-protein βγ-subunits activate the muscarinic-gated atrial potassium channel. *Nature* **368**: 255–257. doi 10.1038/368255a0 pmid:8145826.
Wise RA (2004) Dopamine, learning and motivation. *Nat Rev Neurosci* **5**: 483–494. doi 10.1038/nrn1406 pmid:15152198.
Wise RA (2009) Roles for nigrostriatal—not just mesocorticolimbic—dopamine in reward and addiction. *Trends Neurosci* **32**: 517–524. doi 10.1016/j.tins.2009.06.004 pmid:19758714.
Wolf P, Olpe HR, Avrith D, Haas HL (1978) GABAergic inhibition of neurons in the ventral tegmental area. *Experientia* **34**: 73–74. pmid:202482.
Wulff AB, Tooley J, Marconi LJ, Creed MC (2018) Ventral pallidal modulation of aversion processing. *Brain Res* doi 10.1016/j.brainres.2018.10.010 pmid:30300634.
Wydeven N, Marron Fernandez de Velasco E, Du Y, Benneyworth MA, Hearing MC, Fischer RA, Thomas MJ, Weaver CD, Wickman K (2014) Mechanisms underlying the activation of G-protein-gated inwardly rectifying K+ (GIRK) channels by the novel anxiolytic drug, ML297. *Proc Natl Acad Sci U S A* **111**: 10755–10760. doi 10.1073/pnas.1405190111 pmid:25002517.
Xi ZX, Stein EA (1999) Baclofen inhibits heroin self-administration behavior and mesolimbic dopamine release. *J Pharmacol Exp Ther* **290**: 1369–1374. pmid:10454516.
Xi ZX, Stein EA (2000) Increased mesolimbic GABA concentration blocks heroin self-administration in the rat. *J Pharmacol Exp Ther* **294**: 613–619. pmid:10900239.
Xia Y, Driscoll JR, Wilbrecht L, Margolis EB, Fields HL, Hjelmstad GO (2011) Nucleus accumbens medium spiny neurons target non-dopaminergic neurons in the ventral tegmental area. *J Neurosci* **31**: 7811–7816. doi 10.1523/JNEUROSCI.1504-11.2011 pmid:21613494.
Yamada M, Inanobe A, Kurachi Y (1998) G protein regulation of potassium ion channels. *Pharmacol Rev* **50**: 723–760. pmid:9860808.
Yamaguchi H, Aiba A, Nakamura K, Nakao K, Sakagami H, Goto K, Kondo H, Katsuki M (1996) Dopamine D2 receptor plays a critical role in cell proliferation and proopiomelanocortin expression in the pituitary. *Genes Cells* **1**: 253–268. pmid:9140068.
Yamaguchi T, Qi J, Wang H-L, Zhang S, Morales M (2015) Glutamatergic and dopaminergic neurons in the mouse ventral tegmental area. *Eur J Neurosci* **41**: 760–772. doi 10.1111/ejn.12818 pmid:25572002.
Yamaguchi T, Sheen W, Morales M (2007) Glutamatergic neurons are present in the rat ventral tegmental area. *Eur J Neurosci* **25**: 106–118. doi 10.1111/j.1460-9568.2006.05263.x pmid:17241272.
Yang H, de Jong JW, Tak Y, Peck J, Bateup HS, Lammel S (2018) Nucleus accumbens subnuclei regulate motivated behavior via direct inhibition and disinhibition of VTA dopamine subpopulations. *Neuron* **97**: 434–449.e4. doi 10.1016/j.neuron.2017.12.022 pmid:29307710.

Ye C, Sowell MO, Vassilev PM, Milstone DS, Mortensen RM (1999) G αi2, G αi3and G αoare all required for normal muscarinic inhibition of the cardiac calcium channels in nodal/atrial-like cultured cardiocytes. *J Mol Cell Cardiol* **31**: 1771–1781. doi 10.1006/JMCC.1999.1015.

Yoo J-H, Yang E-M, Lee S-Y, Loh HH, Ho IK, Jang C-G (2003) Differential effects of morphine and cocaine on locomotor activity and sensitization in mu-opioid receptor knockout mice. *Neurosci Lett* **344**: 37–40. pmid:12781916.

Zachariou V, Georgescu D, Sanchez N, Rahman Z, DiLeone R, Berton O, Neve RL, Sim-Selley LJ, Selley DE, Gold SJ, Nestler EJ (2003) Essential role for RGS9 in opiate action. *Proc Natl Acad Sci* **100**: 13656–13661. doi 10.1073/pnas.2232594100 pmid:14595021.

Zarrindast M-R, Khakpai F (2015) The modulatory role of dopamine in anxiety-like behavior. *Arch Iran Med* **18**: 591–603. doi 0151809/AIM.009 pmid:26317601.

Zhang H, He C, Yan X, Mirshahi T, Logothetis DE (1999) Activation of inwardly rectifying K+ channels by distinct PtdIns(4,5)P2 interactions. *Nat Cell Biol* **1**: 183–188. doi 10.1038/11103 pmid:10559906.

Zhang S, Qi J, Li X, Wang H-L, Britt JP, Hoffman AF, Bonci A, Lupica CR, Morales M (2015) Dopaminergic and glutamatergic microdomains in a subset of rodent mesoaccumbens axons. *Nat Neurosci* **18**: 386–392. doi 10.1038/nn.3945 pmid:25664911.

Zhao S, Maxwell S, Jimenez-Beristain A, Vives J, Kuehner E, Zhao J, O'Brien C, de Felipe C, Semina E, Li M (2004) Generation of embryonic stem cells and transgenic mice expressing green fluorescence protein in midbrain dopaminergic neurons. *Eur J Neurosci* **19**: 1133–1140. doi 10.1111/j.1460-9568.2004.03206.x pmid:15016072.

Zhou W, Mailloux AW, McGinty JF (2005) Intracerebral baclofen administration decreases amphetamine-induced behavior and neuropeptide gene expression in the striatum. *Neuropsychopharmacology* **30**: 880–890. doi 10.1038/sj.npp.1300635 pmid:15592348.

Zweifel LS, Argilli E, Bonci A, Palmiter RD (2008) Role of NMDA receptors in dopamine neurons for plasticity and addictive behaviors. *Neuron* **59**: 486–496. doi 10.1016/j.neuron.2008.05.028 pmid:18701073.

Zweifel LS, Fadok JP, Argilli E, Garelick MG, Jones GL, Dickerson TMK, Allen JM, Mizumori SJY, Bonci A, Palmiter RD (2011) Activation of dopamine neurons is critical for aversive conditioning and prevention of generalized anxiety. *Nat Neurosci* **14**: 620–626. doi 10.1038/nn.2808 pmid:21499253.

Appendix

As a graduate student, there have been several papers that I have found exceptionally inspirational and/or helpful, and I would like to highlight them here.

Ref.	Title	What I appreciated about this paper
(Arora et al., 2011; Padgett et al., 2012)	Emerging concepts for G protein-gated inwardly rectifying potassium (GIRK) channels in health and disease	**Review**. Excellent introduction to GIRK channels in the nervous system. I read this paper at the start of my time in the Wickman lab, and continue to return to it to this day. Happily recommend to anyone looking to learn about GIRK channels and only has an hour to spare!
	Structure to Function of G Protein-Gated Inwardly Rectifying (GIRK) Channels Edited by Paul A. Slesinger, Kevin Wickman. International Review of Neurobiology Volume 123, 2015.	**Book.** If you find yourself with more time and interest in GIRK channels, this book is a fantastic resource.
(Lüscher and Slesinger, 2010)	Firing modes of dopamine neurons drive bidirectional GIRK channel plasticity	**Research paper**. This paper describes firing model dependent adaptations in GIRK channel activity in VTA DA neurons, which I think has major implications for as a general mechanism for GIRK channel adaptations.
(Lalive et al., 2014)	Diversity of Dopaminergic Neural Circuits in Response to Drug Exposure	**Reviews**. Collectively, these reviews provide an excellent introduction to the tangled mess of VTA DA neuron subpopulations.
(Juarez and Han, 2016)	Ventral tegmental area dopamine revisited: effects of acute and repeated stress	
(Holly and Miczek, 2016)	Ventral tegmental area: cellular heterogeneity, connectivity and behavior	
(Morales and Margolis, 2017)	Diversity of transgenic mouse models for selective targeting of midbrain dopamine neurons	